PB-228 668

GASIFICATION OF FOSSIL FUELS UNDER OXIDATIVE, REDUCTIVE, AND PYROLYTIC CONDITIONS

A. L. Yergey, et al

Scientific Research Instruments Corporation

Prepared for:

National Environmental Research Center

December 1973

DISTRIBUTED BY:

NTIS

National Technical Information Service
U. S. DEPARTMENT OF COMMERCE
5285 Port Royal Road, Springfield Va. 22151

BIBLIOGRAPHIC DATA SHEET	1. Report No. EPA-650/2-73-042	2.	PB 228 668

4. Title and Subtitle
Gasification of Fossil Fuels Under Oxidative, Reductive, and Pyrolytic Conditions

5. Report Date
December 1973

6.

7. Author(s)
A. L. Yergey, F. W. Lampe, M. L. Vestal, E. J. Gilbert, and G. J. Fergusson

8. Performing Organization Rept. No. SRI 72

9. Performing Organization Name and Address
Scientific Research Instruments Corporation
6707 Whitestone Road
Baltimore, Maryland 21207

10. Project/Task/Work Unit No.
ROAP 21ADD04

11. Contract/Grant No.
68-02-0206

12. Sponsoring Organization Name and Address
EPA, Office of Research and Development
NERC-RTP, Control Systems Laboratory
Research Triangle Park, NC 27711

13. Type of Report & Period Covered
Final

14.

15. Supplementary Notes

16. Abstracts The report contains kinetic reaction data produced in a non-isothermal kinetics laboratory while gasifying selected types of coal under oxidative, reductive, and pyrolytic conditions. Types of coal cover the range, including lignite and anthracite. Evolution of thermal decomposition products under study conditions were investigated at different fuel heating rates and gasification pressures. Gaseous product evolution rates, as the function of temperature, were graphed for different coals exposed to indicated gasification regimes. The evolution of such gaseous species as H_2O, CO, CO_2, O_2, SO_2, NO, H_2, CH_4, H_2S, and C_2H_2 was followed up in conjunction with 13 different coal gasification reactions as identified previously and in the course of this work. The kinetic reaction parameters, such as activation energy and frequency factors for these reactions, were calculated and presented earlier and in this report.

17. Key Words and Document Analysis. 17a. Descriptors
Air Pollution
Coal Gasification
Fossil Fuels
Oxidation
Reduction (Chemistry)
Pyrolysis
Kinetics

17b. Identifiers/Open-Ended Terms
Air Pollution Control

Reproduced by
NATIONAL TECHNICAL
INFORMATION SERVICE
U S Department of Commerce
Springfield VA 22151

17c. COSATI Field/Group 40D, 07D, 13B

18. Availability Statement	19. Security Class (This Report)	21. No. of Pages
Unlimited	UNCLASSIFIED	184
	20. Security Class (This Page) UNCLASSIFIED	22. Price #12.25/1.45

EPA-650/2-73-042

GASIFICATION OF FOSSIL FUELS UNDER OXIDATIVE, REDUCTIVE, AND PYROLYTIC CONDITIONS

by

A. L. Yergey, F.W. Lampe,
M. L. Vestal, E. J. Gilbert, and G. J. Fergusson

Scientific Research Instruments Corporation
6707 Whitestone Road
Baltimore, Maryland 21207

Contract No. 68-02-0206
Program Element No. 1AB013
ROAP No. 21ADD04

EPA Project Officer: L. Stankus

Control Systems Laboratory
National Environmental Research Center
Research Triangle Park, North Carolina 27711

Prepared for

OFFICE OF RESEARCH AND DEVELOPMENT
U. S. ENVIRONMENTAL PROTECTION AGENCY
WASHINGTON, D. C. 20460

December 1973

ia

This report has been reviewed by the Environmental Protection Agency and approved for publication. Approval does not signify that the contents necessarily reflect the views and policies of the Agency, nor does mention of trade names or commercial products constitute endorsement or recommendation for use.

TABLE OF CONTENTS

	PAGE
INTRODUCTION	1
EXPERIMENTAL	3
INSTRUMENTATION AND THEORY	3
IMPROVEMENTS IN EXPERIMENTAL TECHNIQUE	8
ARGON AS DILUENT GAS	8
SAMPLE HOMOGENEITY EXPERIMENTS	9
ON-LINE COMPUTER SYSTEM	10
COMPUTERIZATION OF THE NON-ISOTHERMAL KINETICS LABORATORY	10
SYSTEM HARDWARE	10
SYSTEM SOFTWARE	14
EXPERIMENTAL DATA	17
EVOLUTION CURVES IN OXIDIZING ATMOSPHERES	19
EVOLUTION CURVES IN PYROLYTIC ATMOSPHERES	21
GAS EVOLUTION CURVES IN REDUCING ATMOSPHERES	22
SPECIAL EXPERIMENTS	24
CO_2 + CO REACTIONS	24
AIR OXIDATIONS	25
DISCUSSION	26
KINETIC PARAMETERS	26
OXIDATION REACTIONS	29
HYDROGASIFICATIONS	31
CARBON DIOXIDE - CARBON REACTION	32
SUMMARY	34
APPENDIX A - Gaseous Evolution Data For Oxidative Reactions	35
APPENDIX B - Gaseous Evolution Data For Pyrolysis Experiments	84
APPENDIX C - Gaseous Evolution Data For Reducing Reactions	141
APPENDIX D - Gaseous Evolution Data For ^{13}C Reactions	169
APPENDIX E - Gaseous Evolution Data For Air Reactions	174
BIBLIOGRAPHY	177

LIST OF FIGURES

		Pages
Figure 1	Block Diagram of the Coal Research Facility	4
Figure 2	Schematic of Computer and Peripheral Interconnections	13
Figure 3	Kinetic Parameters for CO Evolution - Oxidizing Atmosphere, SRI Coal No. 5	28
Figures 4 - 47	Oxidation Experiments - Appendix A	40 - 83
Figures 48 - 102	Pyrolysis Experiments - Appendix B	86 - 140
Figures 103 - 128	Reduction Experiments - Appendix C	143 - 168
Figures 129 - 132	^{13}C Experiments - Appendix D	170 - 173
Figures 132 - 133	Air Experiments - Appendix E	175 - 176

LIST OF TABLES

		Pages
TABLE I.	Run Conditions, Representative Sample	9
TABLE II.	Hardware Components of On-Line Computer System	11
TABLE III.	System Software	15
TABLE IV.	Proximate and Ultimate Analysis Summaries	18
TABLE V.	Kinetic Parameters (Oxidation and Reduction Reactions)	27
TABLE VI.	Kinetic Parameters (CO_2 - Coke Reactions)	32
TABLE VII.	Peak Temperatures in Oxidative Gasification of Coal - Appendix A	36
TABLE VIII.	Effect of Water Vapor on Oxidative Gasification of Coal - Appendix A	38
TABLE IX.	Peak Temperatures in Treatment of Coke (SRI-7) with CO_2 in Ar - Appendix A	39
TABLE X.	Peak Temperatures for Pyrolysis of Coals and Cokes Heated at 30^0/min in Argon - Appendix B	85
TABLE XI.	Peak Temperatures in Reducing Atmospheres of Hydrogen at 10 atm Pressure - Appendix C	142

INTRODUCTION

This final report describes our studies on the gasification of coals and related fossil fuels performed under Contract 68-02-0206 with the Environmental Protection Agency.

Contract efforts in the past have resulted in the development of the computerized non-isothermal kinetics laboratory[1], and in the demonstration of the value of the non-isothermal kinetics treatment for the study of chemical reactions related to coal desulfurization[1,2]. The work described in this report clearly demonstrates the ability of the non-isothermal kinetics laboratory to generate large amounts of phenomenological data concerning complex reaction systems. The relatively short times required for data production, the number of different materials which have been used or obviously could be used, and the quality of the data produced indicate the power of the non-isothermal kinetics technique. Possible future importance of the non-isothermal kinetics method can perhaps be fully appreciated for the first time through the results presented in this report. The apparent practical applications of the method to studies of desulfurization, combustion and gasification given here and in past reports could be extended to studies of the practical basis of the chemical industry, heterogeneous reaction kinetics.

Gasification studies have been performed on a variety of bituminous coals, anthracite, lignite, and some chars under a large variety of reaction conditions. Oxidative gasifications have been performed in a range of oxygen concentrations from 0.1% to 20% O_2 by volume at pressures up to 10 atm. Reductive gasifications in pure hydrogen have been carried out routinely at hydrogen pressures of up to 20 atm.

Several experiments which utilize the unique capabilities of the non-isothermal kinetics technique have also been performed. First are a number of fuel pyrolysis studies carried out in an argon atmosphere, and intended to determine the thermal evolutionary behavior of some materials present in these fuels. Second, the non-isothermal kinetics technique permits the study of particular reactions of importance in gasification under conditions where interfering reactions are limited in extent or totally absent. In this fashion, the CO shift reaction with coal chars and coals was studied.

A great deal of progress was made toward the goal of operational on-line data acquisition and storage system using a mini-computer. The computer and its peripherals have all functioned as a system. The interfacing hardware as well as the data acquisition software are in near-final form. The actual operation of the computer/mass spectrometer in an on-line, real-time situation will be deferred until a future date.

EXPERIMENTAL

INSTRUMENTATION AND THEORY

The experimental apparatus and the mathematical treatment of results used in the non-isothermal kinetics method have been fully described in earlier publications[1-5]. During the performance of the research described in this report, the apparatus was used in virtually an unaltered form from that given in the descriptions cited, but important changes in the apparatus are given in a following section. For the sake of completeness, a brief description of the apparatus and a brief theoretical summary are given below.

A block diagram of the non-isothermal kinetics apparatus is shown in Figure 1. Hydrogen or helium, at flow rates selected for an experiment, is passed over a finely ground (100-200 mesh) sample of coal placed into a quartz tube inside the furnace. Temperatures within the furnace are increased linearly with time, and are maintained to within a few degrees of a preselected heating rate by differential controls within the temperature programmer. The heating rates possible within this apparatus can vary from about 1^0C/min to 100^0C/min.

The sweep gases used in this work also serve as chemical ionization[6] reagent gases since their concentrations are much greater than the gaseous reaction products. Source pressures in the mass spectrometer are maintained at about one Torr so that ions formed originally by electron impact undergo mutiple ion-neutral collisions. In the case of hydrogen, this results in H_3^+ being the most abundant ion in the source, as shown in Equations (1) and (2). Ions derived from the desulfurization reaction product gases are formed by a proton transfer from H_3^+ as shown in Equation (3).

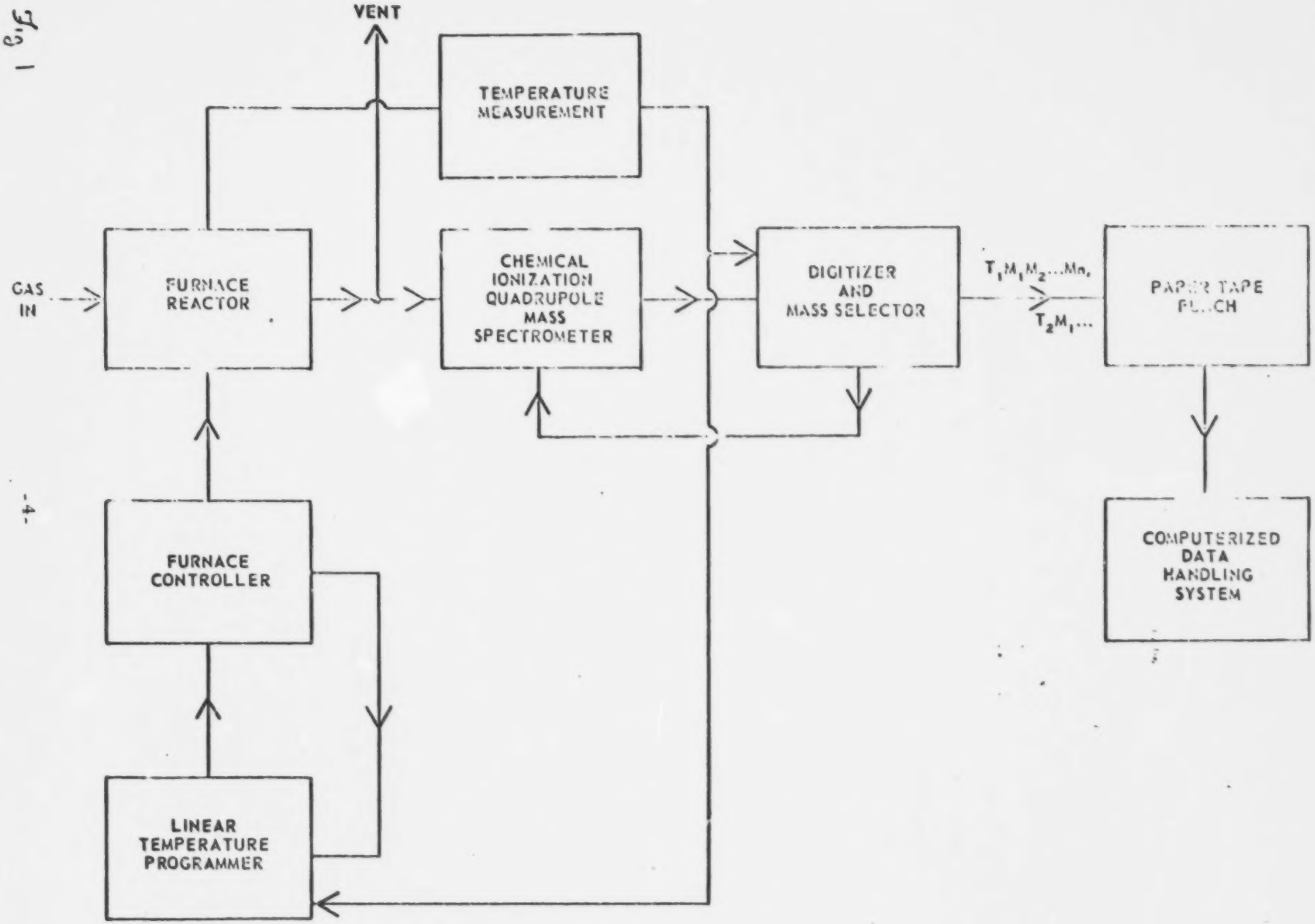

Figure 1 Block Diagram of the Coal Research Facility

$$H_2 + e \rightarrow 2e + H_2^+ \qquad (1)$$

$$H_2^+ + H_2 \rightarrow H_3^+ + H \qquad (2)$$

$$H_3^+ + H_2S \rightarrow H_3S^+ + H_2 \qquad (3)$$

Because the proton affinities of the product gases are higher then that of H_2, the product gases are preferentially protonated, an effect which results in a great sensitivity increase compared with normal electron impact ionization. An analogous situation involving charge transfer occurs when He is used as the reagent gas.

Ions leaving the source region are mass-analyzed in a quadrupole mass filter and their intensities are amplified by an electron multiplier. Signals from both the multiplier and a thermocouple are input to the digitizer and mass spectrometer controller. This device allows the monitoring of the intensities of up to nine peaks in the mass spectrum by stepping the mass filter to appropriate focussing voltages. The rate at which the controller steps through the mass settings and temperature is selected to be comparable to the furnace heating rate, so that intensity versus temperature plots result.

The mathematical treatment of reaction product intensity versus temperature profiles obtained by linear heating of a bed of material can be summarized using a general reaction considered to proceed in the furnace. Consider Equation (4), the reaction of a particular solid species, P, with gas H_2 passing over it. For the purpose of this brief summary, it will be assumed that the reaction is first order in P and zeroth order in H_2 and that gaseous products are swept from the chamber without further reaction.

$$P + H_2 \rightarrow PH_2 \qquad (4)$$

The differential expression of the reaction rate is:

$$-\frac{d[P]}{dt} = \frac{d[PH_2]}{dt} = k[P] \qquad (5)$$

where the reaction rate constant, k, is given by the Arrhenius equation:

$$k = k_0 e^{-E/RT} \qquad (6)$$

where k_0 is the temperature-independent Arrhenius pre-exponential factor, E is the activation energy, and R and T have their usual meaning. Equation (5) can be integrated to yield:

$$\ln \frac{[P]}{[P]_0} = -\int_0^t k\,dt \qquad (7)$$

where [P] is the concentration of the reactant at a time, t, and $[P]_0$ is the initial concentration of the reactant. Consider now a reaction where the temperature may be varied linearly with time as :

$$m = \frac{dT}{dt} \qquad (8)$$

where T , and t are as above and m is the heating rate. When $\frac{dT}{dt}$ =m=0 then k in (7) does not vary with time, and the integration of the right-hand side of (7) becomes trivial. In cases where $m \neq 0$, (6) and (8) are substituted into (7), and the integration limits become those temperatures between which reaction is observed:

$$\ln \frac{[P]}{[P]} = -\frac{k_0}{m}\int_{T_i}^{T} e^{-E/RT}\,dT \qquad (9)$$

The integration of (9) can be completed by use of an approximation for the exponential integral. Making use of an expression for [P] and $[P]_0$ in terms of the volumes of gaseous products, viz:

$$[P] = \alpha(V_0 - V) \qquad (10)$$

where V is the volume of gas evolved up to temperature T, V_0 is the total gas volume evolved and α is a proportionality factor, and then differentiating this expression with respect to T, yields the expression:

$$\frac{dV}{dT} = \frac{V_0 k_0}{\beta} \exp\left[-\left(\frac{k\,RT^2}{\beta E} e^{-E/RT} + \frac{E}{RT}\right)\right] \qquad (11)$$

Equation (11) defines the shape of the intensity versus temperature peaks obtained as data in non-isothermal kinetics experiments. Analysis of these peaks for the kinetic parameters E and k_0 is carried out by taking the temperature derivative of (11) which yields:

$$\ln\left(\frac{\beta}{T_m^2}\right) + \frac{E}{RT_m} = \ln\frac{E}{Rk_0} \qquad (12)$$

where Tm is the absolute temperature of a peak maximum. Plots of (12) using data from experiments conducted at a variety of heating rates, result in determinations of the kinetic parameters desired. A more complete discussion of data analysis, involving reaction orders other than first as well as back reactions, is given in the previously cited references.

IMPROVEMENTS IN EXPERIMENTAL TECHNIQUE

ARGON AS DILUENT GAS

The non-isothermal kinetics laboratory performed quite reliably during the course of the contract in a form virtually unaltered from previous descriptions[1,3]. Several improvements to the experimental techniques have, however, been made.

Previous work in oxidizing atmospheres was done using helium as the carrier gas. Helium, although desirable because of its inertness, has an ionization potential of 24.6 eV, which is sufficient energy to cause extensive fragmentation of sample gases in charge exchange chemical ionization. Argon, with an ionization potential of 15.8 eV, has been used in place of helium as the diluent in oxidizing atmosphere studies because the inertness is attained with considerably reduced fragmentation. Nitrogen, with an ionization potential near argon, and much less expensive than argon, is not useable because the N_2^+ ion has the same mass as CO^+, a crucial product gas in oxidizing experiments, and thus CO production could not be followed. Some fragmentation of CO_2^+ to yield CO^+, a process which occurs at energies higher than 20.5 eV, is seen with the use of argon. This fragmentation is undoubtedly due to the presence of the small amounts of Ar^{++} ion observed in the chemical ionization mass spectrometer. Although at first it would be anticipated that any Ar^{++} formed by electron impact would be quickly eliminated by the large numbers of collisions occurring between the ions and neutrals present in the source at typical operating conditions, nevertheless, this species is observed at high source pressures. Apparently, the mechanisms which exist for the decomposition of the Ar^{++} - Ar collision complex into two argon singly charged ions are very inefficient and sufficient quantities of the doubly charged ion are present to effect some fragmentation in the source.

SAMPLE HOMOGENEITY EXPERIMENTS

An area of continuing concern for experiments performed in the non-isothermal kinetics laboratory has been the reliability of data interpretation when sample sizes of the order of 10-15 mg are used. The well known inhomogeneity of coal, coupled with small samples, could result in interpretations which are based not on the average properties of the coals, but on the properties of a totally unrepresentative portion of the material. On the other hand, the use of small samples in the bed is imperative to the non-isothermal kinetics method, if adequate resolution is to be obtained from sequential evolution of a particular gaseous product.

A series of experiments has been performed to investigate the reproducibility of H_2S evolutions from small samples. Scientific Research Instruments Corporation Coal #10, (Kentucky 4% Sulfur, USBM #110 from bed 14 of the Shamrock mine) was used. The entire quantity of this coal in hand was subjected to a four-fold rifle sampling, resulting in sixteen final samples. Non-isothermal kinetic runs were performed on a portion of each of the eight odd-numbered samples. The standard run conditions are shown in Table I.

TABLE I RUN CONDITIONS, REPRESENTATIVE SAMPLE

Material - SRI Coal #10, Kentucky 4% Sulfur

Weight - 15 mg	Initial Temperature -80°C
Particle Size - 100-200 mesh	Carrier Gas - H_2
Heating Rate - 14°/min	Flow Rate - 100 scc/min

The eight H_2S intensity-temperature profiles resulting from these experiments although not given here, are sufficiently alike in all respects for seven of the eight experiments, that recognition of the material used in the experiments would be readily accomplished. It appears that the use of small carefully chosen samples can reflect with some confidence, the average behavior of the material chosen for a non-isothermal kinetics experiment.

ON LINE COMPUTER SYSTEM

COMPUTERIZATION OF THE NON-ISOTHERMAL KINETICS LABORATORY

The non-isothermal kinetics laboratory has been computerized to some extent in past years[1]. The results of this computerization are demonstrated by the bulk of this report, in that substantial quantities of data have been produced. The computerization of the past has been an off-line raw data reduction system with additional programming necessary for data analysis. The computerization, as it is presently structured, however, has several drawbacks. There is an upper limit for a data acquisition rate, a lower limit on data reduction time, and a high long-term cost. The first computerization of the non-isothermal kinetics laboratory involved data recording on punched paper tape. Because the paper tape is limited in speed, data acquisition rates for non-isothermal kinetics experiments are limited to speeds corresponding to heating rates of about 100°/min. Recent incremental improvements in data reduction software on the time-shared computer being used have permitted data reduction for a given experiment to be done in thirty minutes, but at the cost of an operator's time and useage charges for the time sharing service.

The use of an on-line, real-time mini-computer data acquisition system is seen as solving all three of the problems described above. Data acquisition can be done easily at heating rates that conservatively are on order of magnitude faster than are currently feasible, raw data reduction can be completed simultaneously with the completion of an experiment, and only a single operator will be required for the entire process of experiment supervision and raw data reduction.

SYSTEM HARDWARE

An evaluation of cost, programming ease, and quality resulted in the choice of a Varian 620/L computer with 12K, 16 bit core, a paper tape reader, and 1.17M, 16 bit word disc for the task of interfacing with the non-isothermal kinetics laboratory. The hardware components of this system are listed in Table II.

TABLE II. HARDWARE COMPONENTS OF ON-LINE COMPUTER SYSTEM

Varian Components

620/L Central Processor with 12,288 words of 16-bit core, 1.8μ sec cycle time, 130 member instruction set, 4 operational and 5 buffer registers.

Buffered Interlace Controller (BIC) allows programmable block data transfers

Real Time Clock (RTC) at 400 Hz

Power Fail/Restart (PF/RS) interrupts programs at power failure and automatically restarts upon power recovery

Priority Interrupt Module (PIM) allows branching and return to programs based on the status of external signals such as real-time data ready or internal function complete signals.

Moveable Head Disc with capacity for 1.17 M 16-bit words formatted into 8 sectors and 203 tracks on two sides of a magnetic oxide medium, 10 operations with interrupt capability, and a 92K 16-bit word transfer rate.

Buffered I/O Controller allows interfacing to SRIC Digitizer and Mass Spectrometer Controller

Universal Asynchronous Series Controller allows use of Typagraph plotting teletype in place of standard teletype

300 cps Paper tape Reader

Other Components

(used previously in non-isothermal kinetics laboratory)

Tally 60 cps Paper Tape Perforator

Typagraph Model 3 Plotting Teletype Terminal (TTY)

The first seven items listed along with the controllers for the last four items are located in two CPU console chassis, while the remaining items, two being peripheral devices, are contained in separate chassis.

Figure 2 shows a schematic representation of the functional connections between various components in the system. The CPU is the main control device and supervisor for the entire system. Information transfer between the CPU and various peripherals is carried out along the I/O lines, although block word transfers for the paper tape system and the disc can be effected through the BIC. The PIM is a very necessary and a very useful device for the optimum ionization of other kinds of programming. In data acquisition for example, such as a raw data reduction/analysis program, the PIM interrupts a program whenever the SRIC digitizer has data to transfer. When the transfer is complete, the program execution continues from the point of interruption. A similar operation can be used in the copying of information from one peripheral to another or between a peripheral and core. The latter case is important because of the wide disparity in rates which exist between core and any peripheral. If interrupt signals are received by the PIM from two devices simultaneously, they are dealt with in a hierarchical fashion with number 1 on Figure 2 having the highest priority. The PF/RS acts as the PIM does, but only for the specific case of power failures and restarts. In addition, it has a priority higher than any of those in the PIM. The RTC is used in establishing a time-base for the acquisition of data in a real-time experiment, or for the execution of particular operations at predetermined real-time points.

Considerable difficulty was encountered in bringing the hardware to a functioning state. The principle components of the system were delivered one month after the date agreed upon with the manufacturer, but in addition, final delivery of the correct system components was not accomplished until five months after the original delivery date. A fully functioning system is virtually accomplished but due to delays incurred principally by disc hardware malfunctions,

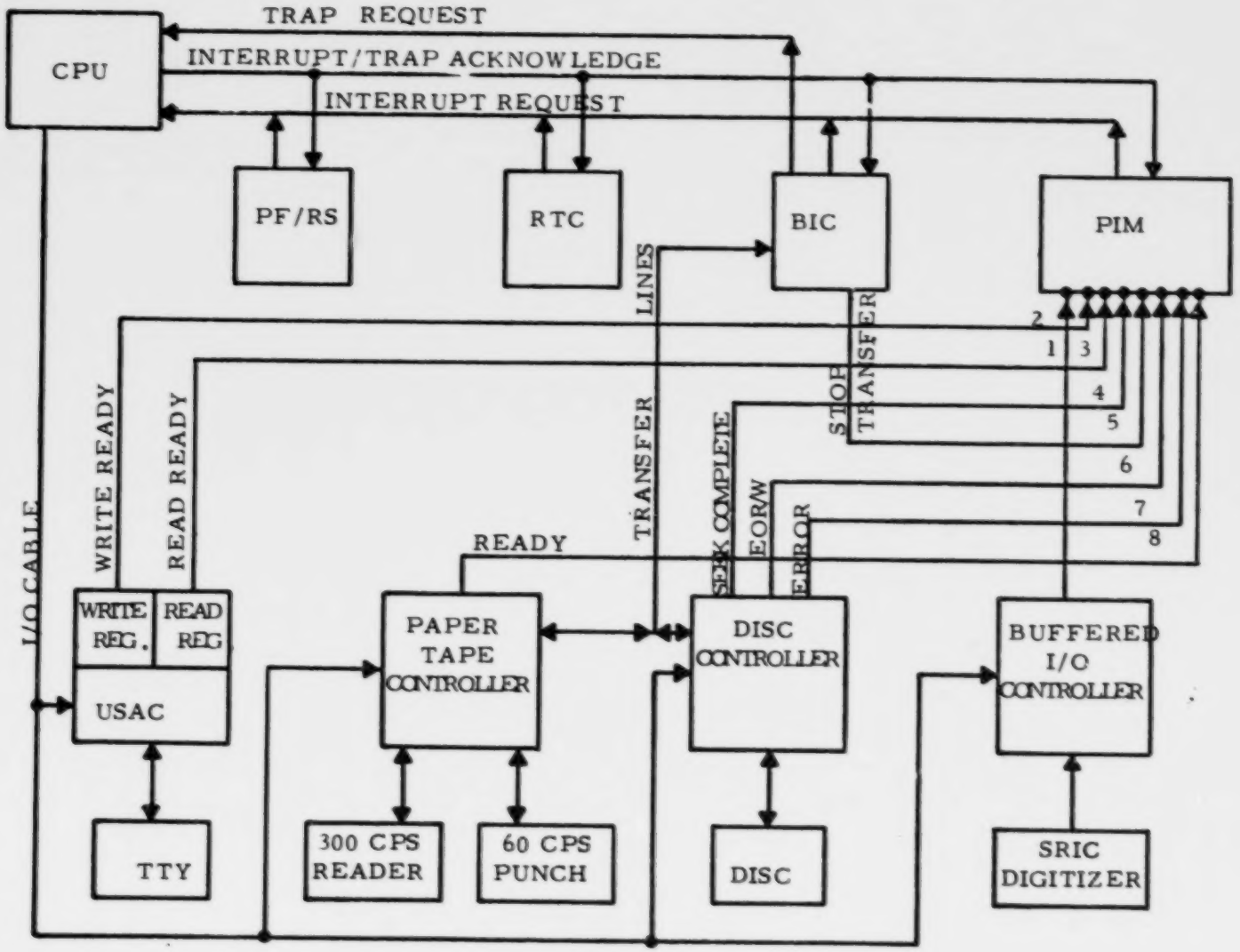

FIGURE 2. Schematic of Computer and Peripheral Interconnections

software development allowing full system integration was slowed considerably from initial projections. Use of the buffered I/O controller in the interrupt mode will be deferred until a future date.

SYSTEM SOFTWARE

Software intended for use for the on-line computer connection to the non-isothermal kinetics laboratory is grouped in two large sections. One section is that supplied by the computer manufacturer, and the other section is that developed by Scientific Research Instruments Corporation. Table III lists the software in each of these catagories.

The Varian software is a necessary tool that was used in developing the software for executing the real task assigned to the computer. The existance of MOS and the disc hardware, in addition to being required for data acquisition should have eased the entire job of applications software development. To a large extent, this was true, especially in the later development stages where program modules were assembled and then stacked together for execution. The difficulties involving hardware, that were described above, limited the usefulness of MOS. In addition, there was an acutely felt lack in the MOS software package for an easy-to-use line editor. The editor present in MOS was found to be slow, difficult to operate, and inconvenient. Aside from this lack, however, the remaining utility software, the assembler, compiler, loader, and executive, was found to be adequate. The other Varian software listed in Table III was found to be satisfactory for its intended purposes, and thus very valuable at particular times.

Although development of the SRIC software package was hampered by the hardware failures encountered and by the lack of a useable MOS editor, the programs listed in Table III have all been written, and have been tested to some extent with the exception of VEZGRAF. This particular program requires some experimentation to detemine the optimum size of pieces which can be handled by 12K of core storage.

TABLE III. SYSTEM SOFTWARE

Varian Software	
Name	**Purposes**
MOS	Operating System for Disc useage. Includes an assembler, compiler for FORTRAN, loader, disc executive, and the ability to manipulate peripherals.
MAINTAIN	Family of diagnostic programs used for locating failures in the CPU or any peripherals. Also used in checking for correct functioning of apparatus after completion of interfacing.
AID	Stand-alone debugging program, permanently resident in high core locations.
BLD	Stand-alone load and dump program for use with binary information only. Permanently located in high core.
SRIC Software	
ACQI	Data acquisition and raw data reduction program
LINED	Source code editor for any language in any format.
FLIM	Disc file management program which converts disc to a random access device.
VEZGRAF	Modified form of Typagraph program EZGRAF, which enables a computer of limited core size to drive the plotting teletype
MTM, etc.	Translated forms of previously written SRIC data analysis programs to permit data analysis with on-line systems.

The protocol of software development was to use the excellent editor available to us in a time-shared computer service to develop the LINED program. LINED is an extremely versatile line and source code editor which can then be used to develop the other programs in the SRIC package. Future plans call for the elimination of the MOS editor from the disc system file and replacing it with the LINED programming.

The FLIM program is intended to alter the formatting of the disc so that it can be considered a random access device. This is very necessary for the efficient storing of data files on the disc. It utilizes the concept of a disc table of contents permitting the addition and subtraction of files without the necessity of operator bookkeeping required by MOS. FLIM is the beginning of a random access MOS package also slated for future development.

ACQI is the real time data acquisition programming for the on-line computerized non-isothermal kinetics laboratory. As such, it takes data from the SRIC digitizer and mass spectrometer controller at any time in an experiment when such digital information is ready, by using the PIM described above. In the long intervals, by computer time standards, between sequential data presentations, ACQI creates separated intensity versus temperature profiles for each species monitored in the experiment, corrects for heating ramp linearity and temperature skewing, and stores the data files via block data transfers through the BIC, on the disc. At the end of an experiment, ACQI writes an end-of-file after the stored data and updates the indexing of FLIM. The use of ACQI replaces MULT, MODFILE, CAFILE and PIP used with the time shared computer[1] to read-in data from punched paper tapes , and then separate it into individual data files. The programs such as MTM, LSTS and CURVE[1] are retained in the on-line configuration of the computerized non-isothermal laboratory because translation between two Fortran dialects permits these valuable data analysis programs to be used.

EXPERIMENTAL DATA

A major objective of the experimental program during the past year has been to utilize the computerized non-isothermal kinetic laboratory[1] to obtain as much kinetic data as possible pertinent to the oxidative gasification, pyrolysis, hydrogenation , and desulfurization of representative coals and cokes. With this objective in mind, we have studied the evolution of a variety of gases from three typical coals, from cokes derived from these coals, from an anthracite and from a lignite, as these solid materials are heated at various rates from room temperature to 1400°K under oxidative conditions, under reducing conditions and under purely pyrolytic conditions. Proximate and Ultimate analysis summaries of these materials appear in Table IV.

In this section we present the results of our non-isothermal experiments in terms of computer-drawn evolution curves of the most significant gases evolved from the various coals and cokes under the various conditions of treatment. The evolution curves are presented as plots of the mass spectrometric ion-currents of ions derived from chemical ionization of the pertinent gases as functions of the absolute temperature of the bed of coal or coke. The currents of the various ions are presented in the plots in terms of arbitrary units whose magnitude is proportional to the instantaneous concentration of evolved gas in the gas stream leaving the solid bed of coal or coke. For example, under oxidative conditions in which the treatment gas consists of 99% argon and 1% oxygen, the H_2O^+ ion-intensity is proportional to the concentration of water in the gas stream. On the other hand, under reducing condition in which the treatment gas is pure hydrogen, the H_3O^+ ion-intensity is proportional to the concentration of water in the gas stream leaving the bed of solid coal or coke.

It is useful to point out here at the outset that blank runs, in which only the quartz wool plugs are present in the reactor, show evolution peaks of CO^+, H_2O^+, and CH_3^+ at low temperatures ($\sim$520°K). Therefore, little

TABLE IV

PROXIMATE AND ULTIMATE ANALYSIS SUMMARIES

Material	Mine	Bed	Proximate			Ultimate (dry basis)					
			%Nominal S	% Volatiles	%Fixed C	%C	%H	%N	%S	%Ash	%O*
SRI Coal 5 Illinois ISGS: 32-11.60F	Little Dog	Seam 6	4.5	40.8	44.1	69.35	5.67	1.24	4.23	9.73	9.78
SRI Coal 7 Maryland USBM: 106	Royal	Franklin	3	20.5	62.8	75.64	4.73	1.47	3.13	13.67	1.36
SRI Coal 10 Kentucky USBM: 110	Shamrock	No. 14	4	31.3	46.5	65.30	4.67	1.39	3.20	17.31	8.13
Anthracite			.67	9.0	76.0	84.23	2.64	1.20	0.75	7.10	4.08
Lignite	North Beulah		.55	30.1	33.0	60.47	7.04	0.93	0.54	8.83	22.19

* by difference

if any, significance should be attached to the appearance of these peaks in the non-isothermal treatments of the coals and cokes.

EVOLUTION CURVES IN OXIDIZING ATMOSPHERES

The evolution of gases from the coal designated as SRI-5, when this coal is heated from 300-1400°K at a heating rate of 30 °/min gas stream containing 99% argon and 1% oxygen, may be seen by reference to Figures 4-9. These are typical evolution curves that show the concentration of H_2O, CO, NO, CO_2, SO_2, and O_2, respectively, as a function of temperature. The oxygen is a reactant gas in these studies and the inverted peaks shown in Figure 9 indicate a decrease in intensity of O_2^+ in the ion source of the mass spectrometer detection system. As will be discussed in the next section, this may mean that the O_2 concentration in the gas leaving the solid reactant bed has been lowered; however, this conclusion may be made only with caution, since it is possible that the experimental artifact of O_2^+ reaction in the ion-source with a product gas may be responsible for the apparent decrease in O_2 concentration in the gas stream. The flow rate of gas through the coal sample in the experiments shown in Figures 4-9 was 200 cc/min.

It is clear from Figures 4-9 that (1) the evolution of H_2O exhibits peaks at 605°, 715° and 869°; (2) peaks in the concentration of CO are found at 766° and 840°; (3) a single peak at 828° is found for the concentration of NO; (4) two peaks at 566° and 888° are observed for CO_2; (5) a single peak at 829°K is observed for the evolution of SO_2. As mentioned earlier, the studies depicted in Figures 4-9 were carried out at a heating rate of 30° /min When the reactions are studied at different heating rates similar peaks are observed but at different temperatures. In fact, as shown in an earlier report[1] it is this shift in location with heating rate that permits the determination of activation energy for the process involved in production of the peak. Rather than show the individual curves such as in Figures 4-9 for all heating rates studied, these data will be shown when appropriate in an equivalent but more refined form in activation energy plots.

In Figures 10-15, the concentrations of H_2O, CO, NO, CO_2, SO_2, and O_2, respectively, from an identical treatment (1% O_2 in Ar, 30°/min heating rate) of the coal designated as SRI-7 are shown as functions of the absolute temperature.

The concentrations of H_2O, CO, NO, CO_2, SO_2, and O_2 in the gas stream leaving a solid reactant bed of the coal designated as SRI-10, respectively, as functions of the temperature are shown in Figures 16-21.

Similar plots for the concentrations of the same gases observed when anthracite and lignite are treated under the same conditions, are shown in Figures 22-27 and 28-33 respectively.

The concentrations as functions of temperature of H_2O, CO, CO_2, and O_2 in the gas stream leaving a solid bed of a coke prepared from SRI-5 when this solid is treated identically (1% O_2 in Ar, 30°/min) are shown in Figures 34-37 respectively. Figures 38-43 show the concentrations of H_2, H_2O, CO, NO, CO_2, and O_2 respectively, observed when a coke prepared from SRI-7 is treated with 1% O_2 in Ar but at a slightly lower heating rate of 20°/min.

Finally, we show in Figures 44-47, the concentrations of H_2O, CO, CO_2, and O_2, respectively, as a function of temperature observed from the oxidation treatment of a coke prepared from the coal designated as SRI-10. In this set of experiments, the conditions of 1% O_2 in Ar and a heating rate of 30°/min were employed.

While Figures 4-47 present a rather complete experimental picture of the non-isothermal oxidative treatment of coals SRI-5, SRI-7, SRI-10 for a particular heating rate, the most pertinent information, namely the location of peaks as functions of heating rates, is shown in Table VII , Appendix A.

The effect of adding water (at its vapor pressure at room temperature) to the stream of 1% oxygen in argon may be seen in Table VIII. Each coal was examined at only two heating rates, namely 15 and 40°/min and analyses were made only for CO, CO_2, and O_2.

Since the oxidative gasification of coal or coke required oxygen in some form to be delivered to the solid reactant, a number of experiments were conducted in which a coke prepared from SRI-7 coal was treated non-isothermally with a gas stream of 0.1% CO_2 in Ar. The results, in terms of peak temperatures for H_2, H_2O, CO, NO, "CH_3" and CO_2 are given in Table IX. The "CH_3" refers to the appearance of $\frac{m}{e}15$ and represents a fragment ion from a hydrocarbon. This probably comes from quartz wool as it was also observed in blank experiments.

EVOLUTION CURVES IN PYROLYTIC EXPERIMENTS

In order to differentiate between actual oxidative processes and those due to pyrolysis in the experiments described in which the oxygen and carbon dioxide reactants are contained in a great excess of argon, experiments were conducted in which the gas evolution from a pure argon stream was examined. These were studied at only one heating rate, namely 30°/min.

The results for coals SRI-5, SRI-7, and SRI-10 are given in Figures 48-54, 55-61, and 62-68, respectively; those for anthracite and lignite are shown in Figures 69-75 and 76-82 respectively; and those for cokes prepared from coals SRI-5, SRI-7, and SRI-10 are shown in Figures 83-89, 90-95, and 96-102, respectively.

The peak temperatures for the various evolved gases are tabulated for convenience in Table IX.

GAS EVOLUTION CURVES IN REDUCING ATMOSPHERE

Studies have also been conducted on the evolution of CH_4, H_2O, C_2H_6, and H_2S from the same solid reactants when these are heated from 300°-1400° in a stream of hydrogen. The studies have been carried out with hydrogen pressures of 1, 10, and 20 atmospheres. Under such conditions the predominant ion in the ion source of the detecting mass spectrometer is H_3^+ and the ions derived from the gases being evolved from the solids in the reactor are produced via reaction of these gases with H_3^+. We believe that the most reliable analytical results will be obtained when H_3^+ is sufficiently abundant that no depletion of H_3^+ will be observed when other gases evolved by the coal are present to react with it. With the size of the coal samples used (15 mg) very significant depletion of H_3^+ is observed when H_2 at 1 atmosphere and 200 cc/min is employed. However, at 10 atm of H_2 and 2000 cc/min and above, as will be seen, the intensity of H_3^+ remains constant throughout the run, and is taken as being indicative of satisfactory and reliable analyses.

As an example of the above consider the dependence of H_3^+ intensity on temperature shown in Figures 103 and 104. The curve in Figure 103 refers to H_2 reactant at 1 atm and the scatter of points indicates most probably, consumption of H_3^+ via reaction with evolved gases. On the other hand, as shown in Figure 104 the H_3^+ intensity remains constant throughout when H_2 at 10 atm and 2000 cc/min are employed. We take the behavior of reagent gas ion, H_3^+, shown in Figure 104 to indicate more reliable data and, have presented the evolution curves for the conditions embodied therein.

The evolution curves of CH_4 (CH_5^+), H_2O (H_3O^+), and C_2H_6($C_2H_5^+$) from the coal designated as SRI-5 are shown in Figures 105-107. The variation of H_3^+ intensity with temperatures in the experiments with Coal SRI-7 is shown in Figure 108 and the evolution curves for CH_4, H_2O, C_2H_6, and H_2S are given in Figures 109-112. The corresponding curves for Coal SRI-10, Anthracite and Lignite are given in Figures 113-116, 117-119 and 120-123, respectively. The corresponding curves for a coke prepared from SRI-7 are given in Figures 124-128 although these refer to a heating rate of 15°/min rather than the 40°/min pertaining to the other solid samples.

It is to be noted in Figure 127, that even at 10 atm very significant depletions of H_3^+ occur when the coke sample is treated with hydrogen. This signifies the presence of much more evolved gas from the coke samples then from the non- pretreated coal samples.

SPECIAL EXPERIMENTS

CO_2 + C REACTIONS

In the oxidative gasification of coal or coke in O_2-containing atmospheres there is, of course, no question that the carbon in the evolved CO originates in the solid reactant. However, in the oxidative gasification experiments in which the solid reactant is treated with CO_2 it is by no means certain that the CO observed as a product contains any carbon derived from the solid.

To investigate this question in an unambiguous fashion we have treated a carbon sample containing ^{13}C with a gas mixture consisting of 1% $^{12}CO_2$ in argon and have observed the temperature dependence of the concentrations of $^{12}CO^+(\frac{m}{e}\ 28)$ and $^{13}CO^+(\frac{m}{e}\ 29)$.

Figure 129 and 130 show the use of the non-isothermal method in analyzing the isotopic content of the carbon sample. These figures show, respectively, the production of $^{13}CO_2$ and $^{12}CO_2$ in an experiment in which the carbon sample was treated with a gas mixture consisting of 1% O_2 in Ar. The intensities of the peaks indicate that the carbon sample is 57% ^{13}C; an identical conclusion is reached by examination of the ^{12}CO and ^{13}CO evolved.

Figures 131 and 132 show the temperature dependence of the ^{13}CO and ^{12}CO concentrations, respectively, when the carbon sample is treated with a gas mixture consisting of 1% $^{12}CO_2$ in argon. It is clear from these figures that the ratio of the amounts of ^{13}CO to ^{12}CO evolved is unity and reflects the isotopic abundance in the solid as given by Figure 129 and 130.

AIR OXIDATIONS

A number of experiments were performed using air at one atmosphere passing over the coal beds. The results from all of these experiments were similar in nature, and Figures 133 and 134 are presented as examples. The CO_2 evolution shown in Figure 133 shows an extremely sharp spike in CO_2 production during which time the CO_2 concentration swamps the signal amplifier. Somewhat similar behavior is exhibited by the water evolution shown in Figure 134 although this plot shows a preliminary dehydration before the spike.

It is apparent that as a particular temperature is reached, a very rapid oxidation, quite probably an explosive oxidation, occurs. The stoichiometry of the experimental arrangement is such that an excess of oxygen is present, a 2 to 1 molar excess of oxygen per minute compared to a 10 to 1 deficit present in the previously presented oxidative studies. Commercial gasification stoichiometry is much closer to the conditions present when 1% O_2 in Ar is the reactant gas. During this rapid oxidation, the temperature of the coal sample in the furnace is undoubtedly not that shown on the temperature axis of Figures 133 and 134. The usual experimental conditions utilize low stoichiometric amounts of oxygen coupled with gas flow rates to maintain average sample temperatures near the furnace temperature, even though surface temperatures of the sample may be quite different from the average. The rapidity of the air oxidation will not permit these controlling conditions to be obtained thereby resulting in the average temperatures and surface temperatures being unknown.

DISCUSSION

The large number of experiments performed during this contract research by using the computerized non-isothermal kinetics laboratory has resulted in an extremely large data output. Careful cataloging of the detailed behavior of a variety of fossil fuels under a number of reaction conditions, was performed in the previous section of this report. A cursory study of that data is sufficient to demonstrate the complexity of the reactions resulting in gasification. The interpretation of non-isothermal kinetics data offered in the remainder of this report will be only the beginnings of understanding of this material.

KINETIC PARAMETERS

Table V presents the kinetic parameters of activation energy and frequency factor for a number of important carbon gasification reactions occurring in coals and cokes. These parameters are the result of analysis of the temperature maxima of the various gas evolutions according to the procedure outlined in the discussion of equation 12, and presented in detail elsewhere[1]. It includes parameters for gasifications from both oxidation and reduction studies. An example of a typical plot is presented as Figure 3.

The occurence of several evolution maxima for a particular product gas are a routinely observed phenomenon, as seen by inspection of the data in the previous section. The complexity of the gasification kinetics, however, often makes it difficult to identify a particular reaction by a progressive increase in Tm when experiments are performed at several heating rates. This difficulty in identifying reactions can be seen quite well by inspection of Table VII, VIII, and IX, Appendix A. Nevertheless, thirteen reactions have been identified in the studies of coal with oxygen, oxygen/water, and hydrogen. These reactions, six producing CO, three yielding CO_2, two each producing methane and ethane, are summarized in Table V. Reactions, although involving identical reactants and products, are classified as separate based on differences in temperature and maxima occurrance.

TABLE V KINETIC PARAMETERS

Oxidizing Atmosphere	CO Evolution $1/2\ O_2 + C \rightarrow CO$			CO_2 Evolution $O_2 + C \rightarrow CO_2$		
	Tm (30°/min)	E (kcal/mole)	log k_0	Tm (30°/min)	E (kcal/mole)	log k_0
SRI Coal No. 5	835°K	14.0	3.0	883°K	14.8	3.1
SRI Coal No. 7	752	21.2	5.8	1075	10.0	1.0
	900	27.0	6.1			
	1180	30.0	5.0			
SRI Coal No. 10	752	21.2	5.8			
SRI Coke No. 7	1000	10.0	1.1	1075	10.0	1.0

Reducing Atmosphere	CH_4 Evolution $2H_2 + C \rightarrow CH_4$			C_2H_6 Evolution $3H_2 + 2C \rightarrow C_2H_6$		
	Tm (40°/min)	E (kcal/mole)	log k_0	Tm (40°/min)	E (kcal/mole)	log k_0
Three bituminous coals (SRI Nos. 5, 7, 10	850°K	11.7	2.2	774°K	11.3	2.7
	1031	21.5	4.0	880	20.5	4.5

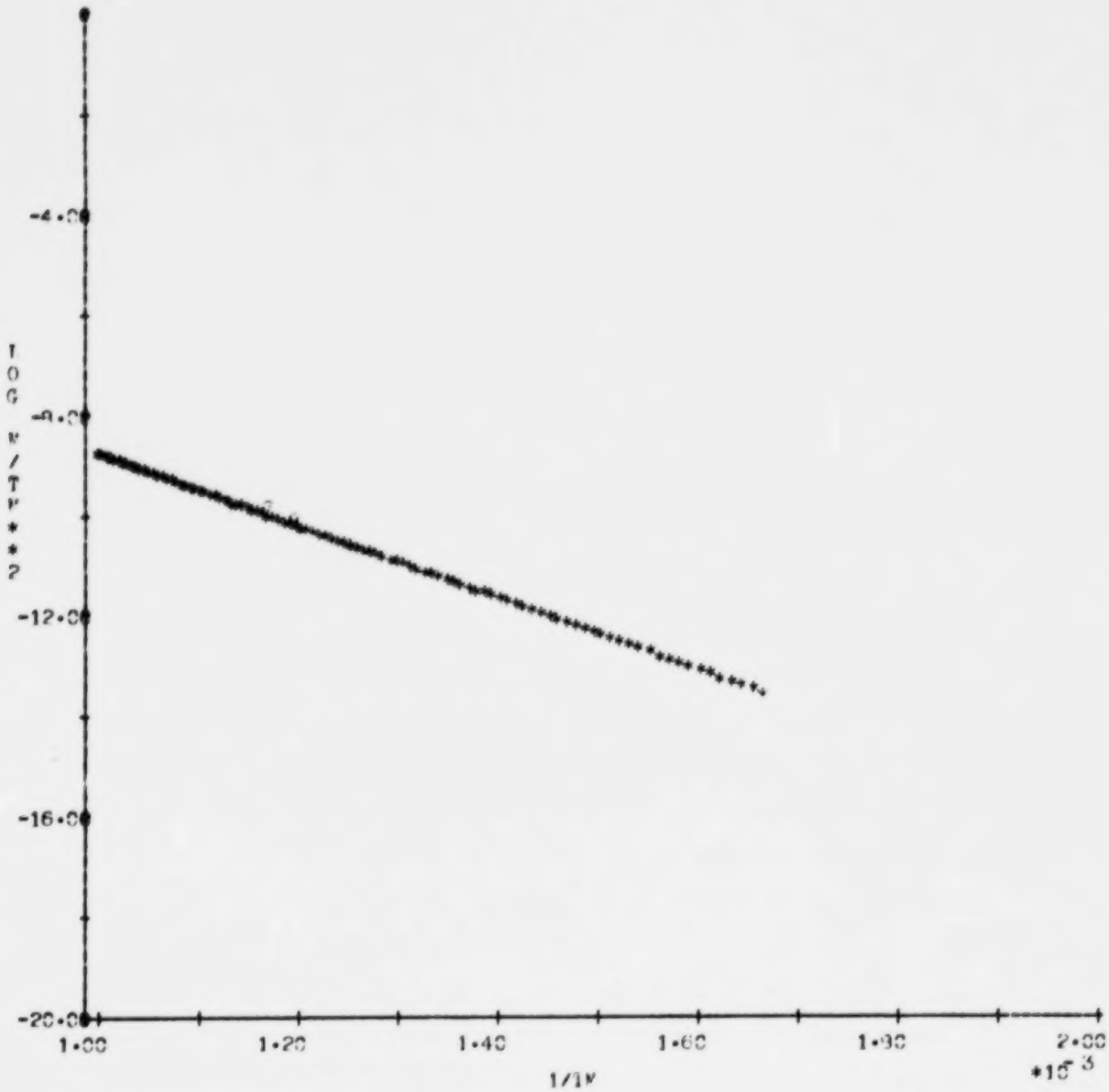

SYMBOL	NO.PTS.	LEGEND
@	4	KINETIC PARAMETERS FOR CO EVOLUTION-OXIDIZING ATM--COAL # 5
*	100	

Figure 3

OXIDATION REACTIONS

Nine reactions were observed for the evolution of CO and CO_2 from three bituminous coals and coke. The kinetic parameters shown in Table V for these reactions are based on data taken from Table VII and VIII. Kinetic parameter for multiple evolutions are presented for the case of CO from SRI coal no. 7 because it was the only material for which it was possible to clearly identify several trends of Tm increasing as a function of heating rate, although the identity of the third reaction (Tm = at 1180°K) may be doubtful. Confidence in the values reported for these kinetic parameters is increased by the fact that in several cases, evolutions occur at the same temperature in both the oxygen and oxygen water experiments.

An important feature of the kinetic parameters present in Table V is the general lack of coincidence in the occurrence of reactions. With the exception of a single CO evolution from Coals No. 7 and 10, and the evolution of CO_2 from Coal and Coke No. 7, no two reactions coincide. This is quite a remarkable difference in a comparison of these carbon gasification reactions and the desulfurization reactions previously reported[1,2,4]. In the sulfur reactions, five or six desulfurization reactions were common to a total of twelve different fossil fuels.

At the present time, observation of the general lack of coincidence for Tm of oxidation reactions is attributed to differences in the carbon matrices of the coals used for the experiments. Differing reactivity of coal macerals is a well known phenomenon[7] and the predominance of particular maceral types in a given coal sample seems quite reasonable. The fact that several different sets of experimental conditions yield similar Tm values for CO and CO_2 evolutions in particular coals tends to confirm the existence of such macroscopic differences in the coal materials used. The coincidence of one reaction

producing CO in Coal No. 7 with the single identifiable reaction for CO production in Coal No. 10 may indicate that some carbon matrix elements occur in common for these two materials. Also of interest is that although the identified reaction producing CO from Coke No. 7 shows no counterpart in Coal No. 7, the only CO_2 evolution identified in either of these materials yields Tm values which indicate that they are the closely similar processes. At present, no reason can be given for the coking process altering the carbon matrix for one type of reaction and not for the other.

No detailed models are offered for the differing reaction kinetics parameters because of a lack of physical information on the carbon matrices present. An important area of future work would be the development of such models with the use of pore size distributions and petrographic data on these coal materials.

Some comparisons are possible between the data in Table V and activation energies which appear in the literature. Van Krevelen[8] in reviewing Oreshko's work for which a thermo-balance technique was used, presents activation energies for four different stages of oxidation. In two of the four stages, decomposition reaction products yield CO and CO_2. The first of these is a low temperature decomposition occurring below 425°K and has an activation energy of about 6 kcal/mole, and the second is a higher temperature decomposition with activation energies 25-35 kcal/mole at temperatures higher then 525°K.

Three of the seven different reactions observed for oxidative gasifications appear to be in agreement with Oreshko's activation energies for the combustion stage of oxidation. The reamining four reactions occur with lower activation energies than those discussed by van Krevelen. It is interesting that the higher activation energy reactions occur for CO evolutions only, and then in only two of the four materials shown in Table V. The presence of the low activation energy, higher temperature reactions appears to indicate in another way that several different kinds of carbon sites participate in the oxidative gasification reactions.

HYDROGASIFICATIONS

Two reactions each for methane and ethane evolution yielded kinetic parameters as shown in Table V. The data used to calculate these values came exclusively from hydrogasification studies conducted at 1 atm. Despite the fact that H_2 concentrations may vary under these conditions, the progressions of Tm values with heating rate are more apparent for the 1 atm experiments. The The Tm values at a particular heating rate, consistently separate into four different temperature ranges for each of the three bituminous coals used. Kinetic parameters for these hydrogasification reactions in the three coals must all be nearly equal, and the calculations done were based on this assumption.

A quite remarkable, and we feel quite significant, coincidence of values is noted in the kinetic parameter values for hydrogasification. Nearly identical values of activation energy and frequency factor are obtained for the evolution of methane and ethane for both the high and low activation energy processes yielding these gases. More remarkable, however, is that methane is evolved at much higher temperatures than ethane in both cases. A similar kind of coincidence is observed in the evolution of CO and CO_2 from SRI Coal No. 5 and from the coke of SRI Coal No. 7.

These kinetic parameter data for oxidative and hydro-gasification seem to indicate fundamental differences in the mechanisms of hydrogen and oxygen interactions with coals. These differences are no doubt significant to commercial gasification processes, and without a doubt these differences re-emphasize the complexity of gasification reactions. It is hoped that work will be done in the future toward the understanding of these mechanisms.

THE CARBON DIOXIDE-CARBON REACTION

In the oxidative treatment of coke with carbon dioxide, carbon monoxide is observed as a product as may be seen by reference to Table IX. In such a process it is not immediately clear as to whether the carbon in the carbon monoxide product is that originally contained in the carbon dioxide reactant (in which case the carbon monoxide would not be a gasification product) or whether it is derived from the solid coke. Thus if the reactions were

$$CO_2(g) + \text{coke} \rightarrow CO(g) + \text{oxygenated coke} \qquad (13)$$

the CO would obviously not be a coke gasification product. On the basis of previous studies[9] using $^{14}CO_2$ as a radioactive tracer it would appear that (13) is a rapid process at temperatures of 1000°K and above. The conclusions of the study of Bonner and Turkevich[9] may not be directly appliable to the observation here that carbon monoxide is a low temperature product of the oxidation of coke by carbon monoxide (of Table X).

As shown in Figures 131 and 132 when a carbon sample containing 57% ^{13}C is treated with $^{12}CO_2$ in a non-isothermal experiment the CO evolved in the range 520-840°K is 51% ^{13}CO and 49% ^{12}CO. If the process producing CO were

$$CO_2(g) + \text{carbon} \rightarrow CO(g) + \text{oxygenated carbon}$$

$$\text{Oxygenated carbon} \rightarrow CO(g)$$

the observed ^{12}CO could not be less than the ^{13}CO. Hence, the result shows that we may safely conclude CO to be a gasification product.

While coke and coal are of course different solid reactants than the carbon sample upon which this conclusion is based, we see no reason why this conclusion concerning the low temperature gasification may not be safely applied to coke and coal.

The kinetic parameters for two carbon gasification reactions resulting from CO_2 reactions with coke from SRI Coal No. 7 are given in Table VI.

TABLE VI Kinetic Parameters (CO_2 - Coke Reactions)

Tm (30°/min)	E kcal/mole	Log k_0
700°K (estimate)	17.5	5.0
991	25	4.9

SUMMARY

During the past year, gasification studies in a variety of oxidizing and reducing atmospheres were performed on a variety of fossil fuels. In all, a total of 245 non-isothermal kinetics experiments were performed on eight different coals and coal chars.

Representative data illustrating the qualitative differences between each of the coals in each of the gasification conditions is presented in this report.

A total of thirteen different carbon gasification reactions were identified in the course of this work. Included in these reactions is a previously unreported low temperature gasification of carbon by carbon dioxide, itself a gasification product. The kinetic parameters of activation energy and frequency factor for these reactions were calculated.

APPENDIX A: Gaseous Evolution Data for Oxidative Reactions

Table VII : Peak Temperatures in Oxidative Gasification of Coal

Table VIII : Effect of Water Vapor on Oxidative Gasification of Coal

Table IX : Peak Temperatures in Treatment of Coke with CO_2 in Ar

Figures : 4 - 47

TABLE VII

Peak Temperatures in Oxidative Gasification of Coal

Reactant Gas = 1% O_2 in Ar

Solid Reactant Coal	Heating Rate °/min	Temperatures at which Peaks Observed - °K					
		H_2O	CO	NO	CO_2	SO_2	O_2*
SRI-5	15	553	773		551	746	
		681			764		
		798			820		
	30	605	766	828	566	829	576
		715	840		888		847
		869					
	40	704	770		898	680	
		884	888		1240	860	
		992	1277**				
SRI-7	15	553	743	940	547	730	
		732	894		863		
		872			977		
		950					
	30	597	575	924	608	718	567
		718	766	997	697	763	768
		786	905		1100	1068	996
		913	1185				
		1008					
	40	609	588	820	615	740	
		755	790	950	745	790	
		810	942	1040	1103	1088	
		1025	1210**				
SRI-10	15	550	733	870	540		
		702	860		868		
		853					
	30	507	575	938	568	762	577
		726	751		987		932
		900	916				
		960	1066**				
	40	710	768	935	580	775	
		955	882		1160		
		1062	1011		1248		
			1295**				

TABLE VII (continued)

Solid Reactant Coal	Heating Rate °/min	Temperatures at which Peaks Observed - °K					
		H_2O	CO	NO	CO_2	SO_2	O_2*
Anthracite	15	552	542	897	545		542
		916	862		930		900
			962				
	30	586	572	566	565	1048	575
		1040***	927	938	1048		1007
				995			
	40	598	577	578	576	935	578
		817	917	972	938	1050	980
		998	1248		1137	1180	
Lignite	15	583	663	652	687		
		674		742			
	30	619	576	575	553		575
		685	716	775	808		708
		726	1013**				
	40	419	595	586	586		588
		625	716	815	828		730
		742	1025**				

* Negative Peaks
** Peak is actually a shoulder on the high-temperature side of another peak
*** Uncertain

TABLE VIII

EFFECT OF WATER VAPOR ON OXIDATIVE GASIFICATION OF COAL

Reactant Gas: 1%O_2 in Ar, saturated at 300°K with H_2O

Solid Reactant Coal	Heating Rate °/min	Peak Temperatures in °K H_2O	CO	CO_2	O_2*
SRI-5	15	862 1153	803	817	797
	40		863	875 1022	608
SRI-7	15		884	872 976	960
	40		973	1100	1081
SRI-10	15		867	870	879
	40		781 946	955 1042	949
Anthracite	15		911	917 1009	971
	40		961 1158	1132	1080
Lignite	15			690 784	690
	40			745 840 1070	740

*Negative Peaks

TABLE IX

Peak Temperatures in Treatment of Coke (SRI-7) with CO_2 in Ar

(Gas Flow Rate = 150 cc/min)

Heating Rate °/min	Peak Temperatures in °K					
	H_2	H_2O	CO	NO	"CH_3"	CO_2*
5		927				
15	500	520	509	500		500
		868				
20	560	580	564	562		554
	1098	1035	1014			1015
30	585	614	586	580		575
	1100	1046	998			1023
40	595	630	594	590		588
	1080	1093	737			1070
			1048			
60	604	639	605	600		598
	1108	1133	745			1077
			1066			

* Negative Peaks

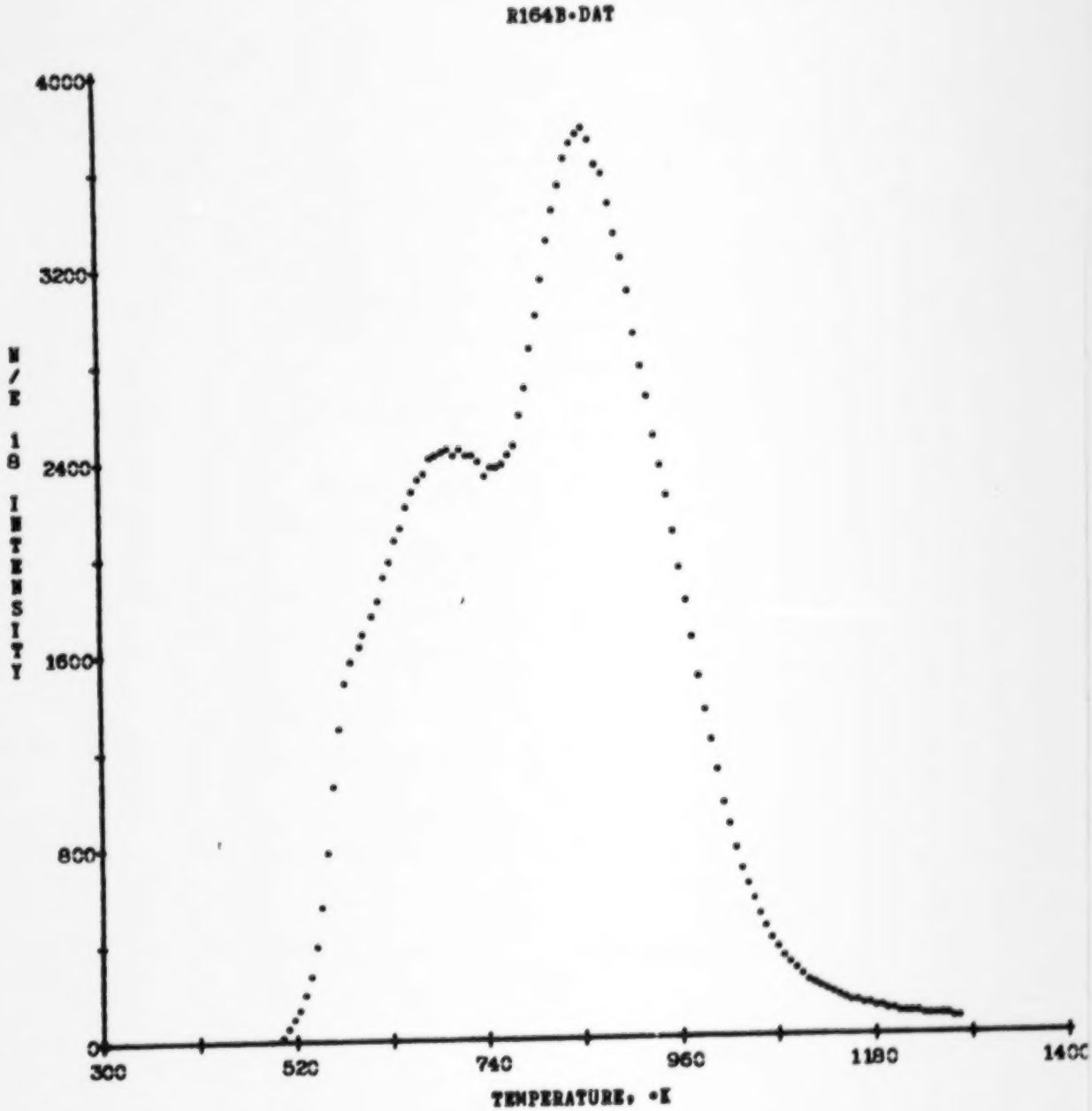

SYMBOL	NO.PTS.	LEGEND
.	113	H2O+ FROM SRI COAL #5, AR+1%O2 AT 200 CC/MIN, 30°/MIN

Figure 4

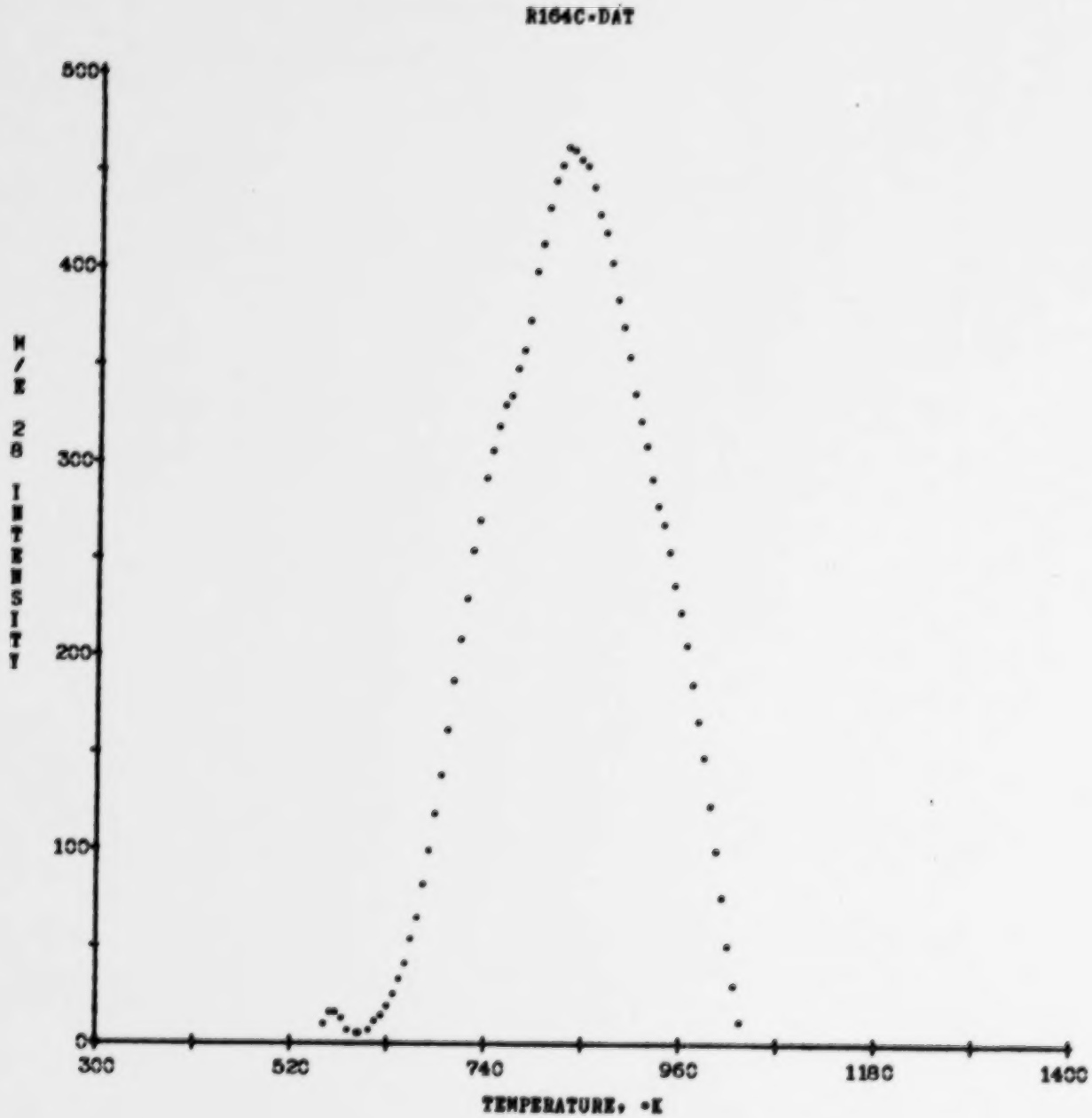

SYMBOL NO.PTS. LEGEND

. 69 CO+ FROM SRI COAL #5, AR+1%02 AT 200 CC/MIN, 30°/MIN

Figure 5

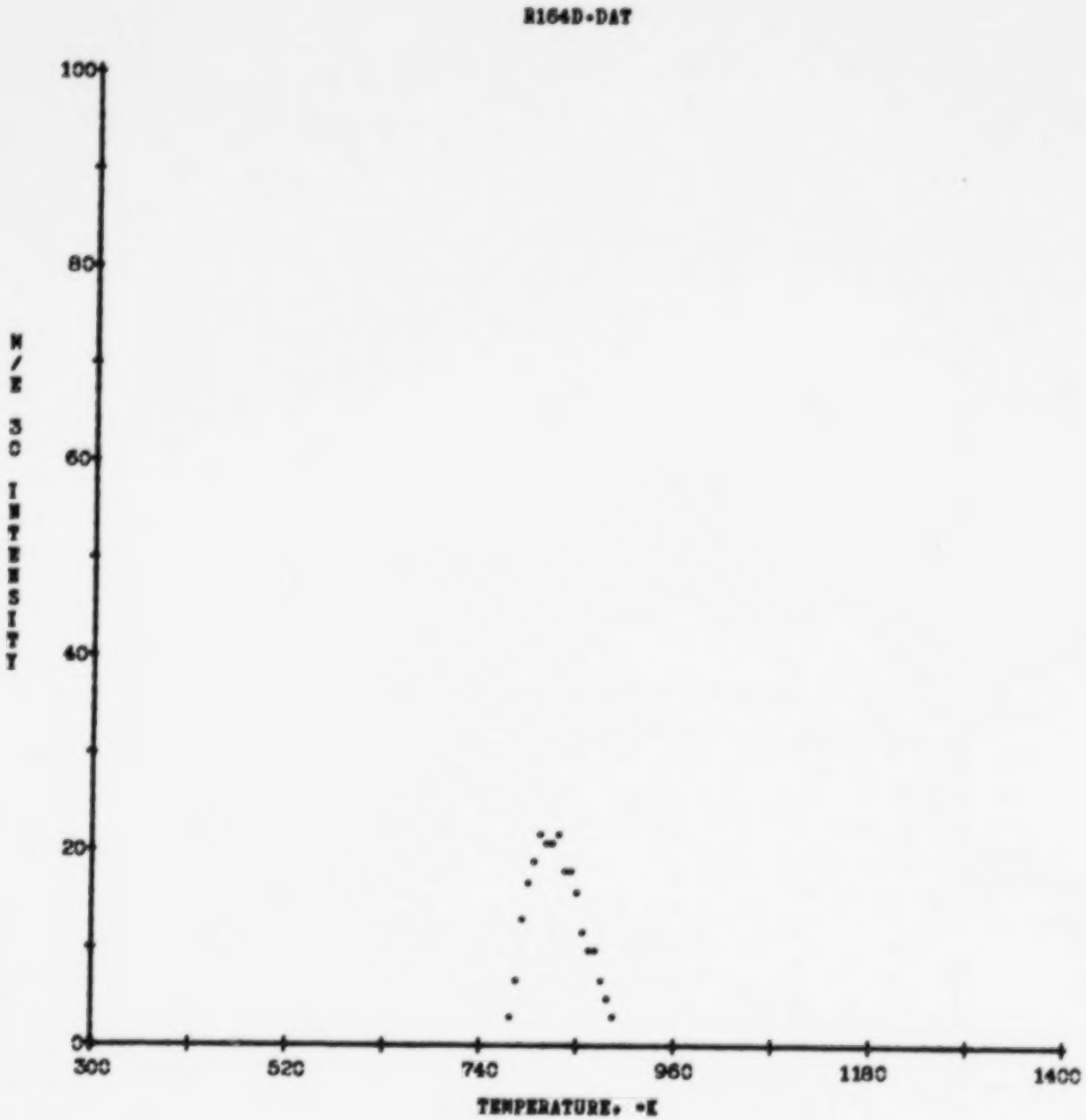

SYMBOL	NO.PTS.	LEGEND
•	18	NO+ FROM SRI COAL #5, AR+1%O2 AT 200 CC/MIN, 30°/MIN

Figure 6

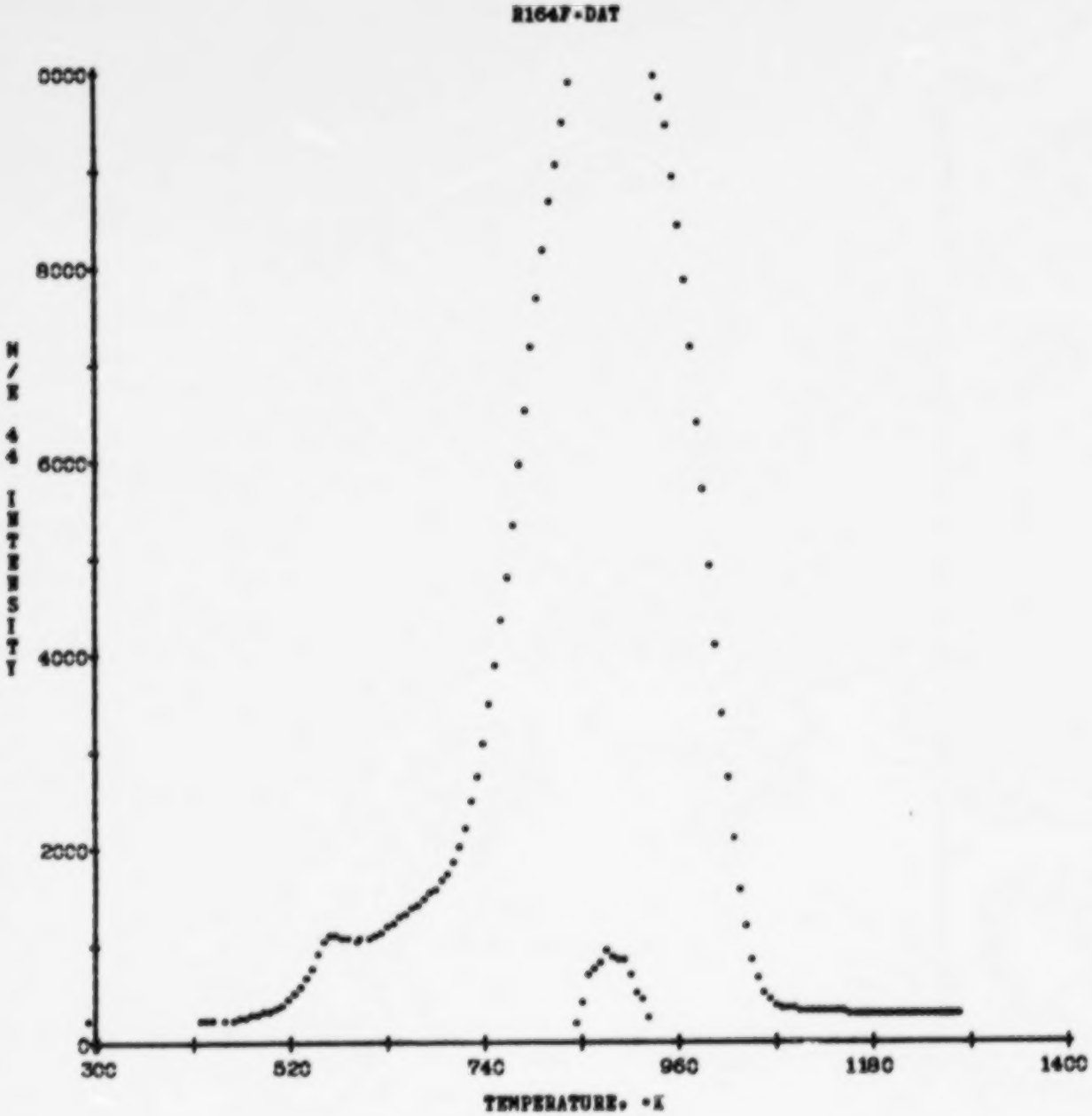

SYMBOL	NO. PTS.	LEGEND
.	125	CO2+ FROM SRI COAL #5, AR+1%O2 AT 200 CC/MIN, 30°/MIN

Figure 7

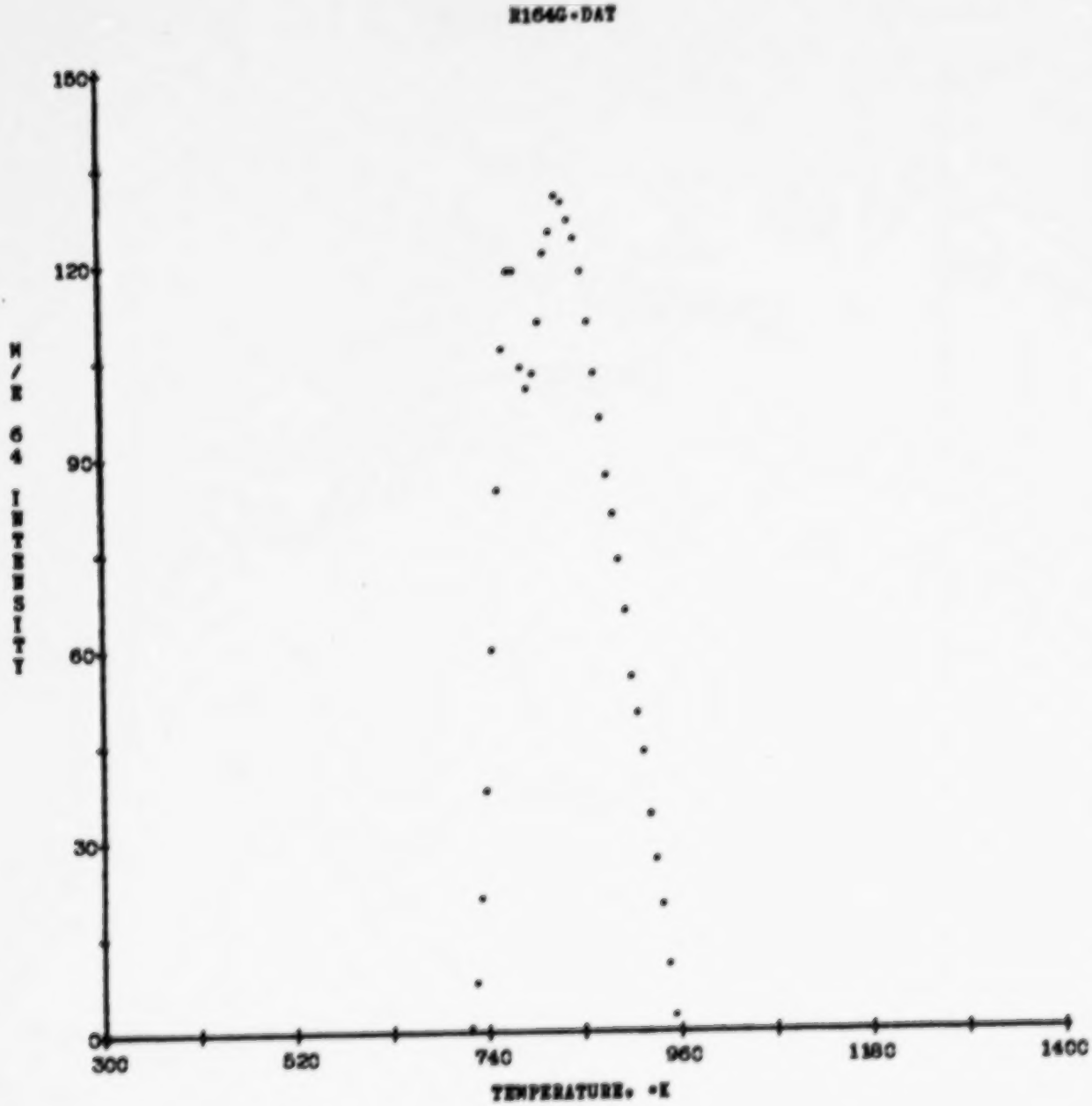

SYMBOL	NO.PTS.	LEGEND
.	35	SO2+ FROM SRI COAL #6, AR+1%O2 AT 200 CC/MIN, 30°/MIN

Figure 8

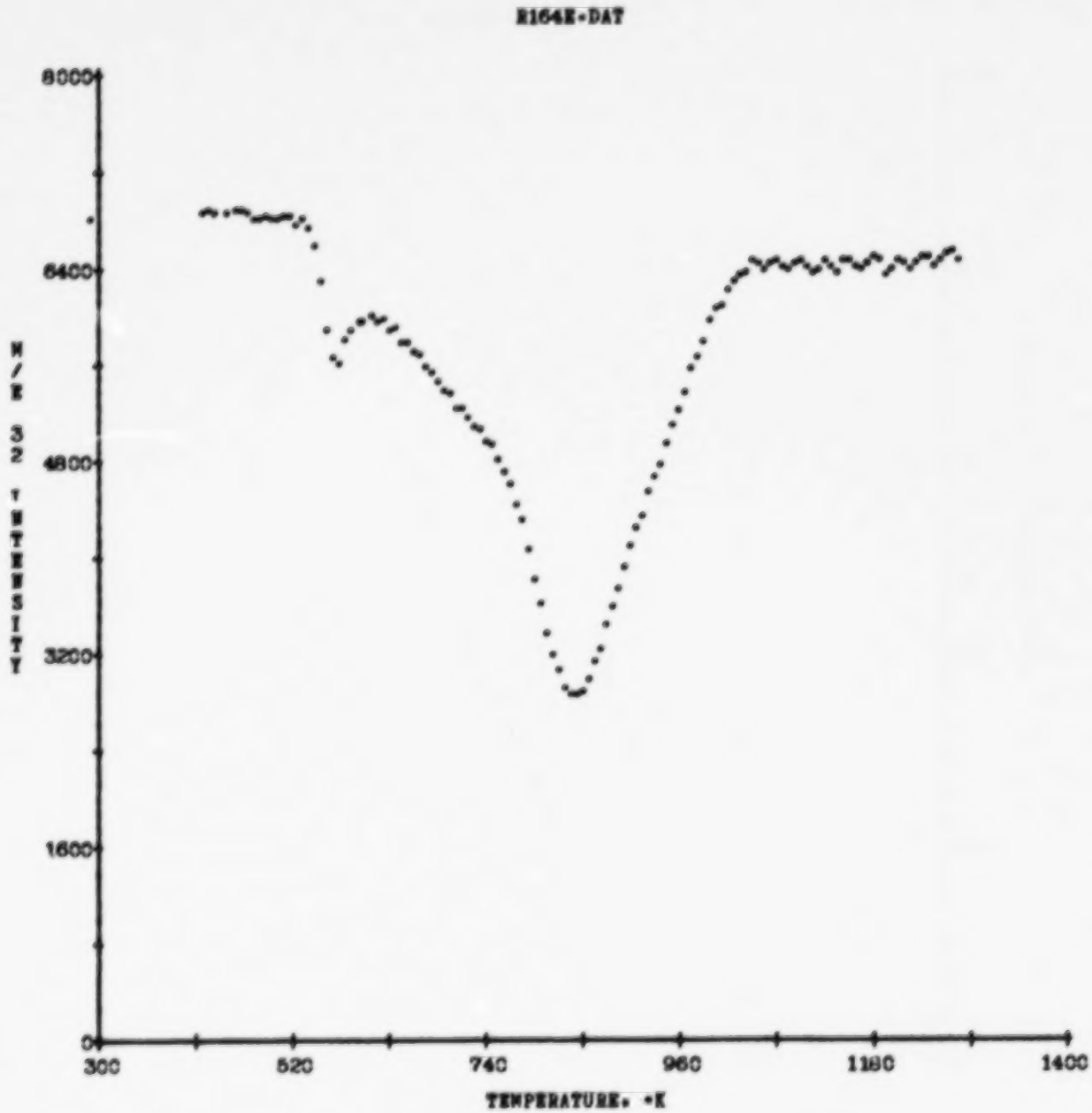

SYMBOL NO.PTS. LEGEND

. 125 O2+ FROM SRI COAL #5, AR+1%O2 AT 200 CC/MIN, 30°/MIN

Figure 9

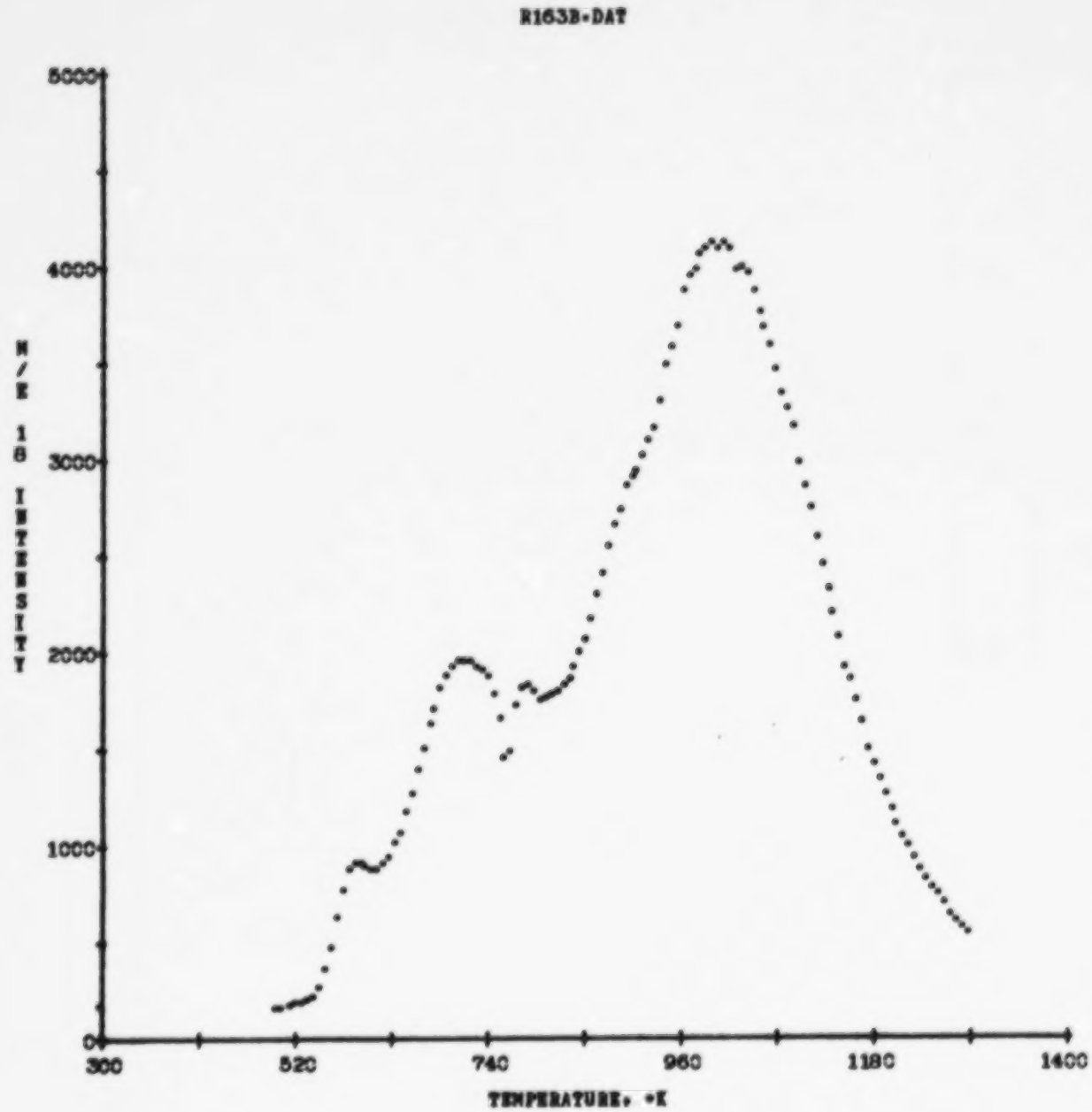

SYMBOL	NO.PTS.	LEGEND
.	121	H2O+ FROM SRI COAL #7, AR+1%O2 AT 200 CC/MIN, 30°/MIN

Figure 10

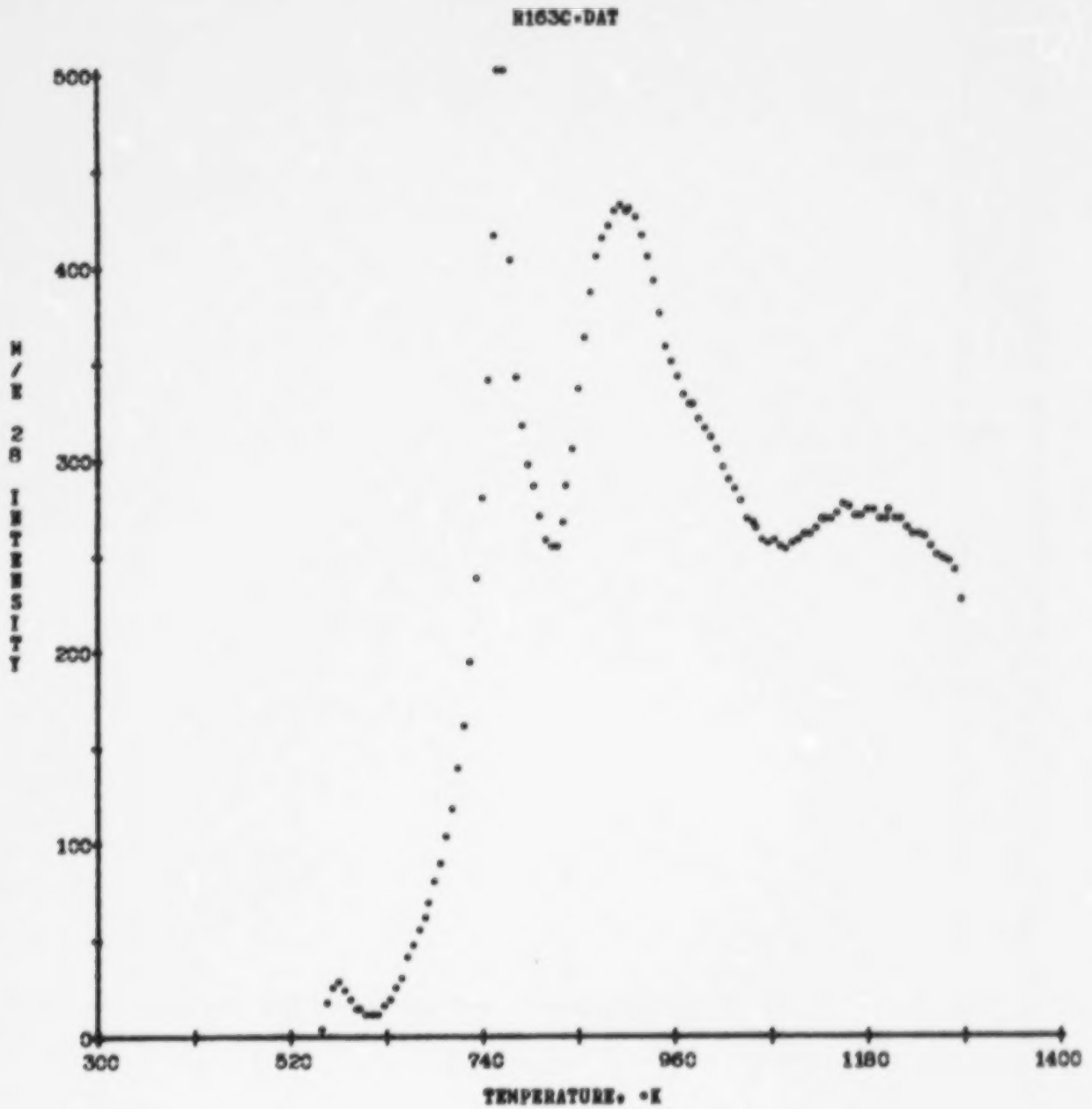

SYMBOL NO.PTS. LEGEND
. 112 CO+ FROM SRI COAL #7, AR+1%O2 AT 200 CC/MIN, 30.4I N

Figure 11

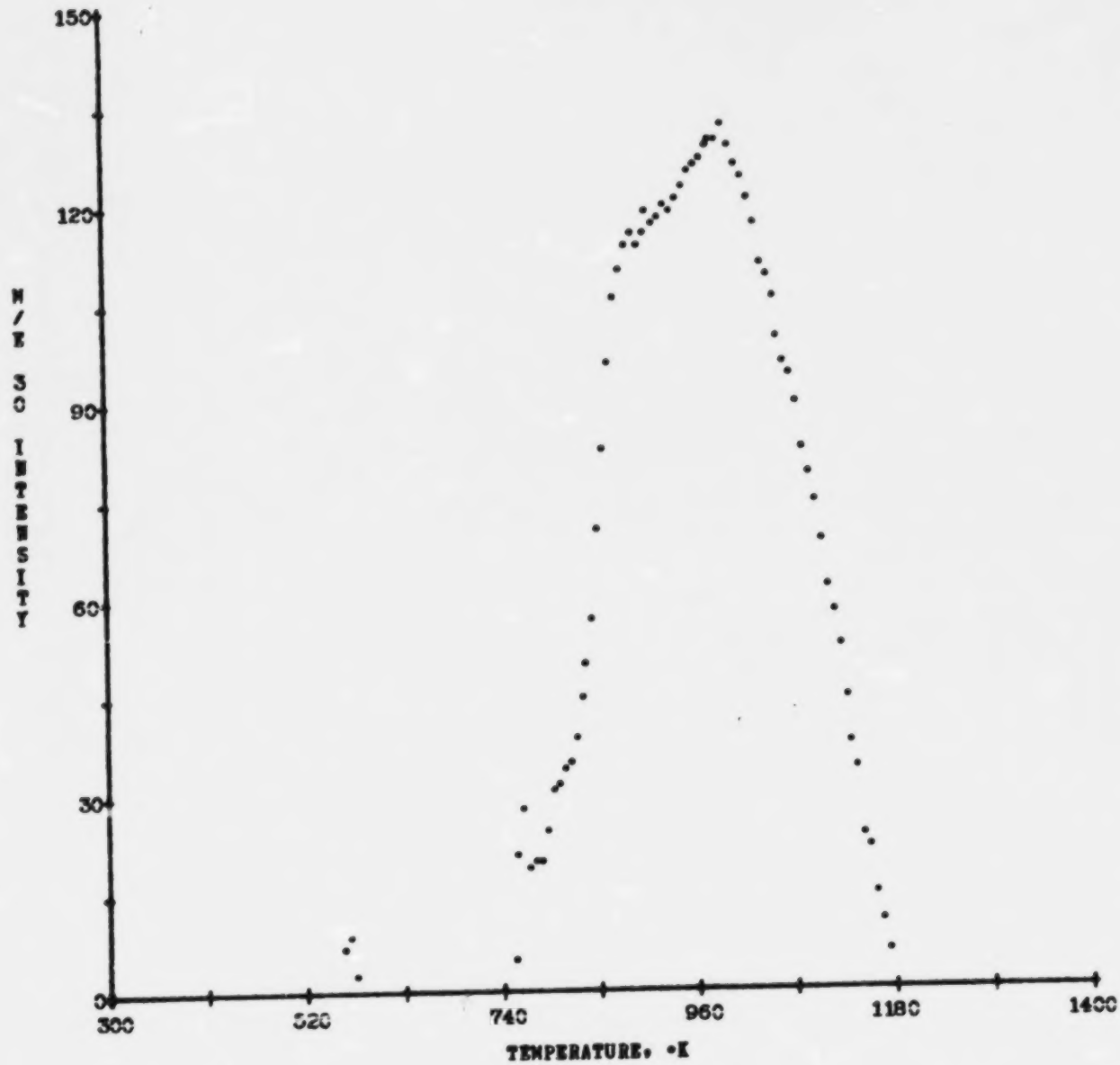

SYMBOL NO.PTS. LEGEND
. 68 NO+ FROM SRI COAL #7, AR+1%O2 AT 200 CC/MIN, 30°/MIN

Figure 12

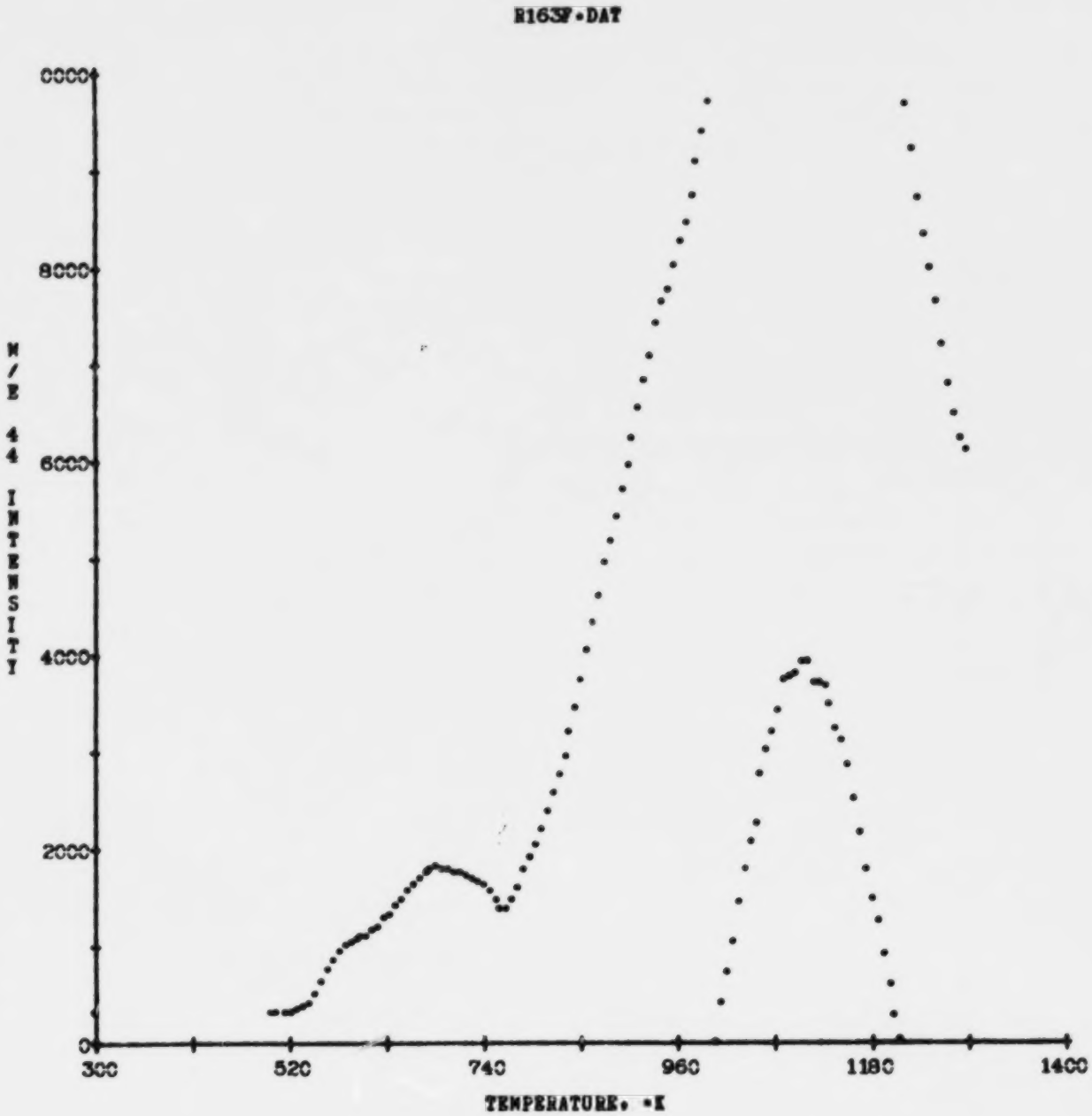

SYMBOL NO.PTS. LEGEND

. 121 CO2+ FROM SRI COAL #7, AR+1%O2 AT 200 CC/MIN, 30°/MIN

Figure 13

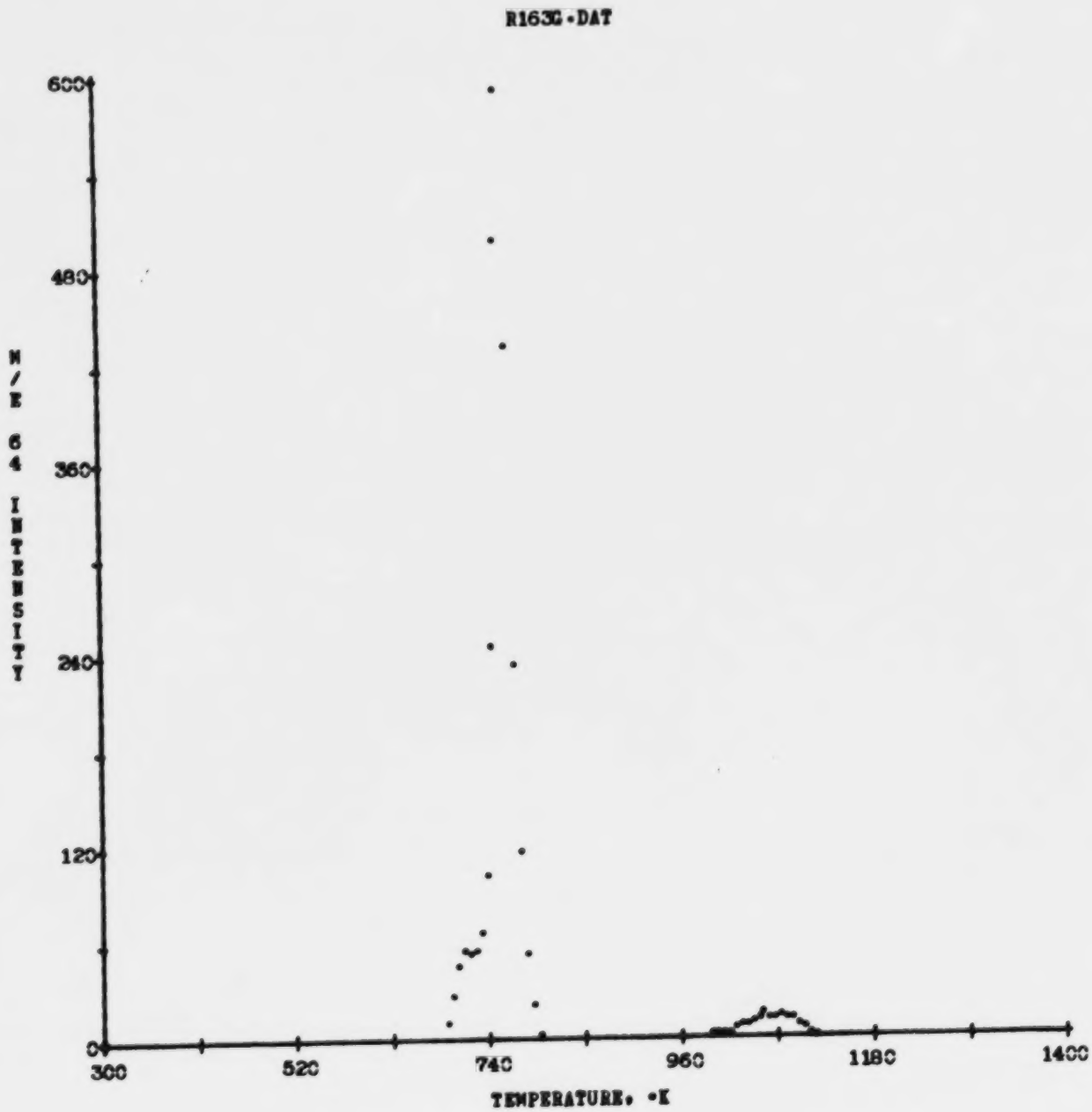

SYMBOL	NO.PTS.	LEGEND
.	36	SO2+ FROM SRI COAL #7, AR+1%O2 AT 200 CC/MIN, 30°/MIN

Figure 14

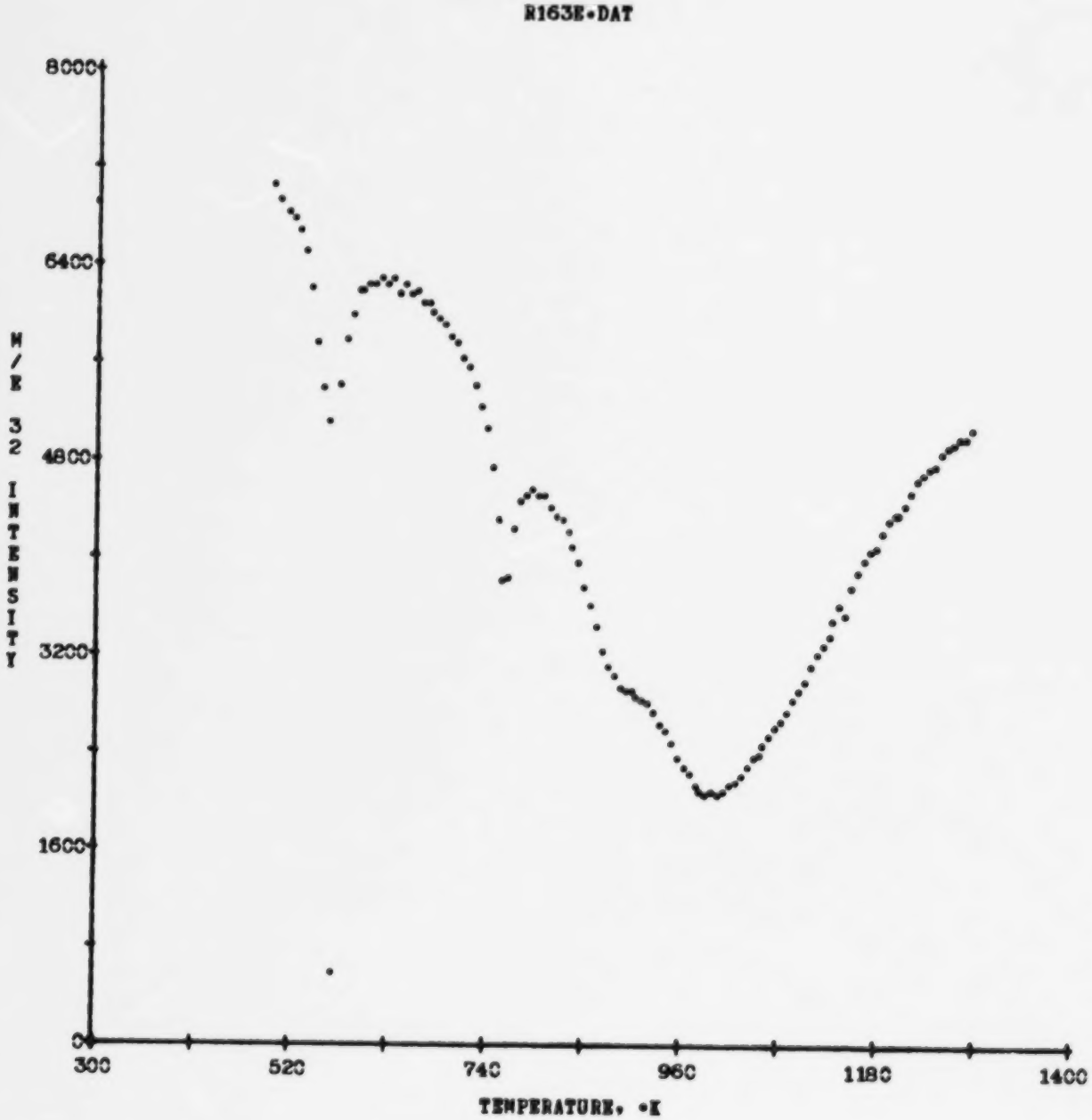

SYMBOL	NO. PTS.	LEGEND
.	121	O2+ FROM SRI COAL #7, AR+1%O2 AT 200 CC/MIN, 30°/MIN

Figure 15

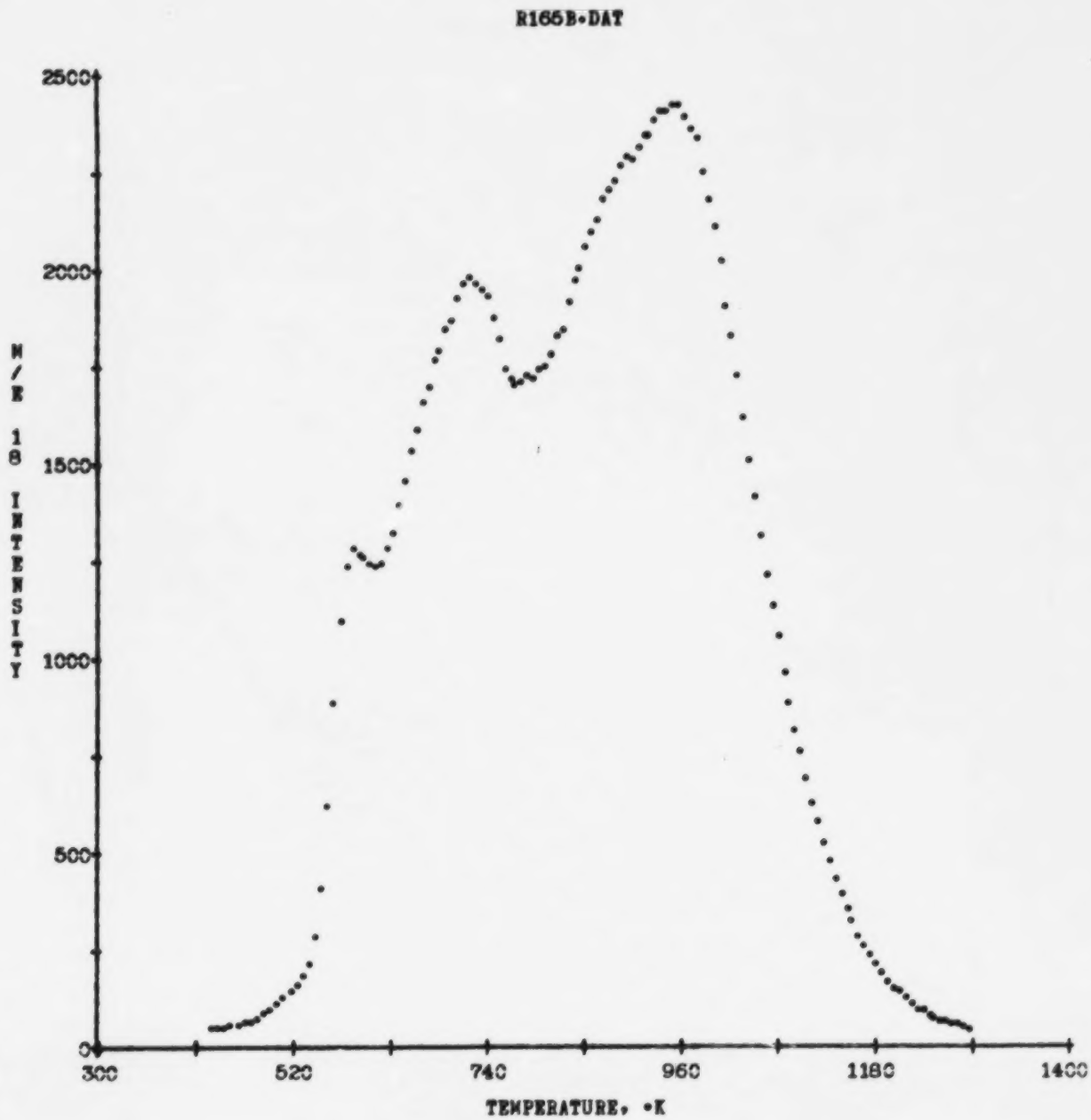

SYMBOL	NO.PTS.	LEGEND
.	129	H2O+ FROM SRI COAL #10, AR+1%O2 AT 200 CC/MIN, 30°/MIN

Figure 16

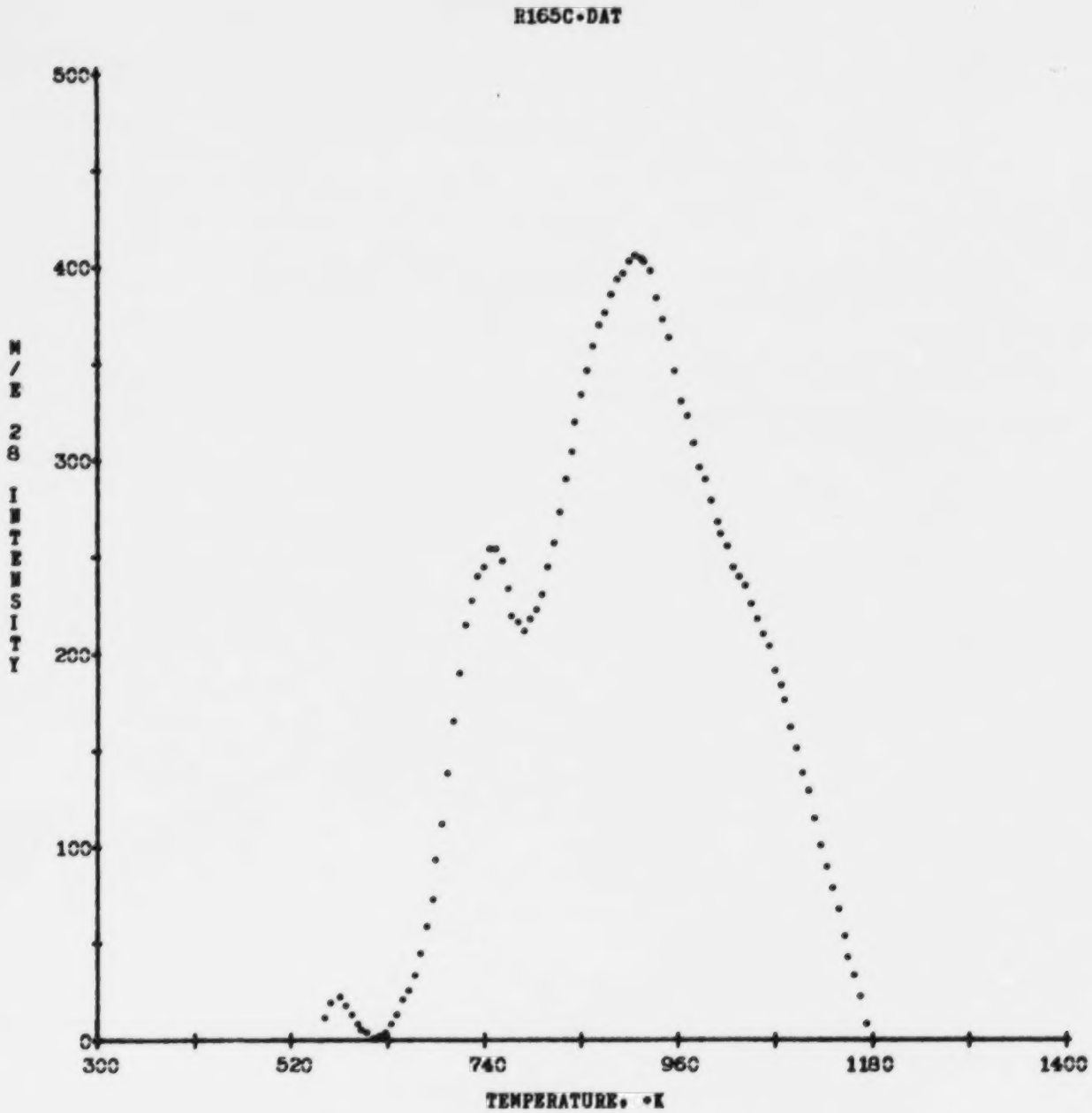

SYMBOL	NO.PTS.	LEGEND
.	94	CO+ FROM SRI COAL #1C, AR+1%02 AT 200 CC/MIN, 30°/MIN

Figure 17

R165D.DAT

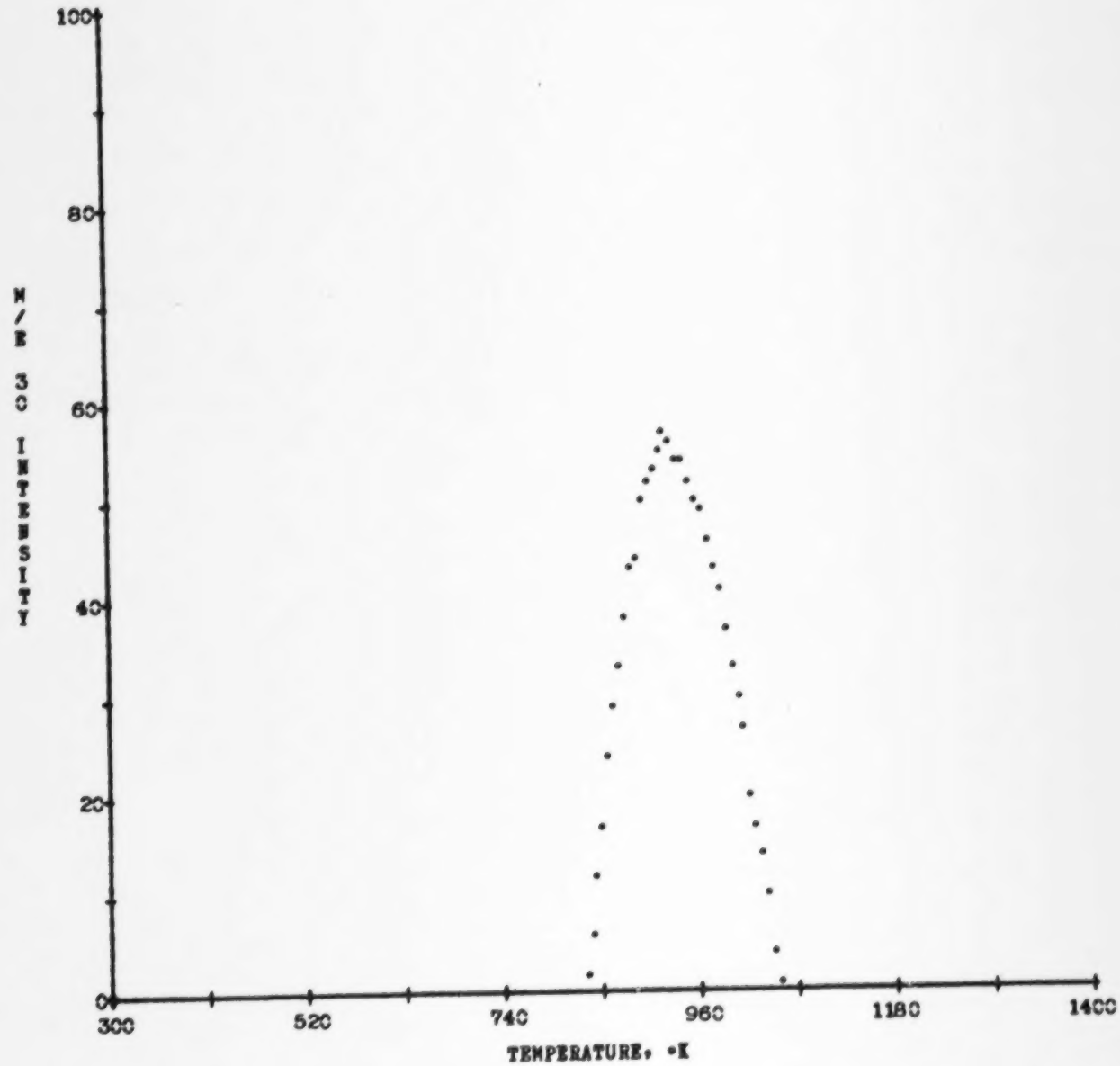

SYMBOL	NO.PTS.	LEGEND
.	34	NO+ FROM SRI COAL #10, AR+1%02 AT 200 CC/MIN, 30°/MIN

Figure 18

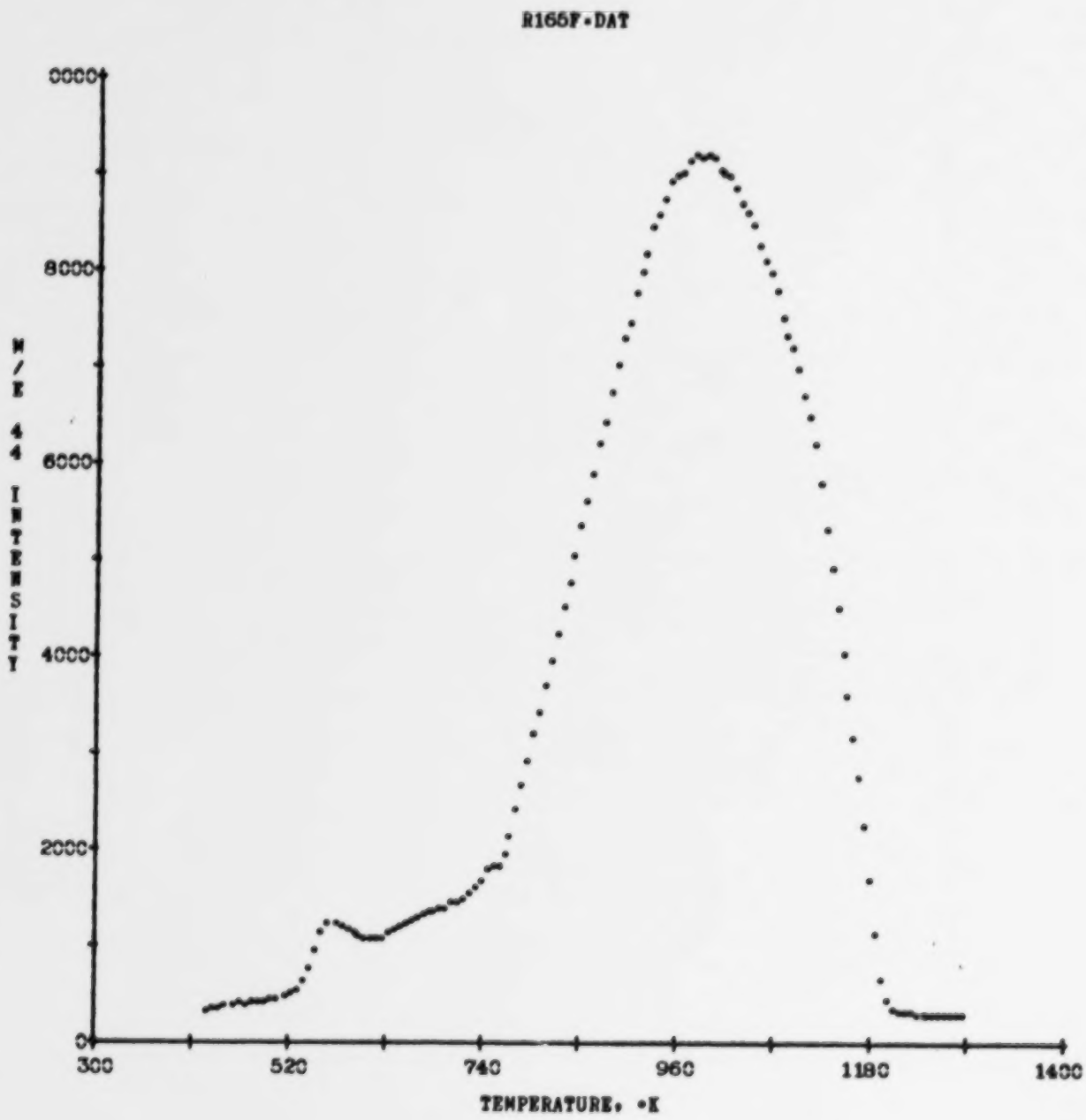

SYMBOL NO.PTS. LEGEND

. 129 CO2+ FROM SRI COAL #1C, AR+1%02 AT 200 CC/MIN, 30°/MIN

Figure 19

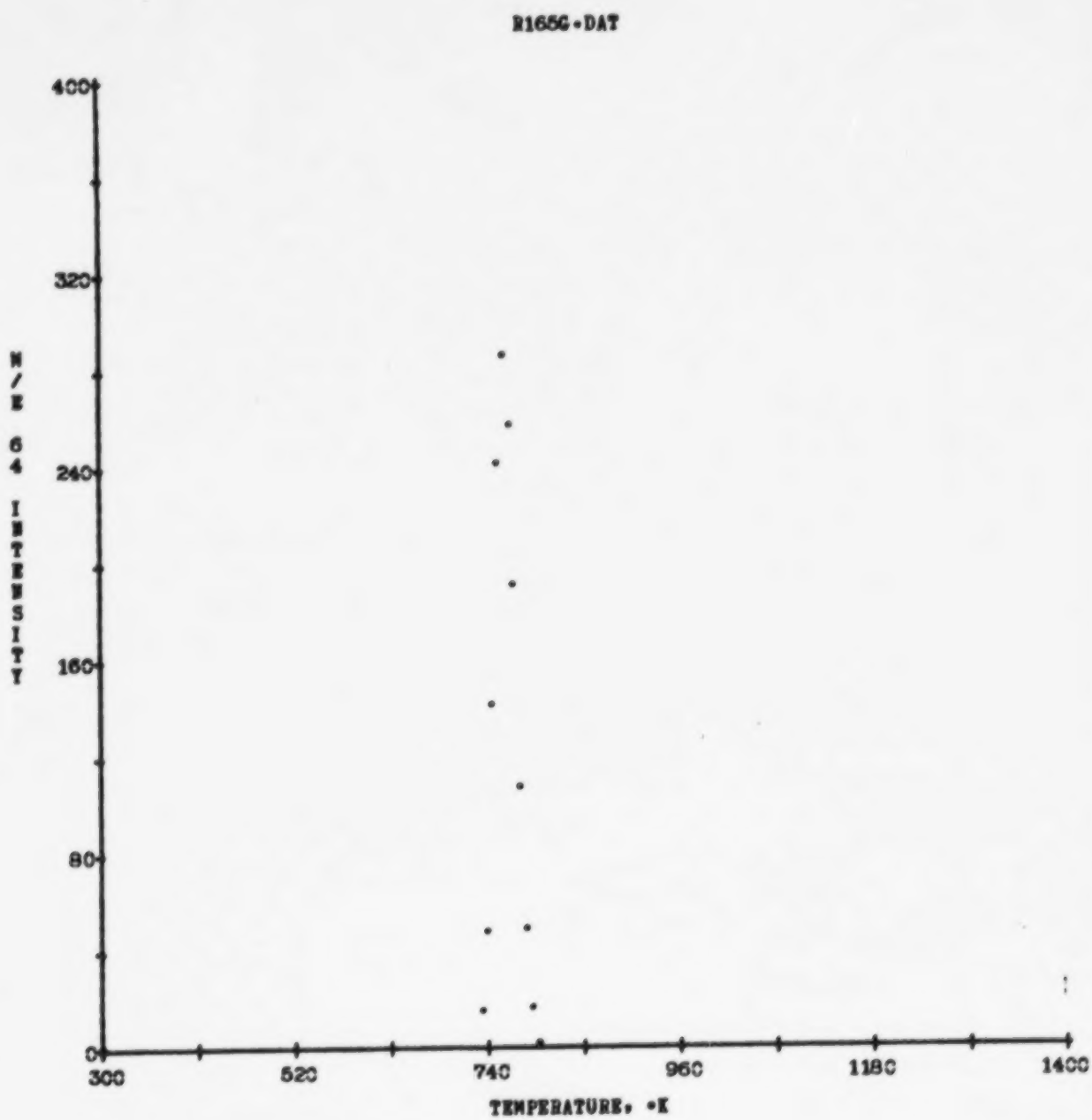

SYMBOL	NO.PTS.	LEGEND
.	11	SO2+ FROM SRI COAL #10, AR+1%O2 AT 200 CC/MIN, 30°/MIN

Figure 20

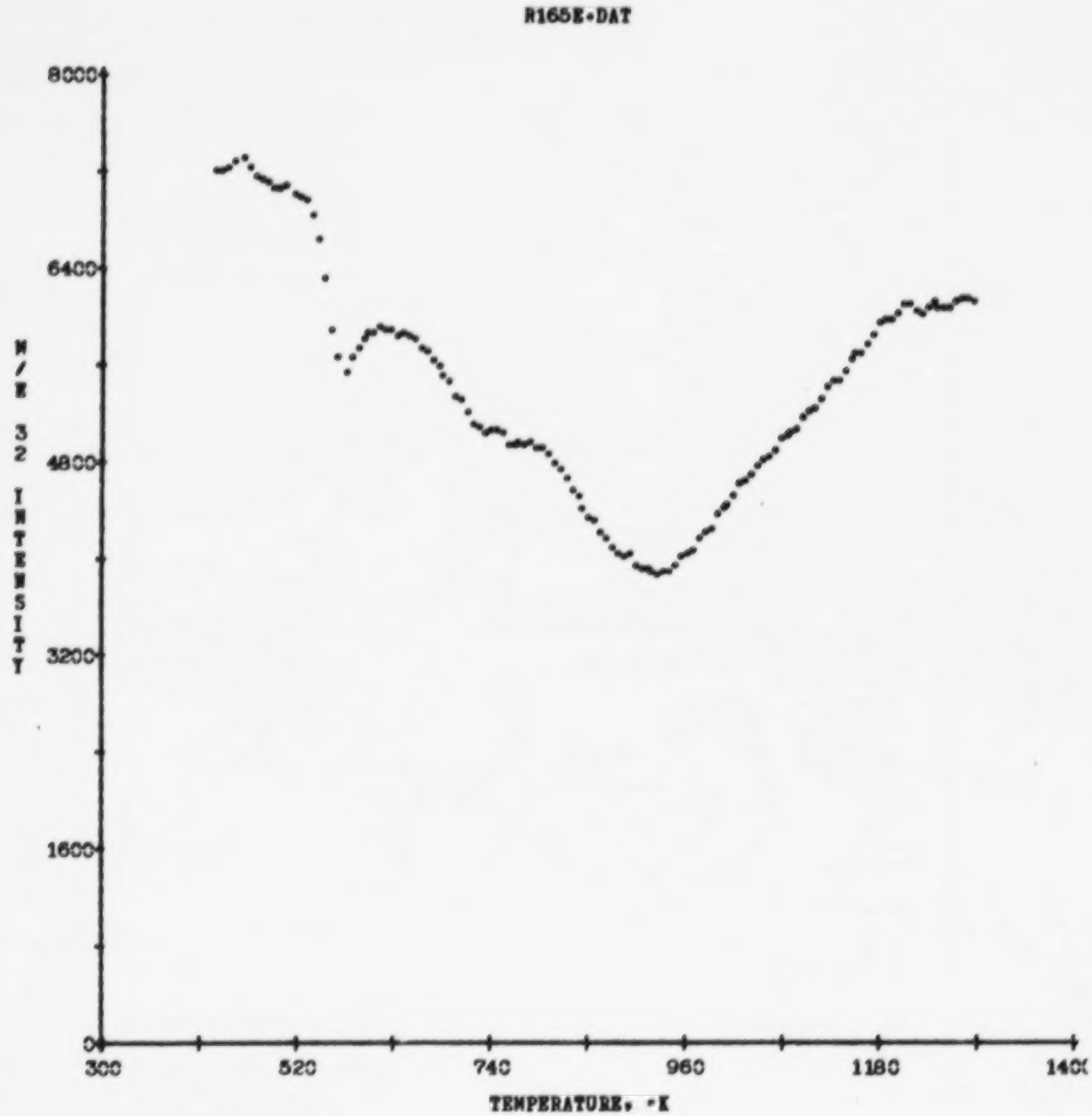

SYMBOL	NO.PTS.	LEGEND
.	129	O2+ FROM SRI COAL #10, AR+1%O2 AT 200 CC/MIN, 30°/MIN

Figure 21

R166B.DAT

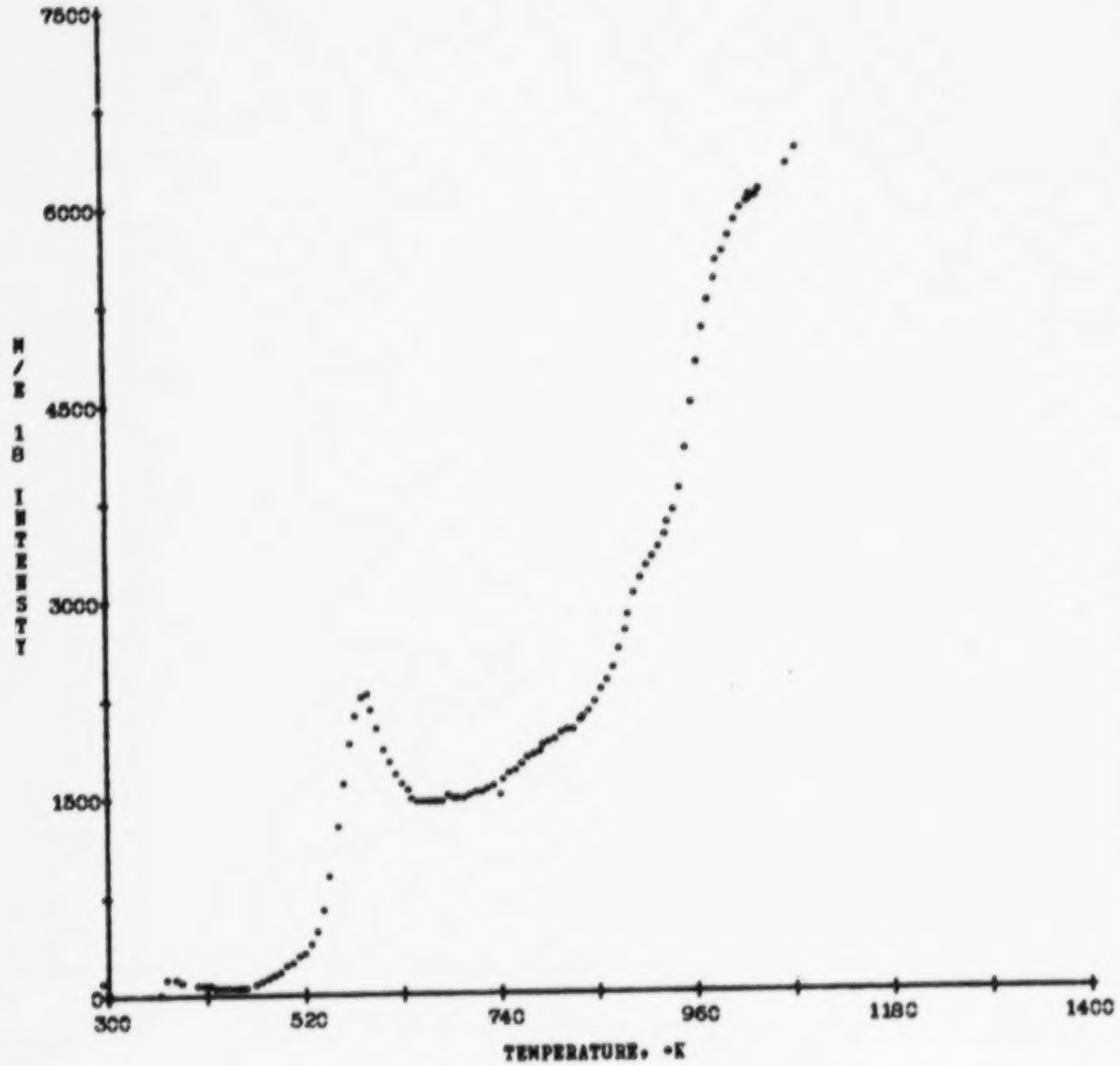

SYMBOL	NO. PTS.	LEGEND
.	106	H2O+ FROM ANTHRACITE, AR+1%O2 AT 200 CC/MIN, 30°/MIN

Figure 22

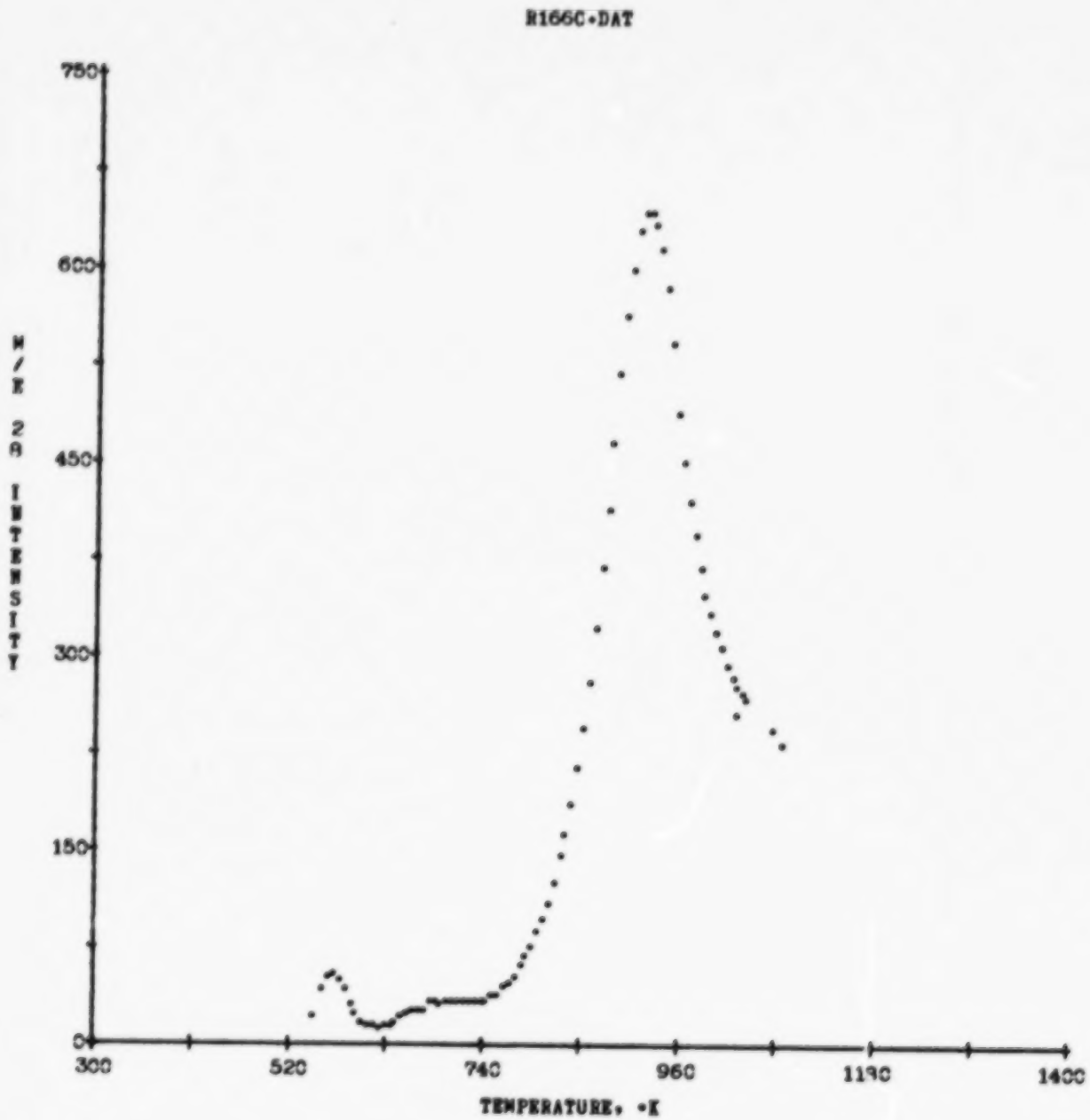

SYMBOL	NO.PTS.	LEGEND
.	80	CO+ FROM ANTHRACITE, AR+1%O2 AT 200 CC/MIN, 30°/MIN

Figure 23

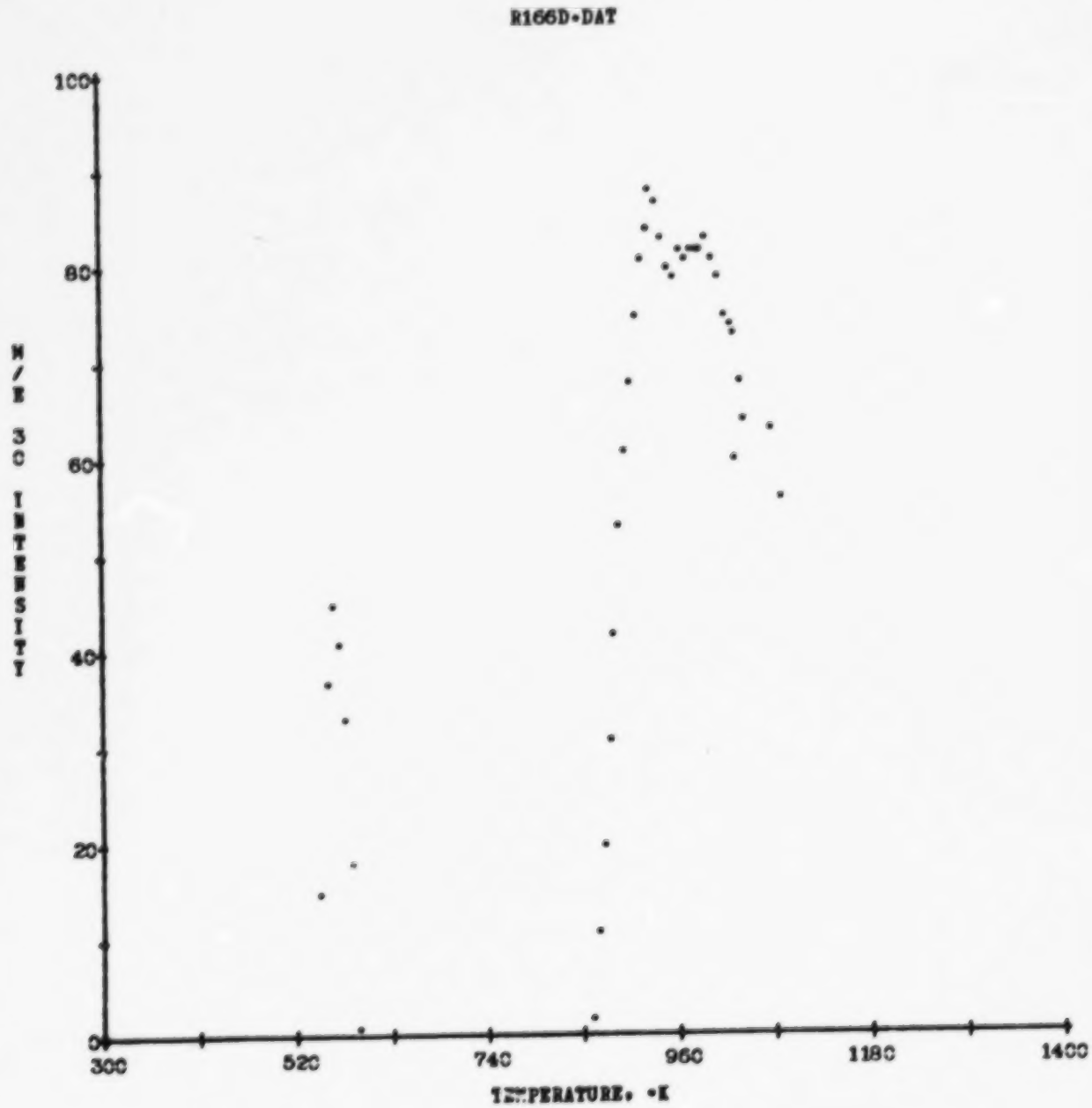

SYMBOL	NO.PTS.	LEGEND
.	39	NO+ FROM ANTHRACITE, AR+1%O2 AT 200 CC/MIN, 30°/MIN

Figure 24

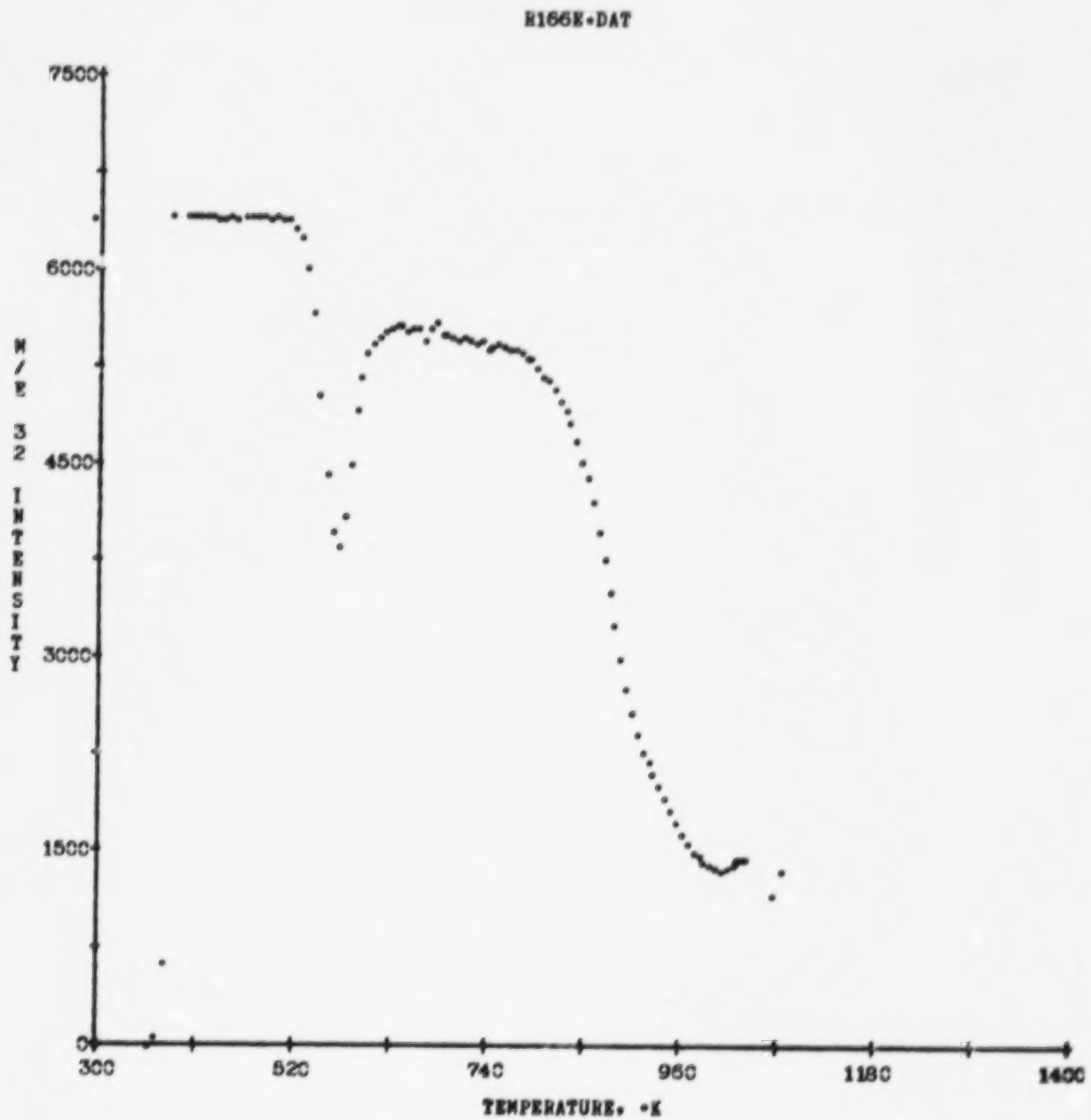

SYMBOL	NO.PTS.	LEGEND
•	106	02+ FROM ANTHRACITE, AR+1%02 AT 200 CC/MIN, 30°/MIN

Figure 25

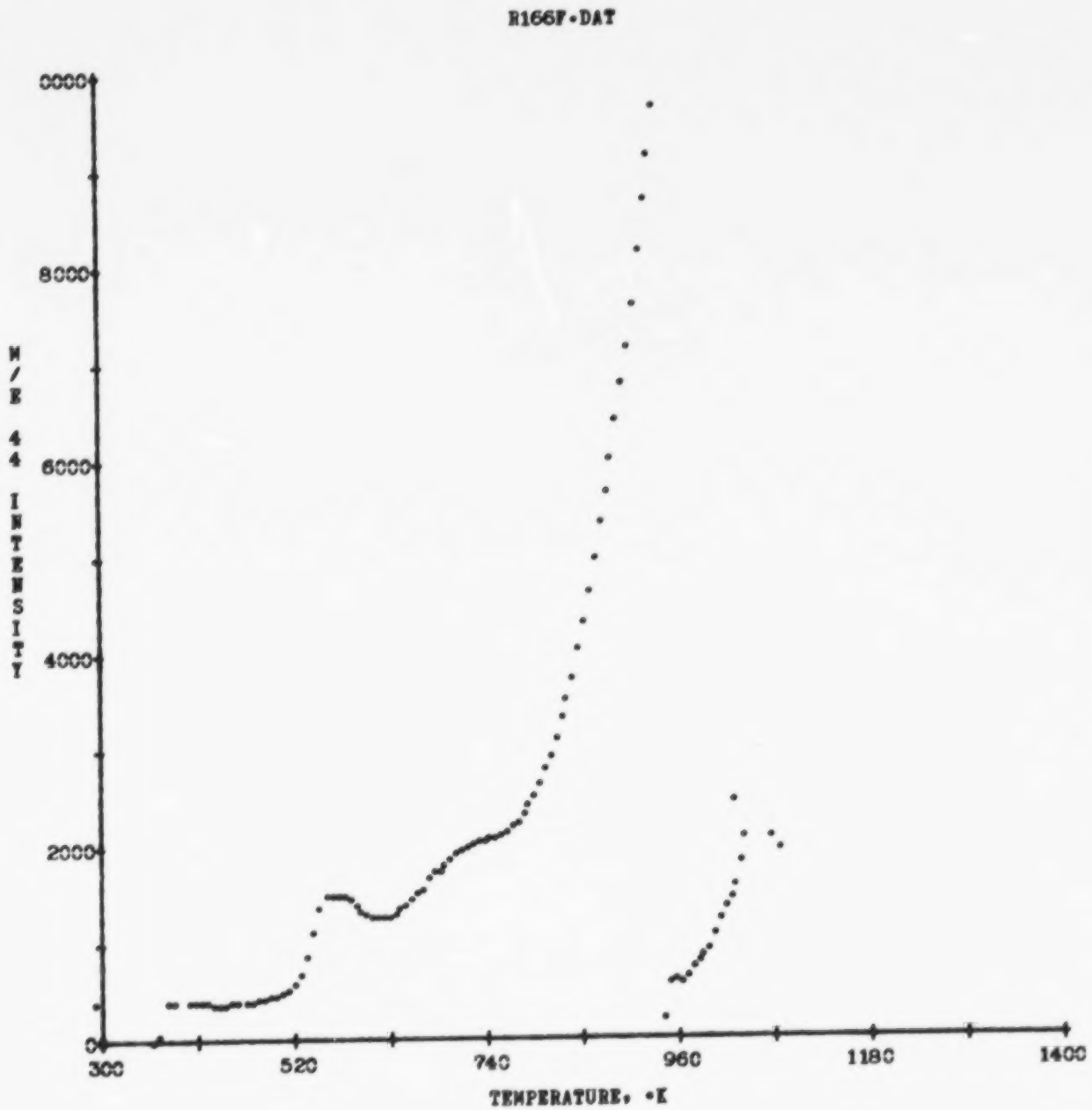

SYMBOL NO.PTS. LEGEND
. 106 CO2+ FROM ANTHRACITE, AR+1%O2 AT 200 CC/MIN, 30°/MIN

Figure 26

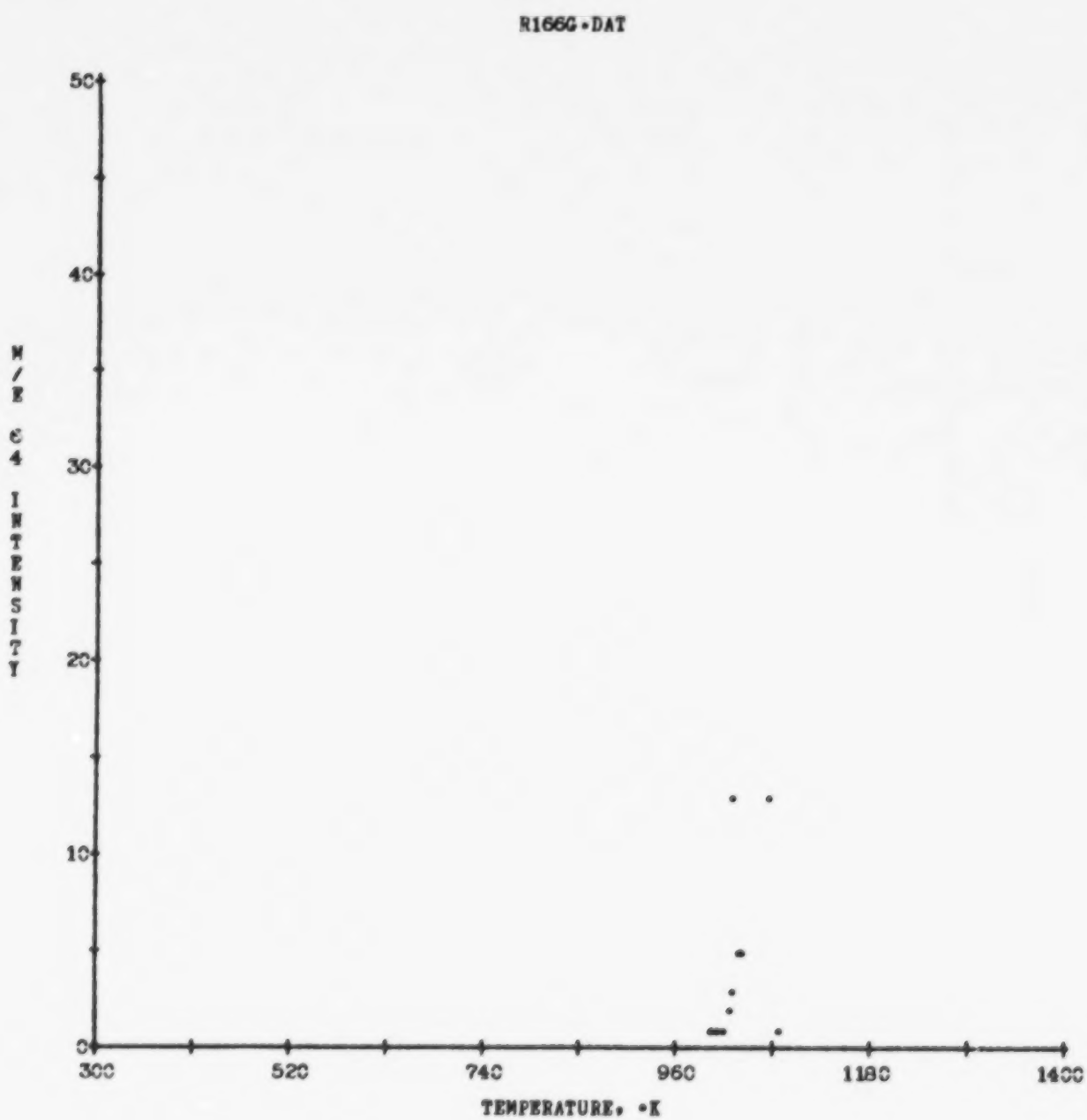

SYMBOL	NO.PTS.	LEGEND
.	11	SO2+ FROM ANTHRACITE, AR+1%O2 AT 200 CC/MIN, 30°/MIN

Figure 27

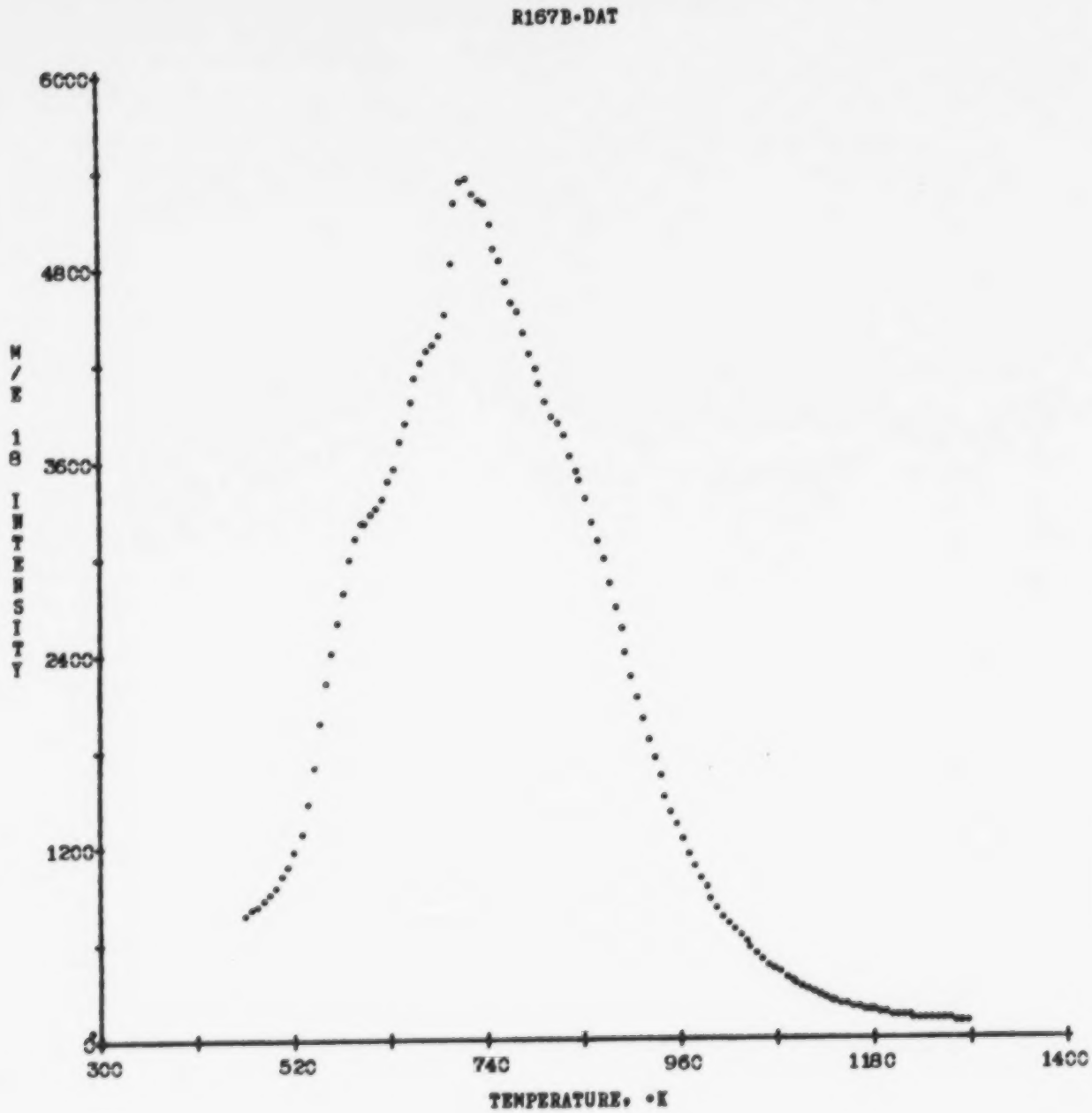

SYMBOL NO.PTS. LEGEND
. 128 H2O+ FROM LIGNITE, AR+1%O2 AT 200 CC/MIN, 30°/MIN

Figure 28

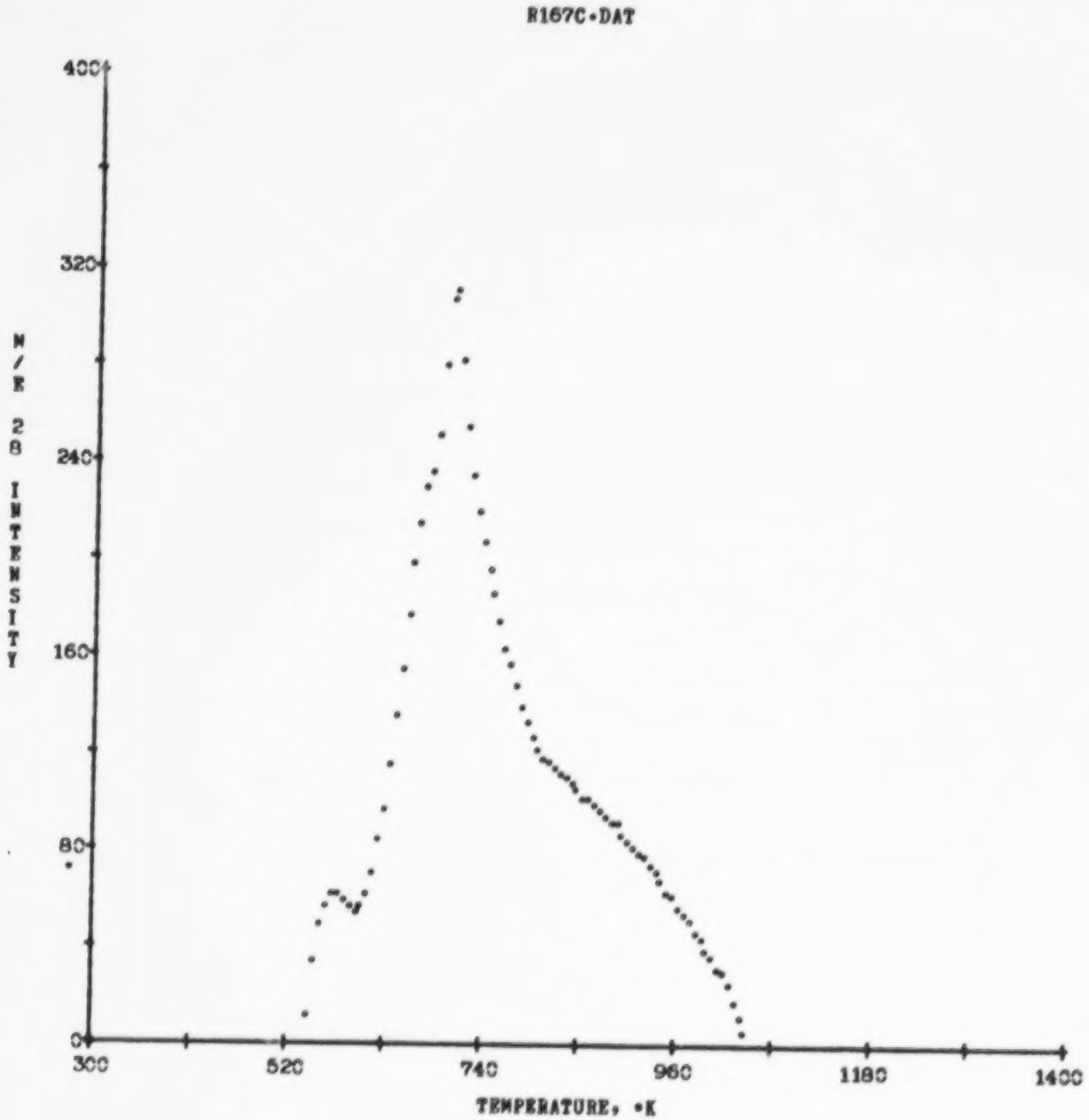

SYMBOL	NO. PTS.	LEGEND
•	81	CO+ FROM LIGNITE, AR+1%O2 AT 200 CC/MIN, 30°/MIN

Figure 29

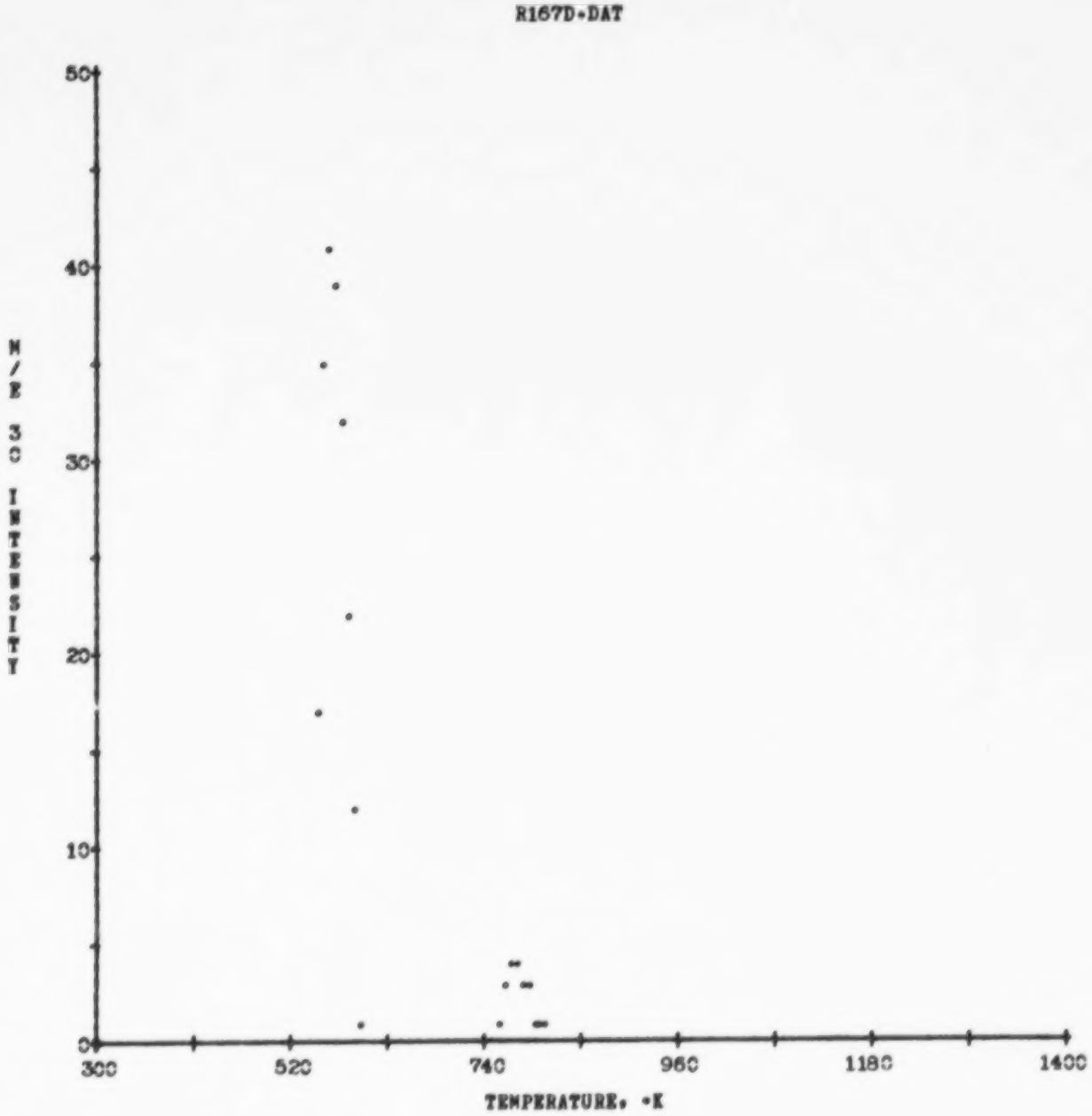

SYMBOL	NO. PTS.	LEGEND
.	17	NO+ FROM LIGNITE, AR+1%O2 AT 200 CC/MIN, 30°/MIN

Figure 30

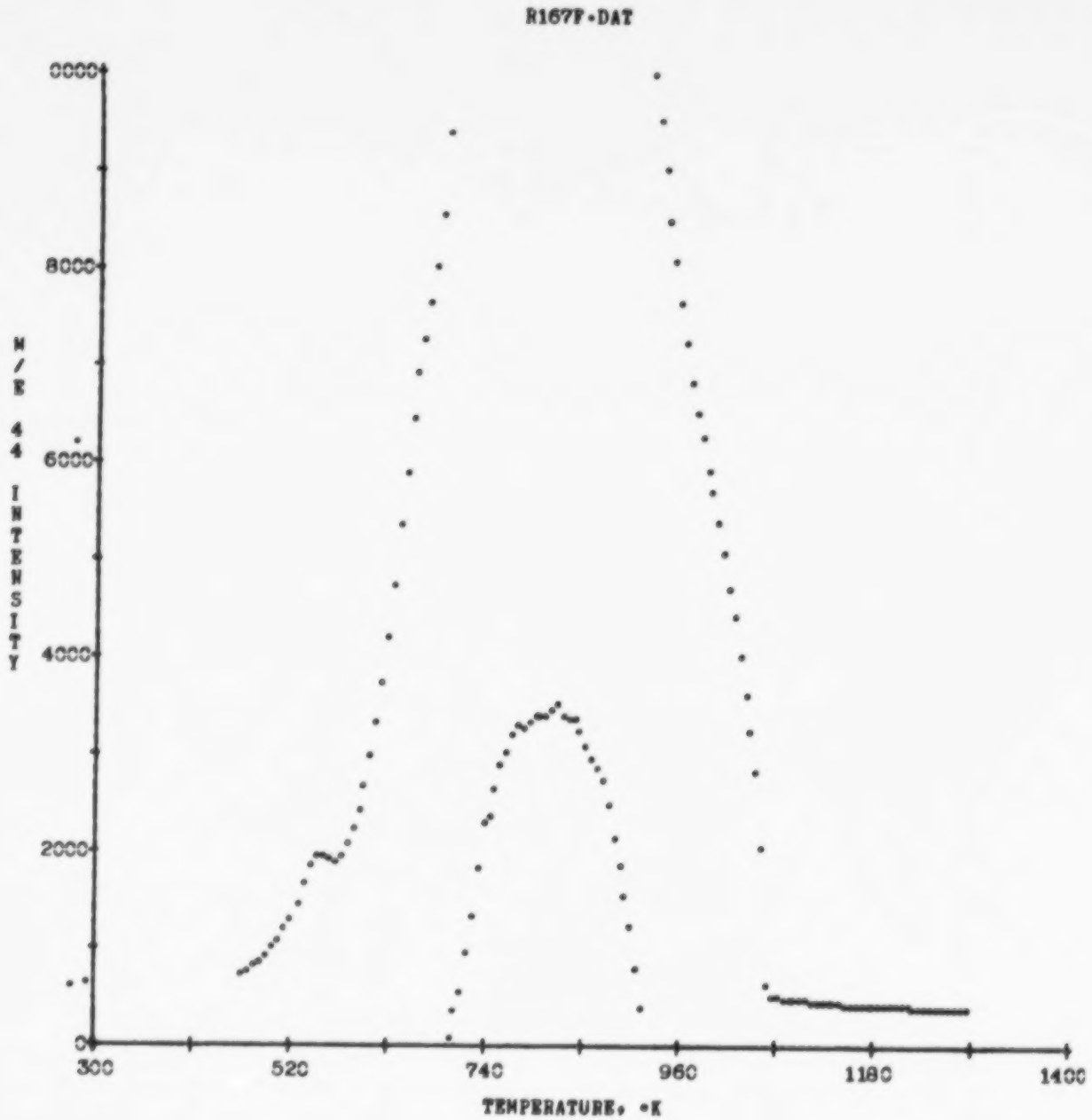

SYMBOL NO.PTS. LEGEND

. 130 CO2: FROM LIGNITE, AR+1%O2 AT 200 CC/MIN, 30°/MIN

Figure 31

R167G.DAT

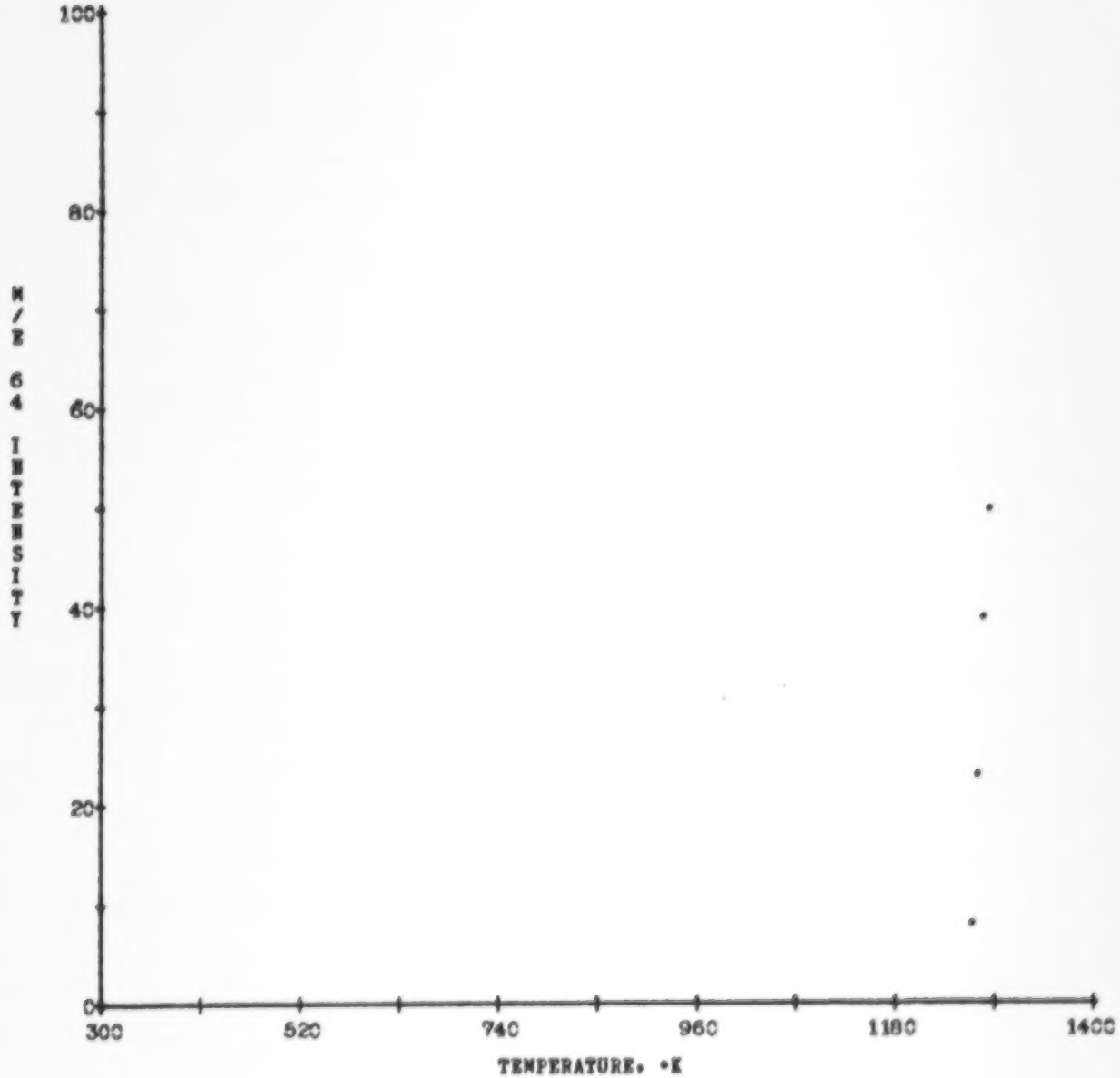

SYMBOL	NO.PTS.	LEGEND
.	6	SO2+ FROM LIGNITE, AR:1%O2 AT 200 CC/MIN, 30°/MIN

Figure 32

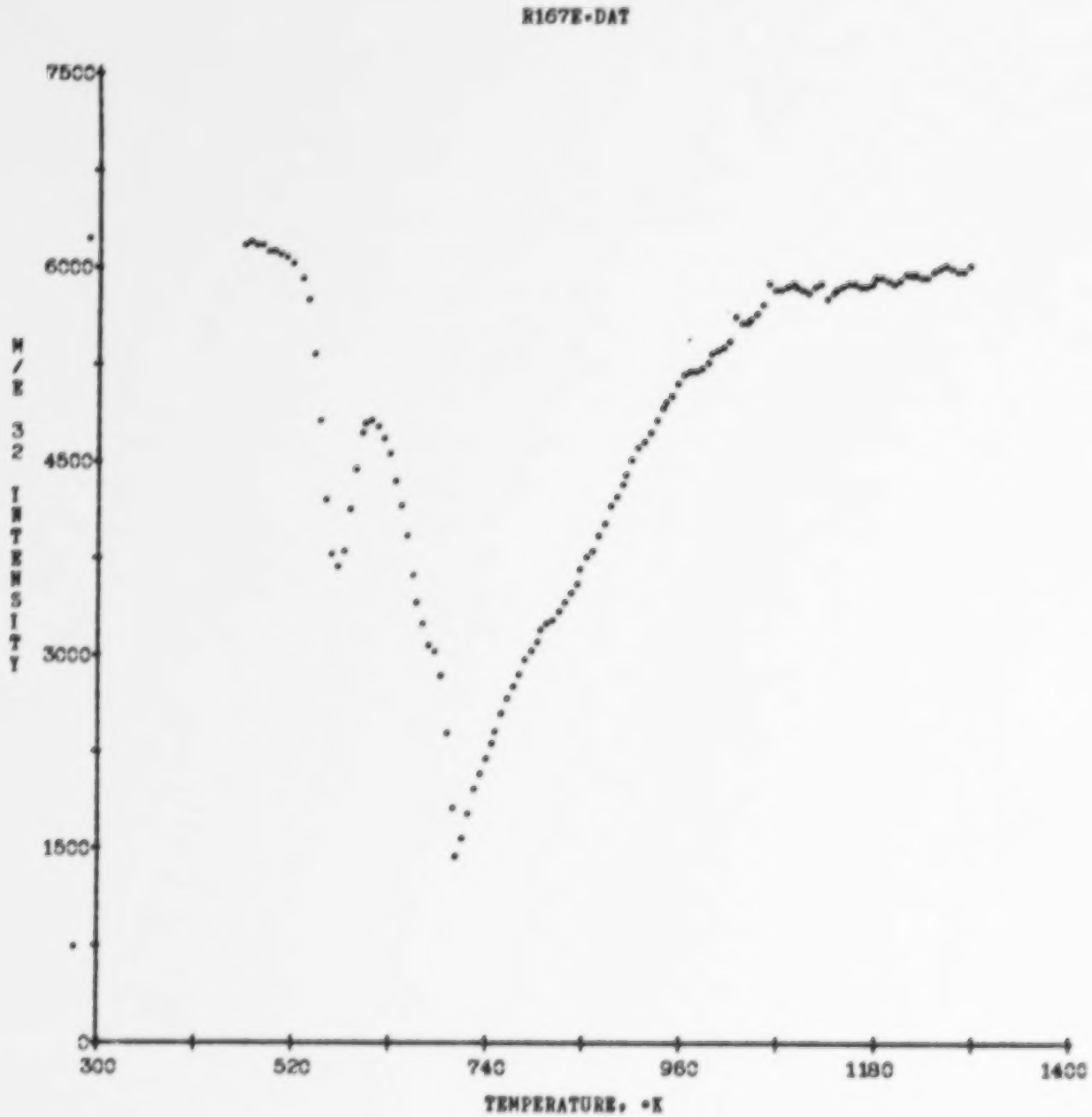

SYMBOL	NO.PTS.	LEGEND
.	129	O2+ FROM LIGNITE, AR+1%O2 AT 200 CC/MIN, 30°/MIN

Figure 33

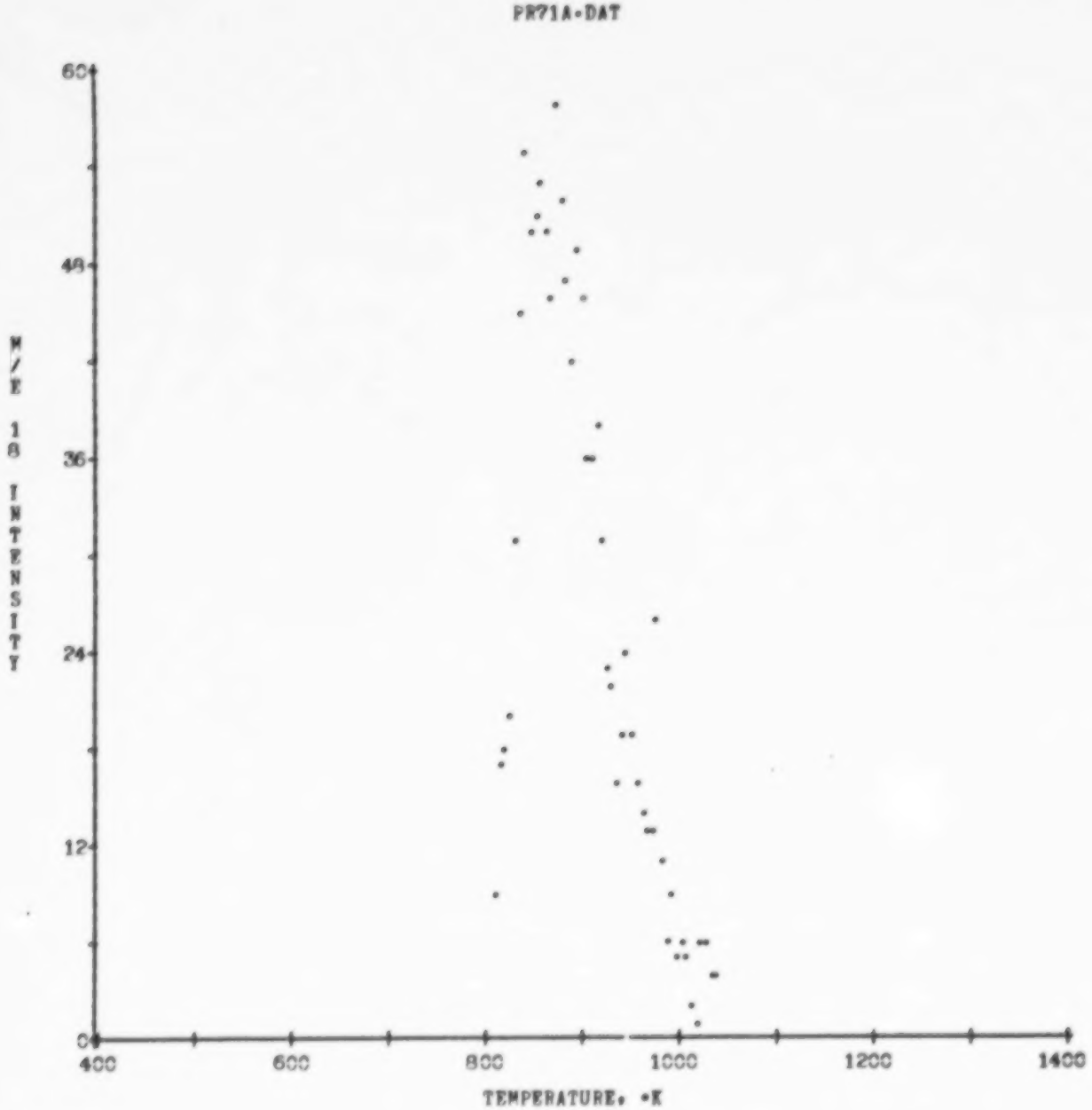

SYMBOL	NO.PTS.	LEGEND
.	47	H2O+ FROM SRI COKE #5, AR+1%O2 AT 100 CC/MIN, 15MG SAMPLE, 30°/MIN

Figure 34

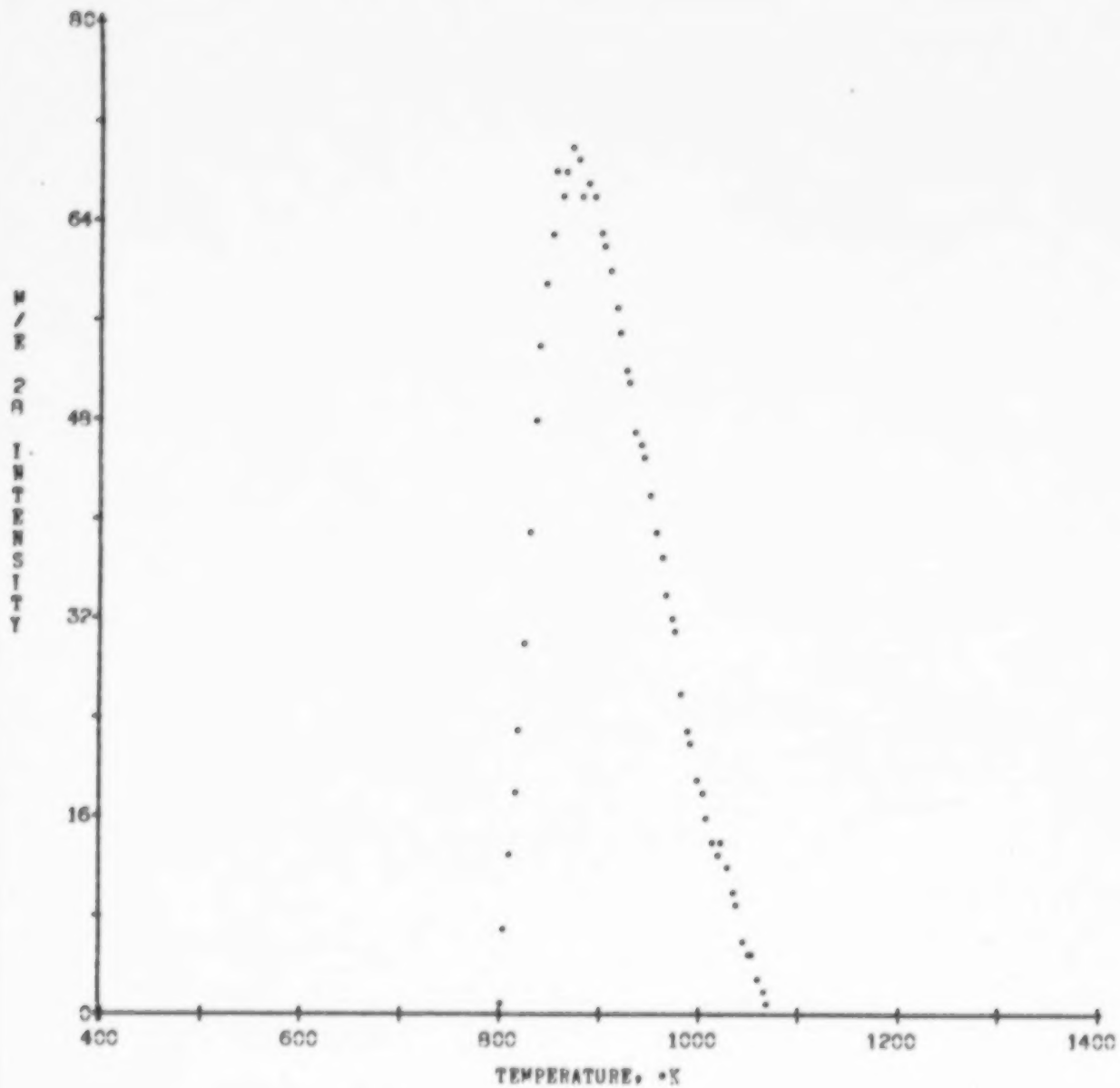

SYMBOL	NO.PTS.	LEGEND
.	53	CO+ FROM SRI COKE #5, AR+1%O2 AT 100CC/MIN, 15MG SAMPLE, 30°/MIN

Figure 35

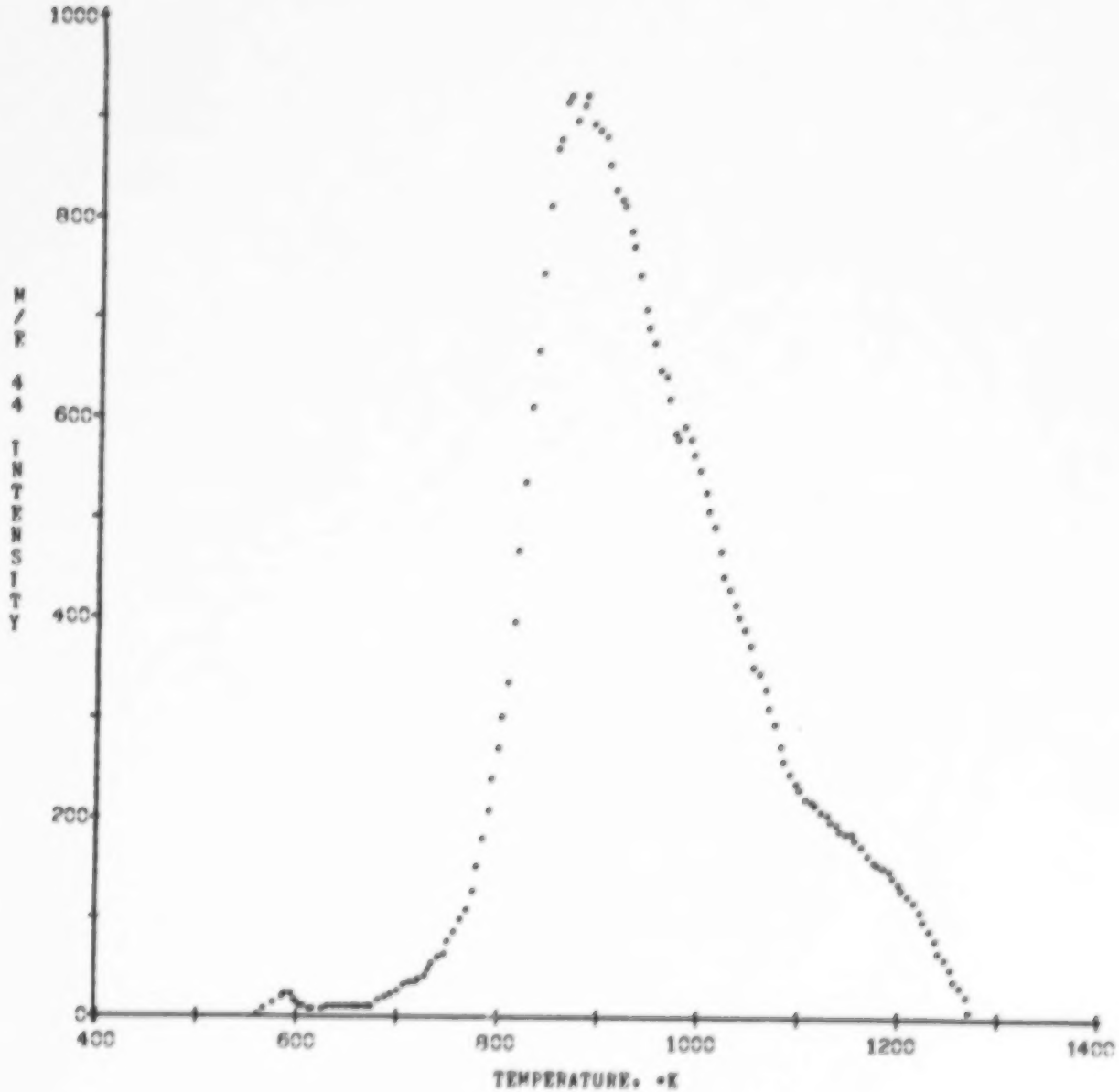

SYMBOL	NO.PTS.	LEGEND
.	137	CO2+ FROM SRI COKE #5, AR+1%O2 AT 100CC/MIN, 15MG SAMPLE, 30°/MIN

Figure 36

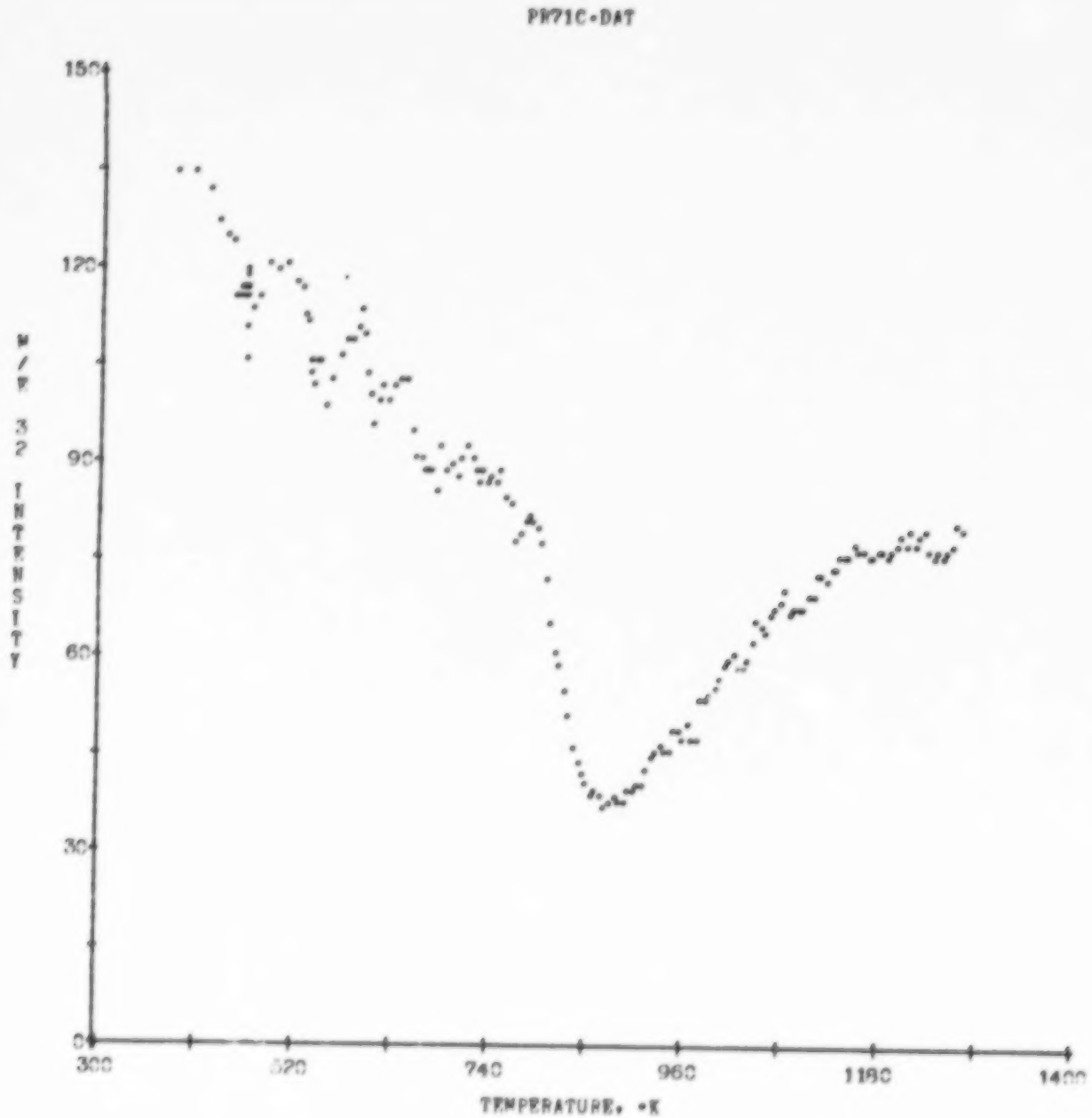

SYMBOL NO.PTS. LEGEND

. 190 02+ FROM SRI COKE #5, AR+1%02 AT 100CC/MIN, 15MG SAMPLE, 30°/MIN

Figure 37

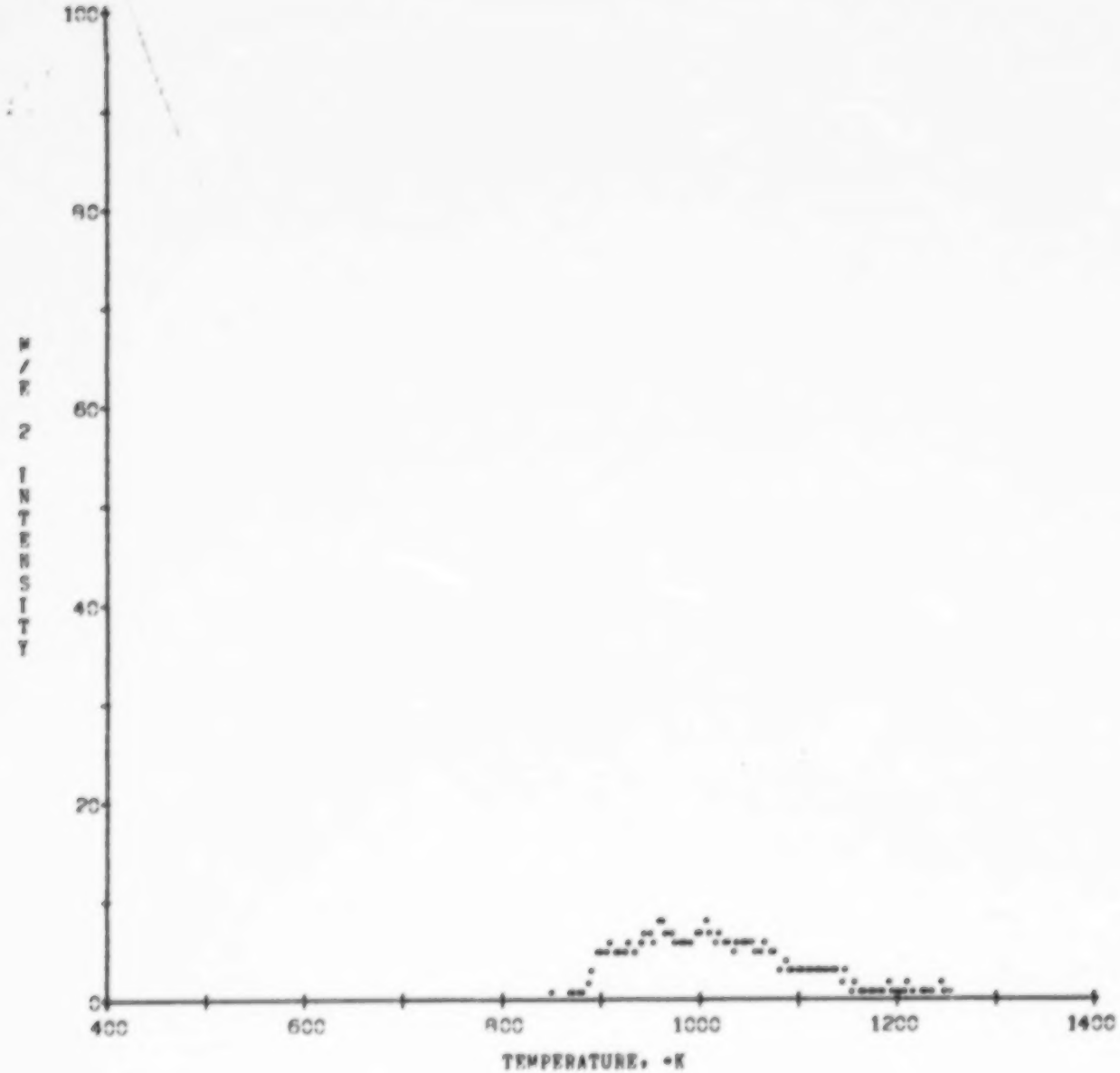

SYMBOL	NO.PTS.	LEGEND
.	92	M2+ FROM SRI COKE #7, AR+1%O2 AT 100CC/MIN, 15MG SAMPLE, 20°/MIN

Figure 38

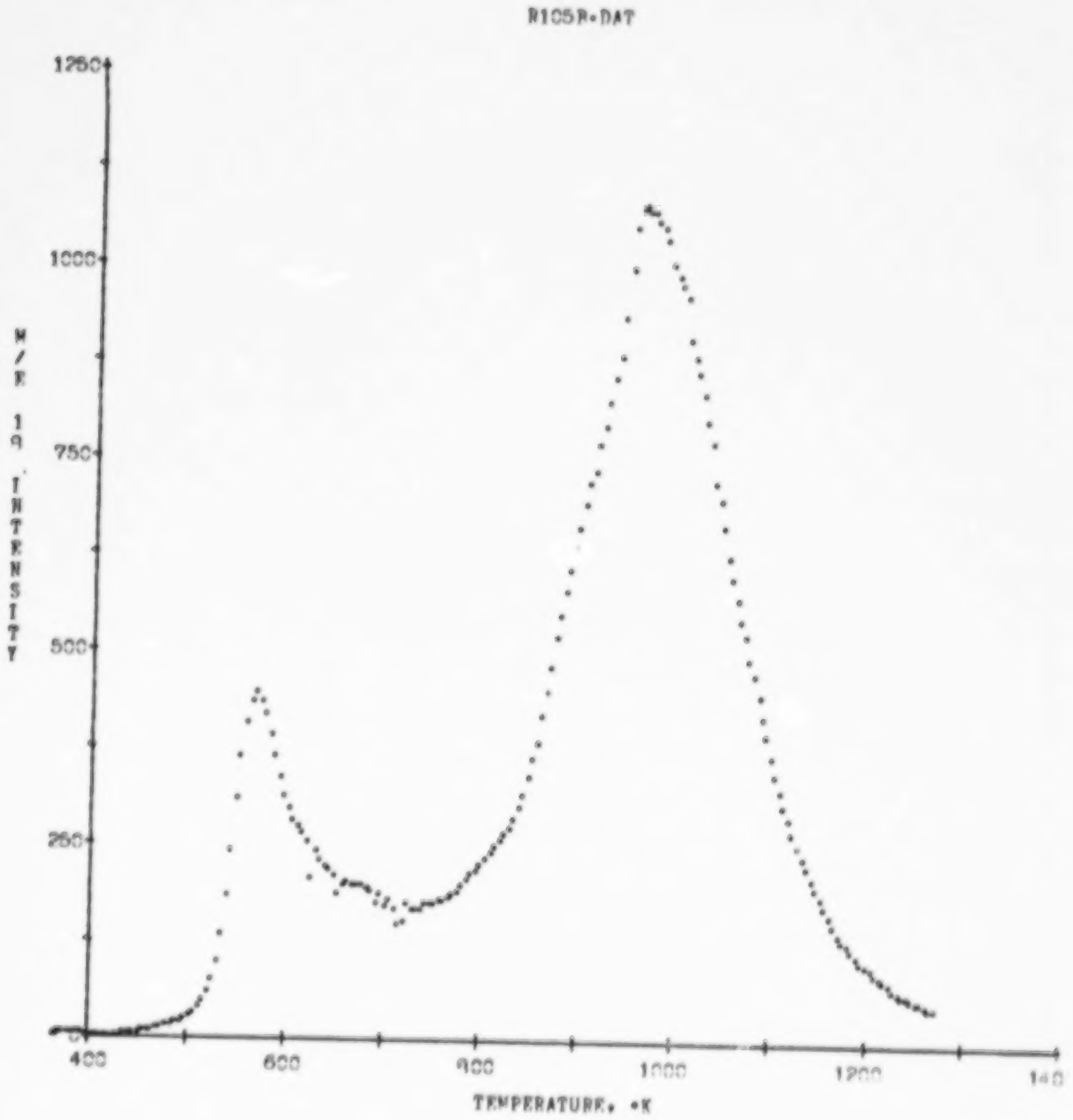

SYMBOL NO.PTS. LEGEND

. 202 H20+ FROM SRI COKE #7, AR+1%02 AT 100CC/MIN, 15MG SAMPLE, 20°/MIN

Figure 39

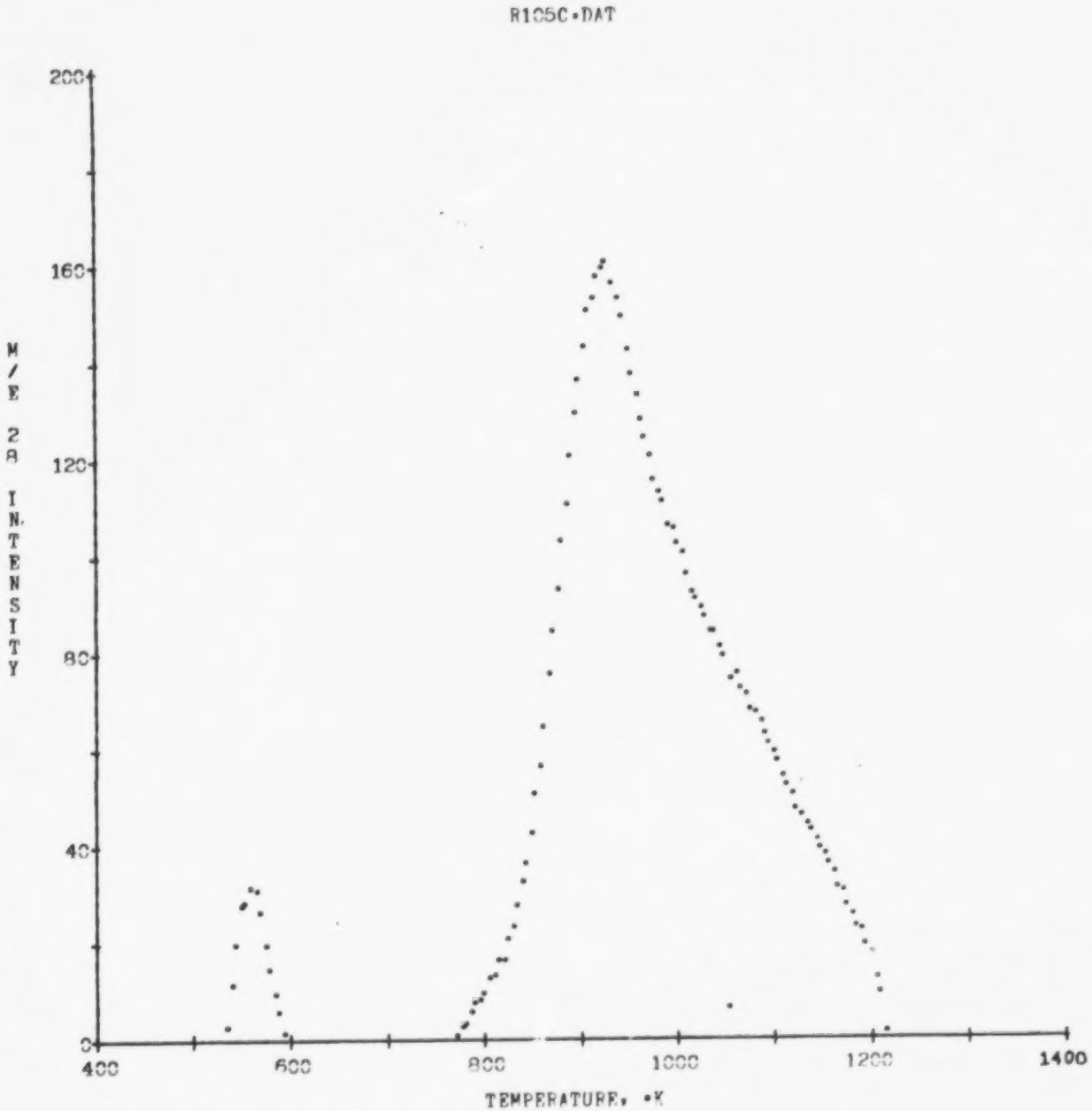

SYMBOL NO.PTS. LEGEND

. 107 CO+ FROM SRI COKE #7, AR+1%O2 AT 100CC/MIN, 15MG SAMPLE, 20°/MIN

Figure 40

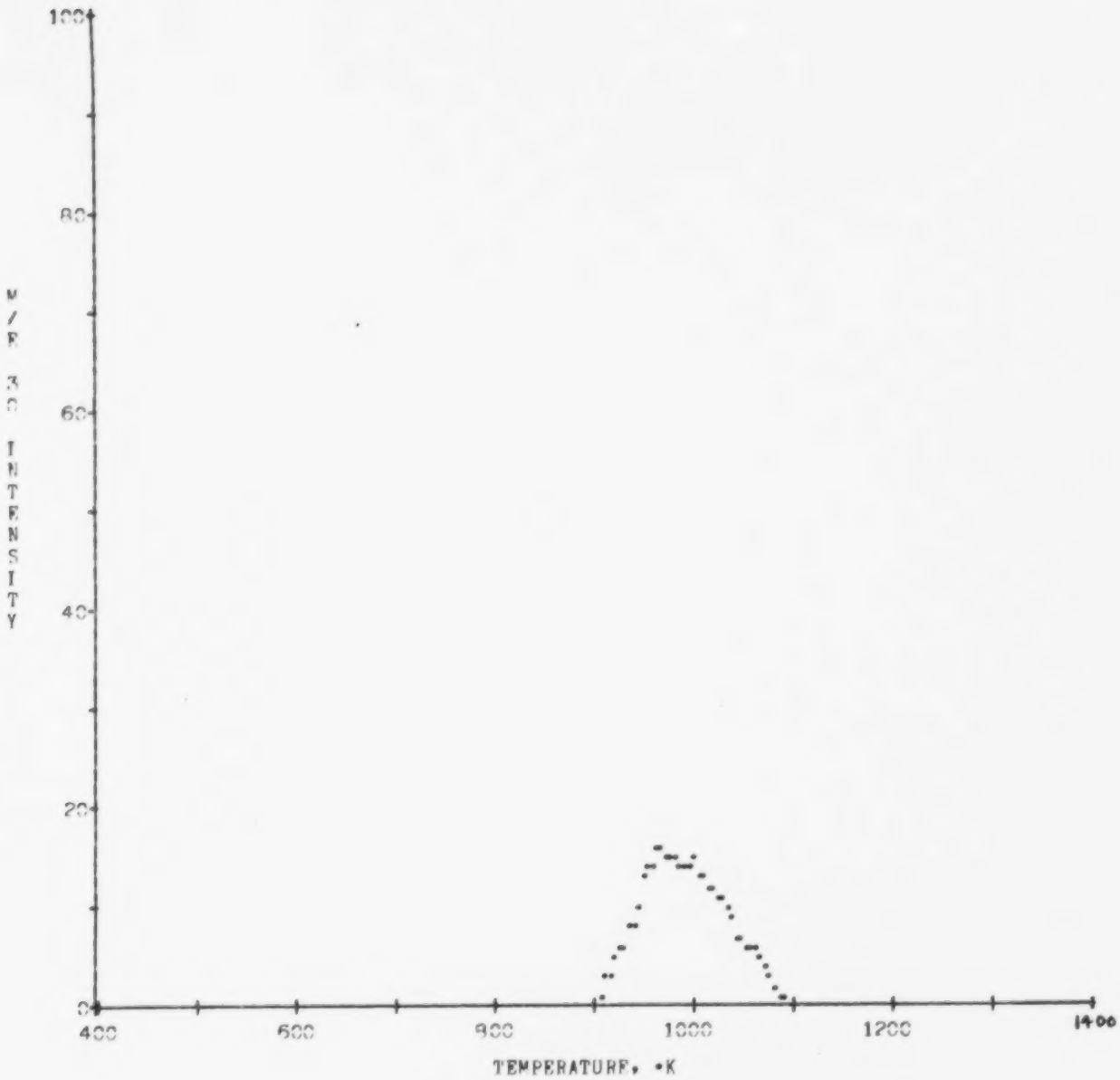

SYMBOL NO.PTS. LEGEND
. 40 NO+ FROM SRI COKE #7, AR+1%02 AT 100CC/MIN, 15MG SAMPLE, 20°/MIN

Figure 41

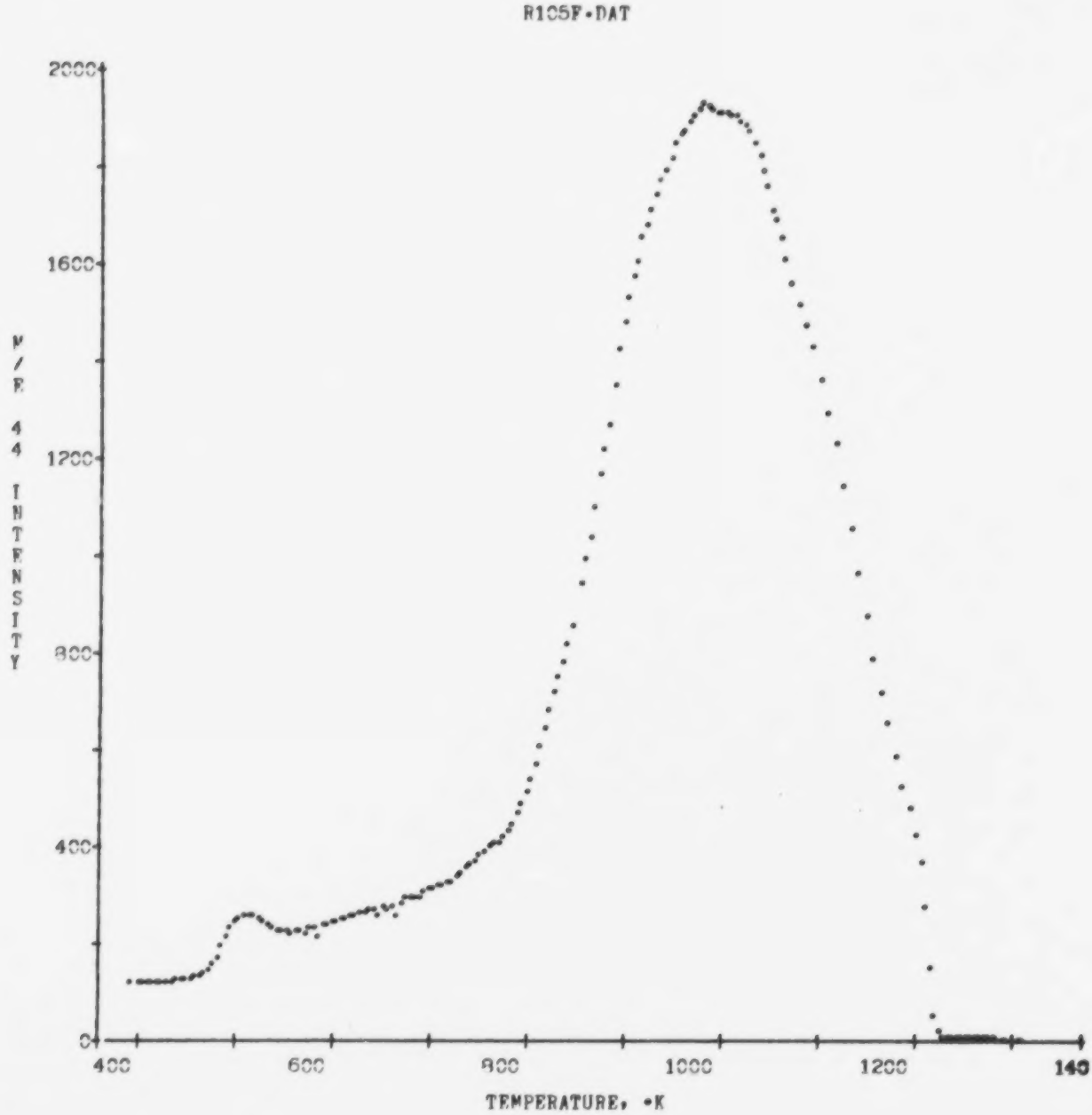

SYMBOL	NO.PTS.	LEGEND
.	181	CO2+ FROM SRI COKE #7, AR+1%O2 AT 100CC/MIN, 15MG SAMPLE, 20°/MIN

Figure 42

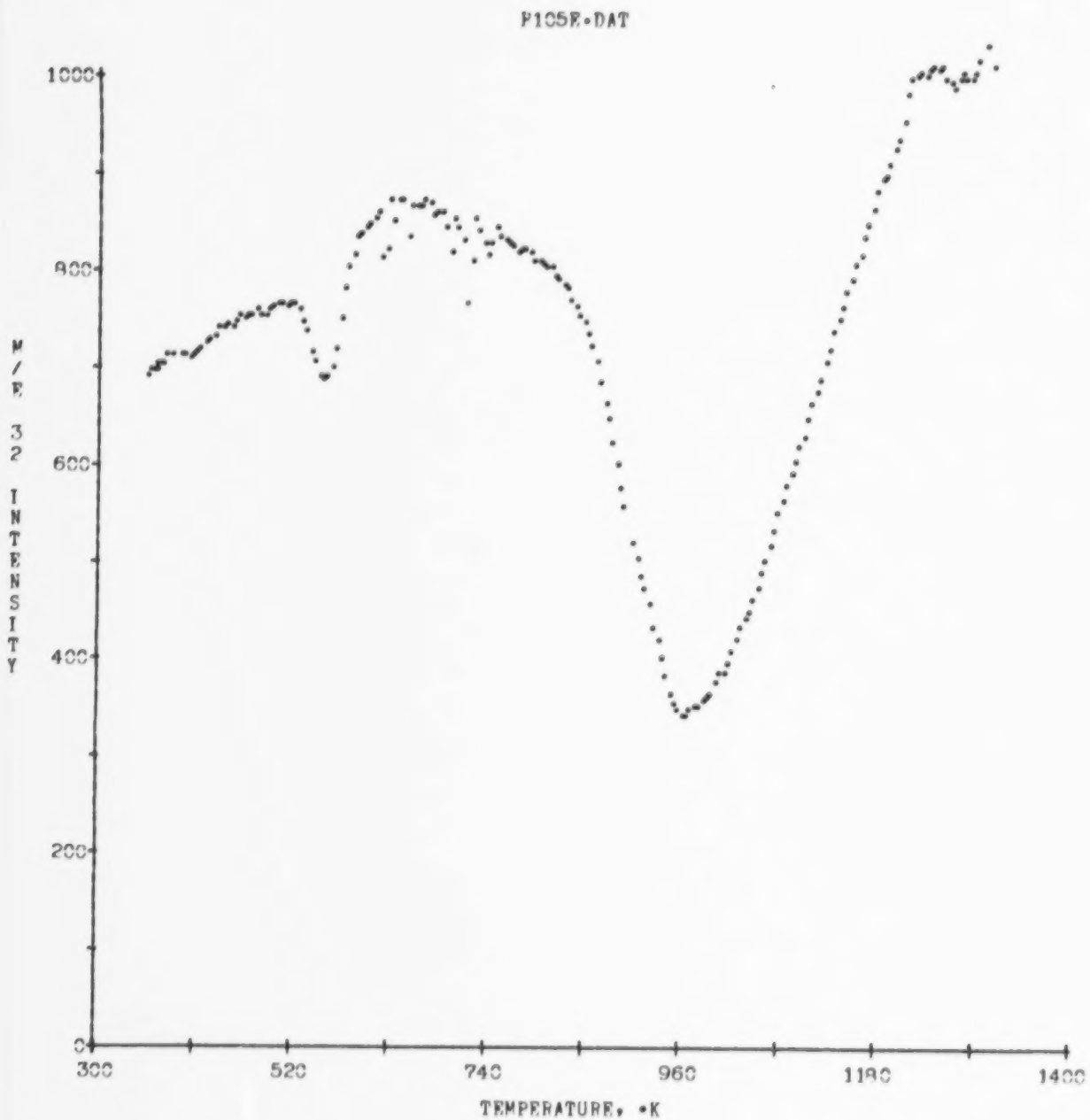

SYMBOL	NO.PTS.	LEGEND
•	202	O2+ FROM SRI COKE #7, AR+1%O2 AT 100CC/MIN, 15MG SAMPLE, 20°/MIN

Figure 43

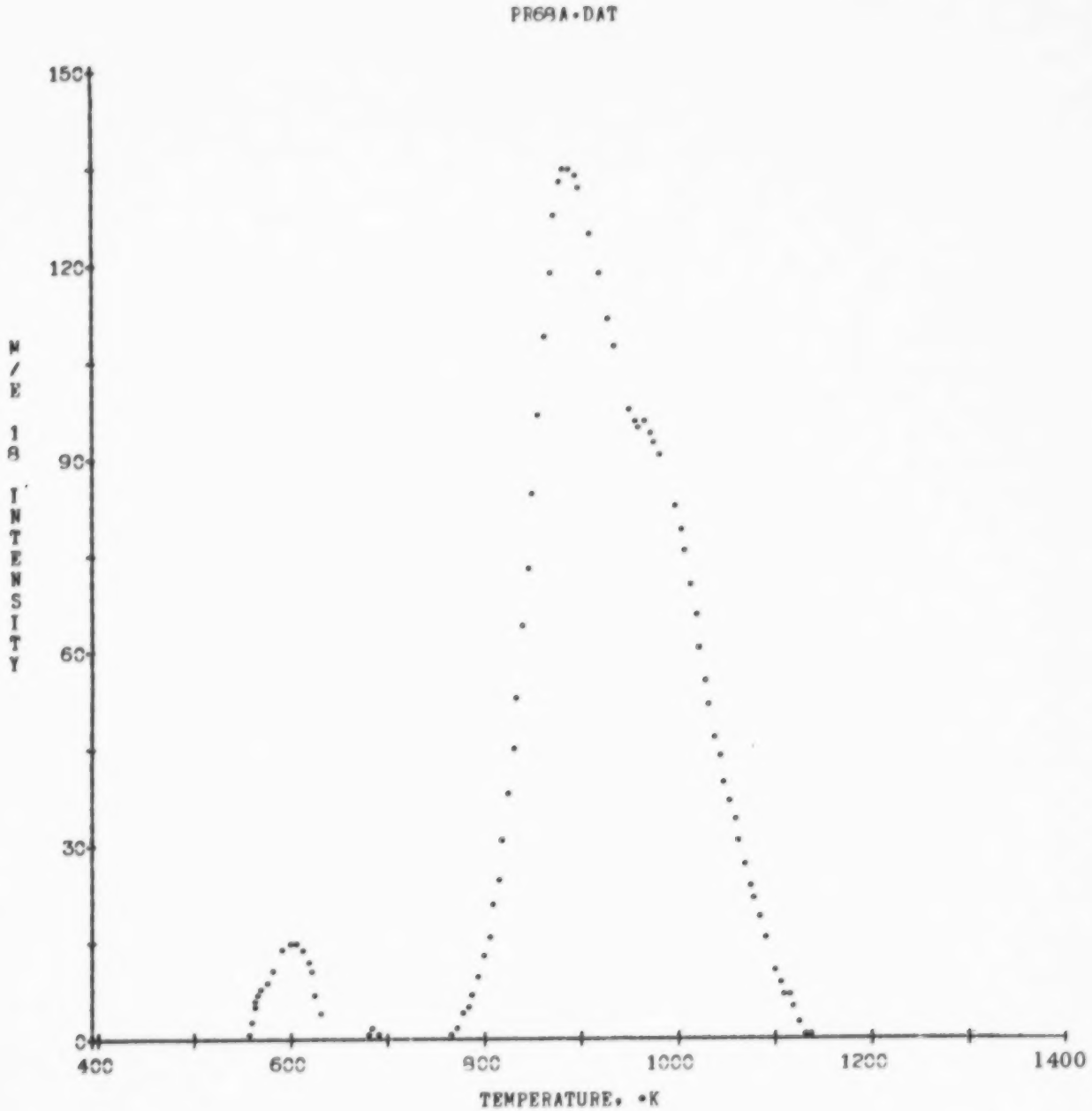

SYMBOL NO.PTS. LEGEND
. 88 H2O+ FROM SRI COKE #1C, AR+1%O2 AT 100CC/MIN,15 MG SAMPLE,30°/MIN
CHANGES FOR NEXT RUN ? ALL

Figure 44

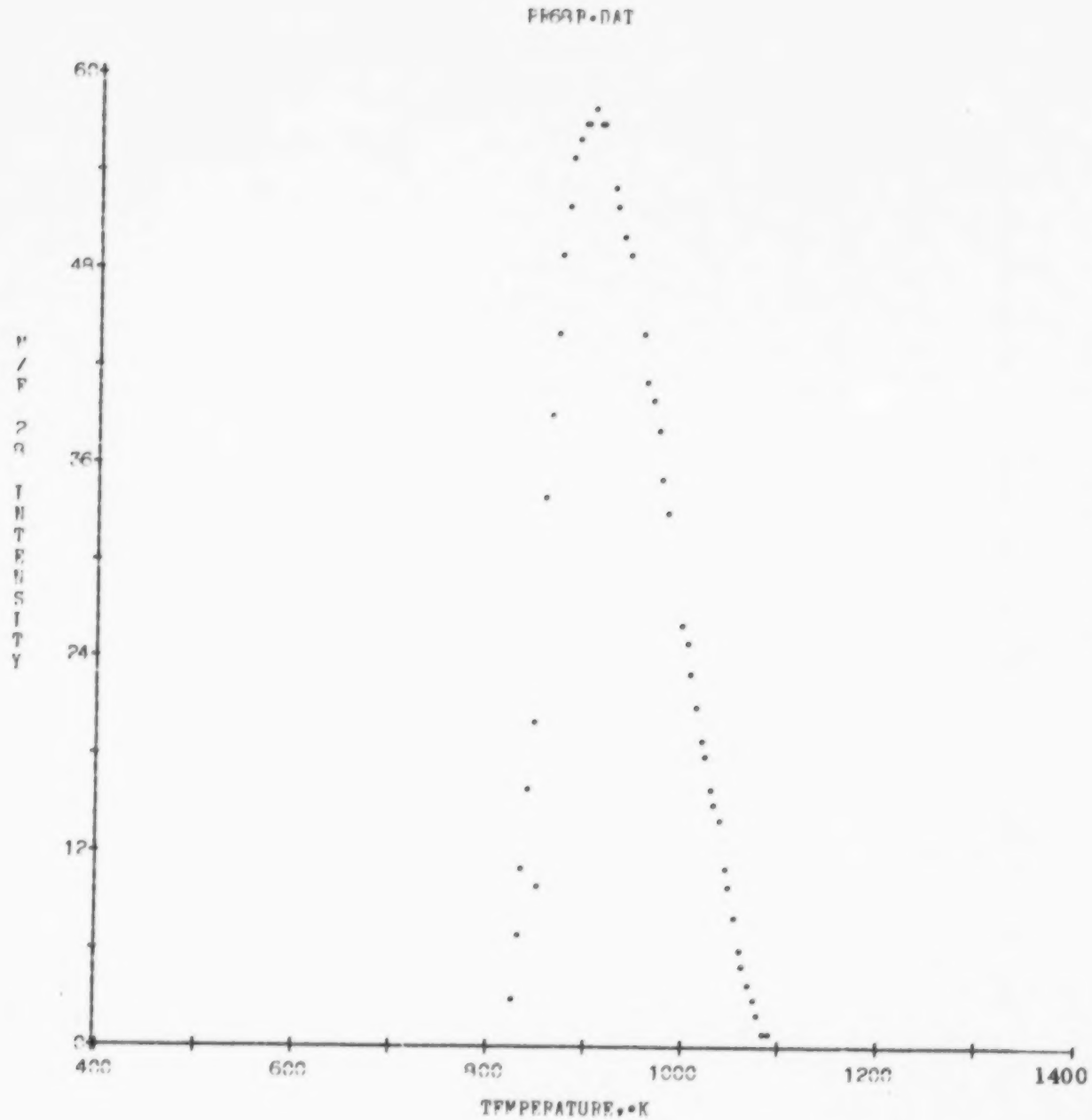

SYMBOL	NO.PTS.	LEGEND
.	50	CO+ FROM SRI COKE #10, AR+1%O2, 100CC/MIN, 15MG SAMPLE, 30°/MIN

Figure 45

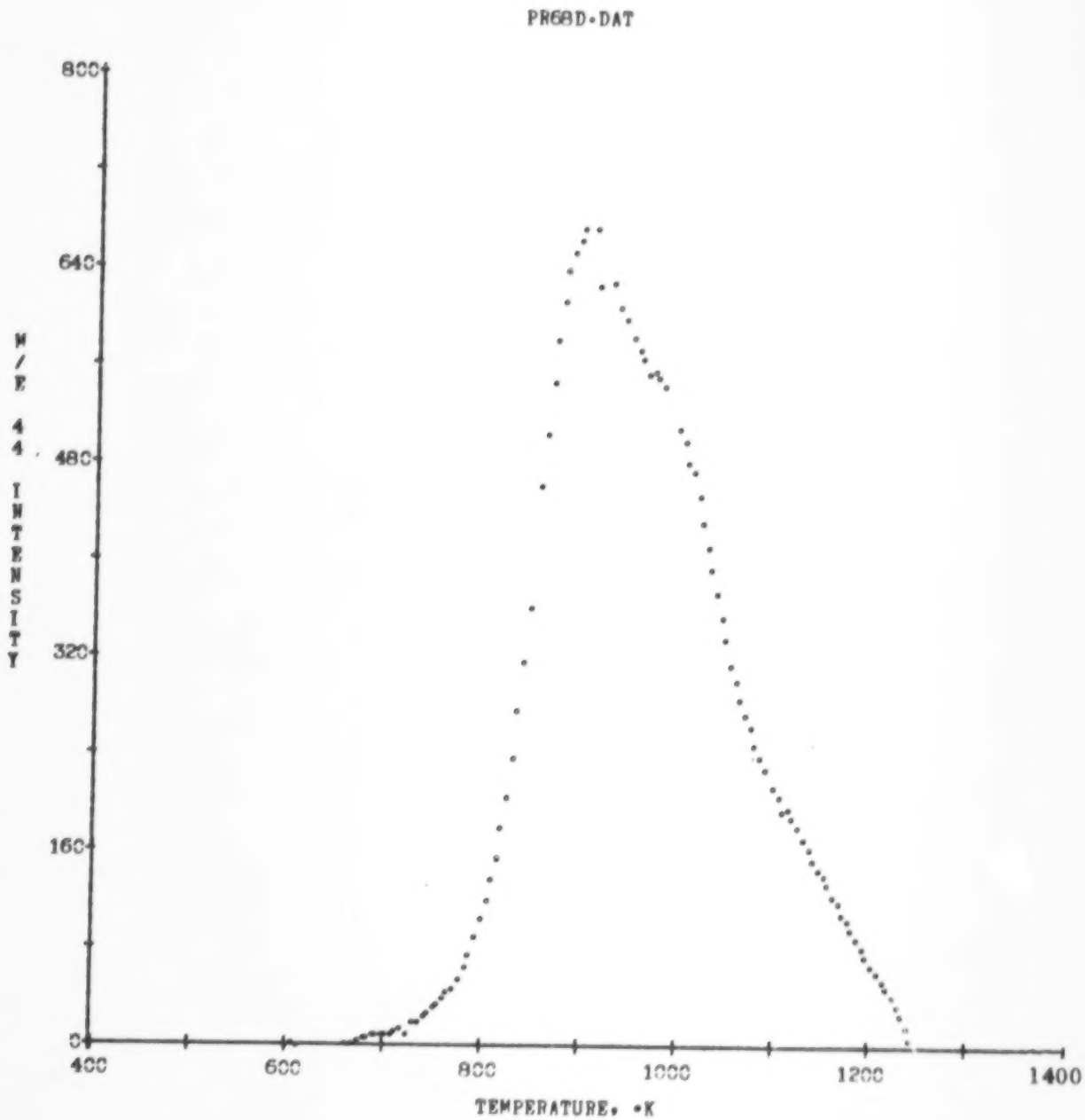

SYMBOL NO.PTS. LEGEND

. 114 CO2+ FROM SRI COKE #1C, AR+1%02 AT 100CC/MIN, 15MG SAMPLE, 30°/MIN

CHANGES FOR NEXT RUN ?

Figure 46

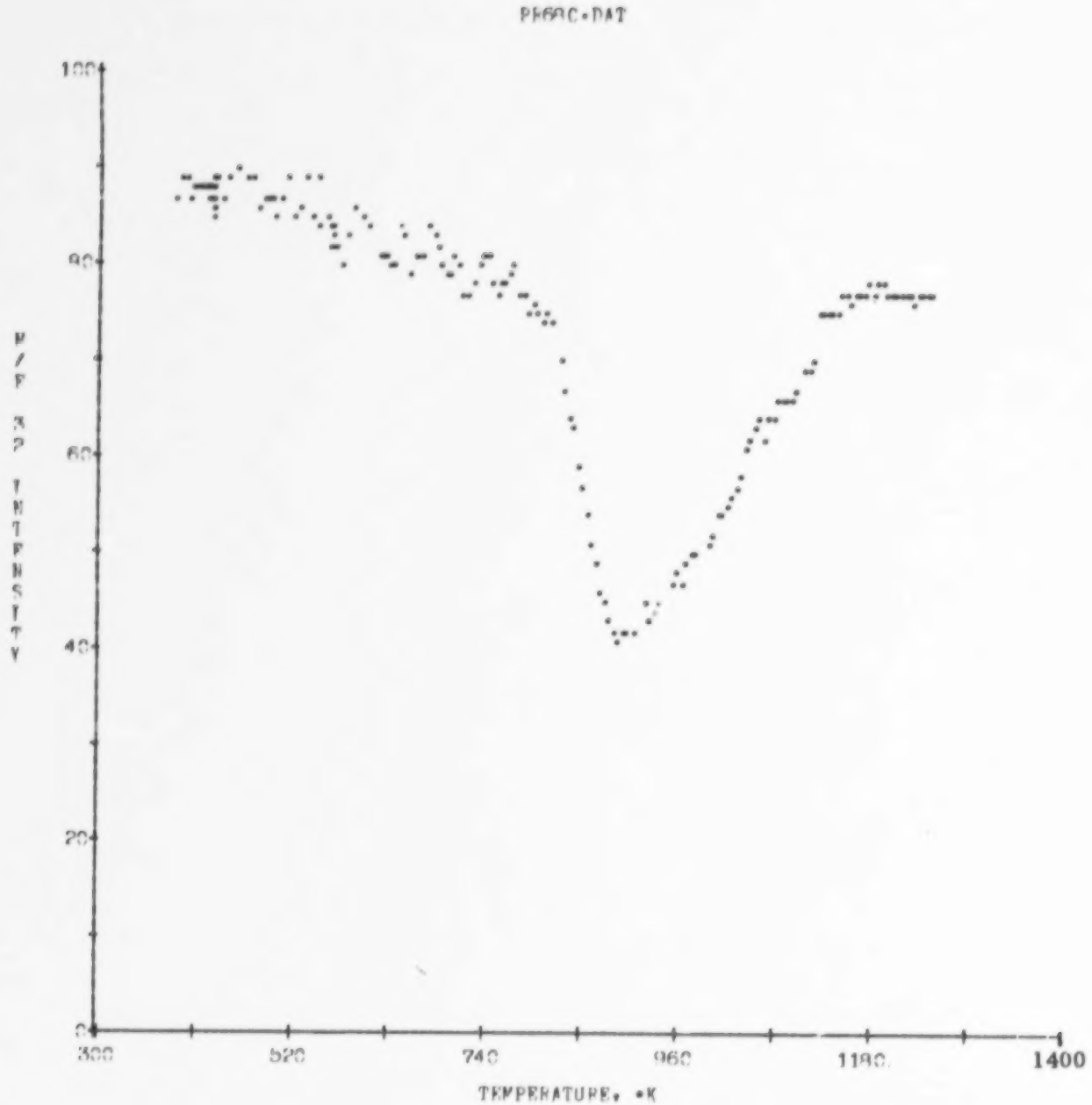

SYMBOL	NO.PTS.	LEGEND
•	178	024 FROM SRI COKE #10, AR+1%O2 AT 1000C/MIN, 15MG SAMPLE, 30°/MIN

Figure 47

APPENDIX B: Gaseous Evolution Data for Pyrolysis Experiments

Table X: Peak Temperatures for Pyrolysis of Coals and Cokes Heated at 30^{0}/min in Argon

Figures: 48 - 102

TABLE X

Peak Temperatures for Pyrolysis of Coals and Cokes Heated at 30°/min in Argon

Solid Reactant	Peak Temperatures in °K						
	H_2	"CH_3"	H_2O	CO	NO	CO_2	SO_2
SRI-5	608	608	629	605	608	610	616
	714	817	726	744	677	700	704
		860	828				805
SRI-7	600	600	632	605	608	607	588
	827	829	741	807	800	810	806
		874	860				
SRI-10	1213	856	751	625	640	674	606
		940	1265	729	730	733	718
				927	994	941	817
				1254	1258		839
							932
Anthracite	608	608	641	603	600	607	599
	947	927	873			760	828
	1082					918	
Lignite	635	628	675	625	634	646	630
	701	704	719	696	690		
		823	817	1010			
Coke-SRI-5	597	598	618	606	603	597	599
		991	1053			970	
Coke-SRI-7	608	600	630	608	608	608	597
	840	850	850	806	806	806	806
							1222
Coke-SRI-10	608	607	641	602	613	610	608
	1092	992	1062				

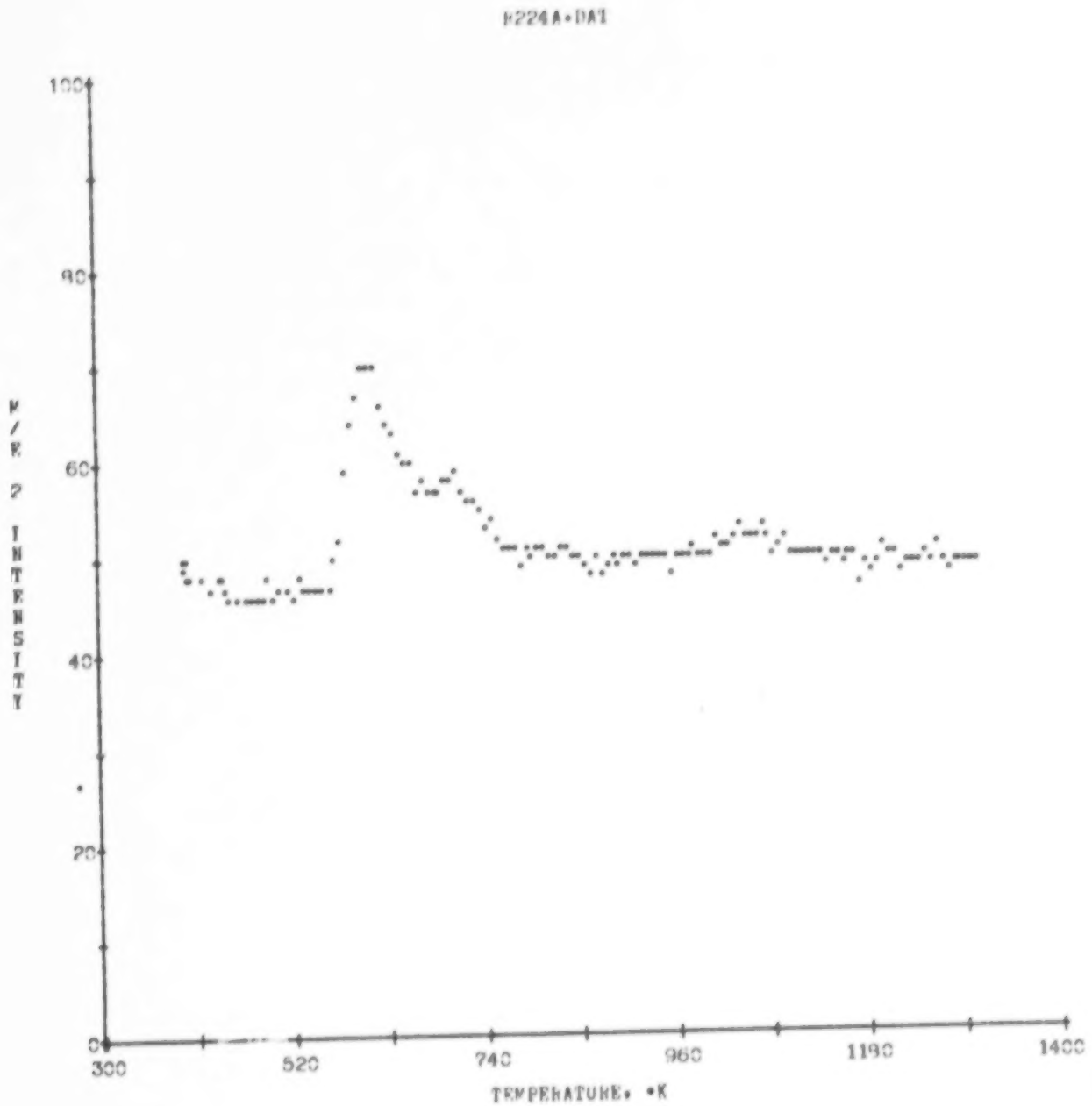

SYMPOL NO.PTS. LEGEND
. 141 H2+ FROM SHI COAL #5, Ah AT 200 CC/MIN, 30°/MIN

Figure 48

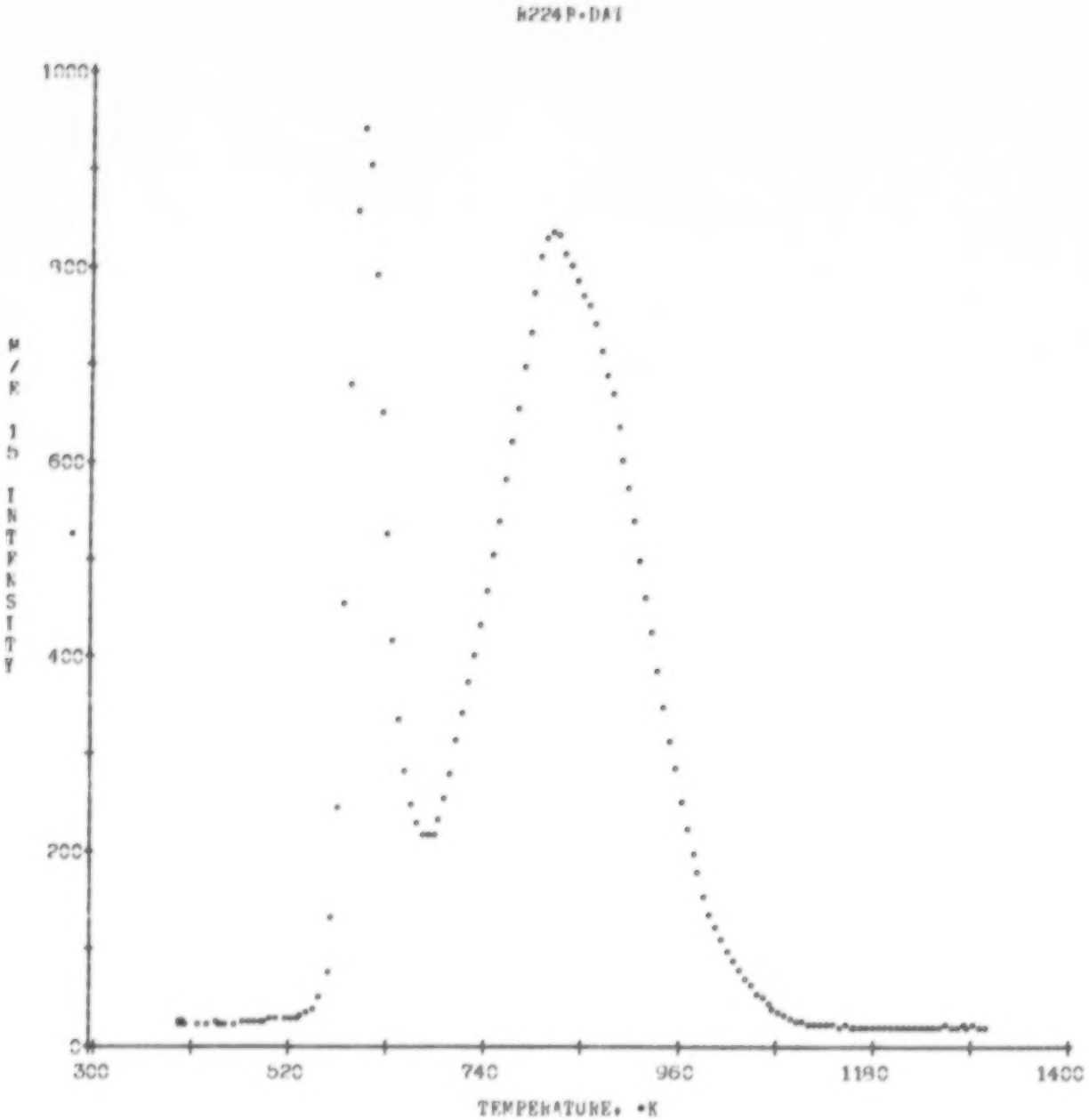

SYMBOL NO.PTS. LEGEND

. 141 CH3+ FROM SHICOAL #5, AR AT 200 CC/MIN, 30°/MIN

Figure 49

9224C.DAT

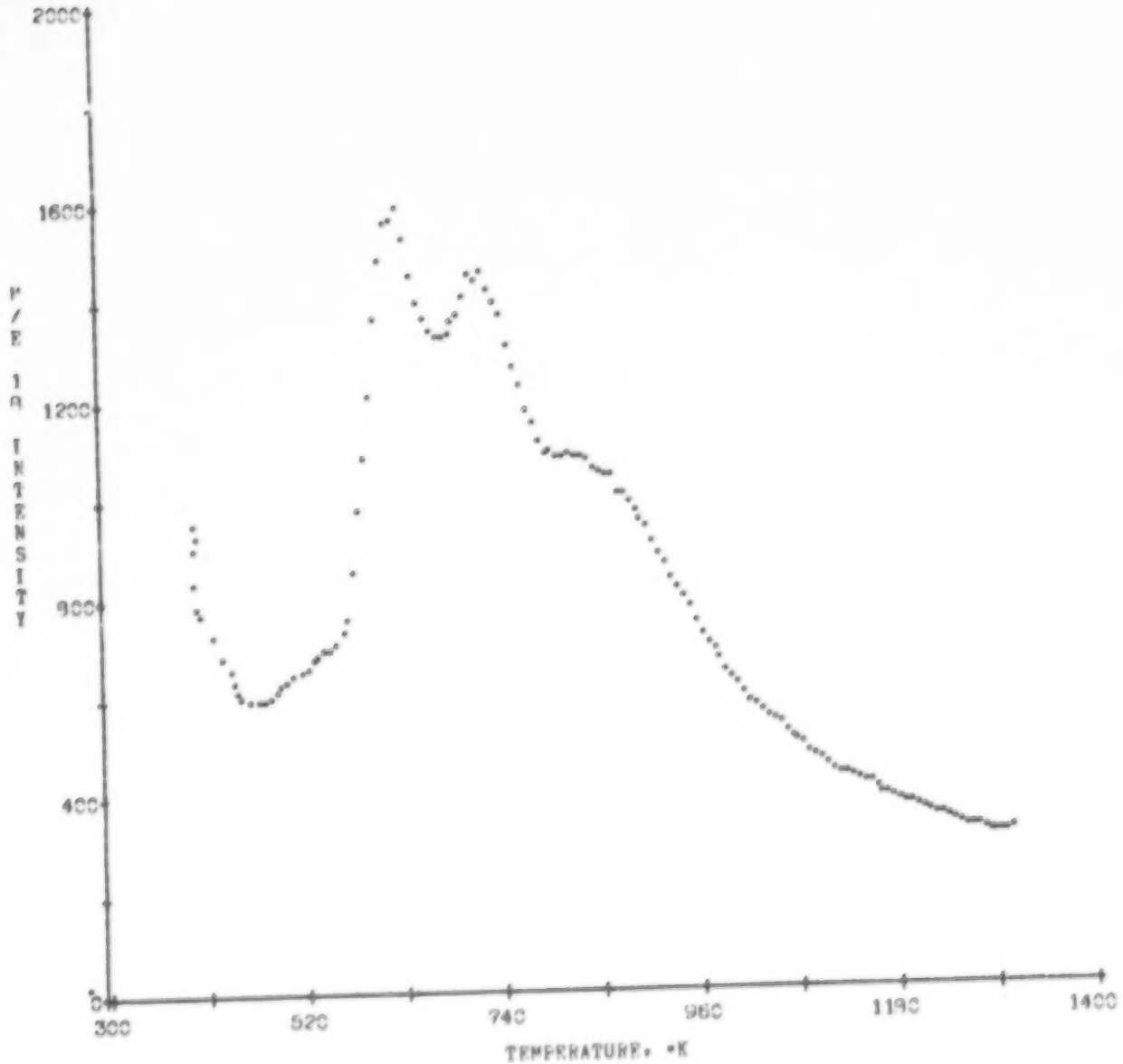

SYMBOL NO.PTS. LEGEND
. 141 9204 FROM SKI COAL #5, AR AT 200 CC/MIN, 30°/MIN

Figure 50

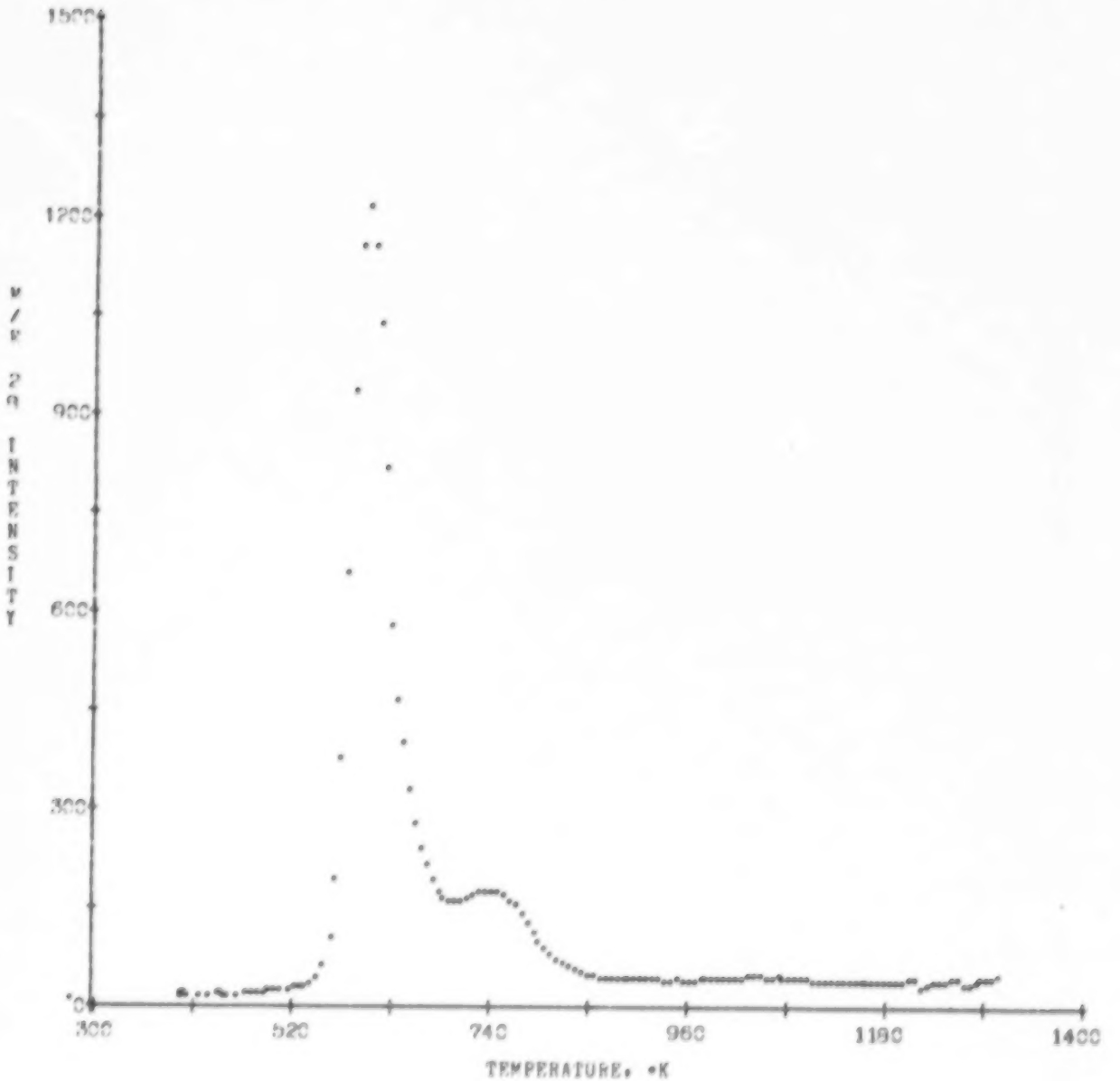

SYMBOL NO.PTS. LEGEND
• 141 CO+ FROM SRI COAL #5, AR AT 200 CC/MIN, 30%/MIN

Figure 51

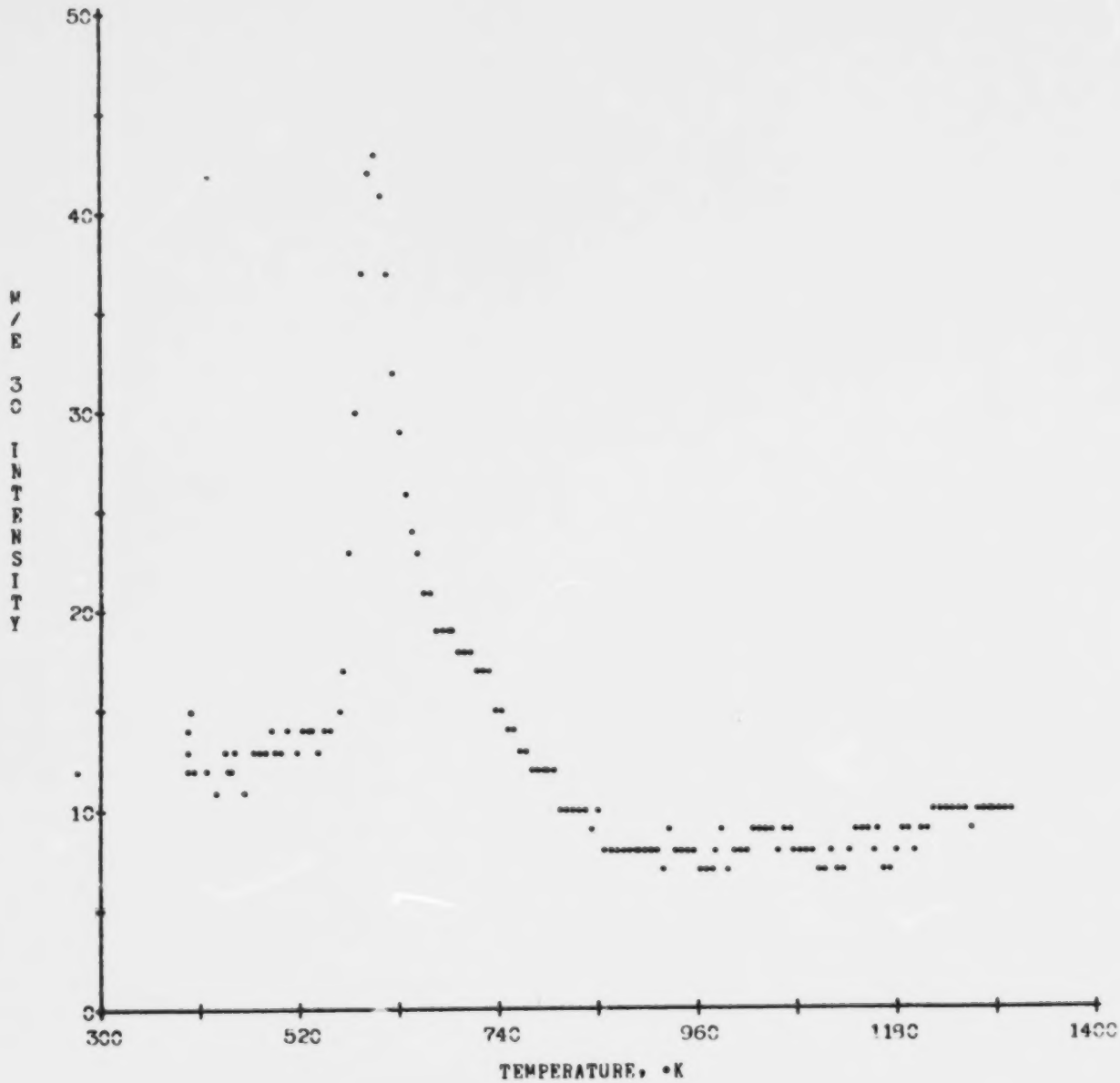

SYMBOL	NO•PTS•	LEGEND
•	141	NO+ FROM SRI COAL #5, AR AT 200 CC/MIN, 30•/MIN

Figure 52

R224F.DAT

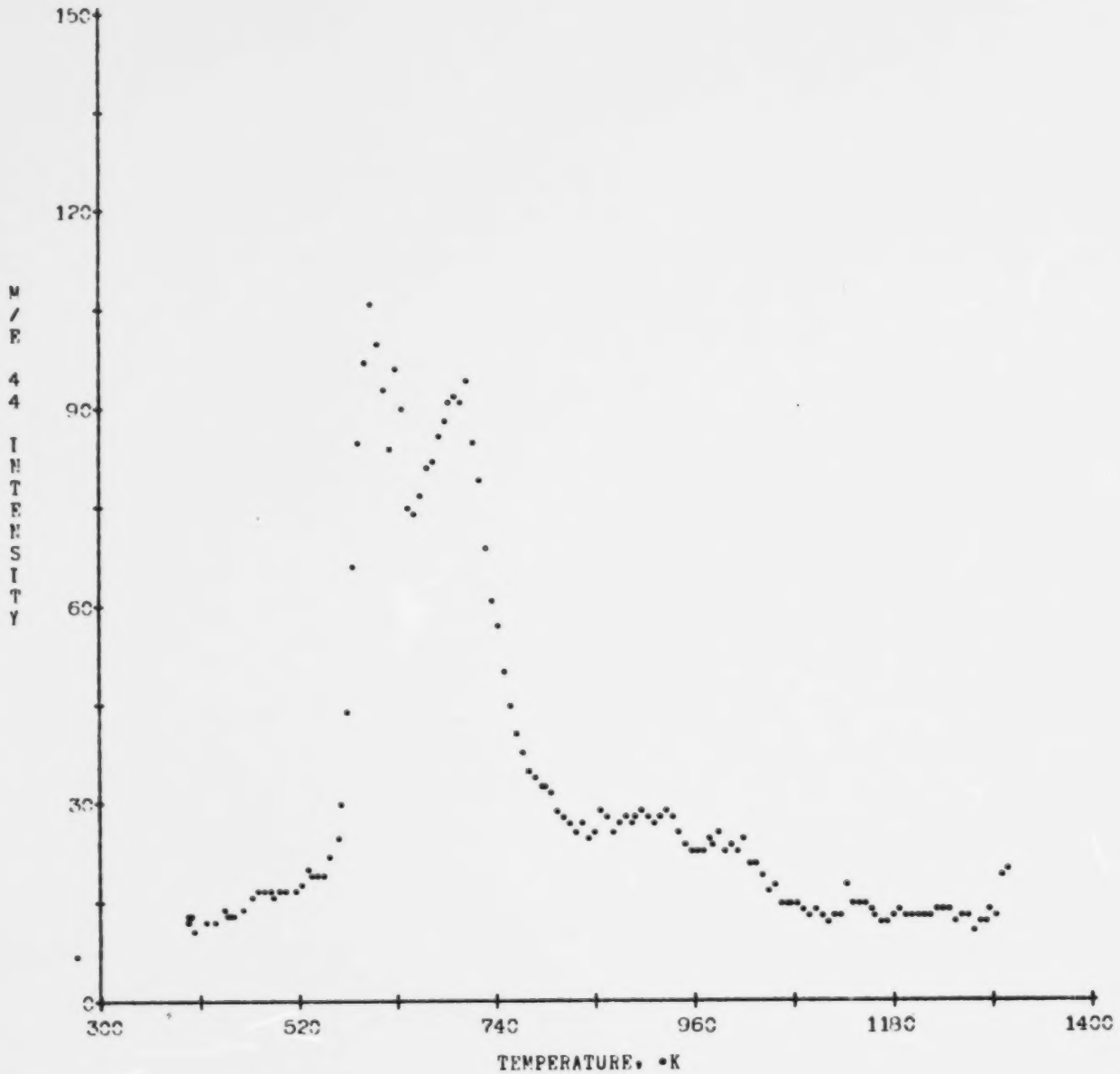

SYMBOL	NO.PTS.	LEGEND
.	141	CO2+ FROM SRI COAL #5, AR AT 200 CC/MIN, 30°/MIN

Figure 53

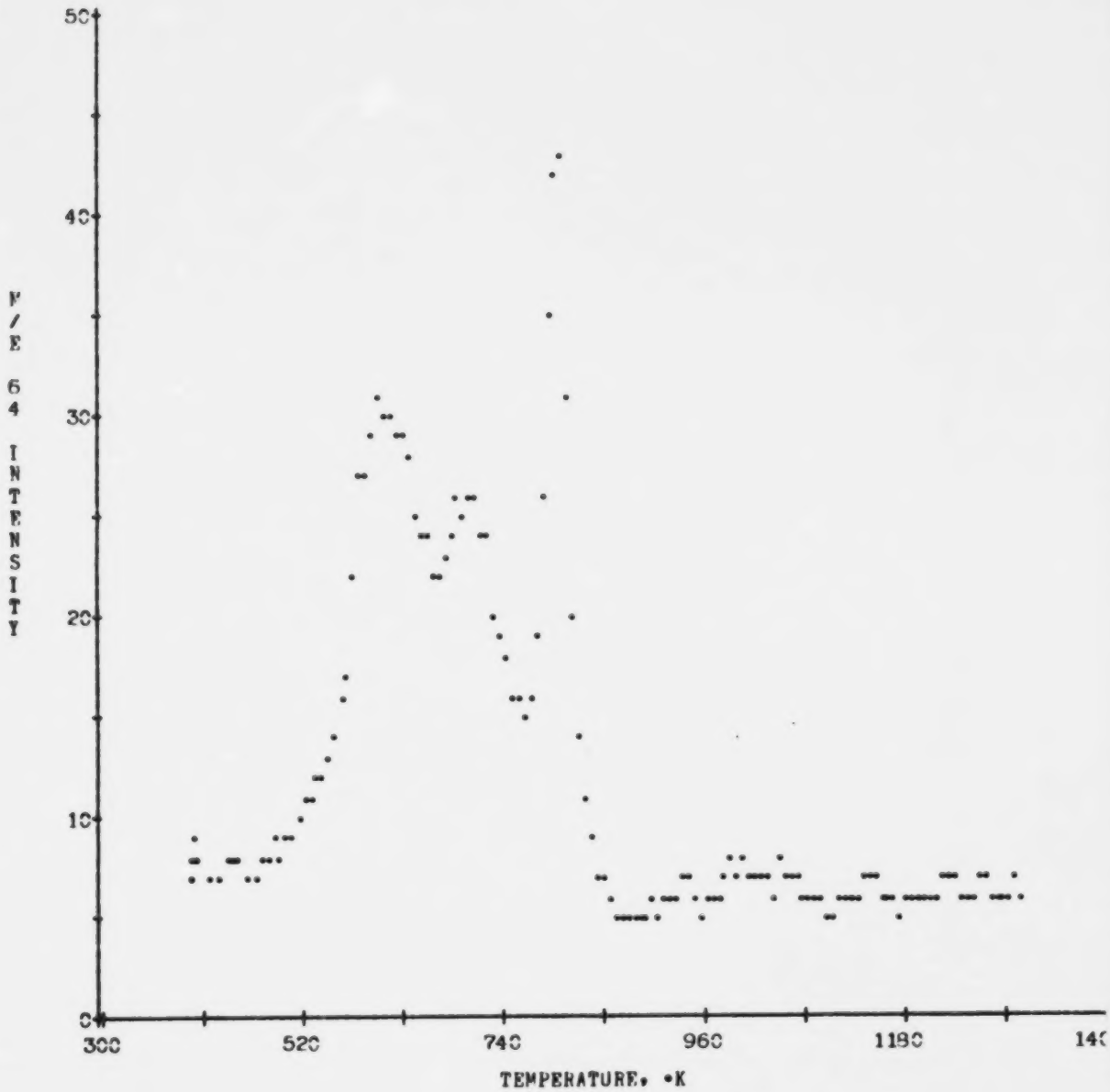

SYMBOL	NO.PTS.	LEGEND
.	140	SO2+ FROM SRI COAL #5, AR AT 200 CC/MIN, 30°/MIN

Figure 54

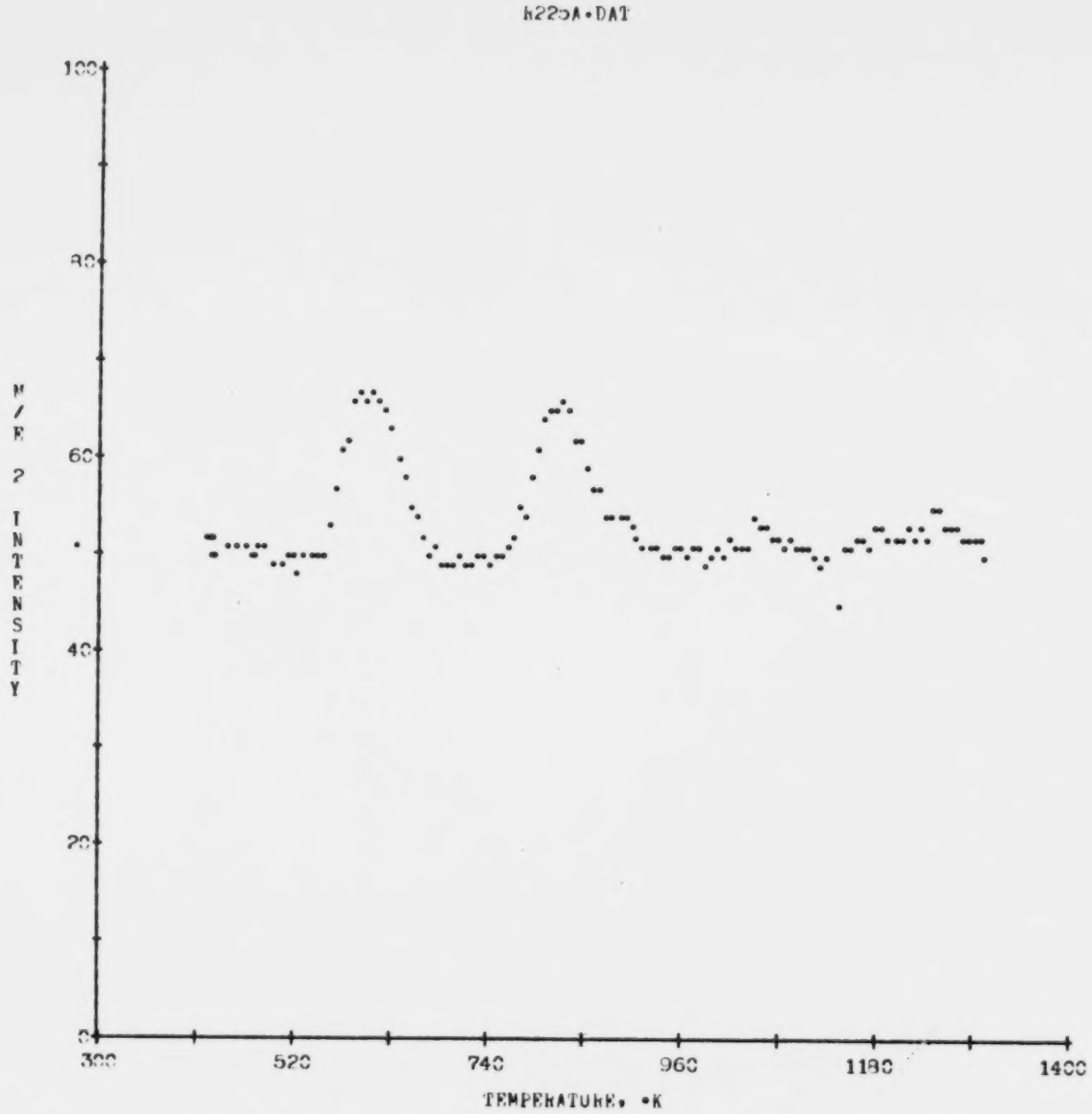

SYMPOL NO.PTS. LEGEND

• 132 H2+ FROM SRI COAL #7, AR AT 200 CC/MIN, 30°/MIN

Figure 55

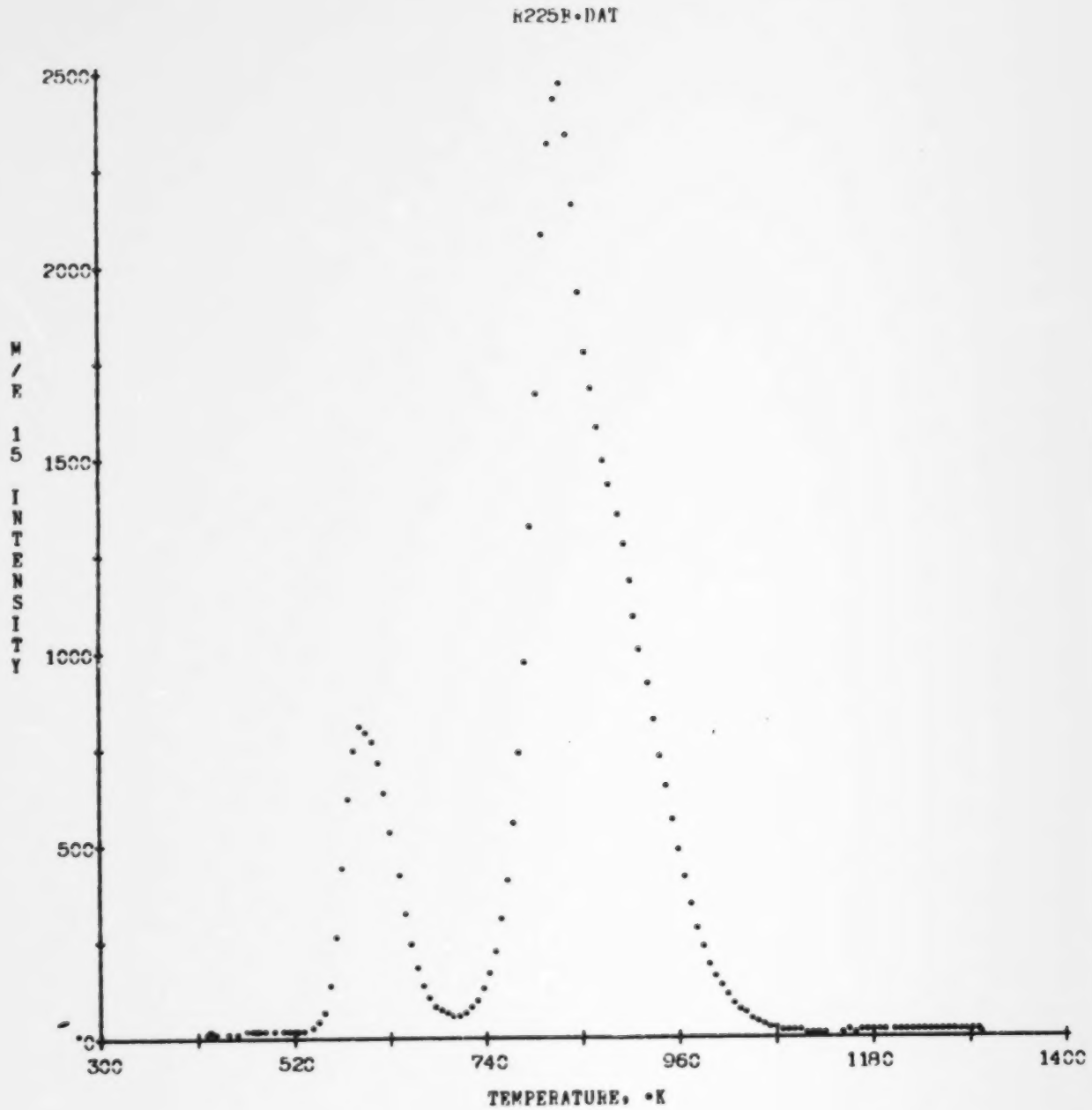

SYMBOL	NO•PTS•	LEGEND
•	130	CH3+ FROM SHI COAL #7, AR AT 200 CC/MIN, 30•/MIN

Figure 56

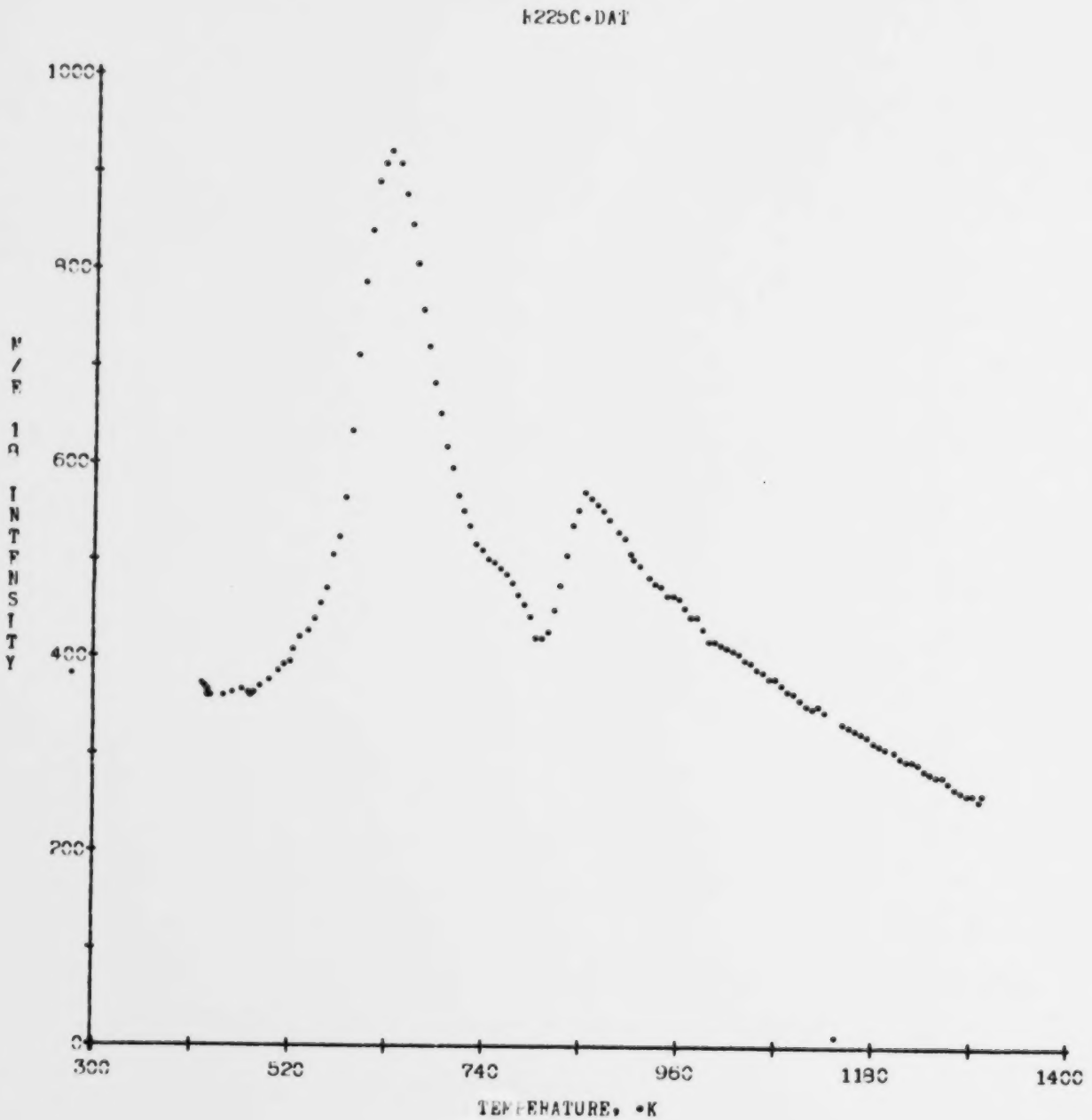

SYMBOL NO.PTS. LEGEND

. 131 H2O+ FROM SRI COAL #7, AR AT 200 CC/MIN, 30°/MIN

Figure 57

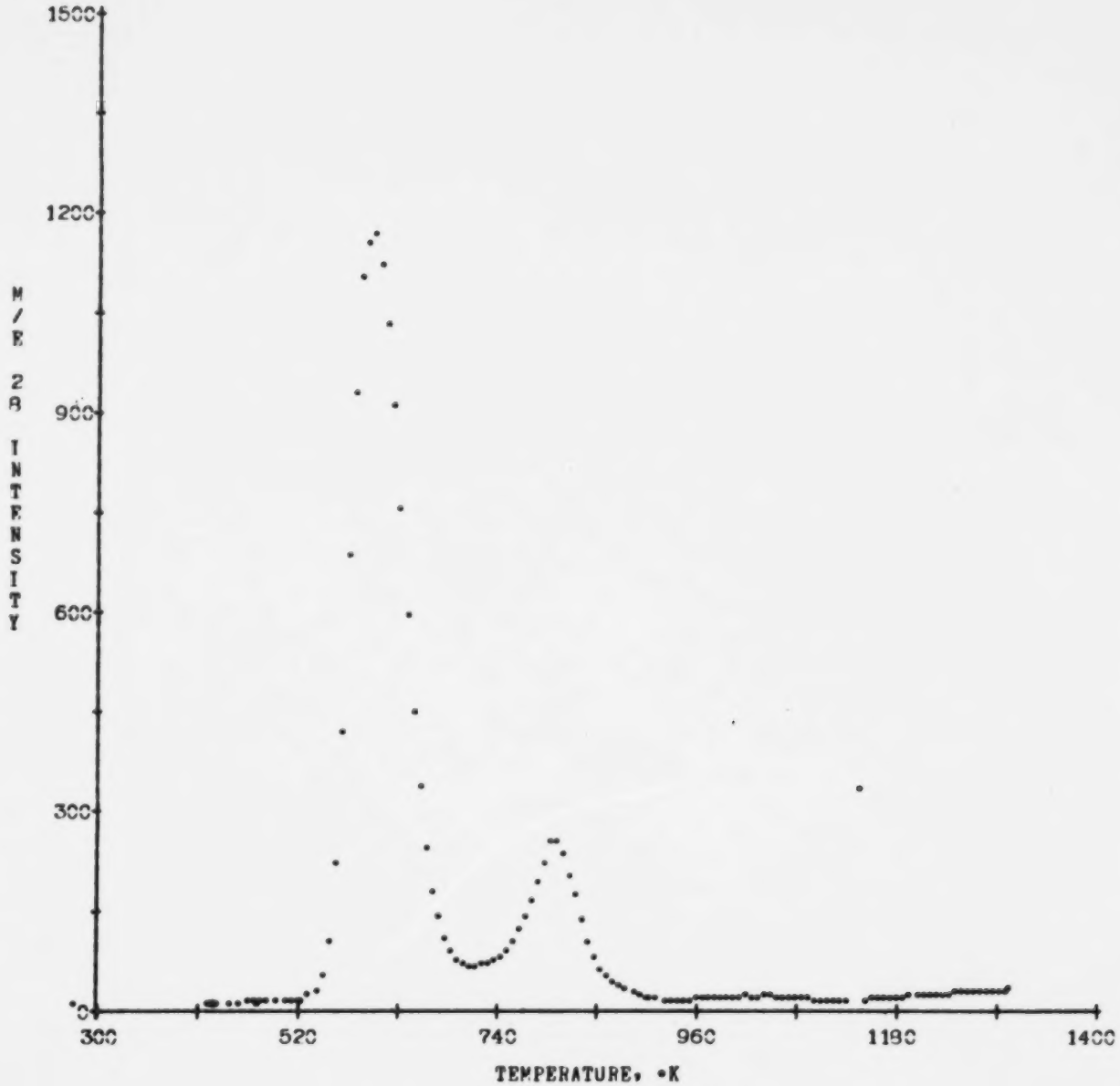

SYMBOL	NO.PTS.	LEGEND
•	131	CO+ FROM SRI COAL #7, AR AT 200 CC/MIN, 30°/MIN

Figure 58

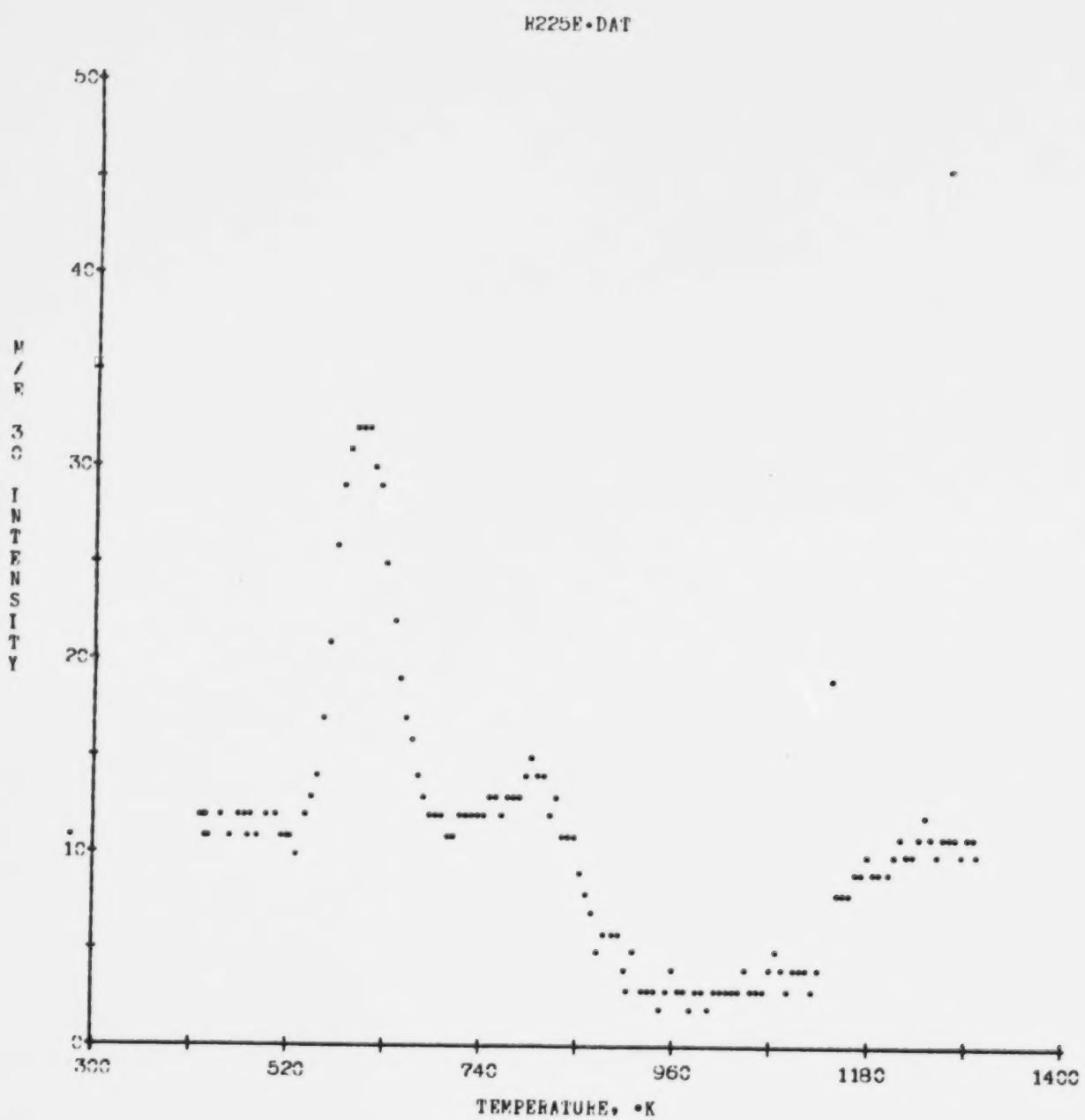

SYMBOL NO.PTS. LEGEND

. 131 NO+ FROM SRI COAL #7, AR AT 200 CC/MIN, 30°/MIN

Figure 59

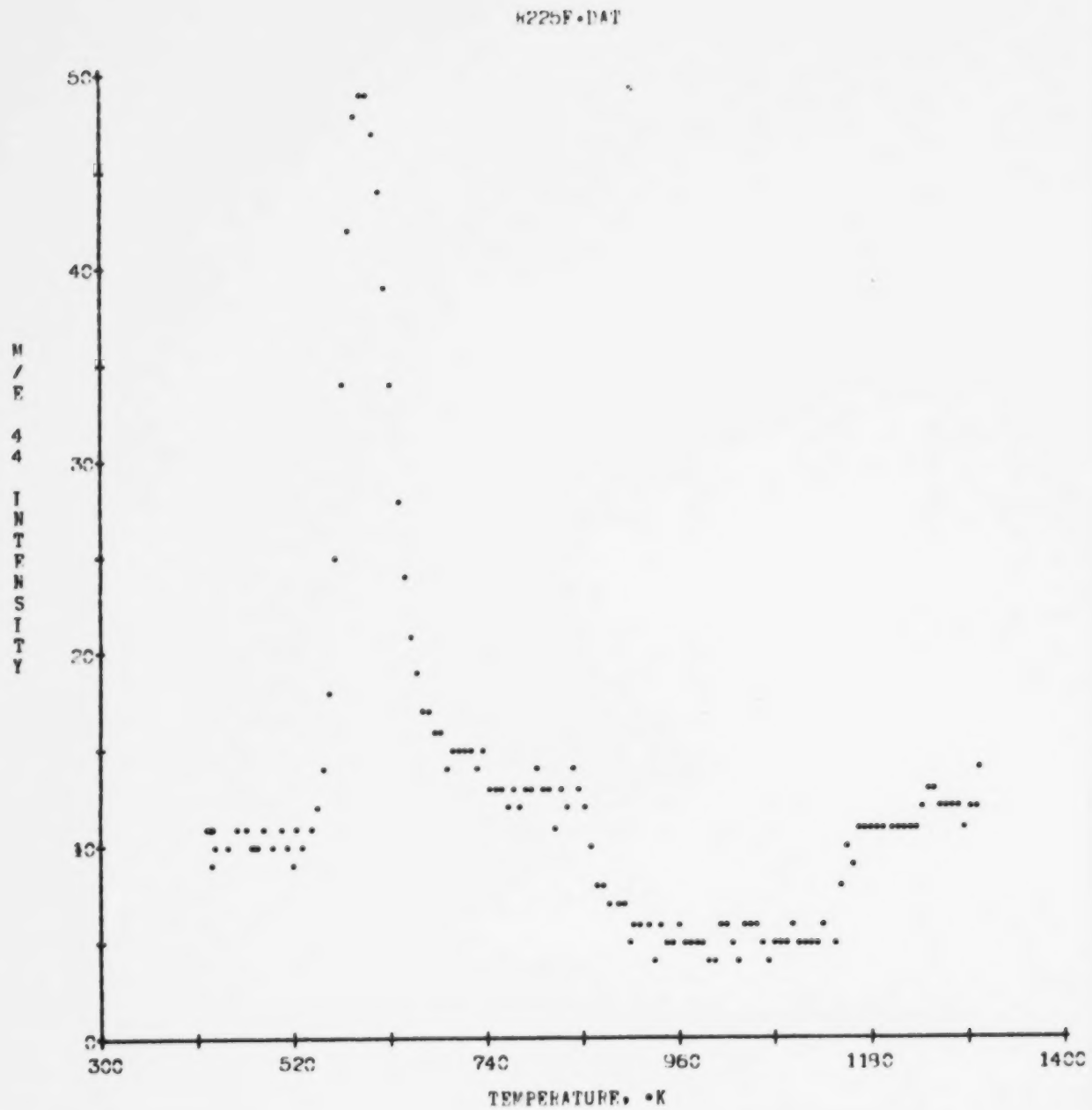

SYMPOL NO.PTS. LEGEND

. 131 CO2+ FROM SRI COAL #7, AR AT 200 CC/MIN, 30°/MIN

Figure 60

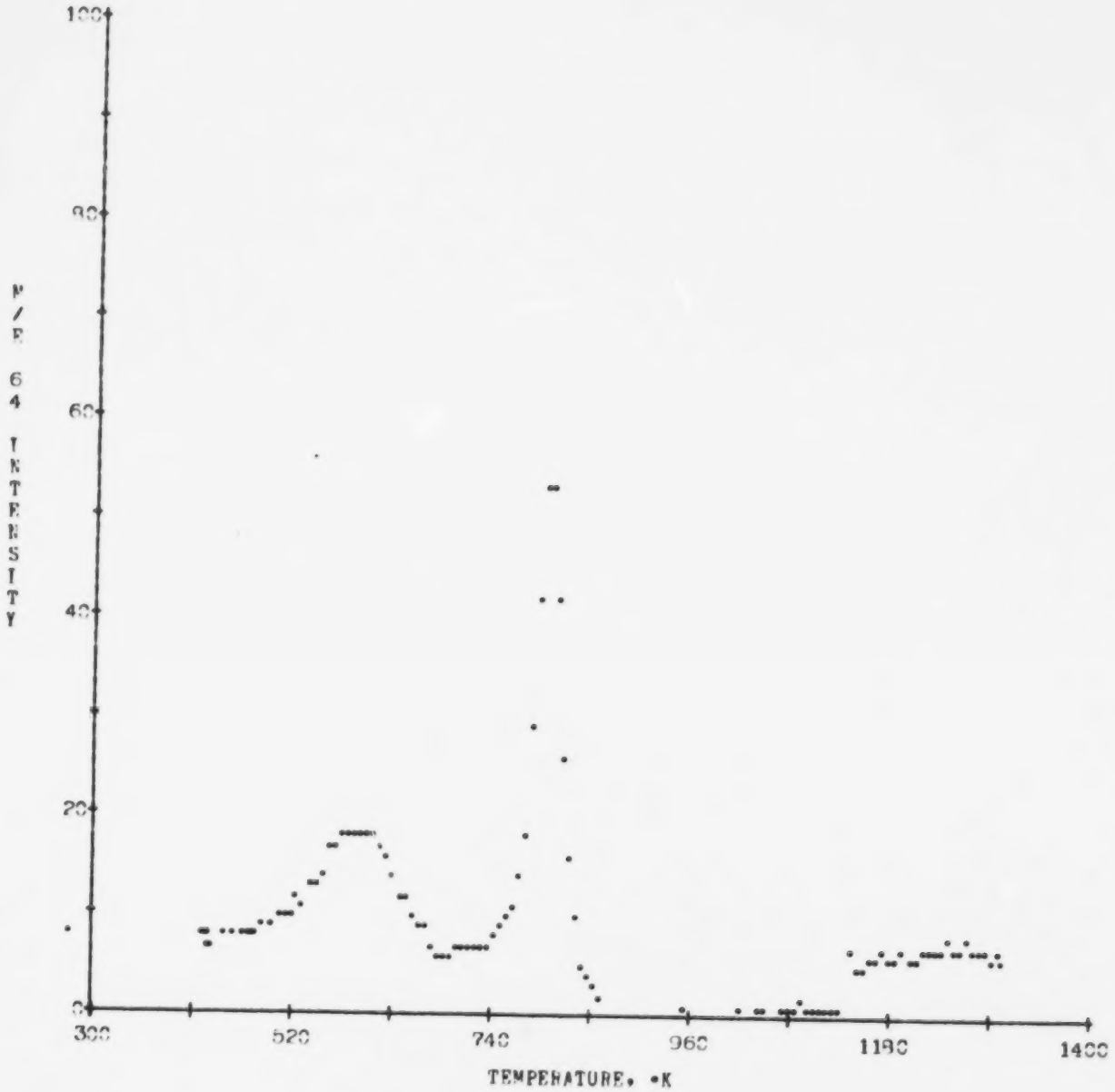

SYMBOL NO.PTS. LEGEND

• 107 SO2+ FROM SEI COAL #7, AR AT 200 CC/MIN, 30°/MIN

Figure 61

H226A.DAT

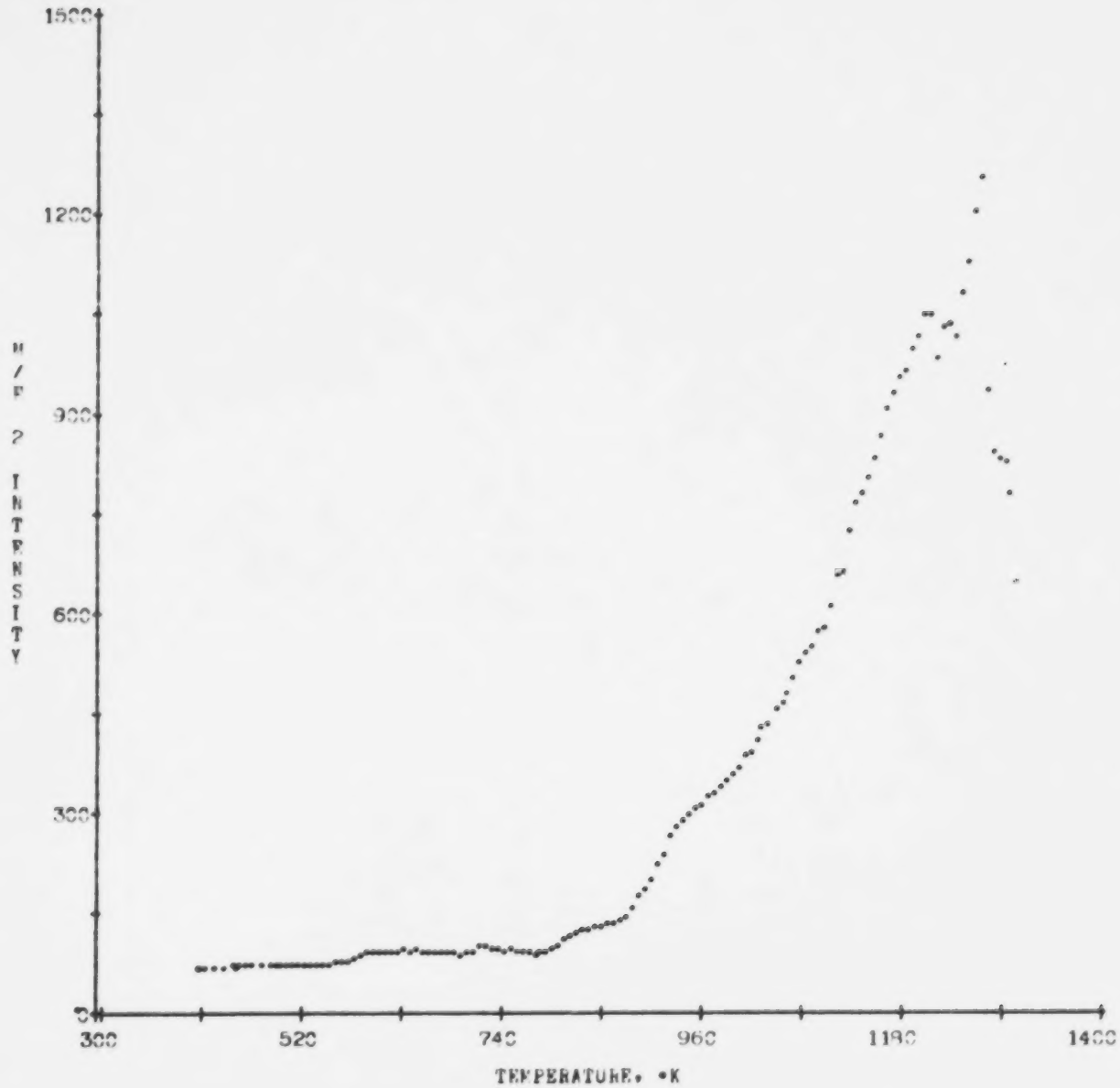

SYMBOL	NO.PTS.	LEGEND
.	136	H24 FROM SBI COAL #10 AR AT 200 CC/MIN, 30°/MIN

Figure 62

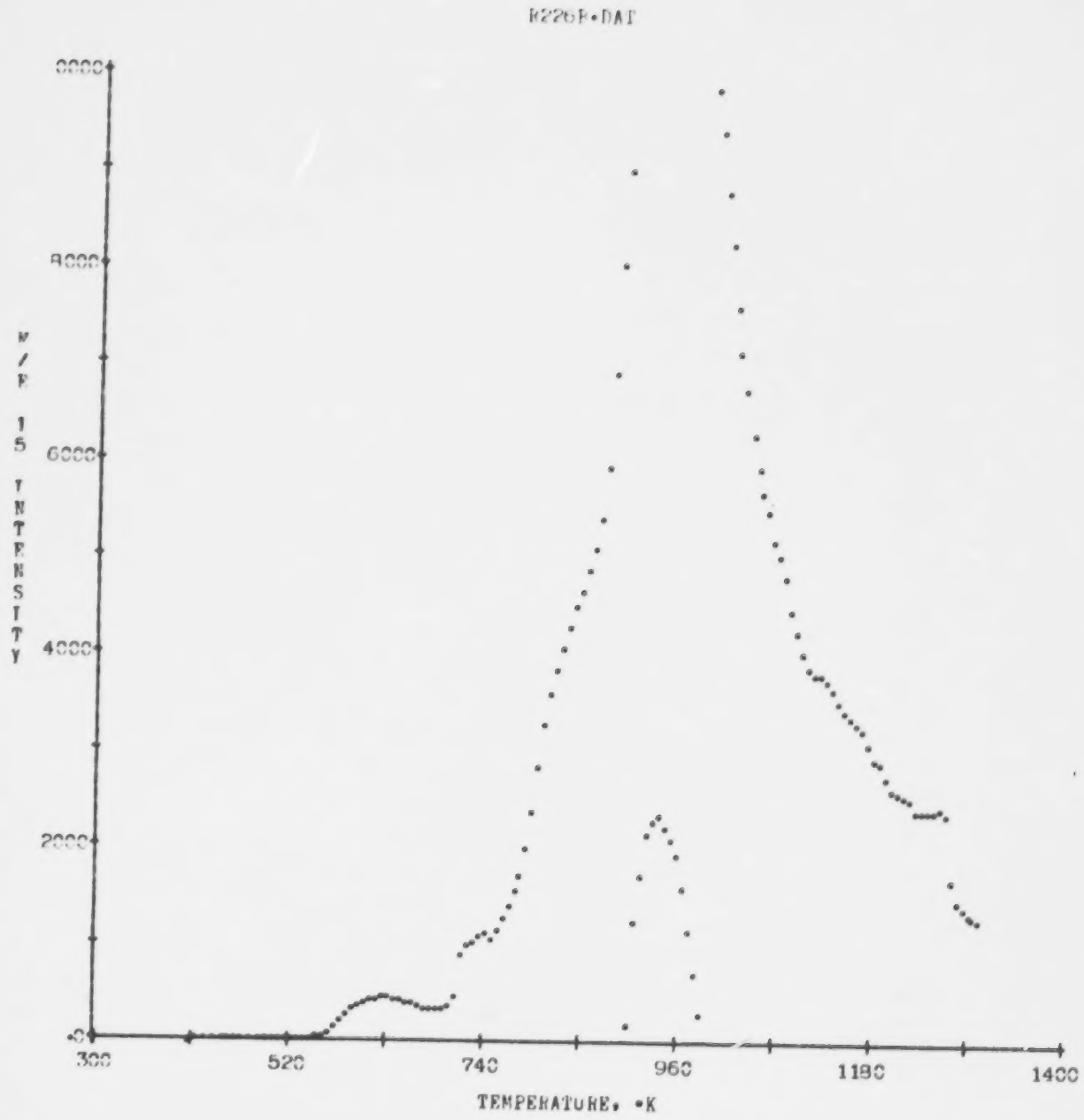

SYMBOL NO.PTS. LEGEND

• 136 CH3+ FROM SHI COAL #10, AR AT 200 CC/MIN 30°/MIN

Figure 63

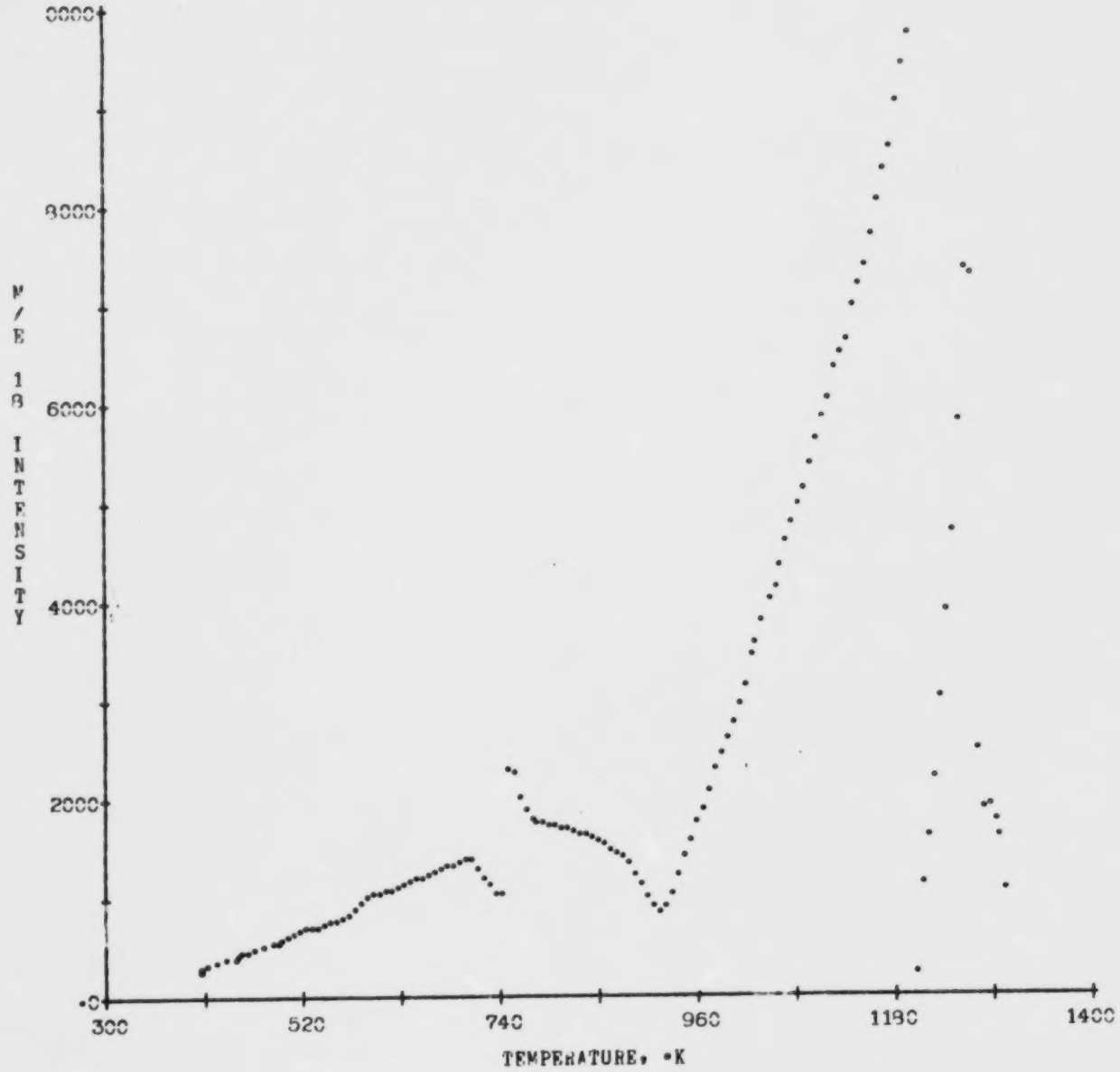

SYMBOL	NO.PTS.	LEGEND
.	136	H2O+ FROM SHI COAL #10, AR AT 200 CC/MIN, 30°/MIN

Figure 64

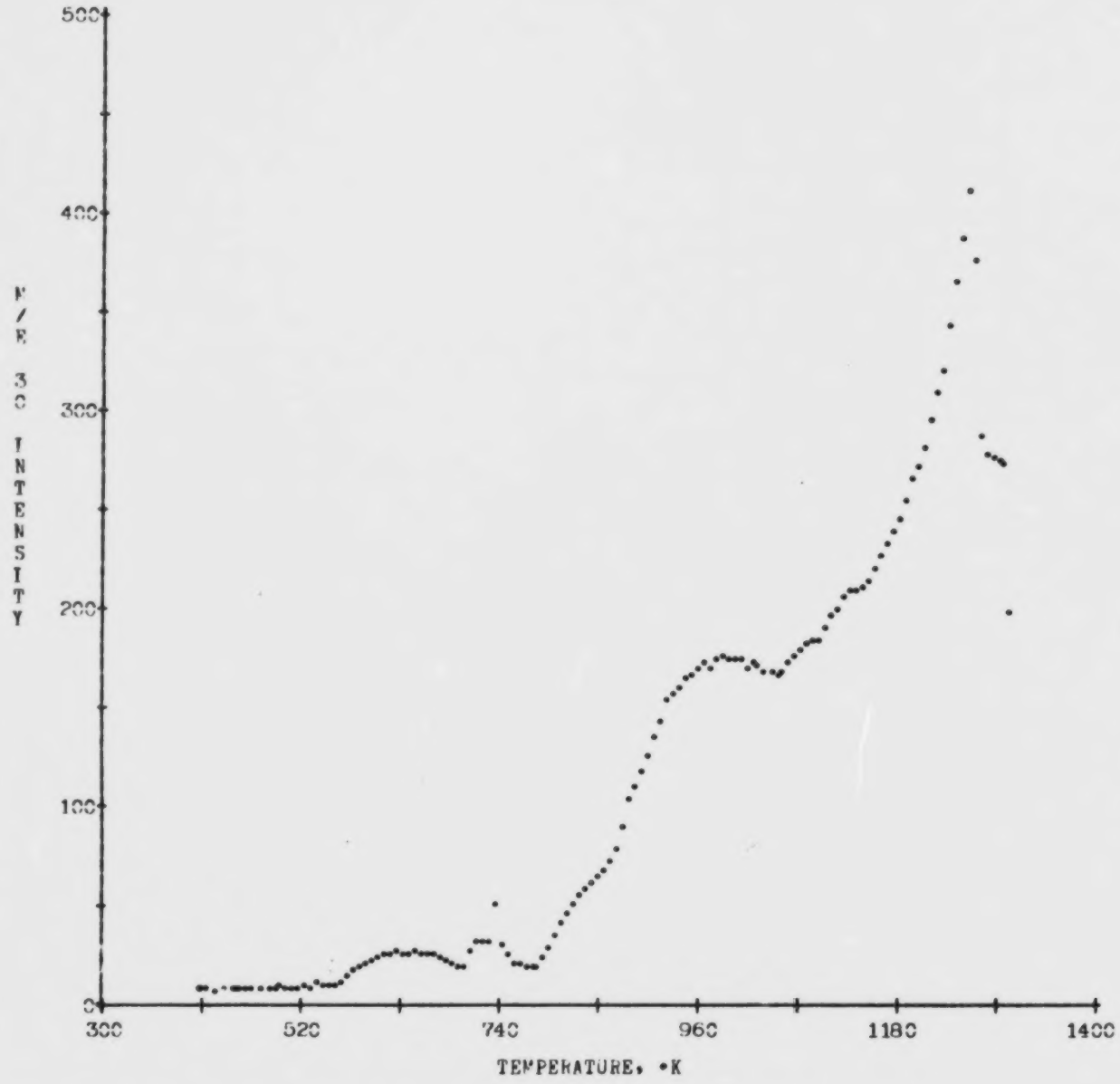

SYMBOL NO.PTS. LEGEND
• 135 NO+ FROM SRI COAL #10, AR AT 200 CC/MIN, 30°/MIN

Figure 65

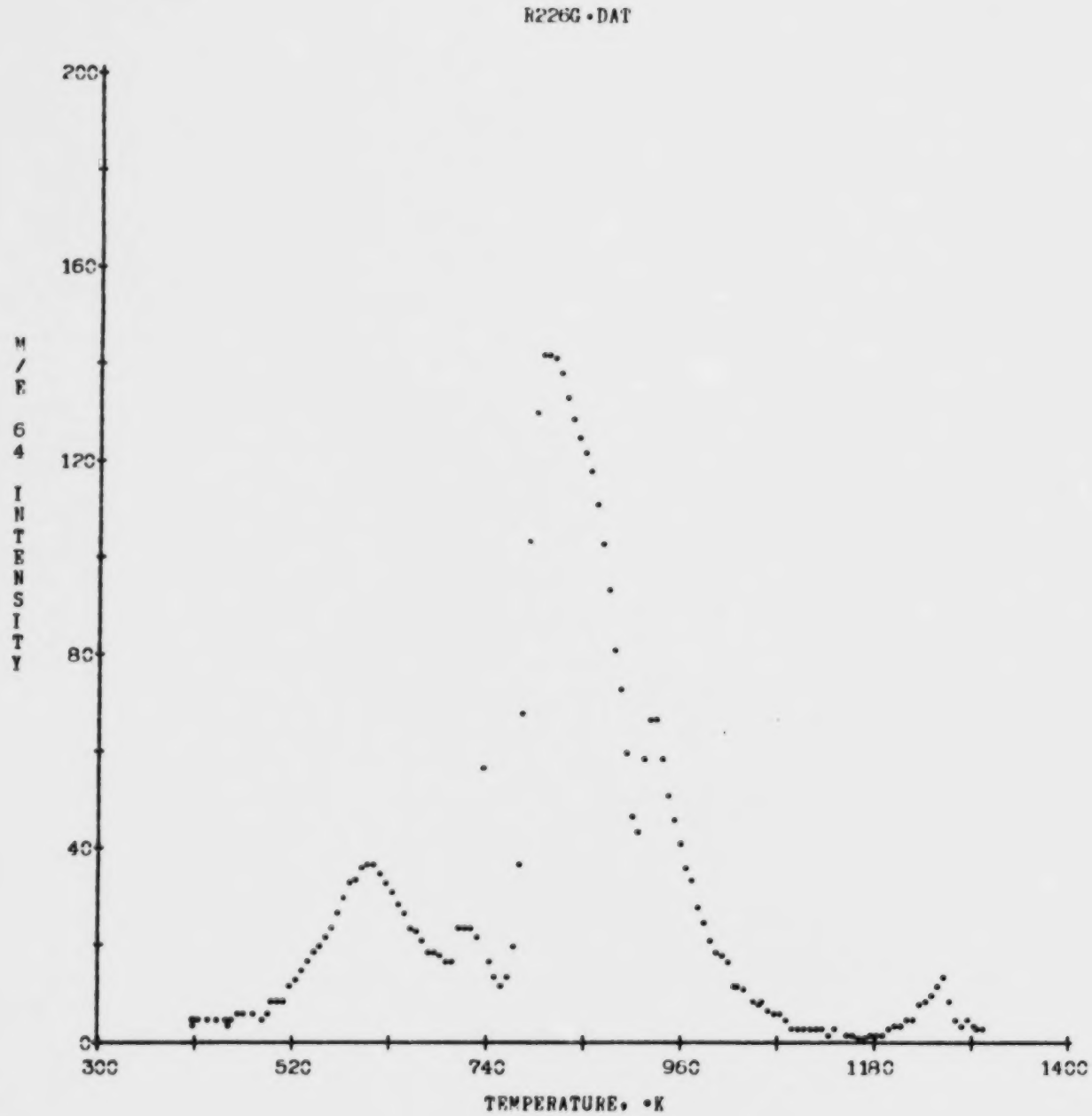

SYMBOL NO.PTS. LEGEND

. 134 SO2+ FROM SRI COAL #10, AR AT 200 CC/MIN, 30G/MIN

Figure 66

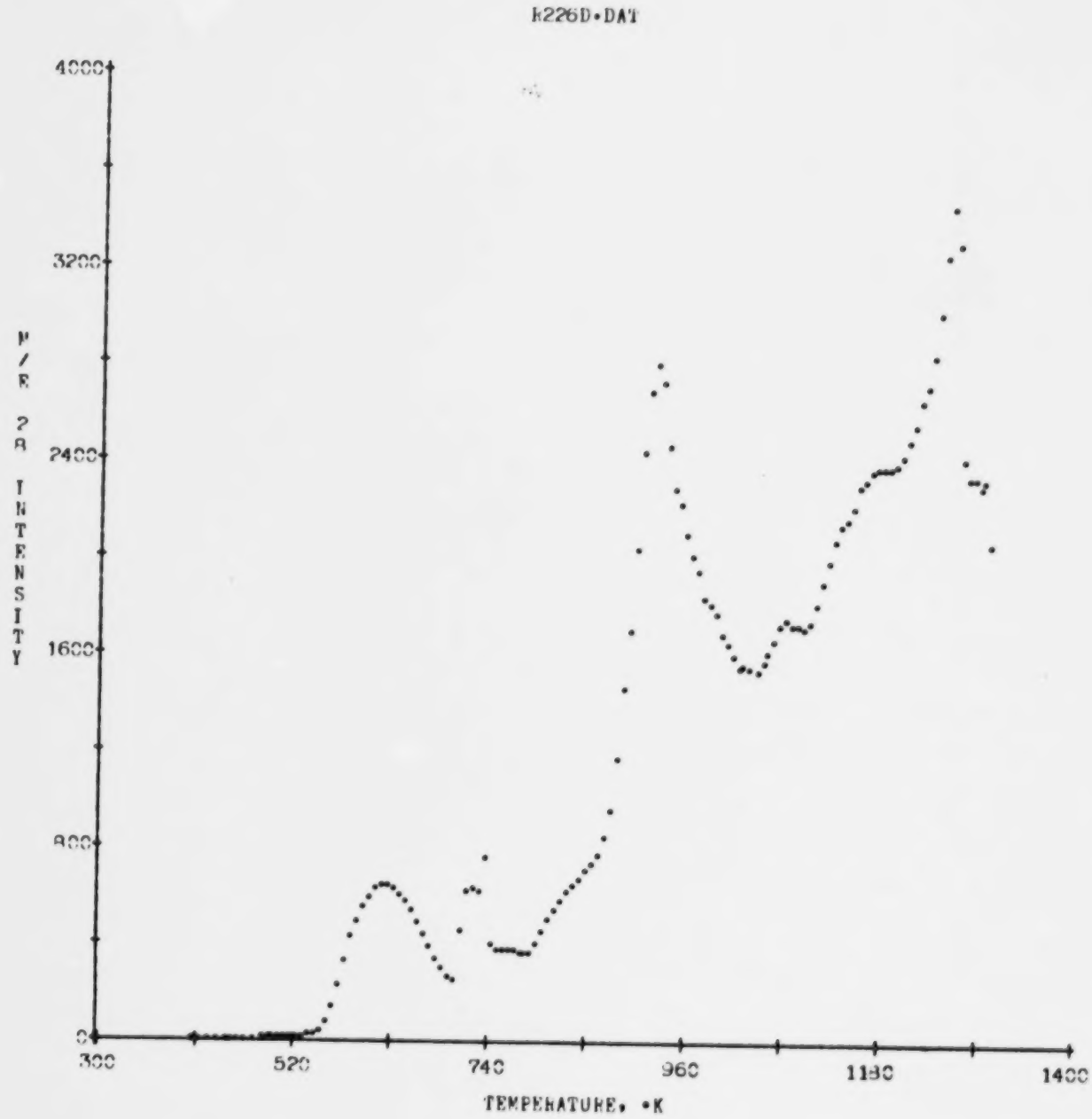

SYMBOL NO.PTS. LEGEND

. 135 CO+ FROM SRI COAL #10, AR AT 200 CC/MIN, 30C/MIN

Figure 67

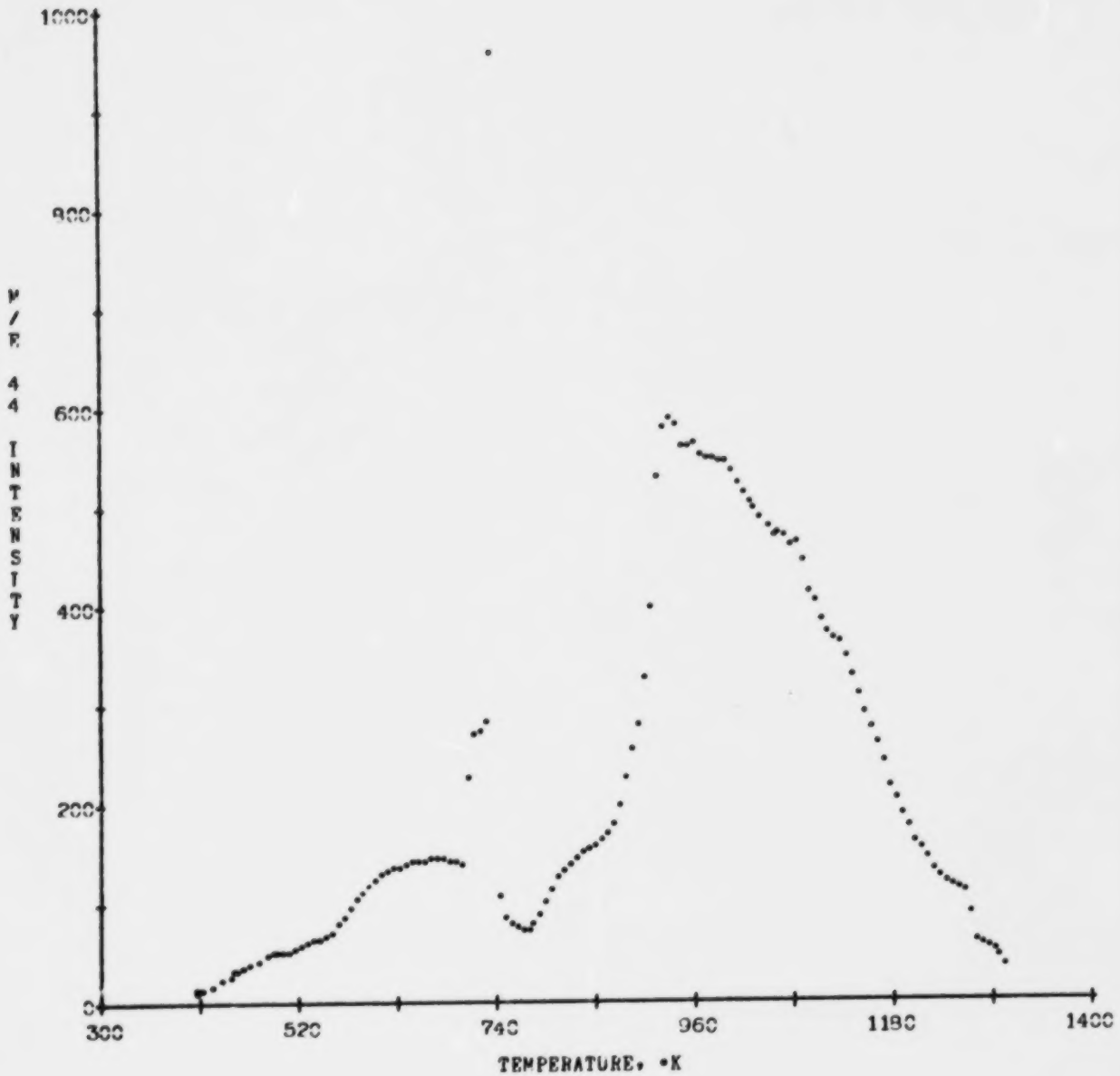

SYMBOL	NO.PTS.	LEGEND
.	135	CO2+ FROM SHI COAL #10, AR AT 200 CC/MIN, 30°/MIN

Figure 68

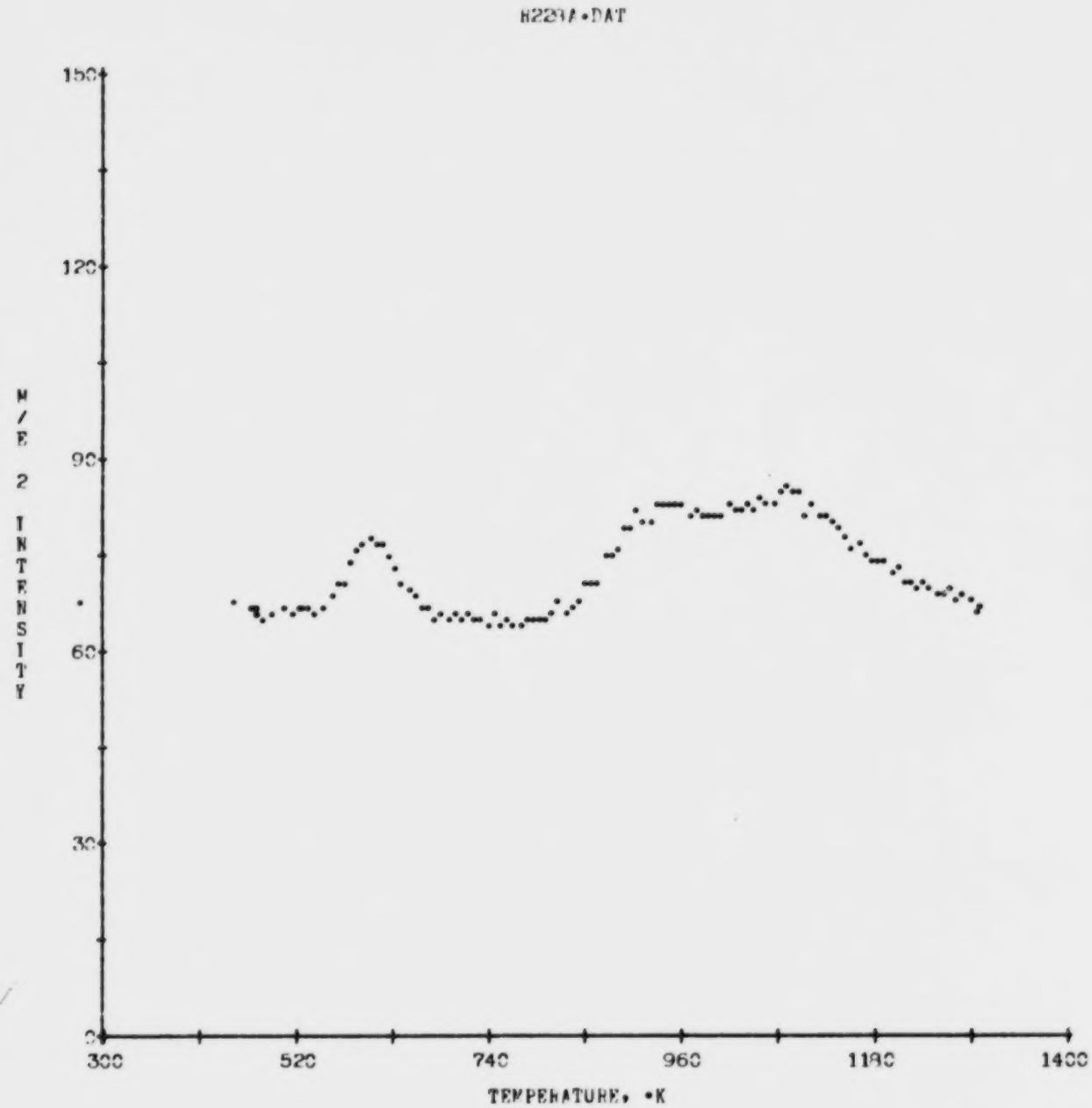

SYMBOL	NO.PTS.	LEGEND
.	119	H2+ FROM SKI ANTHRACITE, AR AT 200 CC/MIN, 30°/MIN

Figure 69

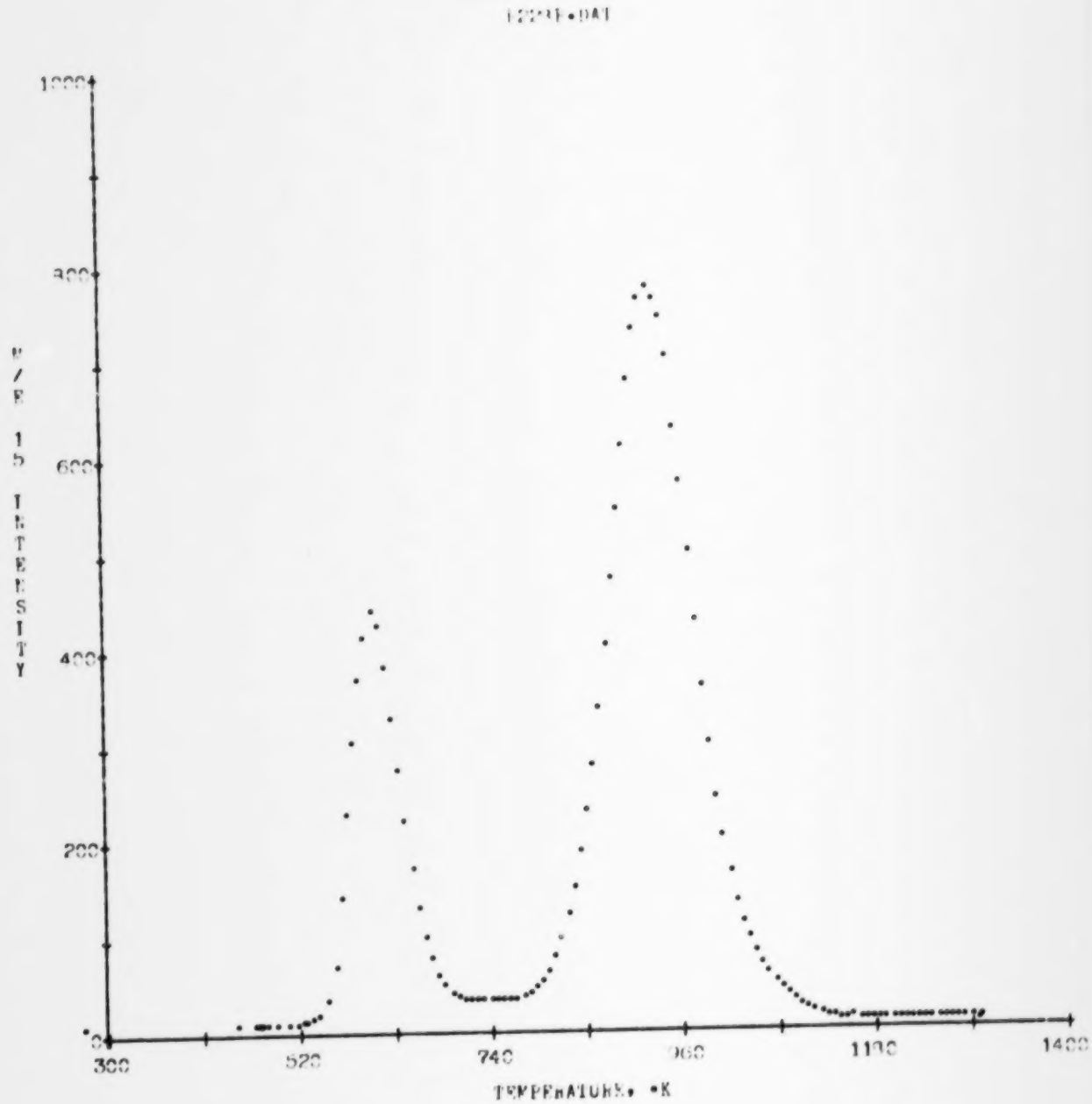

SYMBOL NO.PTS. LEGEND
. 119 CM34 FROM SHI ANTHRACITE, AF AT 200 CC/MIL, 30°/MIL

Figure 70

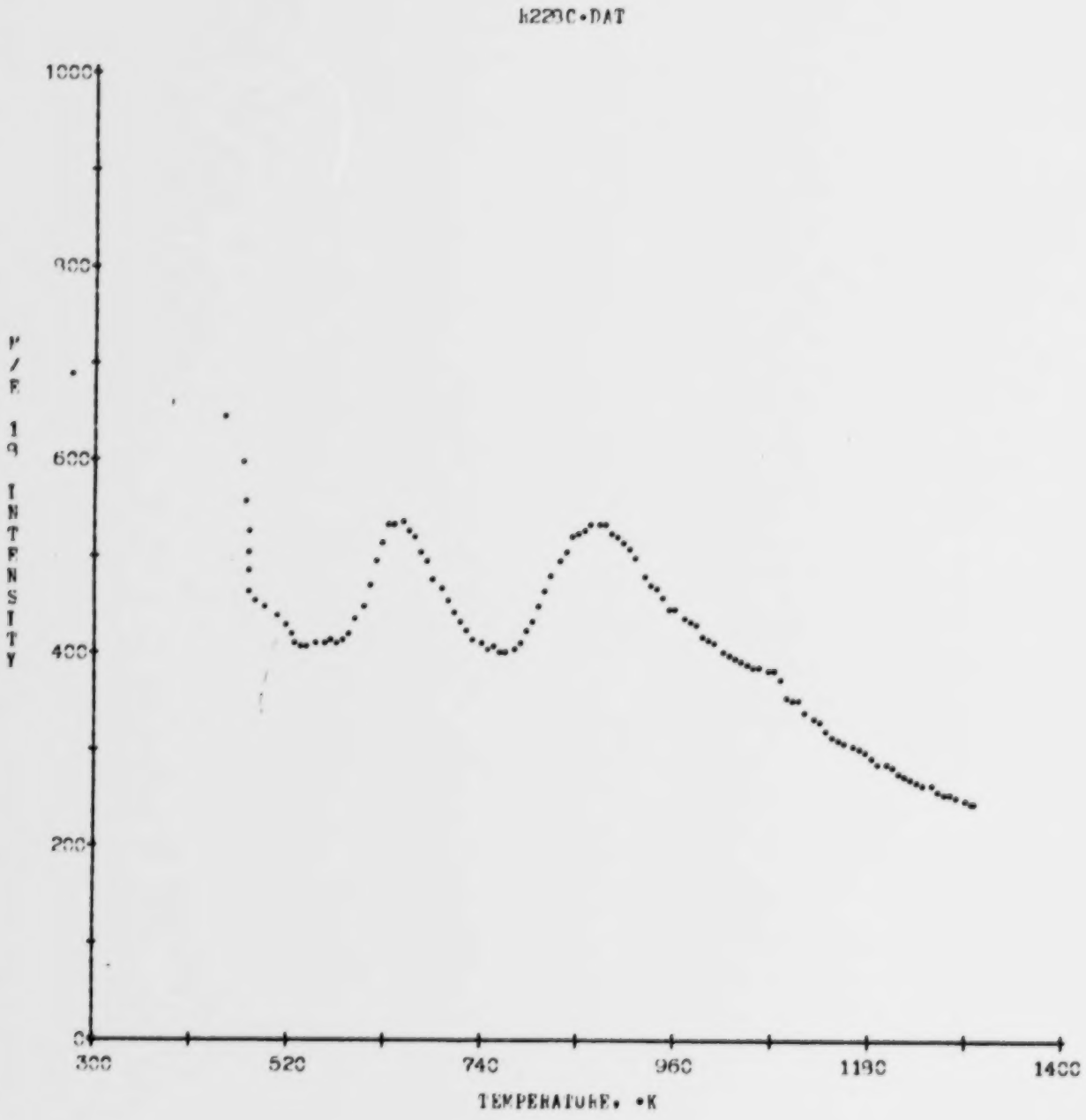

SYMBOL	NO.PTS.	LEGEND
•	119	H20+ FROM SMI ANTHRACITE, AR AT 200 CC/MIN, 30°/MIN

Figure 71

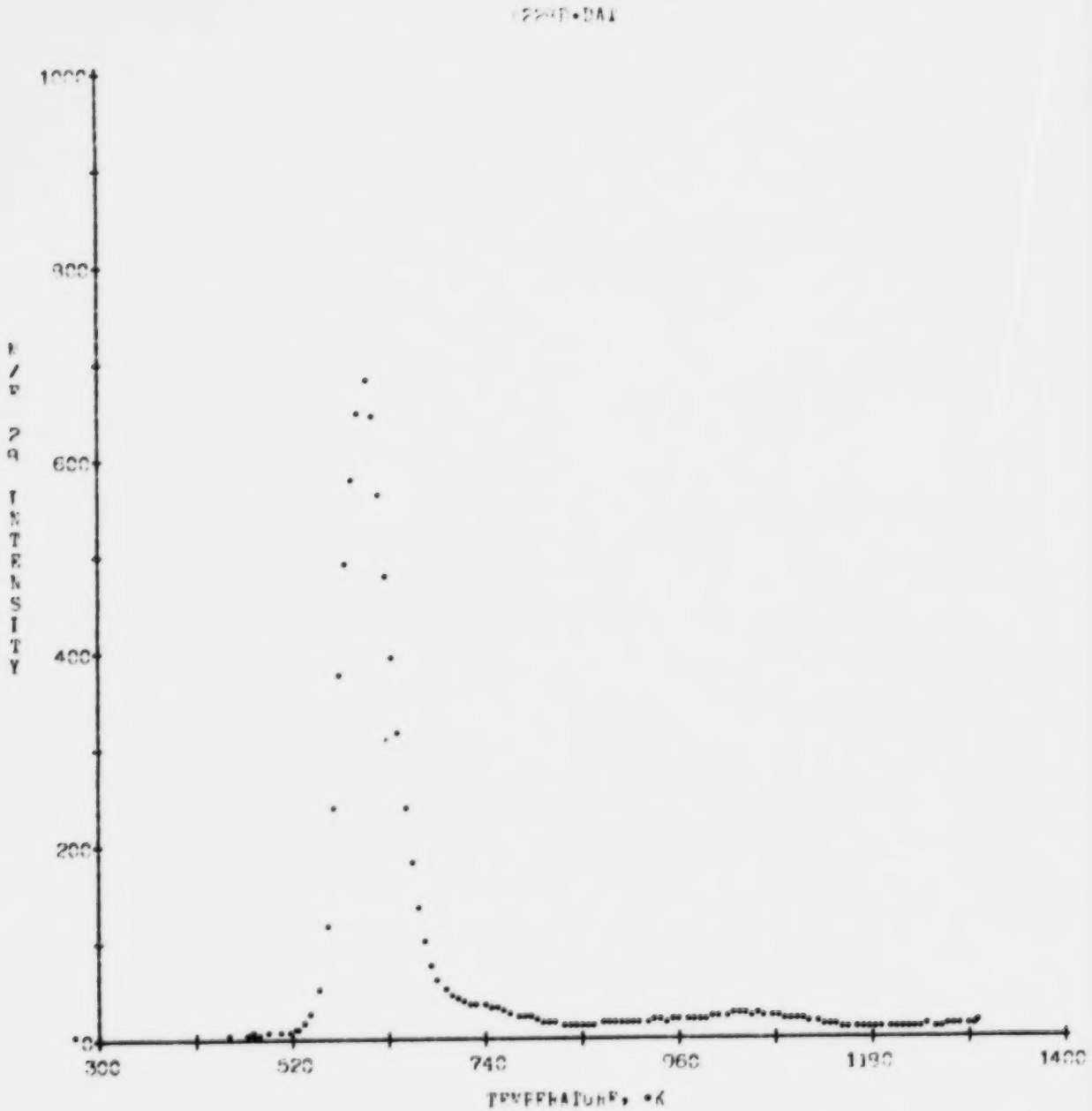

SYMBOL M/E/S LEGEND

• 113 CO+ FROM SAT ALKYLBENZENE, AT AT 200 CC/MIL, 30°/MIN

Figure 72

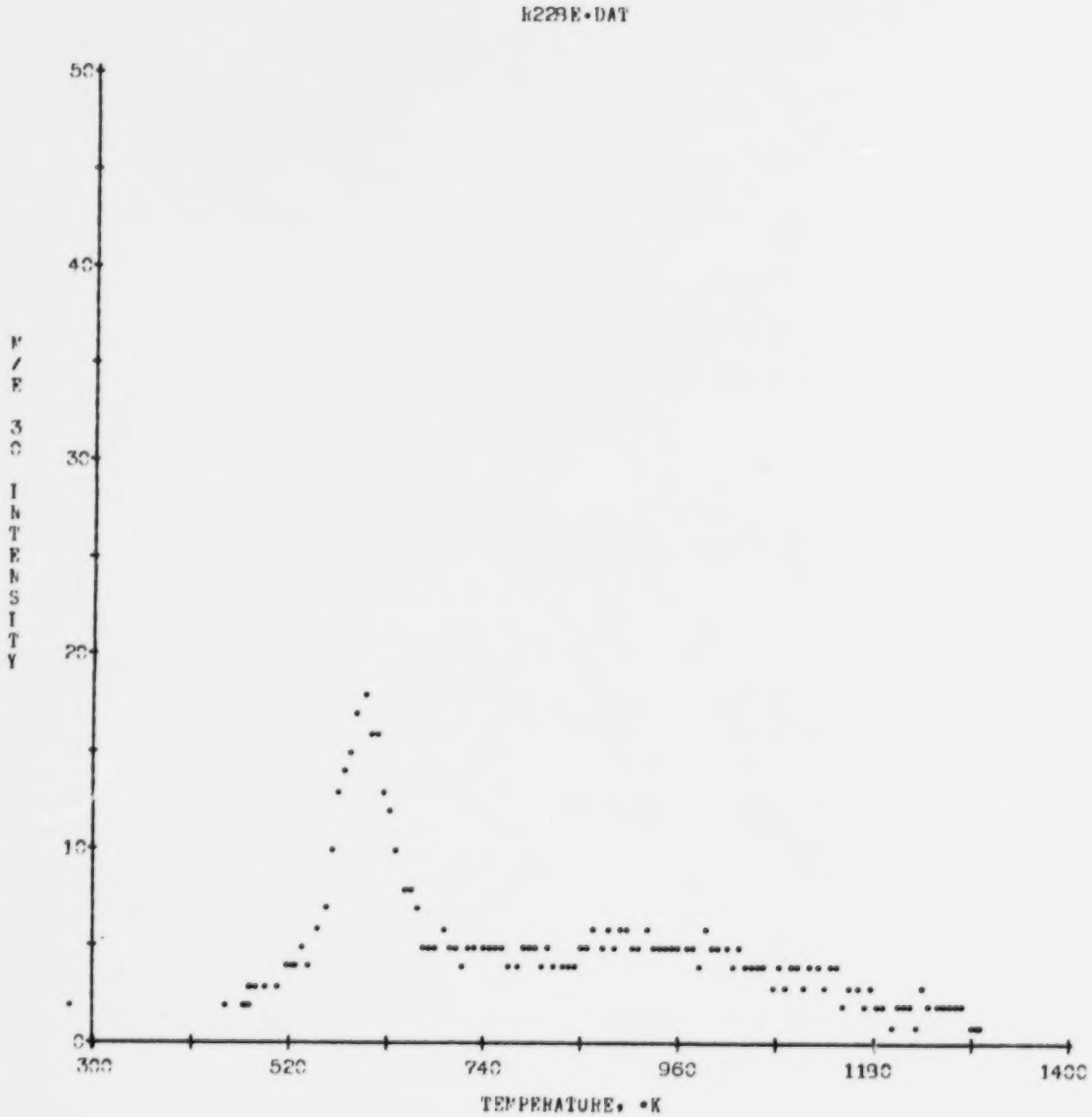

SYMBOL	NO.PTS.	LEGEND
•	119	NO+ FROM SMI ANTHRACITE, AR AT 200 CC/MIN, 30°/MIN

Figure 73

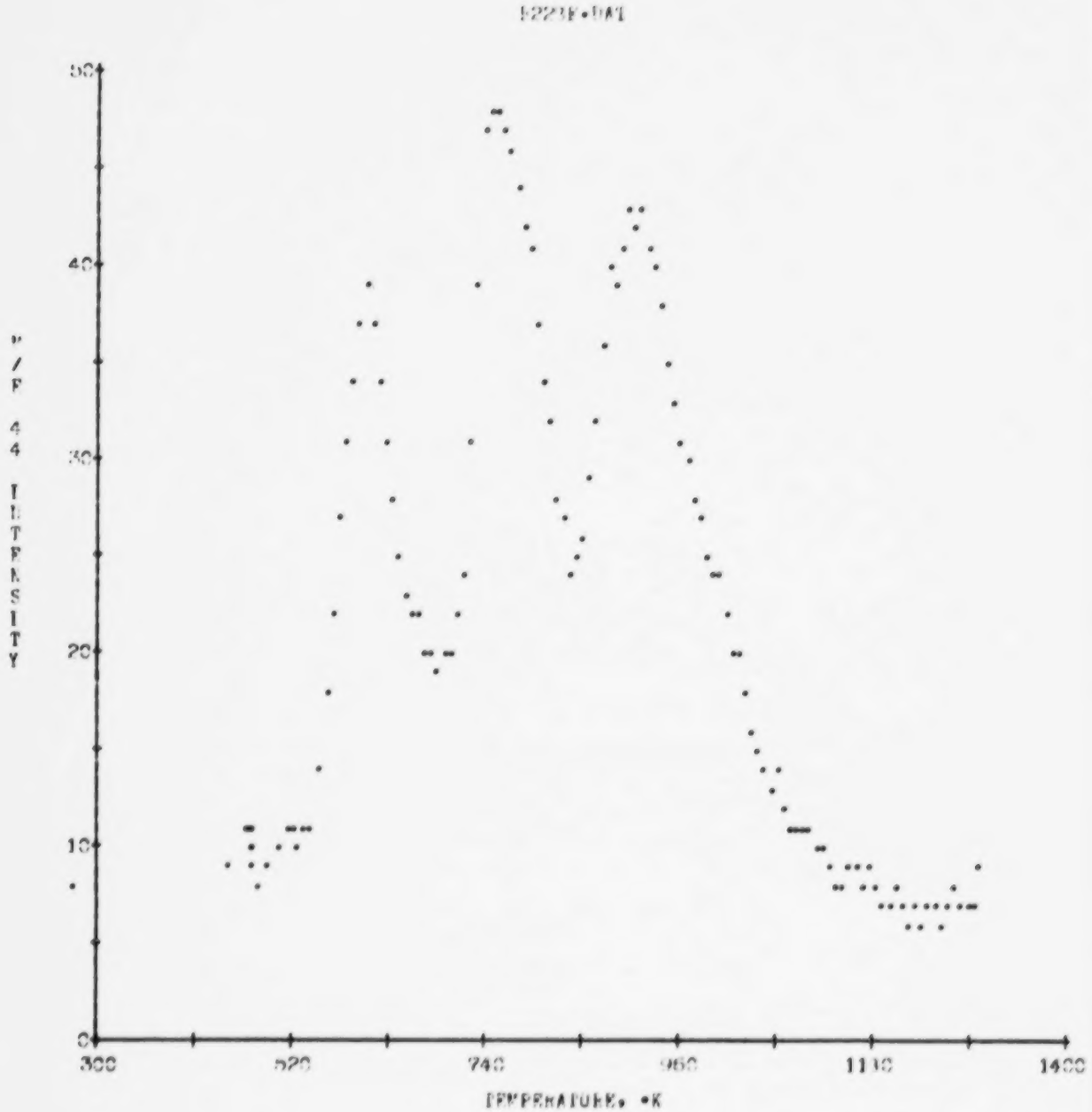

SYMBOL NO.PTS. LEGEND

• 119 CO2+ FROM SIT ALIPHACTIC, Ar AT 200 CC/MIN, 30°/MIN

Figure 74

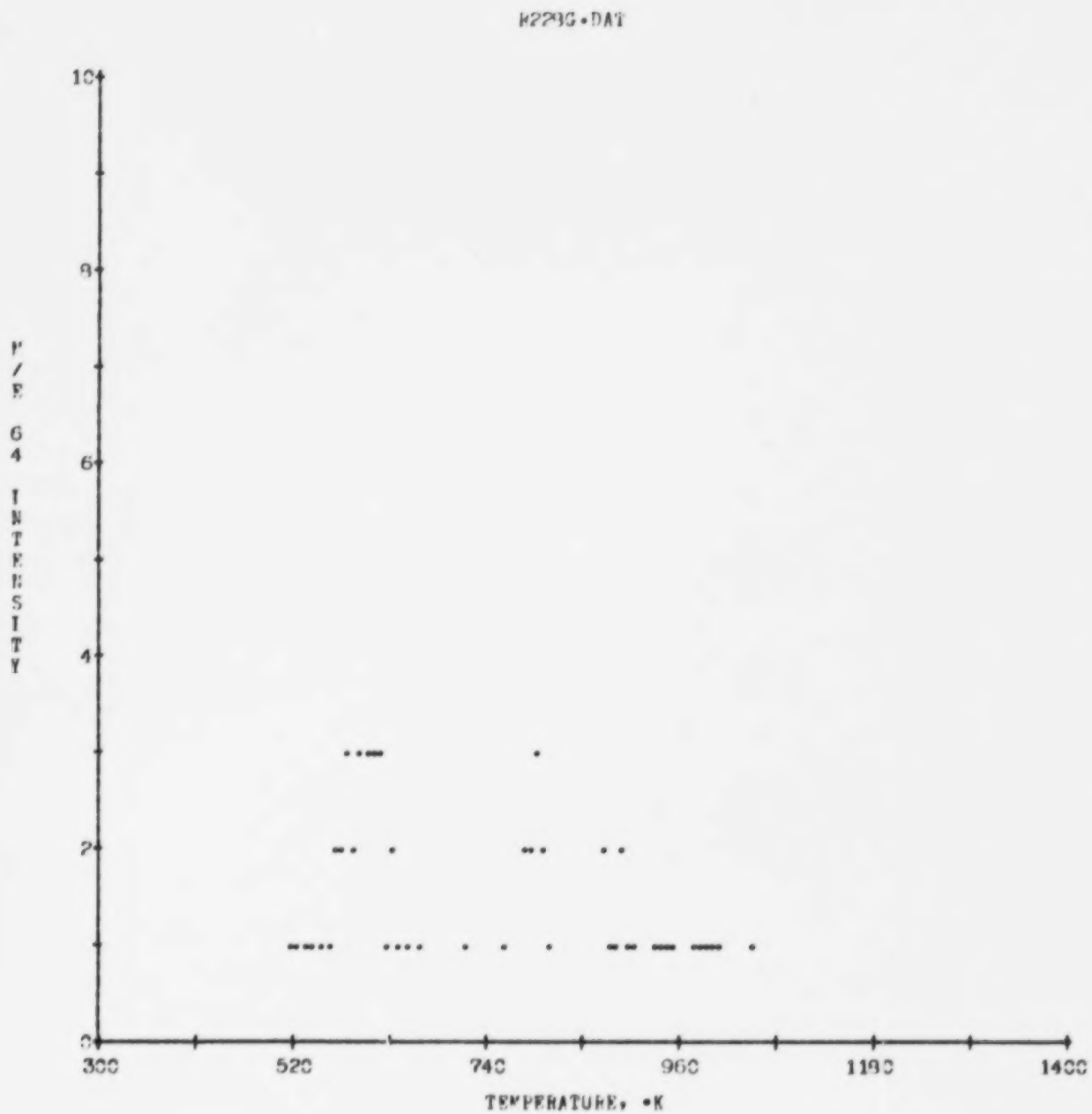

SYMBOL	NO. PTS.	LEGEND
.	42	SO24 FROM SMI ANTHRACITE, AR AT 200 CC/MIN, 30°/MIN

Figure 75

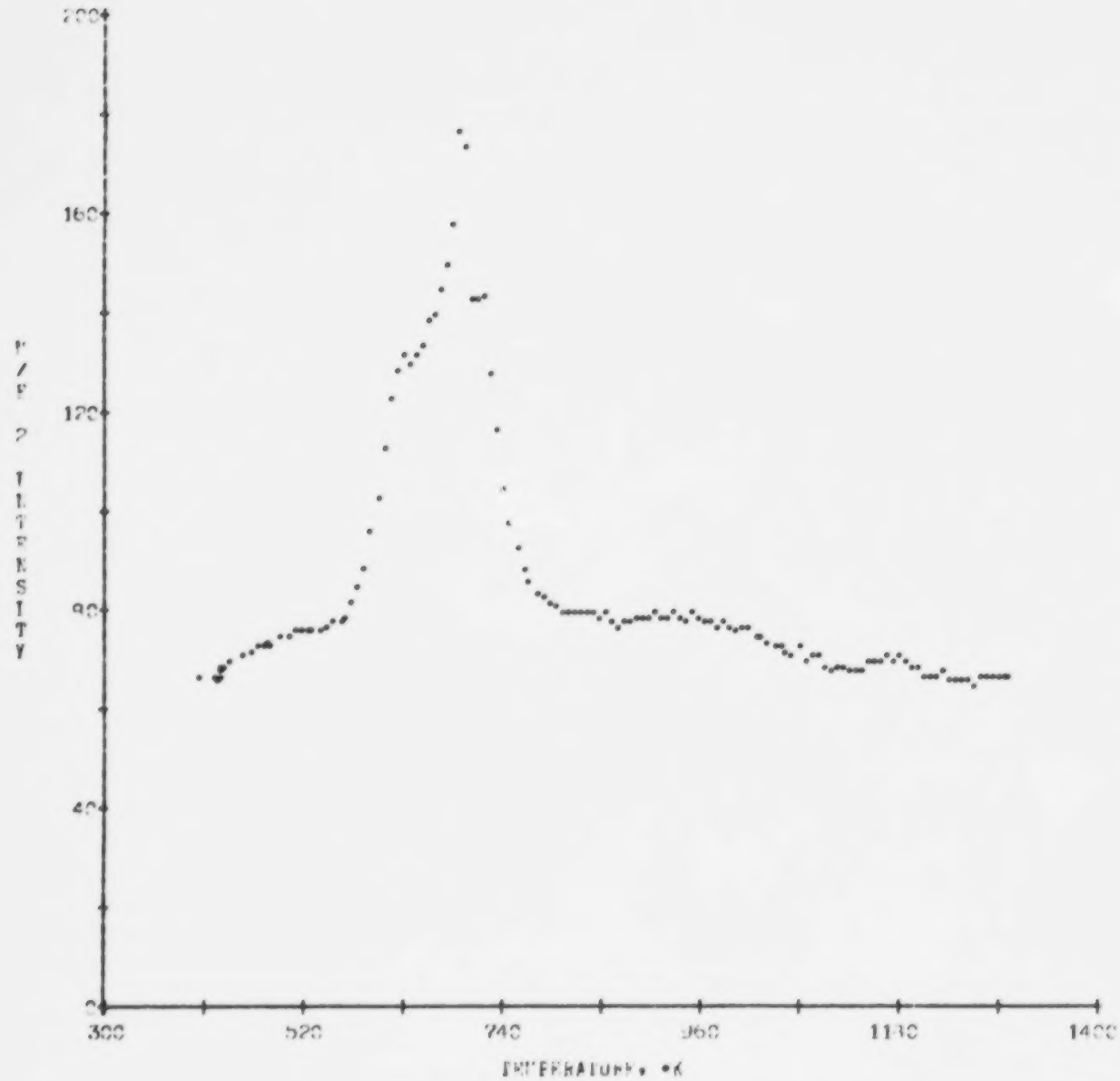

SYMBOL LOADS TEST

• 131 #24 FROM SHT LIGHTS, AT AT 200 CC/MIN, 30°/MIN

Figure 76

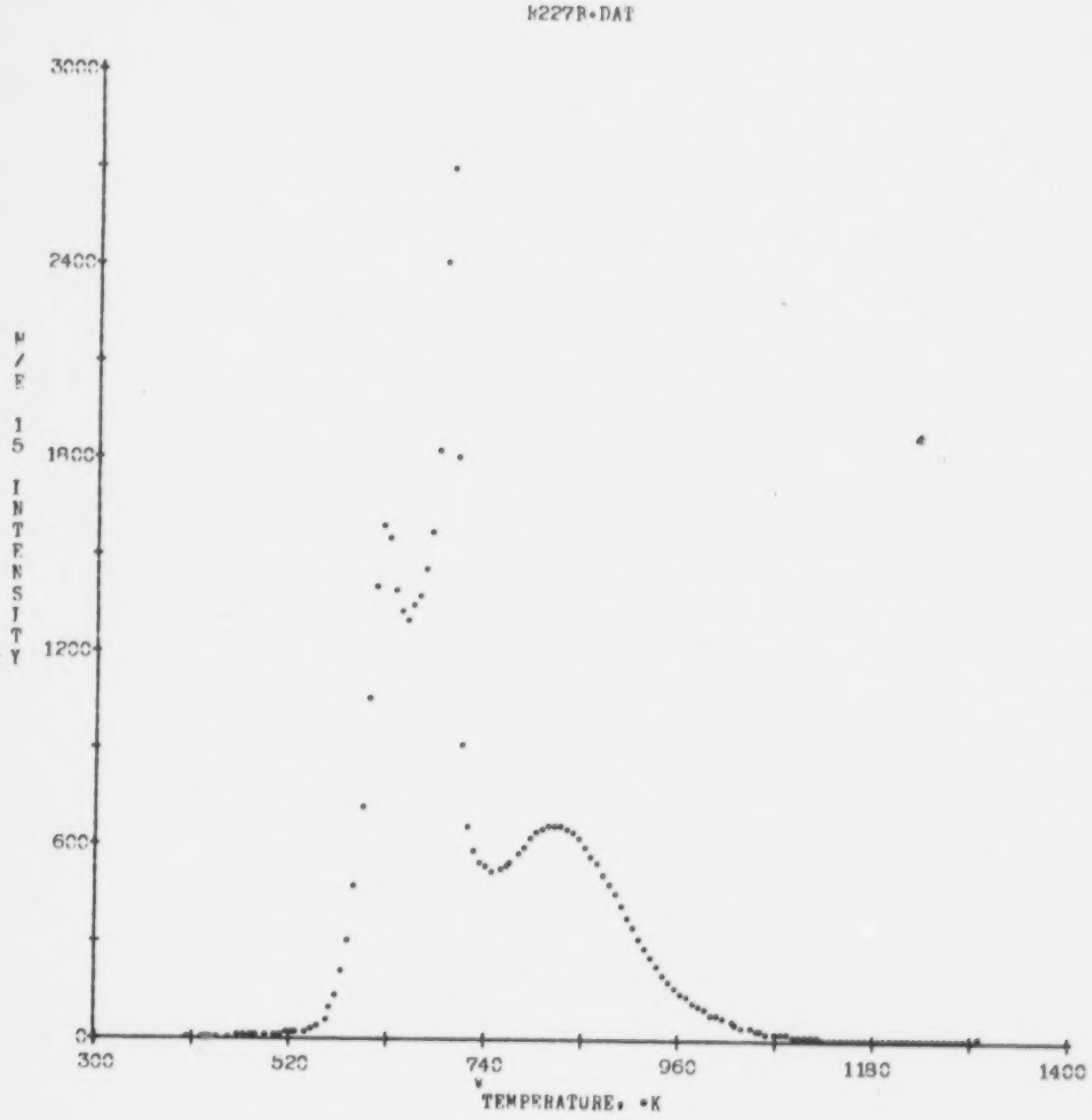

SYMBOL NO.PTS. LEGEND

. 131 CH3+ FROM SRI LIGNITE, AR AT 200 CC/MIN, 30°/MIN

Figure 77

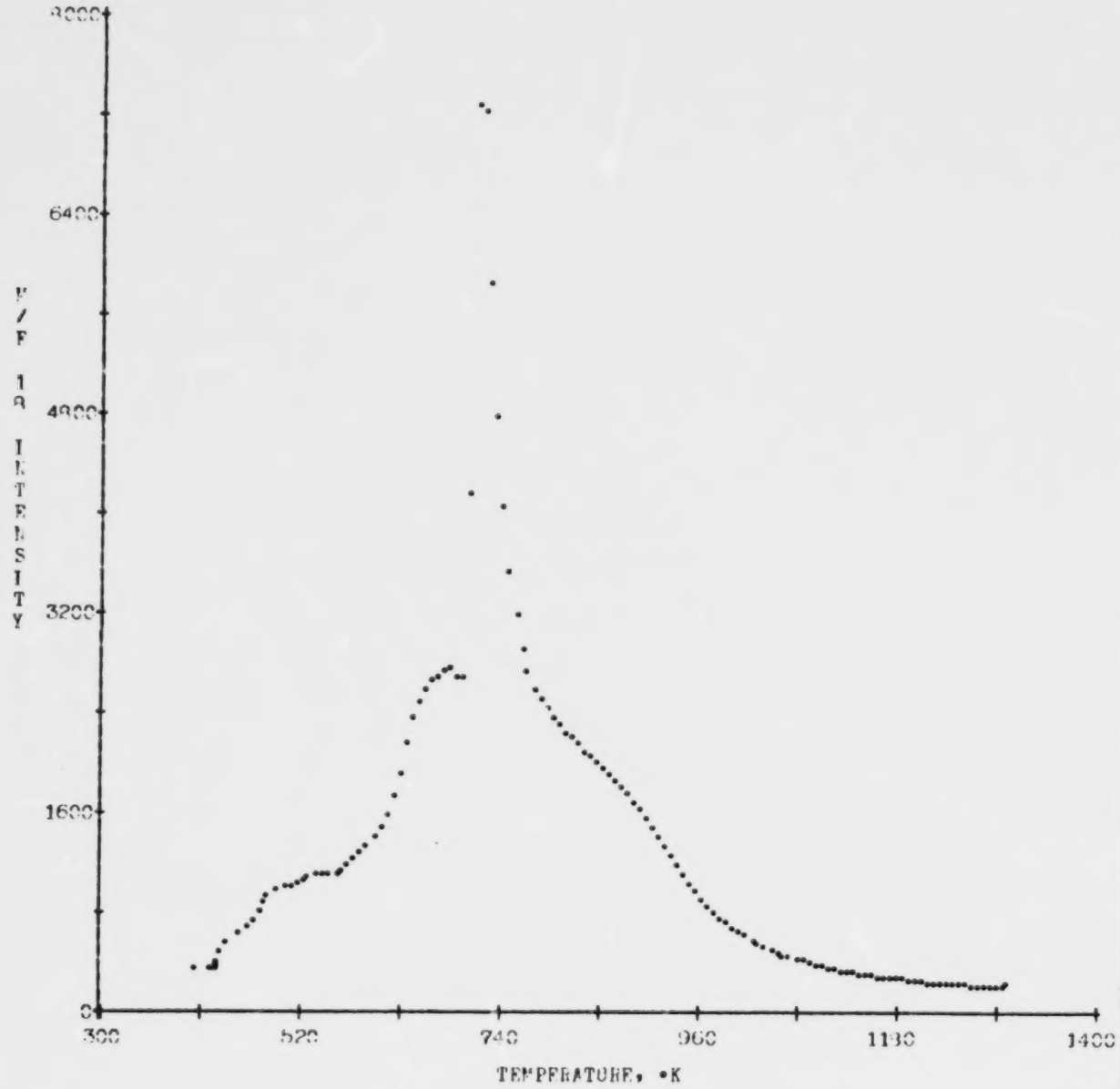

SYMBOL NO.PTS. LEGEND

• 131 H2O4 FROM SnI LIGHTS, Ab AT 200 CC/MIN, 3K°/MIN

Figure 78

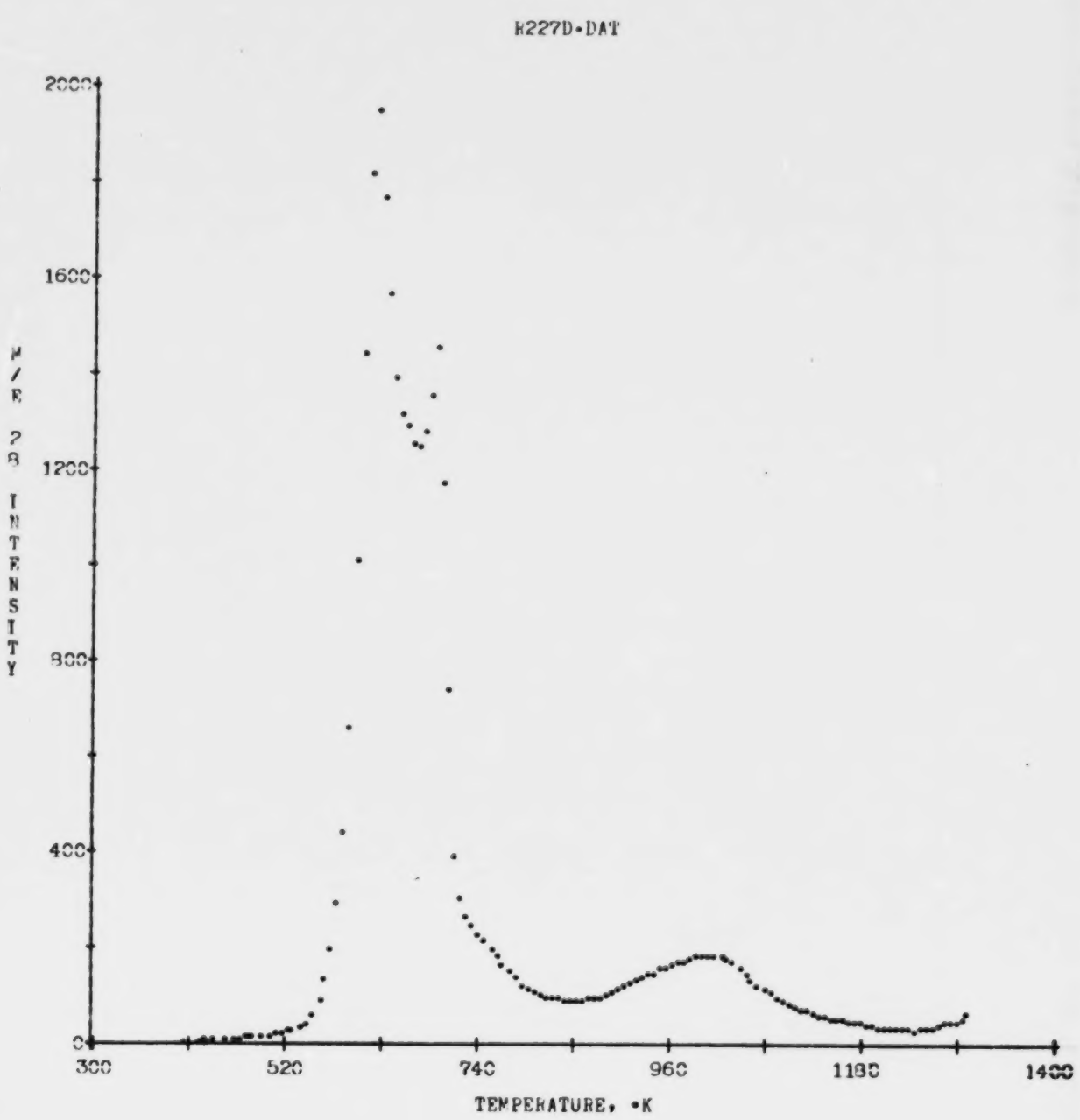

SYMBOL	NO. PTS.	LEGEND
•	131	CO+ FROM SHI LIGNITE, AR AT 200 CC/MIN, 30°/MIN

Figure 79

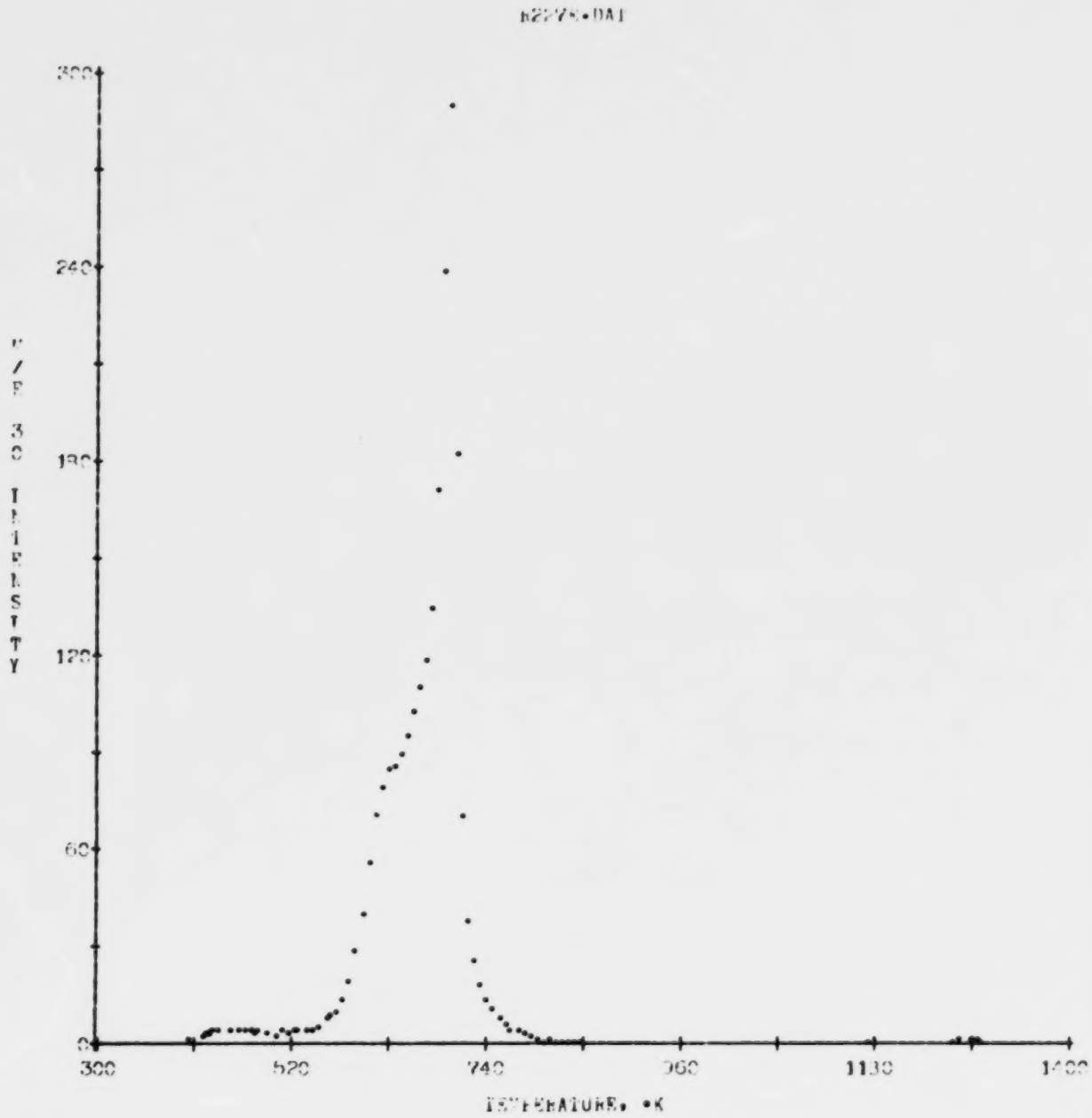

SYMBOL LOTTS. LEGEND
• 72 204 FROM SMI LIGHTS, AR AT 200 CC/MIN, 30°/MIN

Figure 80

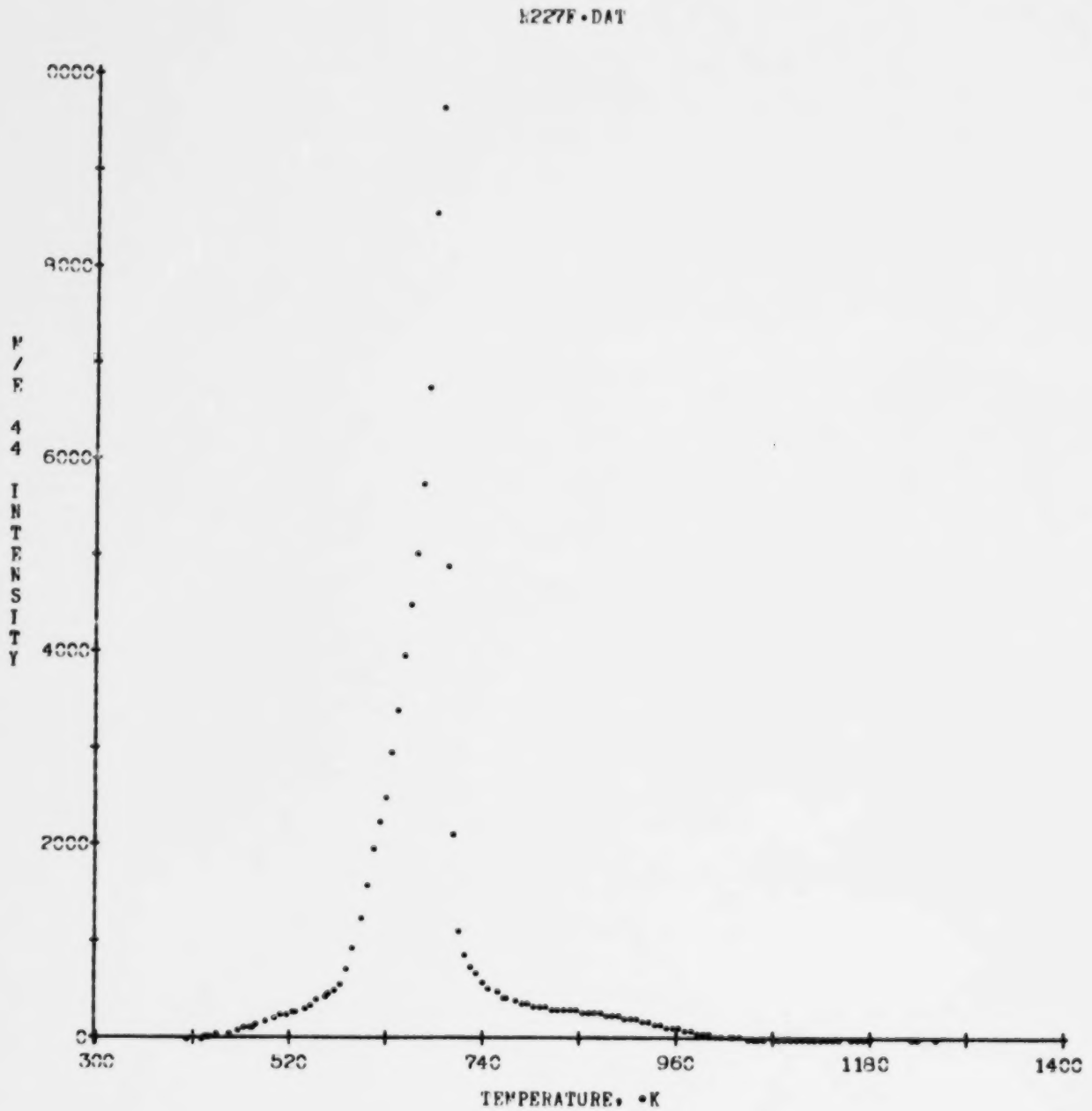

SYMBOL NO.PTS. LEGEND

. 115 CO2+ FROM SMI LIGNITE, AR AT 200 CC/MIN, 30C/MIN

Figure 81

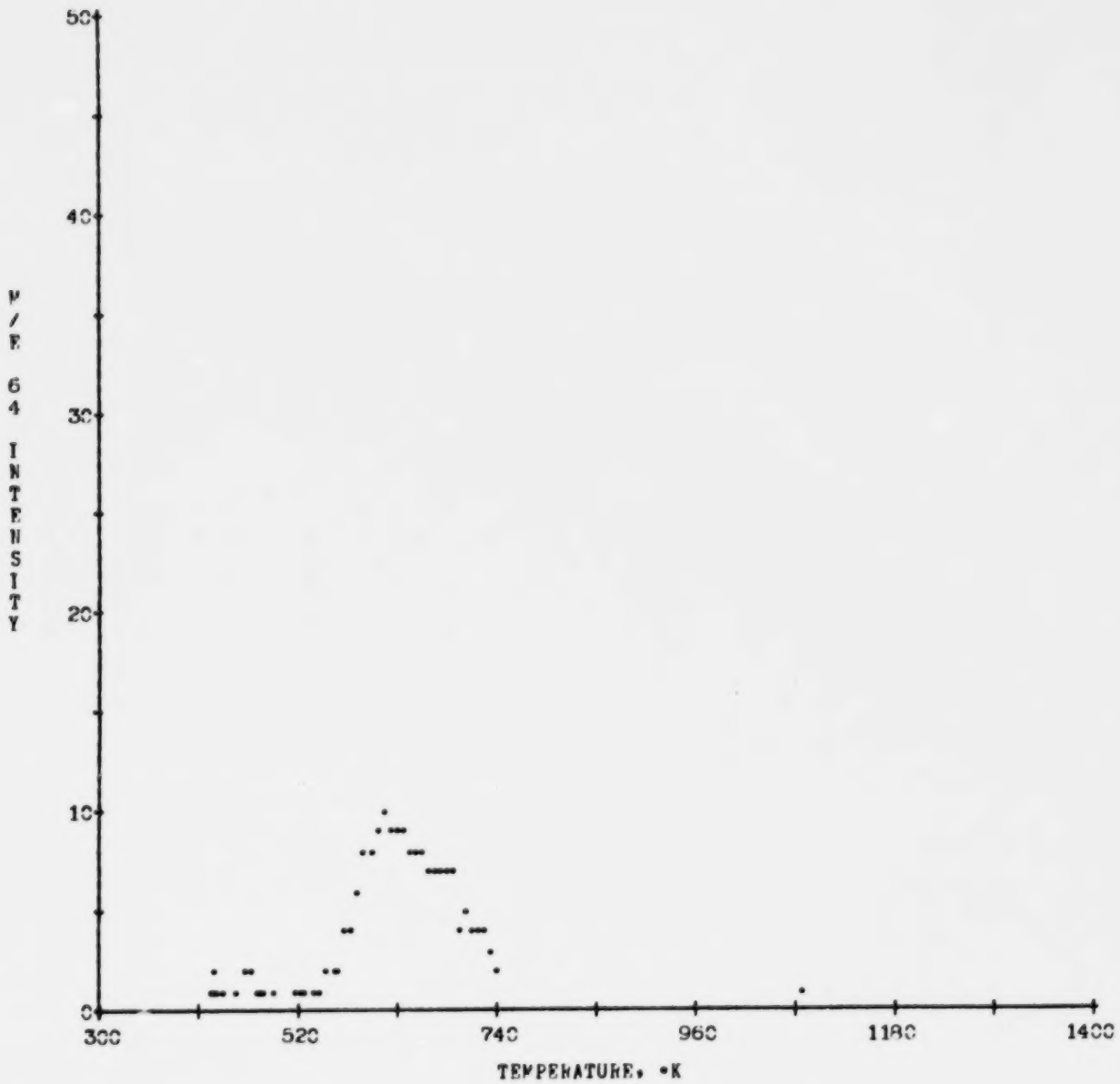

SYMBOL	NO.PTS.	LEGEND
.	46	SO2+ FROM SPI LIGNITE, AR AT 200 CC/MIN, 30°/MIN

Figure 82

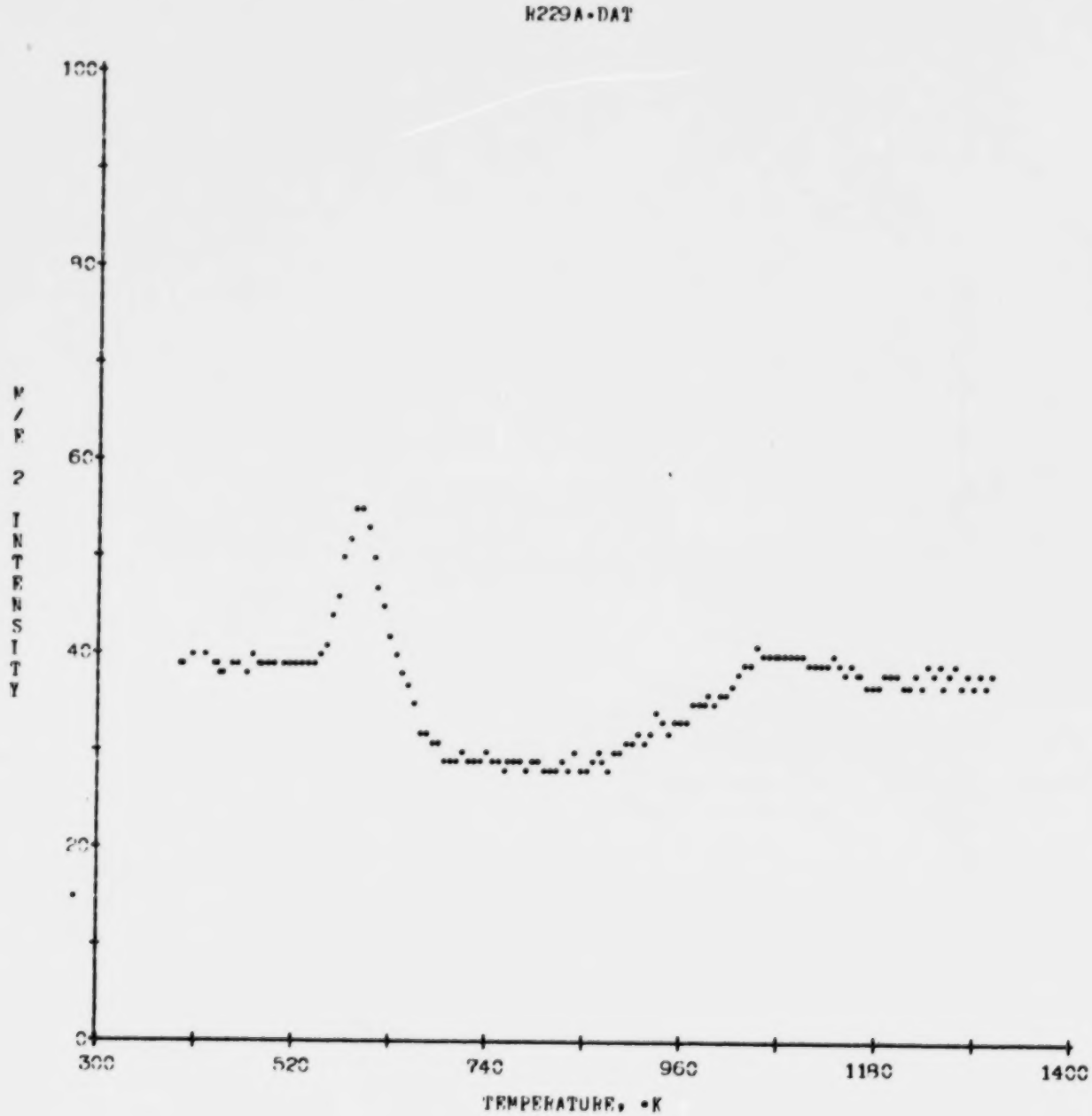

SYMBOL NO.PTS. LEGEND

. 139 H2+ FROM SHI COKE #5, AR AT 200 CC/MIN, 30°/MIN

Figure 83

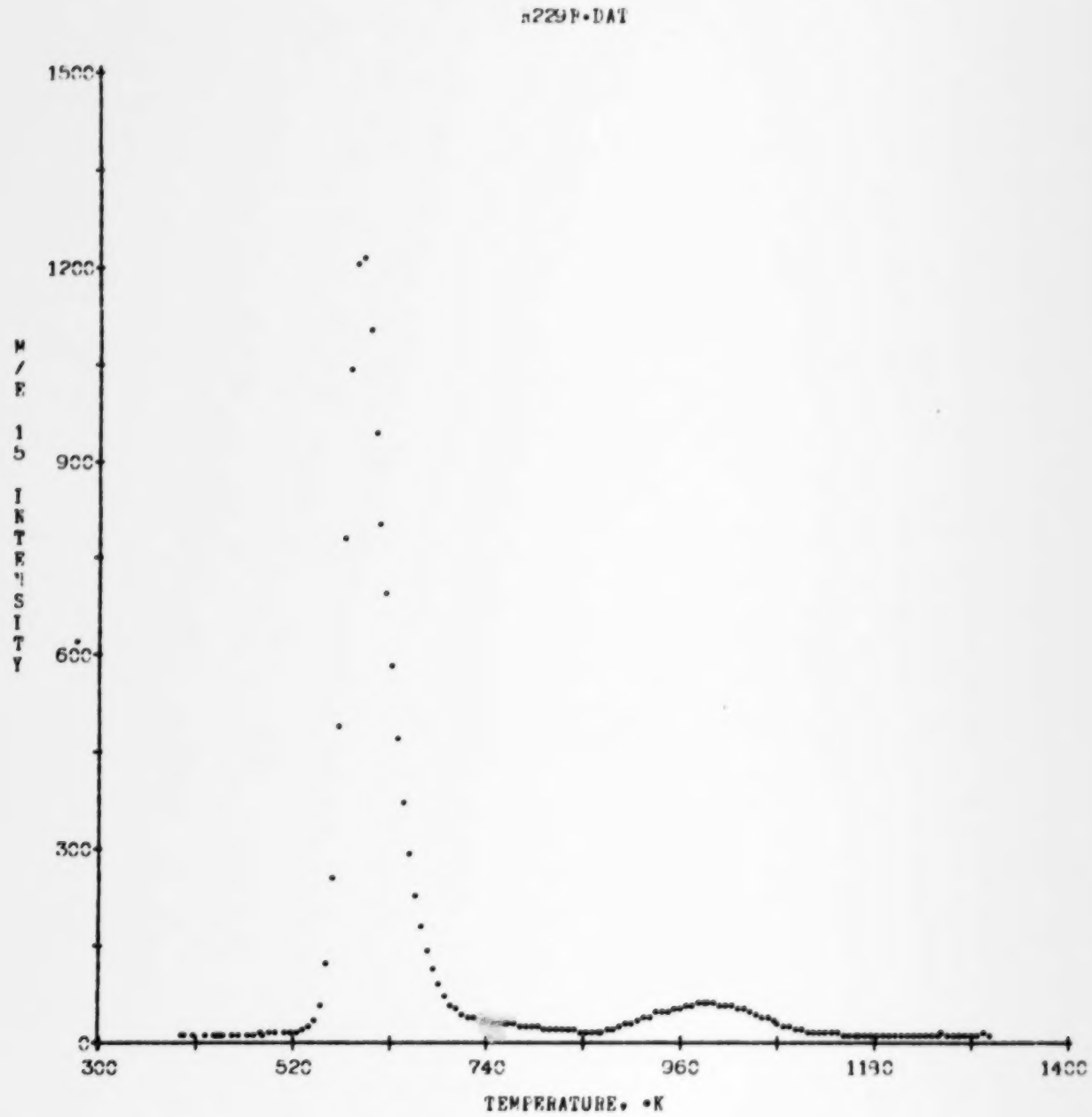

SYMBOL	NO.PTS.	LEGEND
•	139	CH3+ FROM SRI COKE #5, AR AT 200 CC/MIN, 30°/MIN

Figure 84

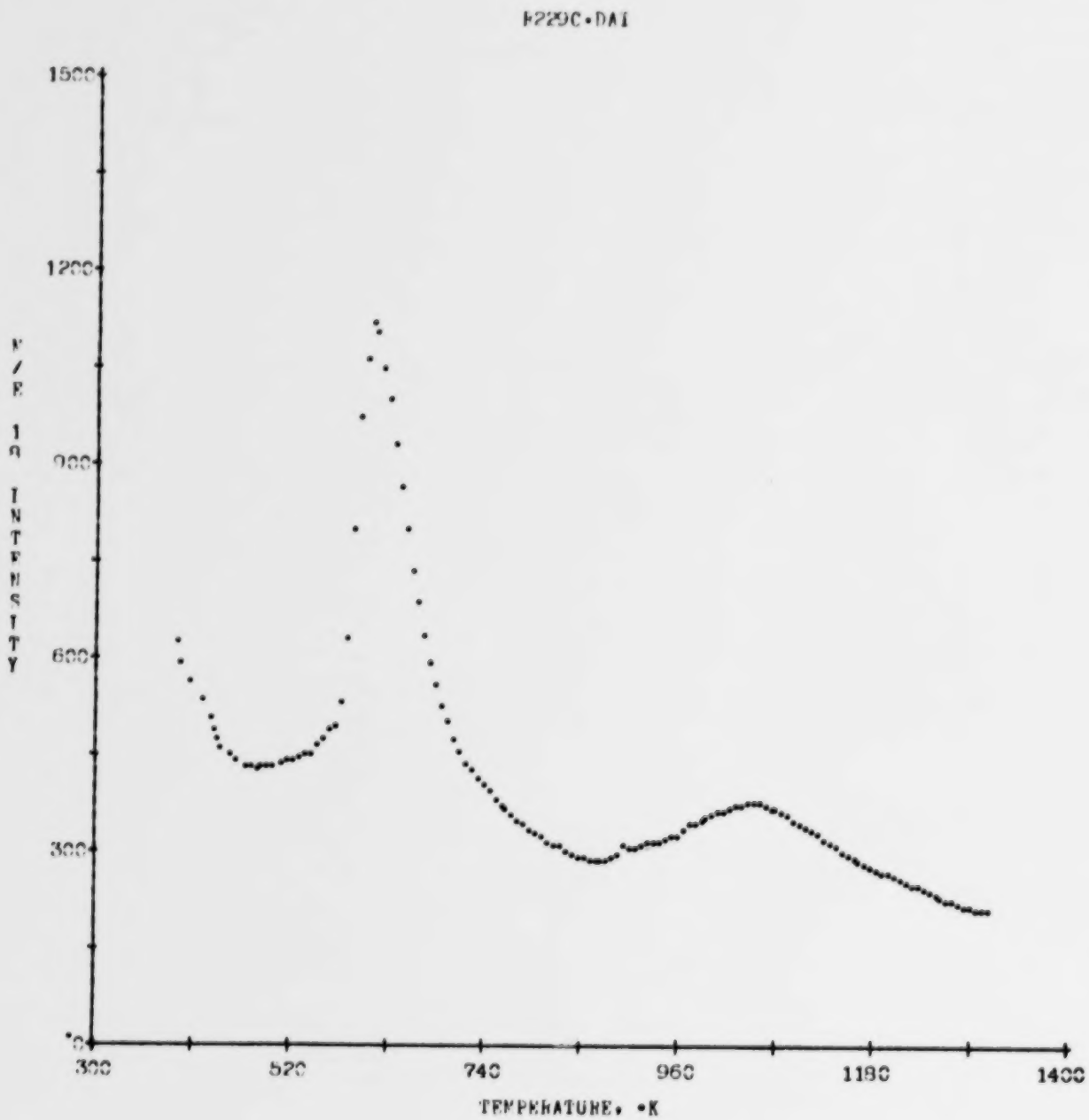

SYMBOL	NO.PTS.	LEGEND
•	138	H20+ FROM SRI COKE #5, AR AT 200 CC/MIN, 30°/MIN

Figure 85

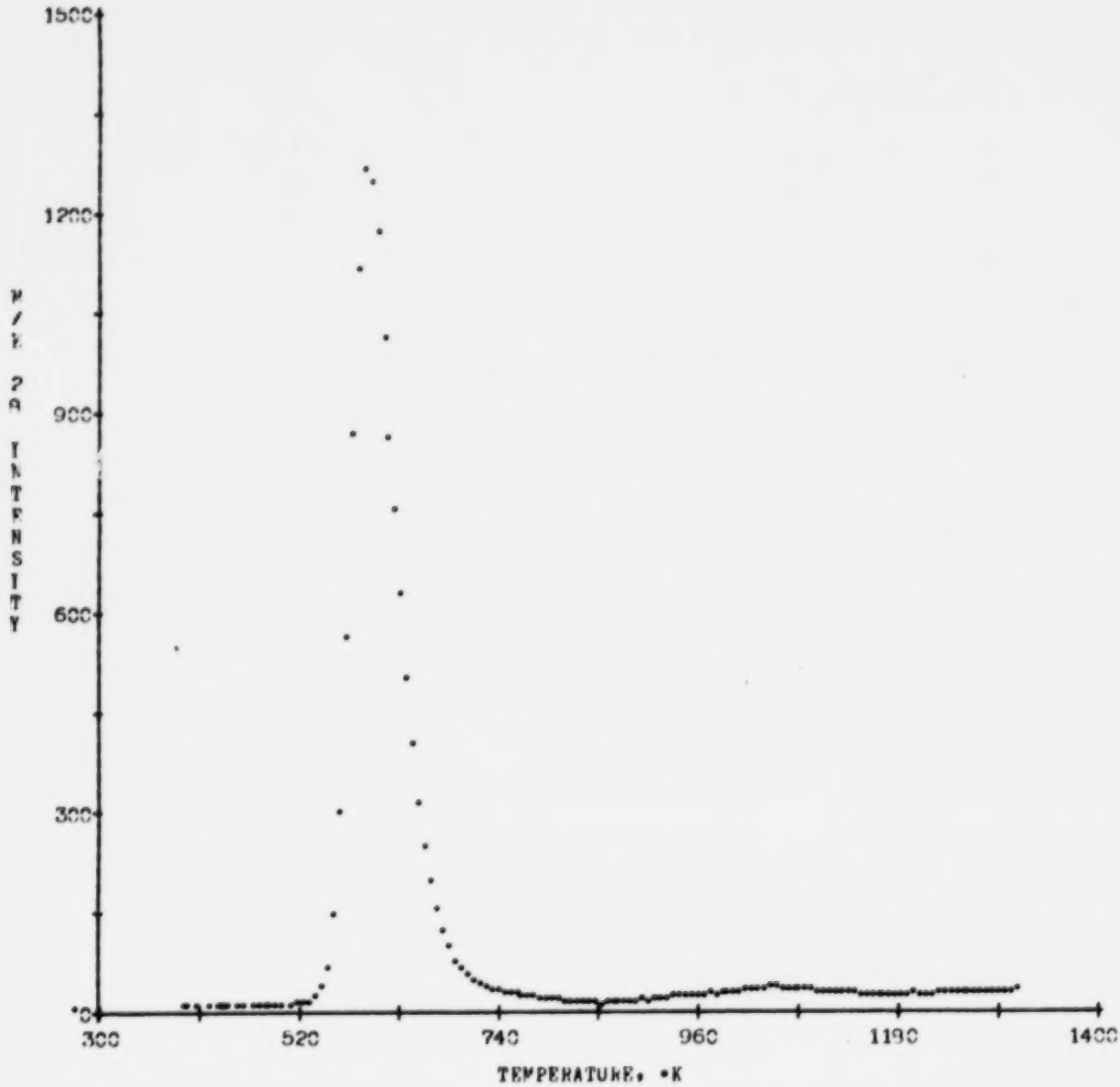

SYMBOL	NO•PTS•	LEGEND
•	130	CO+ FROM SHI COKE #5, AR AT 200 CC/MIN, 30°/MIN

Figure 86

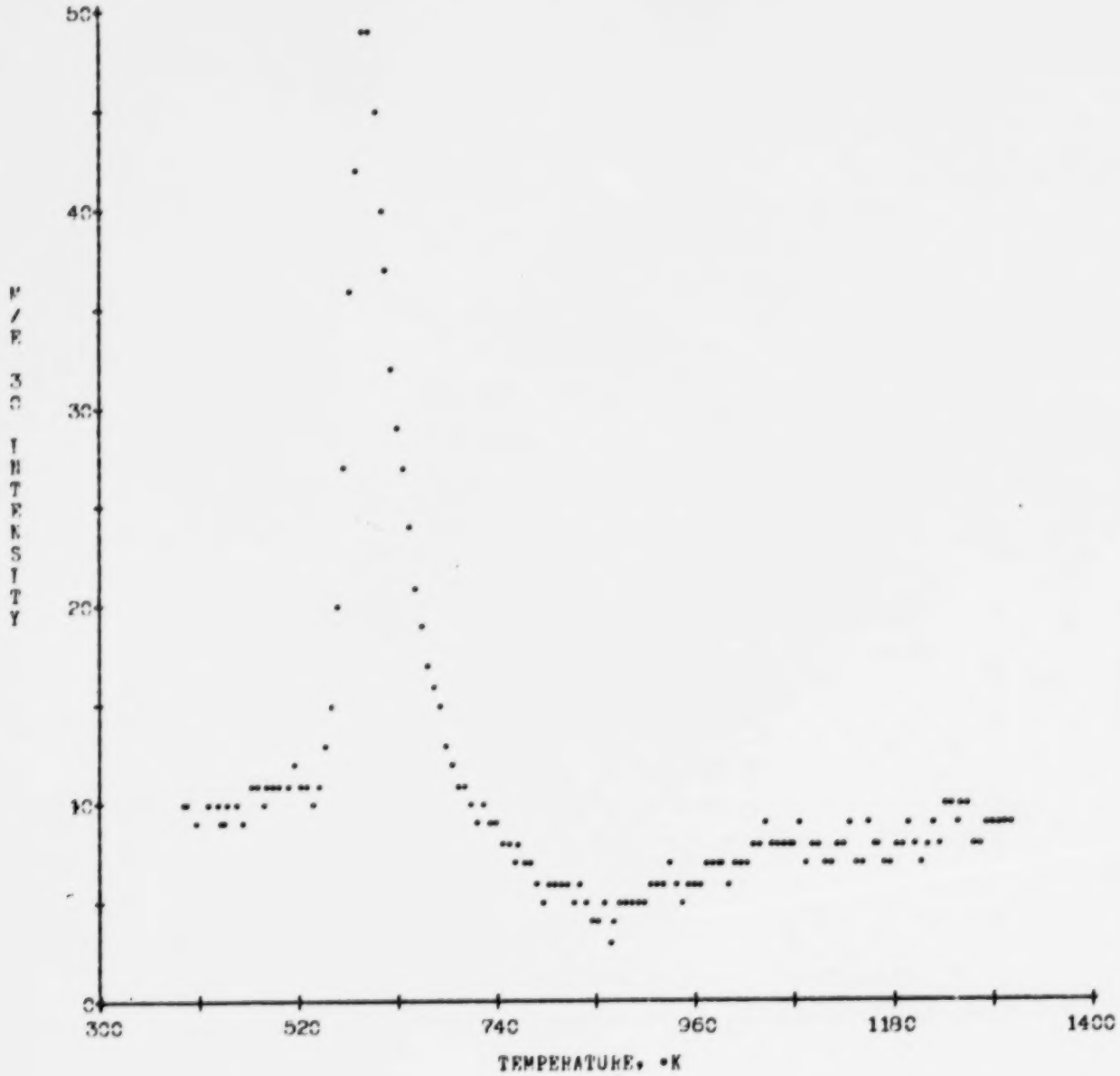

SYMBOL	NO.PTS.	LEGEND
.	139	NO+ FROM SRI COKE #5, AR AT 200 CC/MIN, 30°/MIN

Figure 87

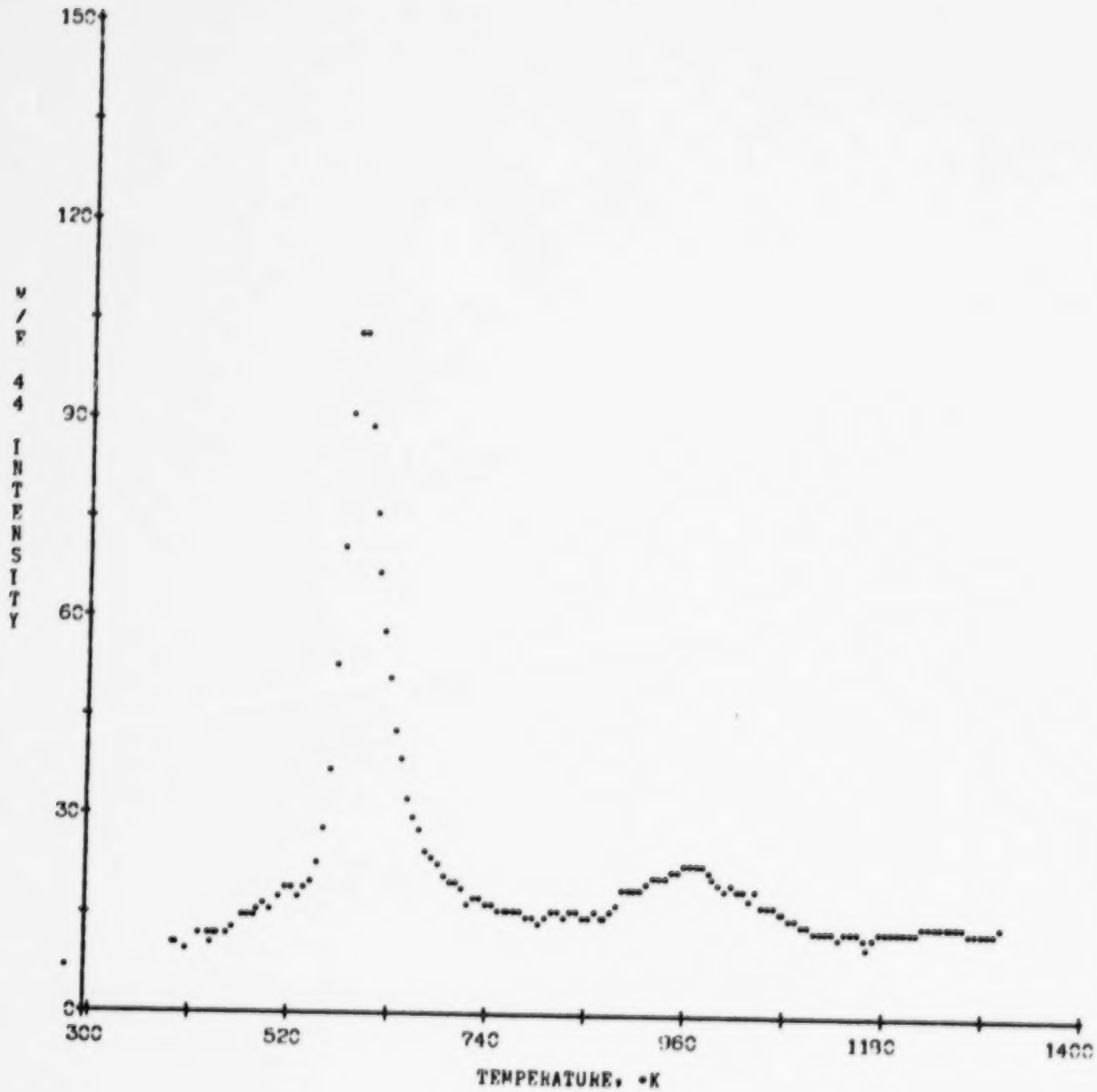

SYMBOL	NO.PTS.	LEGEND
.	139	CO2+ FROM SHI COKE #5, AR AT 200 CC/MIN, 30°/MIN

Figure 88

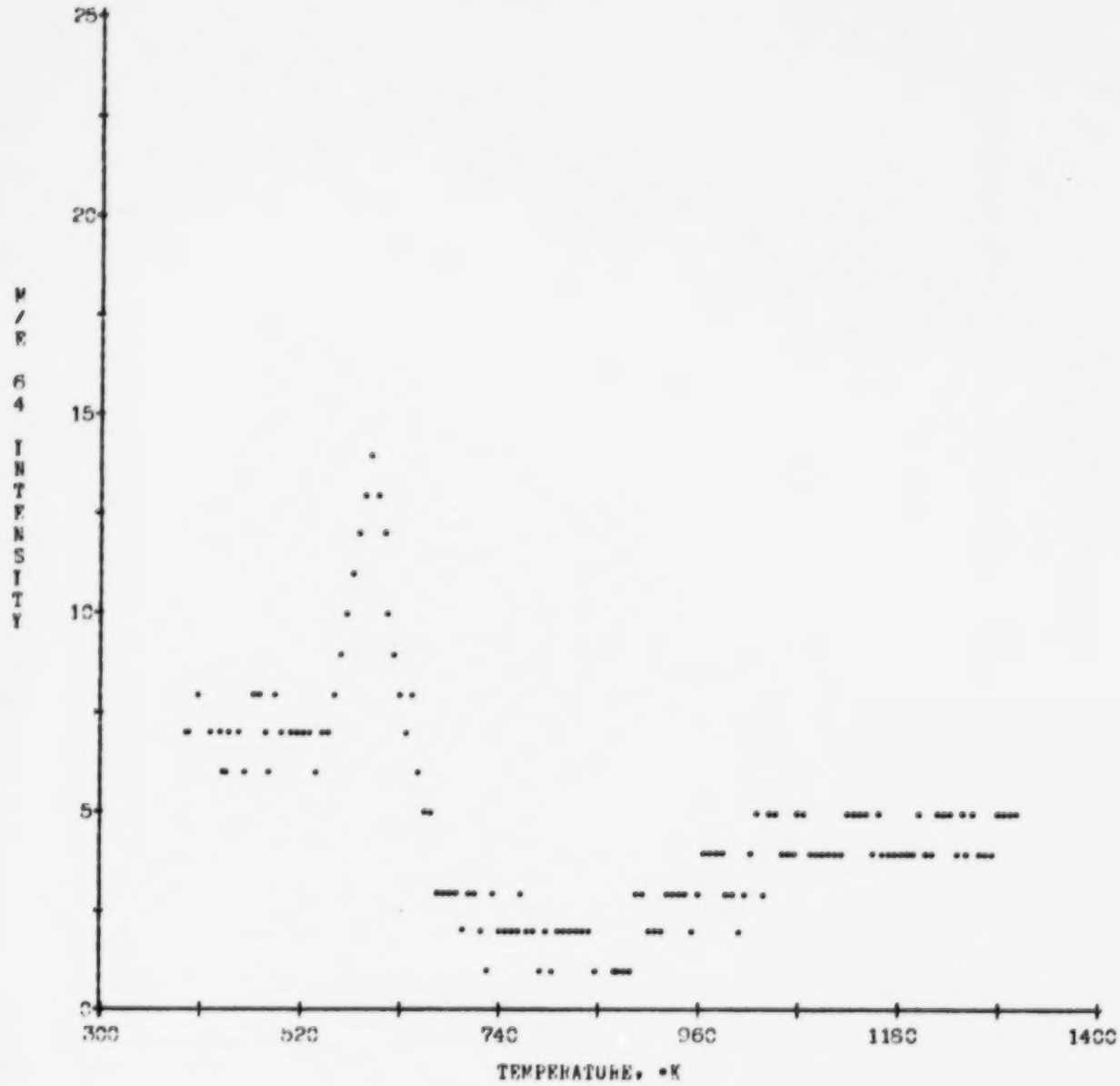

SYMBOL	NO. PTS.	LEGEND
.	135	SO2+ FROM SHI COKE #5, AR AT 200 CC/MIN, 30°/MIN

Figure 89

R152A.DAT

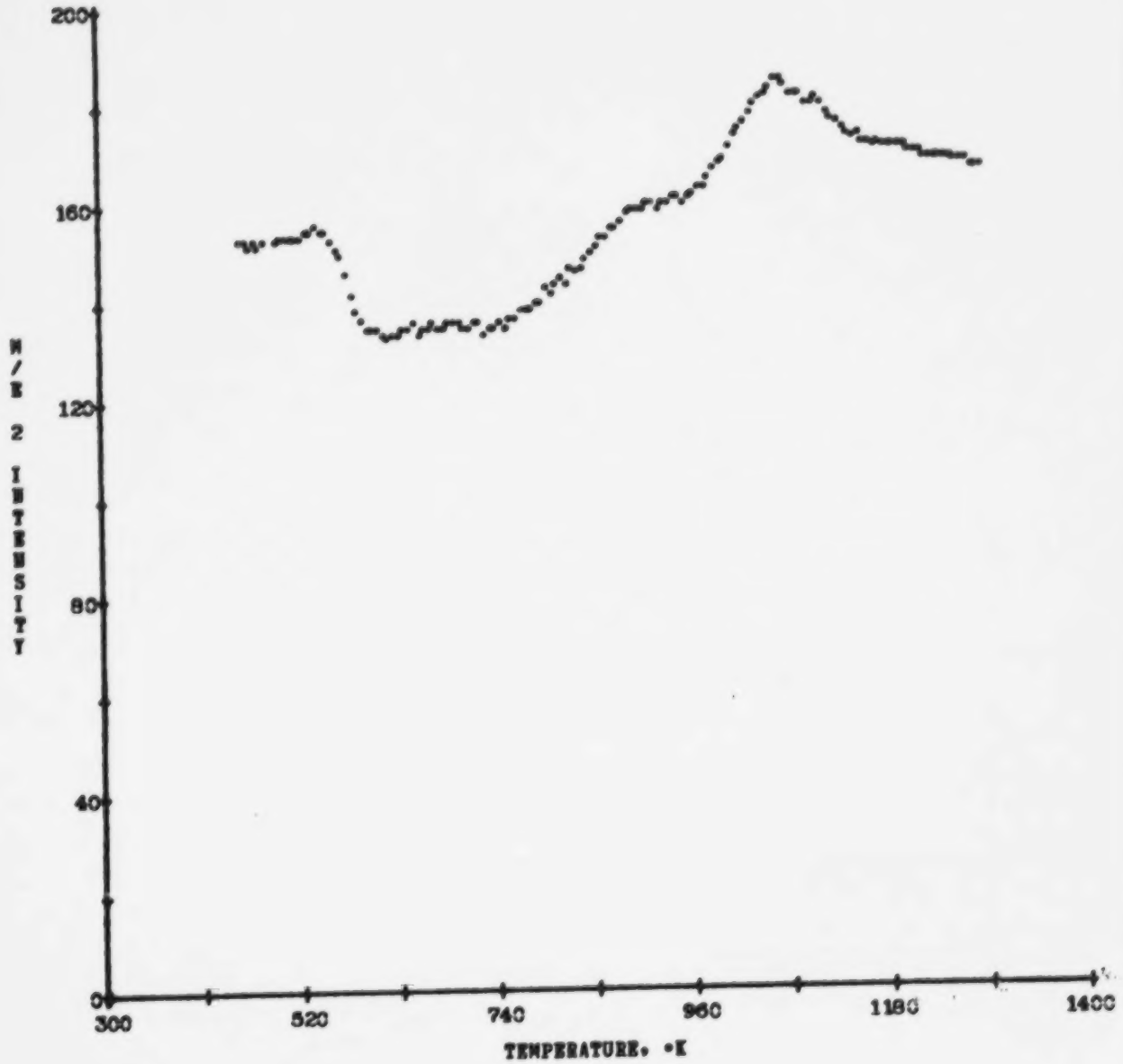

SYMBOL	NO.PTS.	LEGEND
.	145	H2+ FROM SRI COKE #7, AR CARRIER GAS AT 200 CC/MIN, 30°/MIN

Figure 90

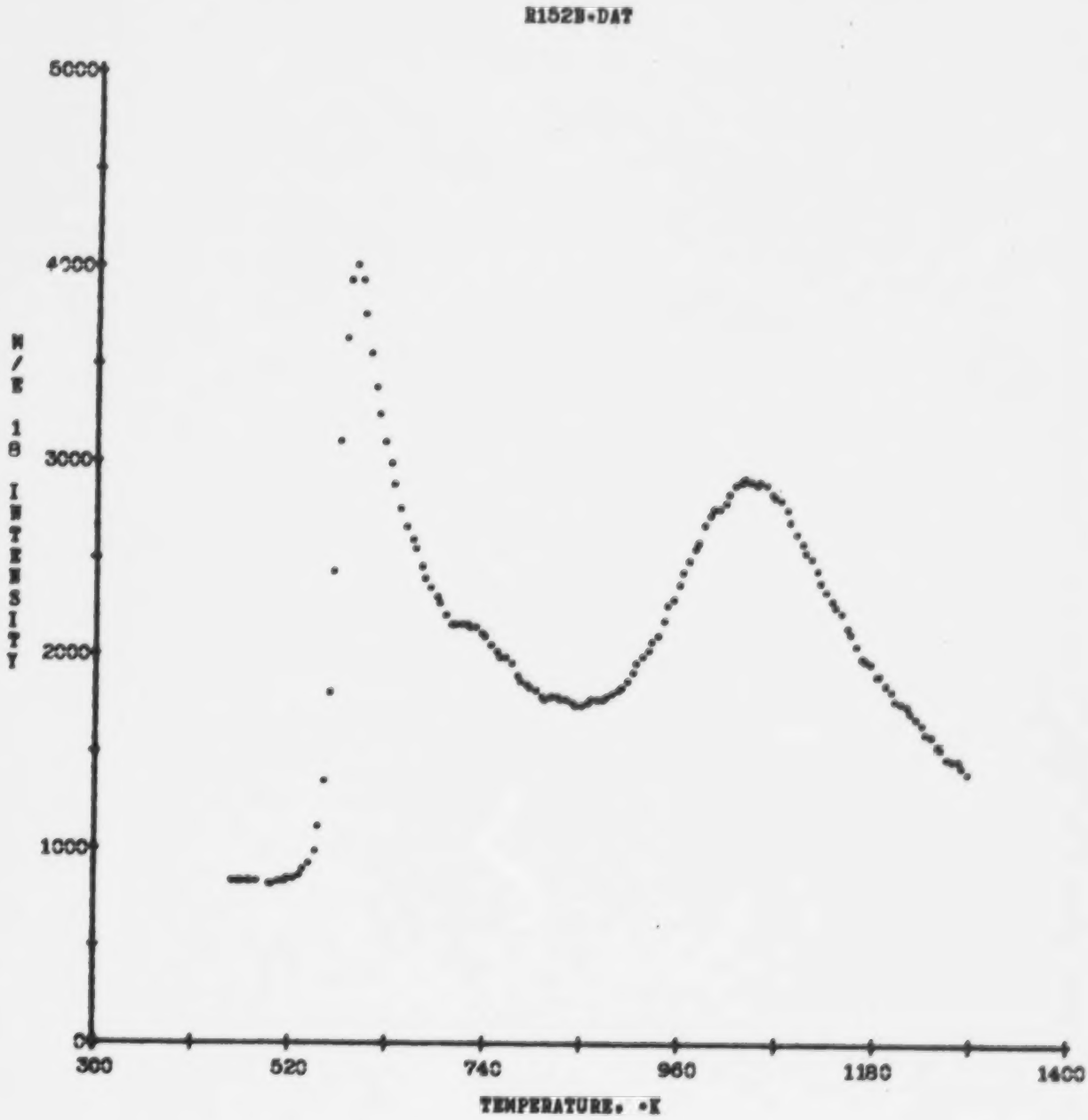

SYMBOL NO.PTS. LEGEND

. 145 H2O+ FROM SRI COKE #7, AR CARRIER GAS AT 200 CC/MIN, 30°/MIN

Figure 91

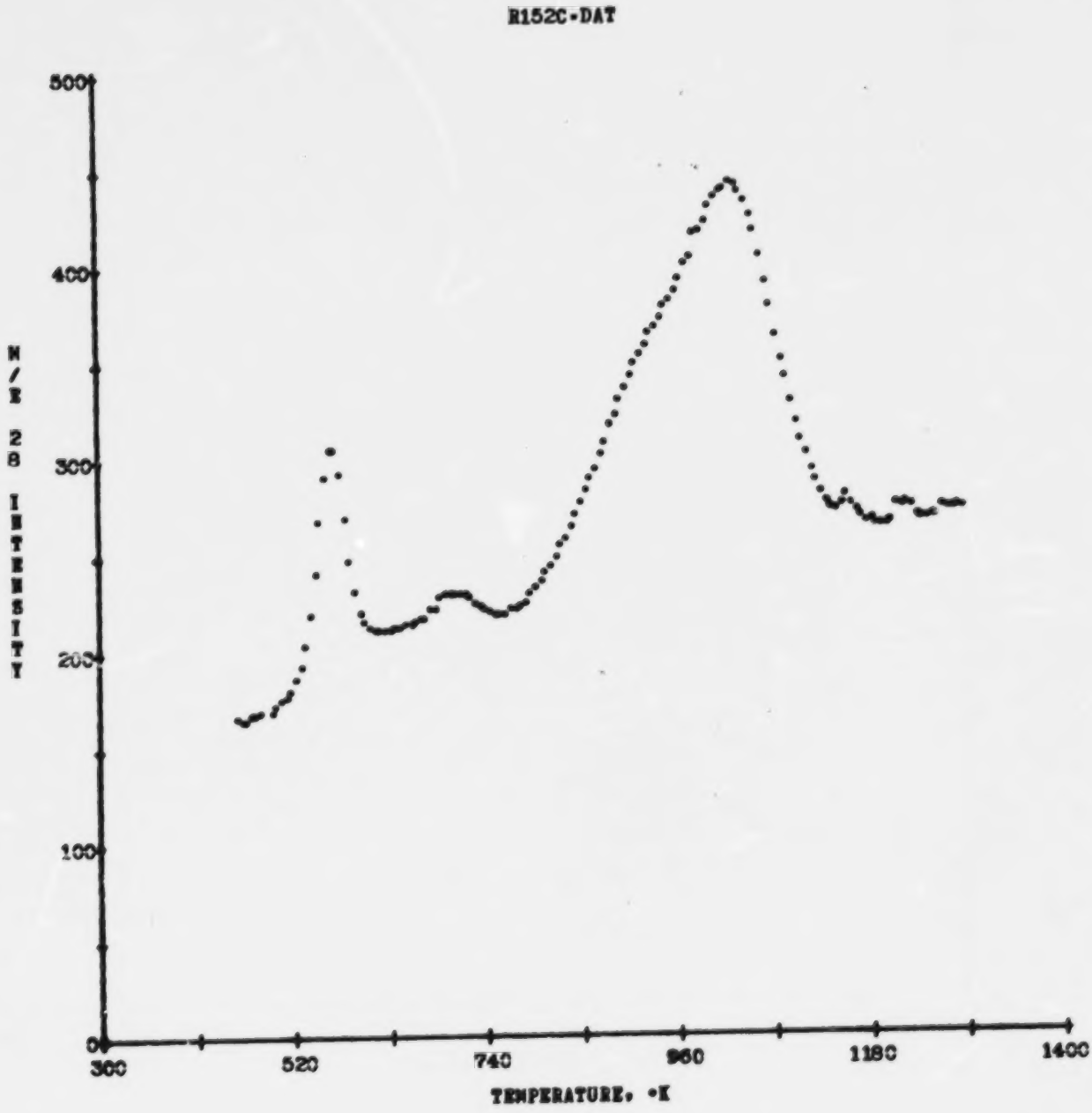

SYMBOL NO.PTS. LEGEND

. 148 CO+ FROM SRI COKE #7, AR CARRIER GAS AT 200 CC/MIN, 30°/MIN

Figure 92

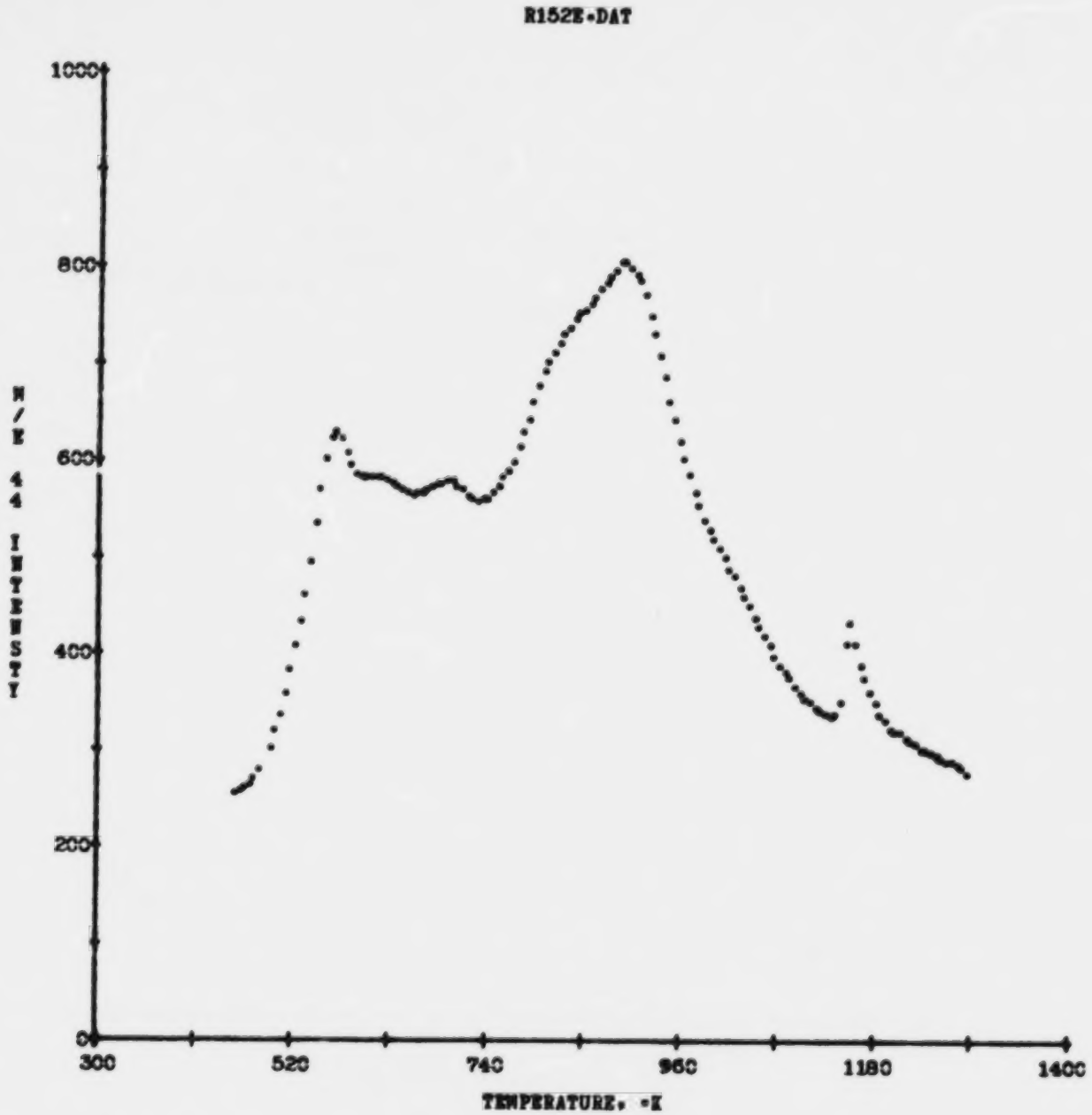

SYMBOL NO.PTS. LEGEND

. 145 CO2+ FROM SRI COKE #7, AR CARRIER GAS AT 200 CC/MIN, 30°/MIN

Figure 93

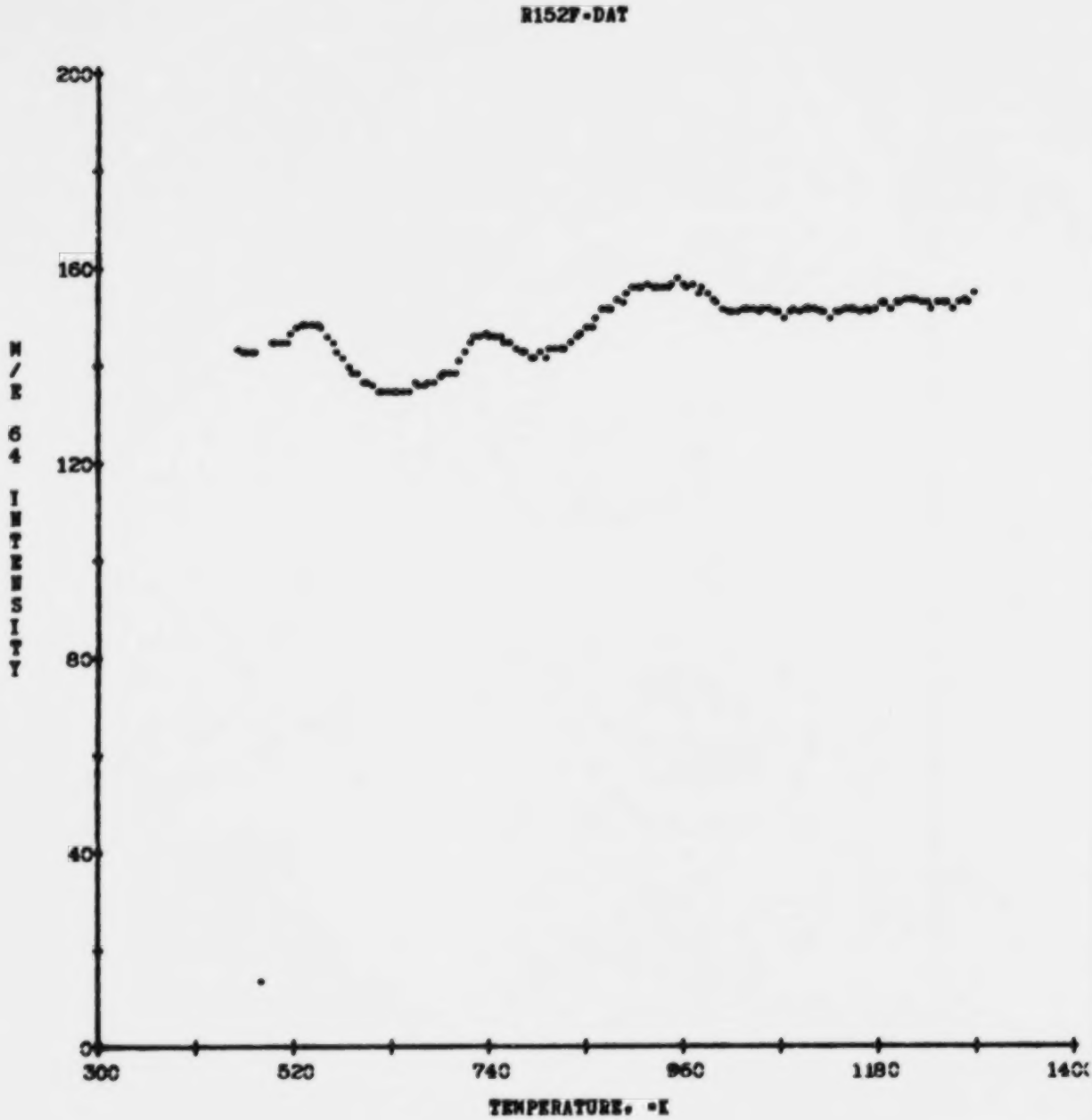

SYMBOL	NO.PTS.	LEGEND
.	145	SO2+ FROM SRI COKE #7, AR CARRIER GAS AT 200 CC/MIN, 30°/MIN

Figure 94

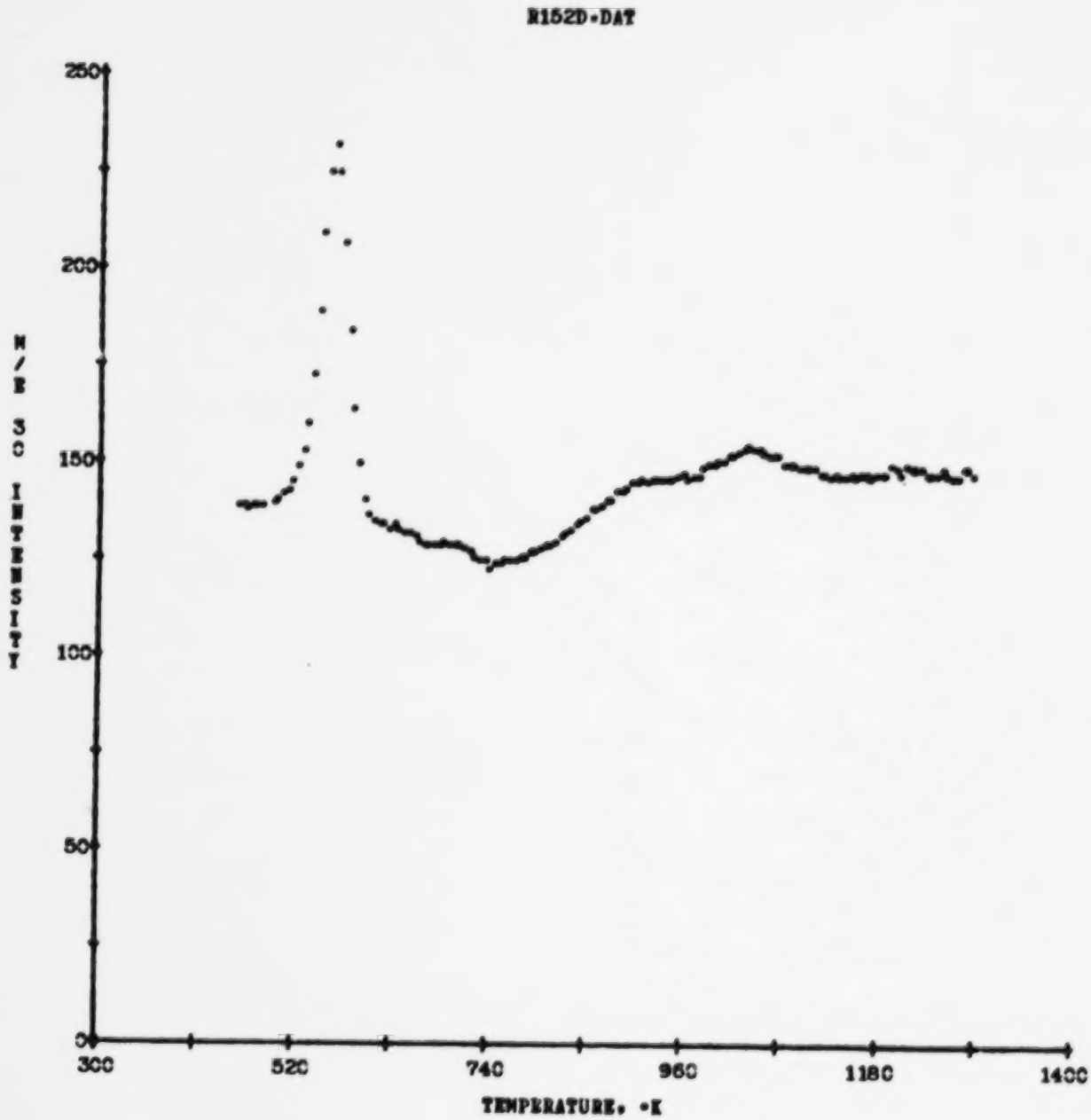

SYMBOL NO.PTS. LEGEND

. 145 NO+ FROM SRI COKE #7, AR CARRIER GAS AT 200 CC/MIN, 30°/MIN

Figure 95

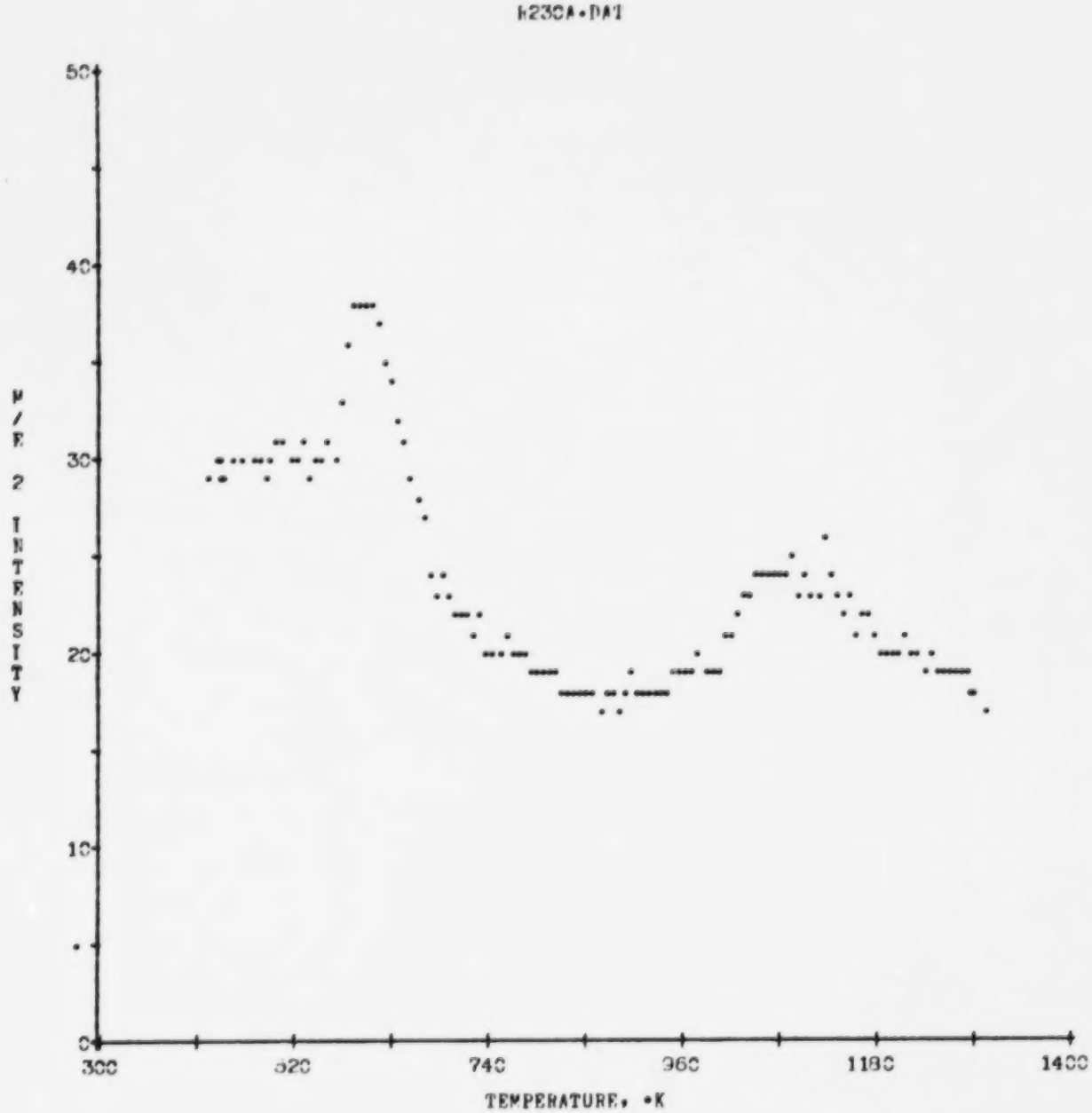

SYMBOL NO.PTS. LEGEND
. 120 H2+ FROM SMI COKE #10, AR AT 200 CC/MIN, 30°/MIN

Figure 96

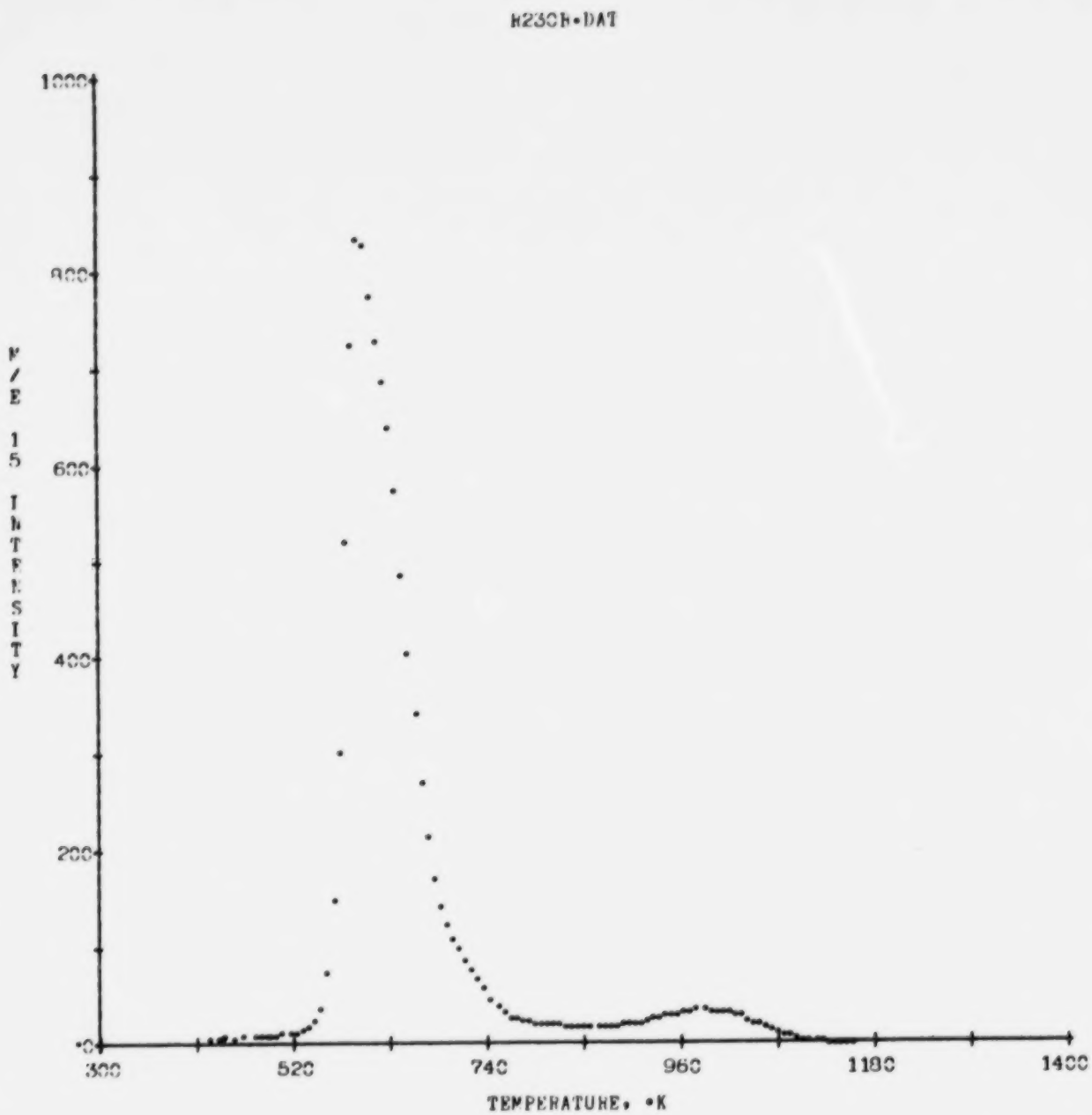

SYMBOL NO.PTS. LEGEND

. 107 CH3+ FROM SHI COKE #1C, AR A T 200 CC/MIN, 30°/MIN

Figure 97

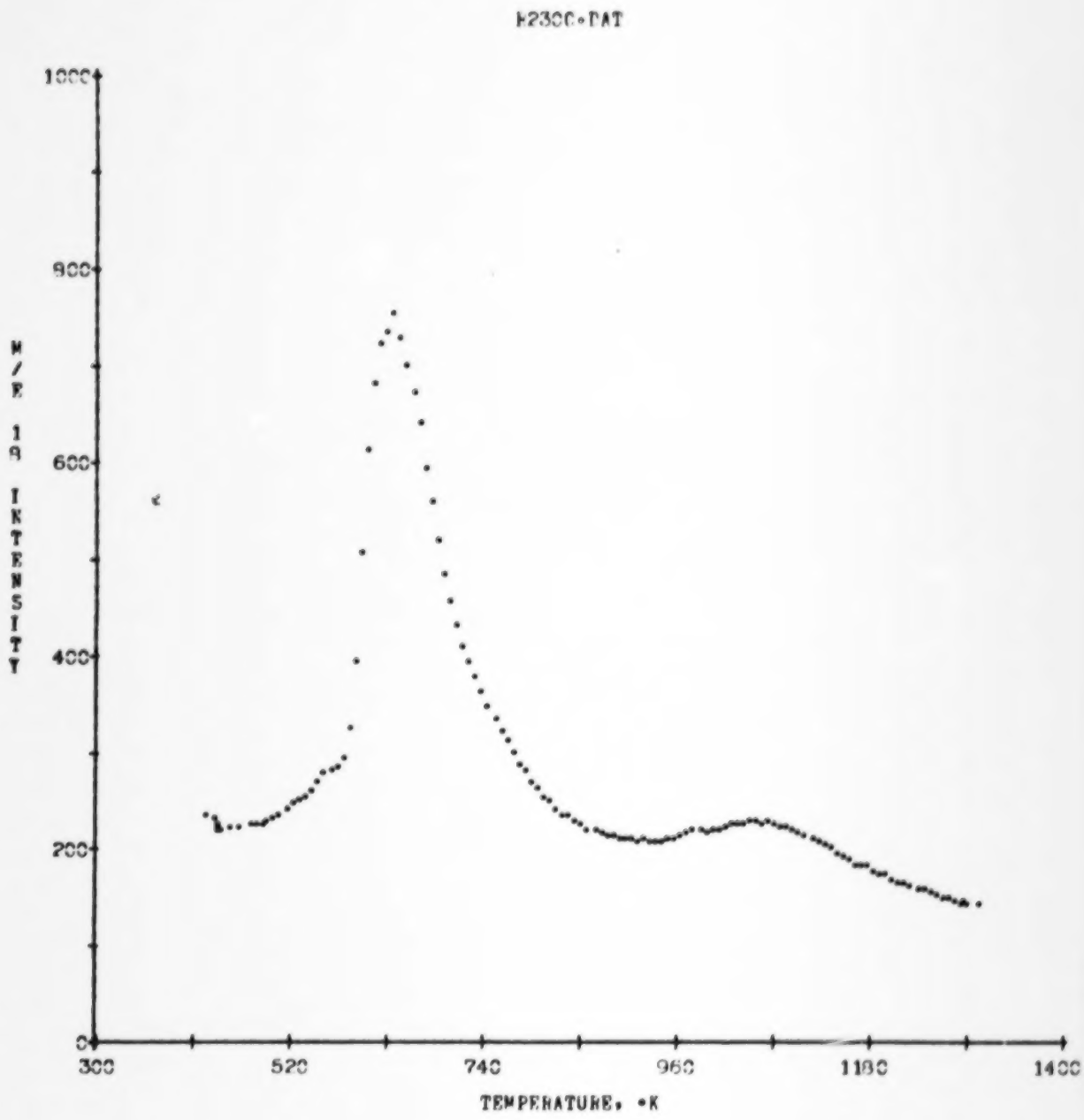

SYMBOL	NO.PTS.	LEGEND
.	127	H2O+ FROM SHI COKE #10, AR AT 200 CC/MIN, 30°/MIN

Figure 98

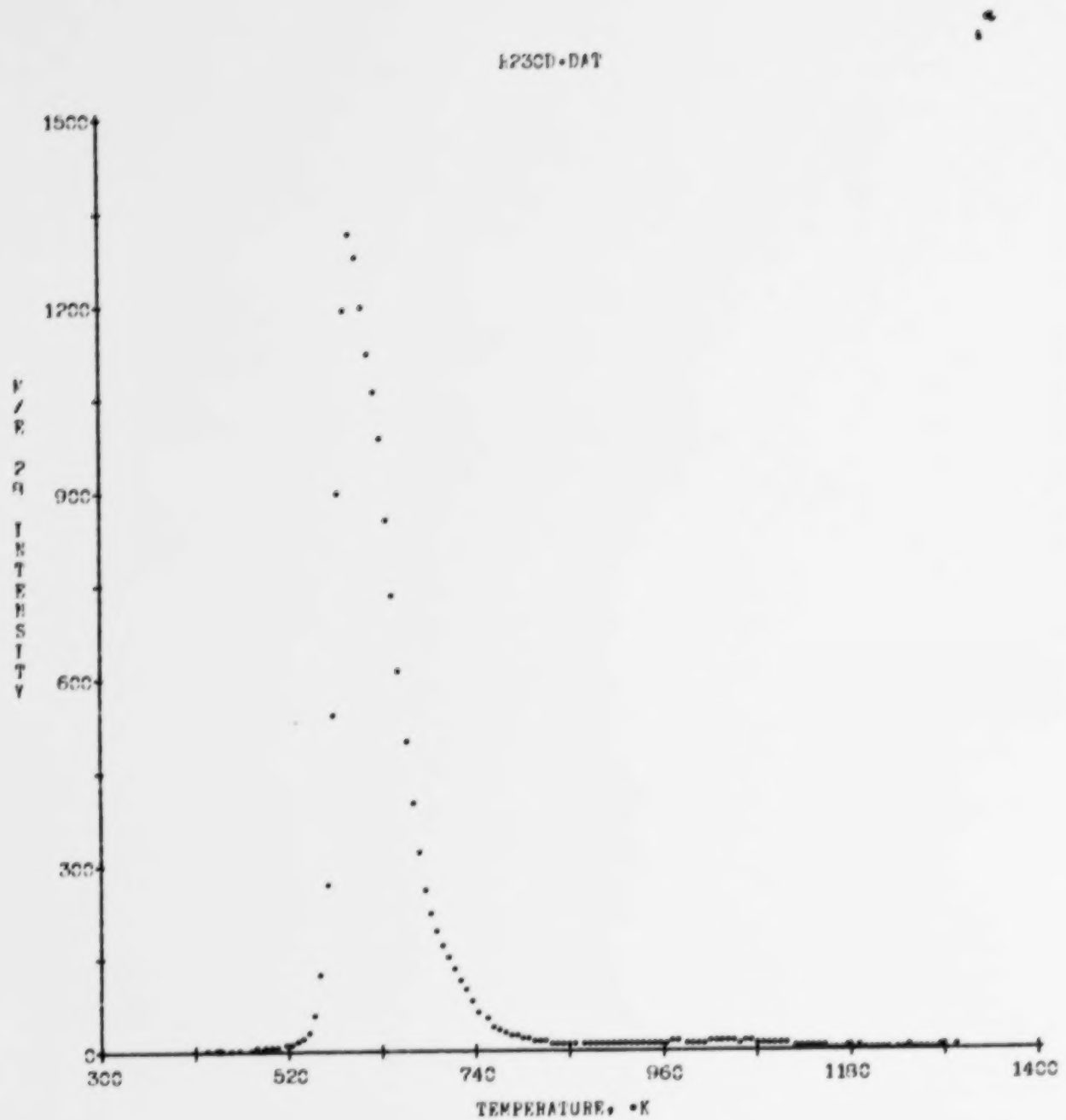

SYMBOL	NO.PTS.	LEGEND
.	127	CO+ FROM SRI COKE #1C, AR AT 200 CC/MIN, 30°/MIN

Figure 99

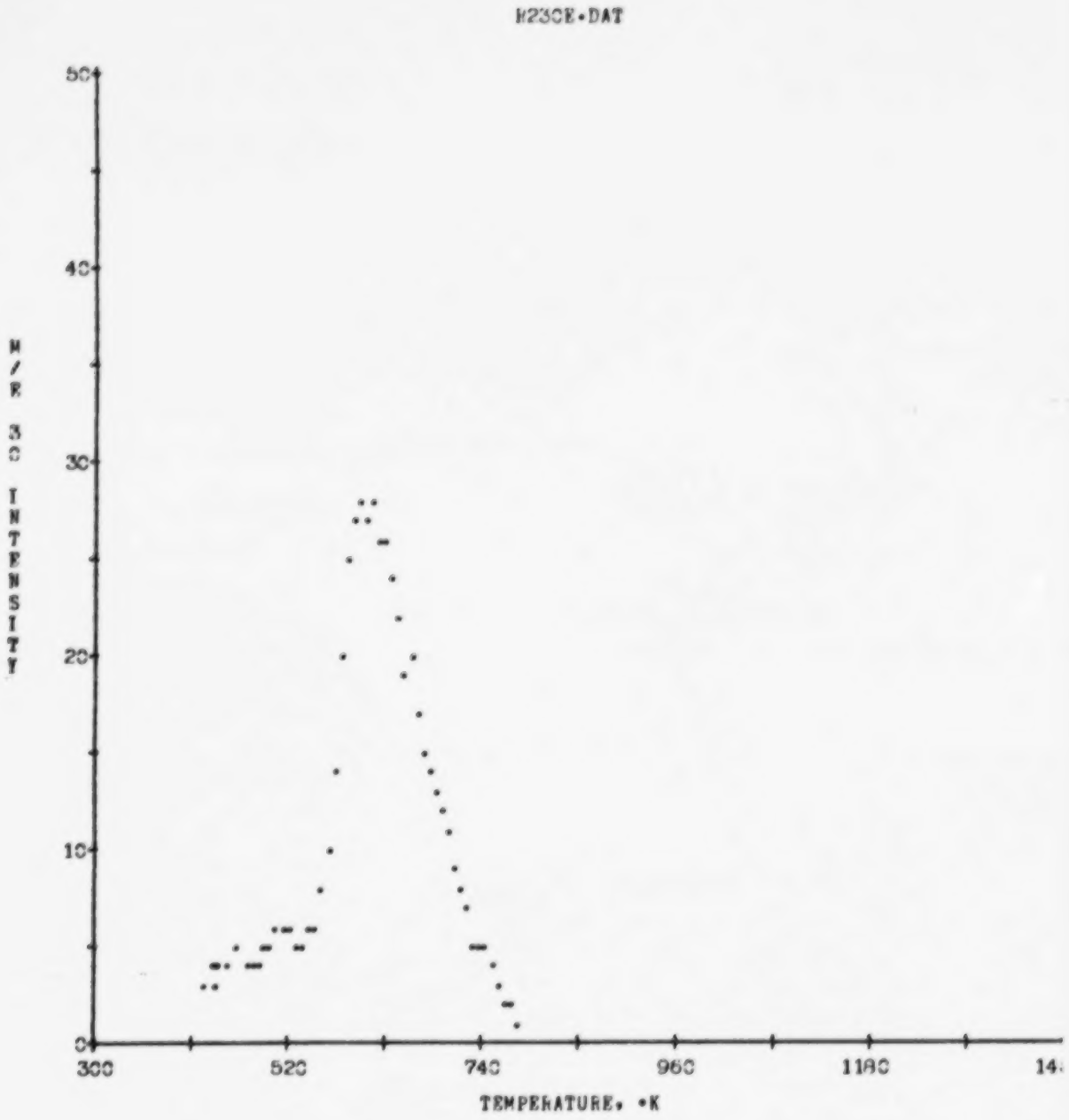

SYMBOL	NO.PTS.	LEGEND
.	53	NO+ FROM SRI COKE #1C, AR AT 200 CC/MIN, 30°/MIN

Figure 100

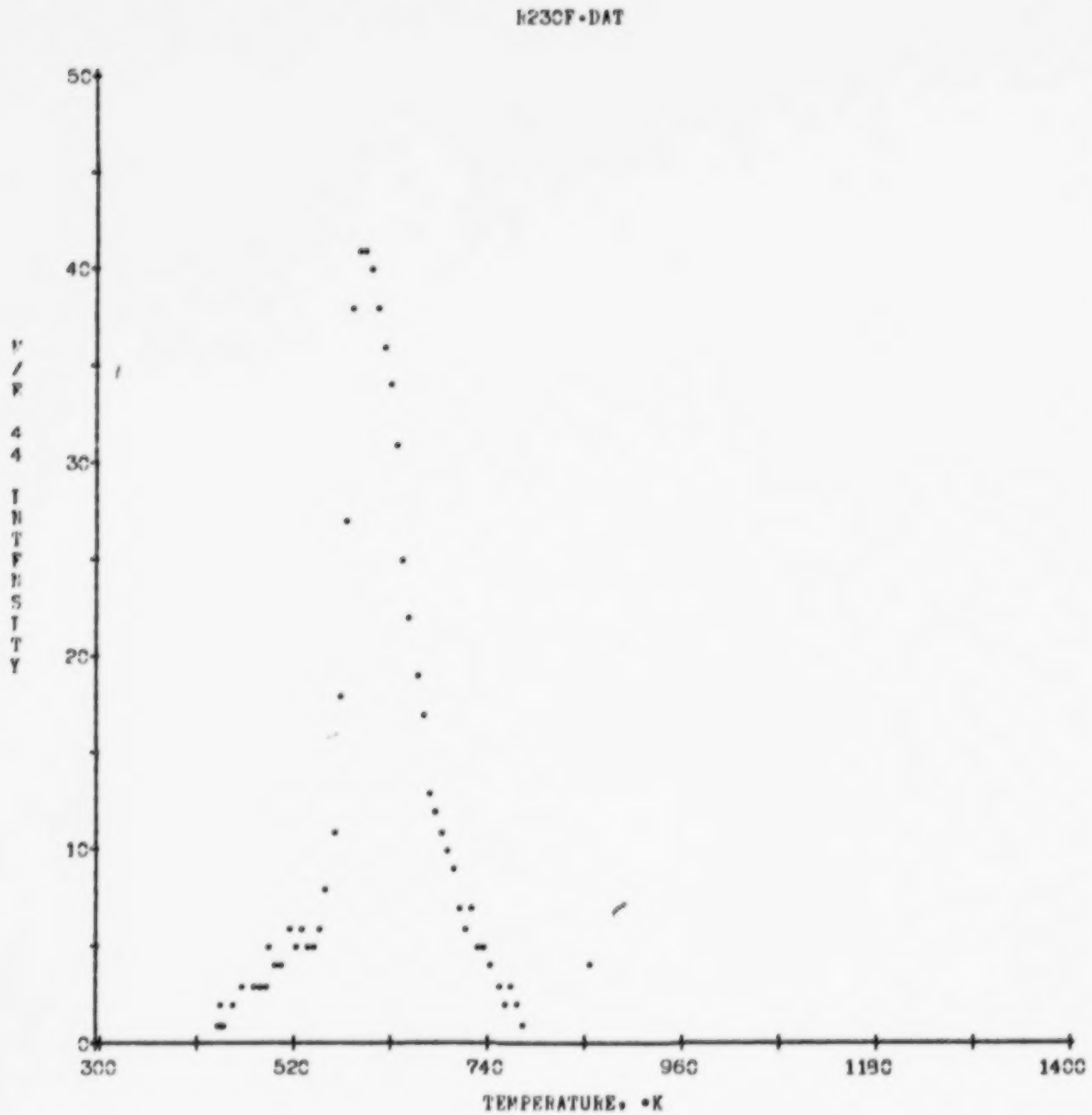

SYMBOL NO.PTS. LEGEND

. 52 CO2+ FROM SHI COKE #1C, AR AT 200 CC/MIN, 3C°/MIN

Figure 101

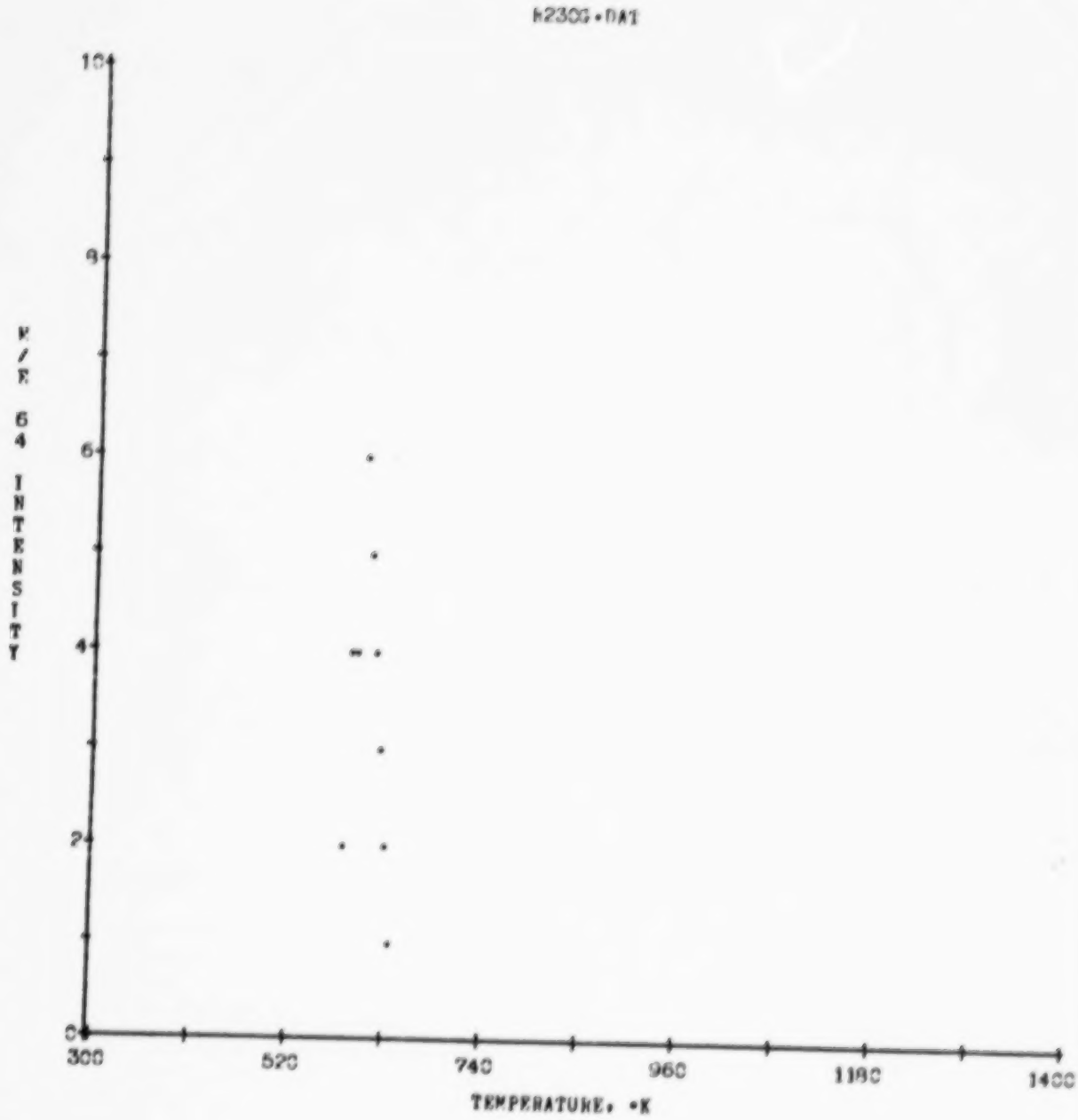

SYMBOL	NO.PTS.	LEGEND
•	9	SO2+ FROM SRI COKE #10, AR AT 200 CC/MIN, 30°/MIN

Figure 102

APPENDIX C: Gaseous Evolution Data for Reducing Reactions

Table XI: Peak Temperatures for Reducing Atmospheres of Hydrogen at 10 atm.

Figures: 103 - 128

TABLE XI

Peak Temperatures in Reducing Atmospheres of Hydrogen at 10 atm Pressure

Solid Reactant Coal	Heating Rate °/min	Temperature of Observed Peaks, °K CH_4	H_2O	C_2H_6	H_2S
SRI-5	15	1148	571		
			685		
			718		
			827		
	40	1200	630	619	
		1322	749	772	
			796		
			888		
SRI-7	15	1068	597		
		1193	773		
	40	814*	640	614	776
		866	817	800	
		1120			
SRI-10	15		585		
			742		
			872		
	40		632	608	
			780	761	
			877		
Anthracite	15		581		
			784		
	40	1169	635		
			826		
Lignite	15	972	577		
			803		
	40	1064	641	610	
			893		

* Uncertain

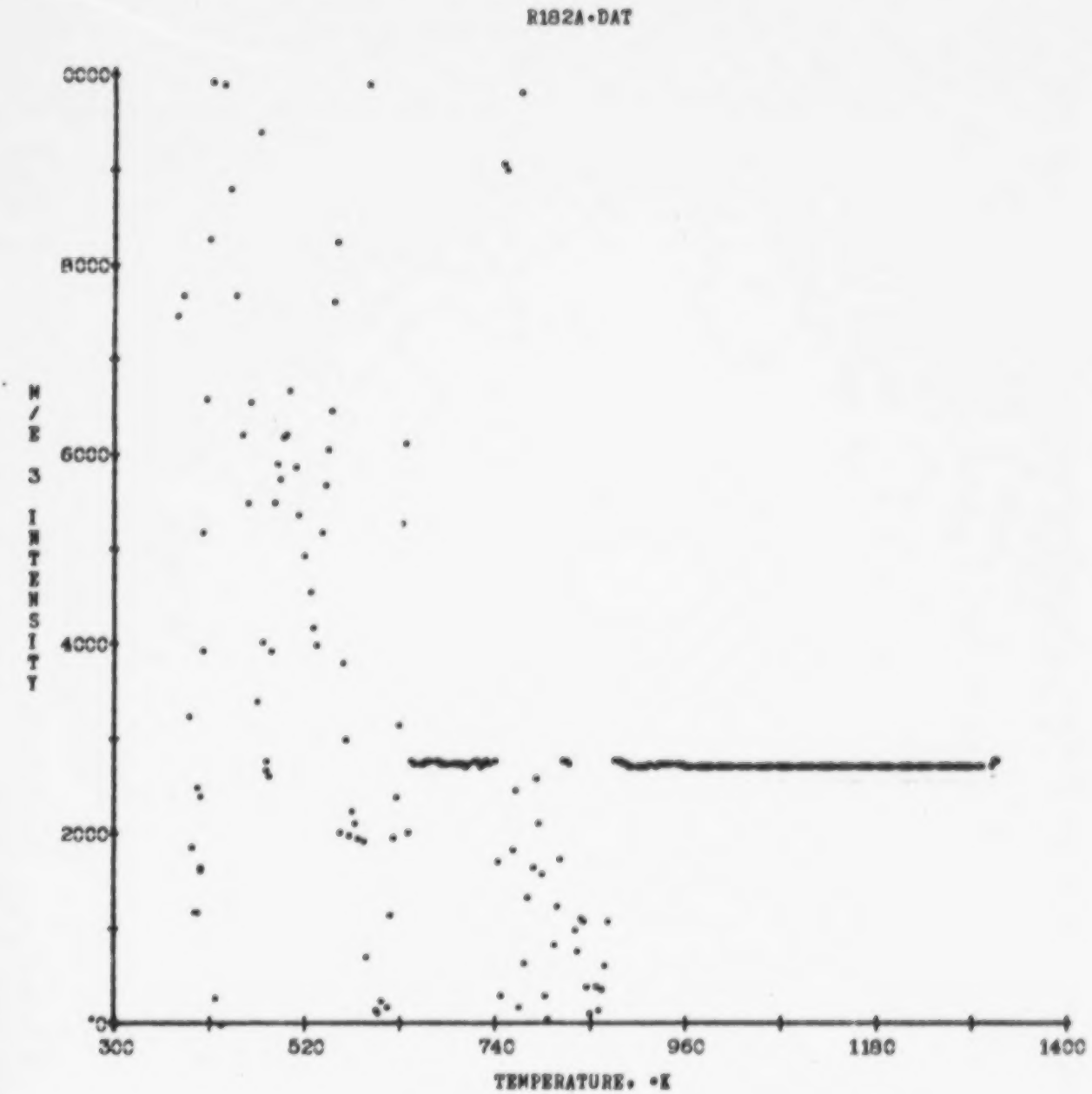

SYMBOL	NO.PTS.	LEGEND
.	278	H3+ FROM SRI COAL #5, H2 CARRIER GAS AT 200 CC/MIN, 40°/MIN

Figure 103

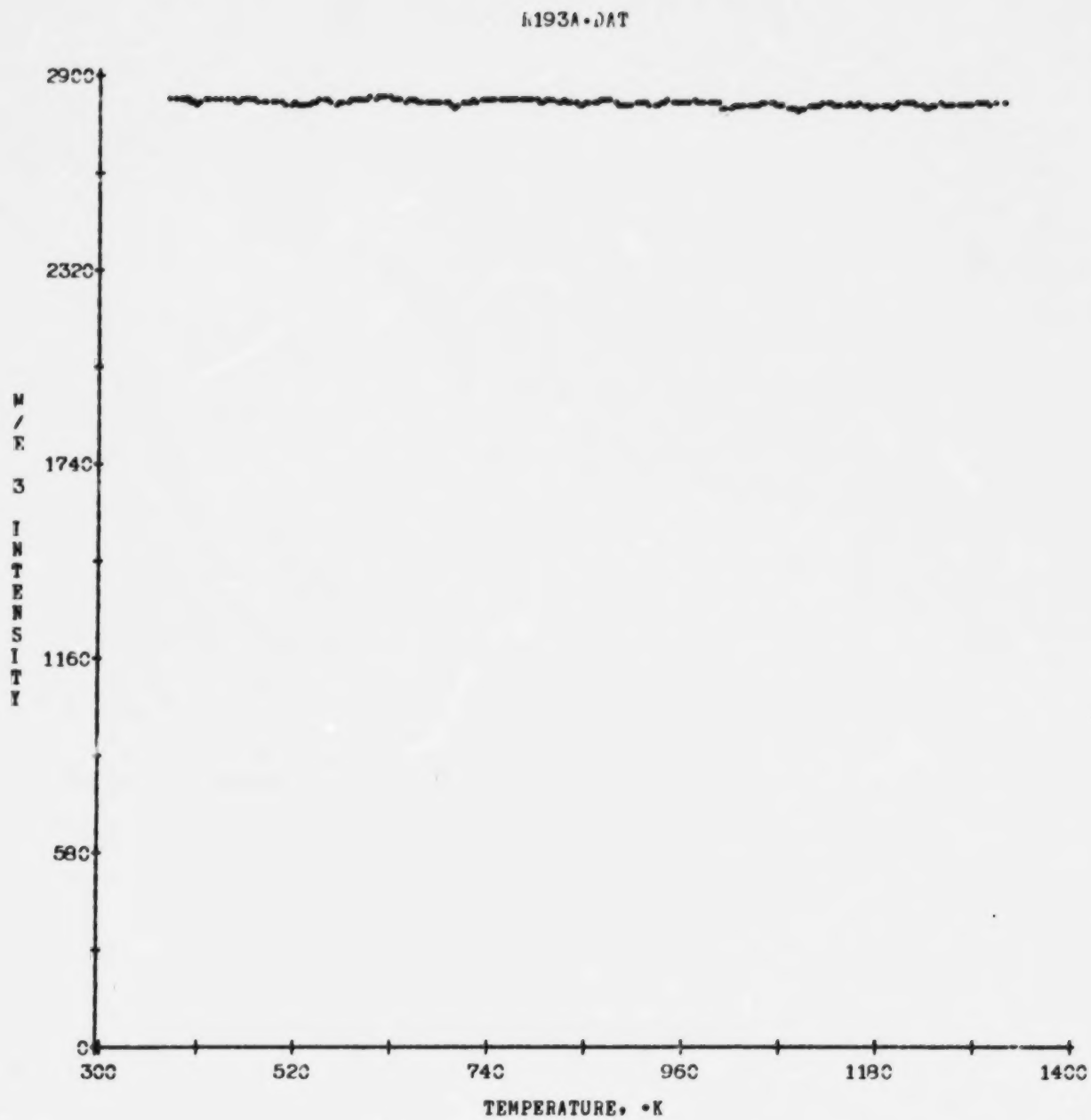

SYMBOL NO.PTS. LEGEND

. 234 H3+ FROM SRI COAL #5, H2 CARRIER GAS AT 2000 CC/MIN, 40°/MIN, 10 ATM

Figure 104

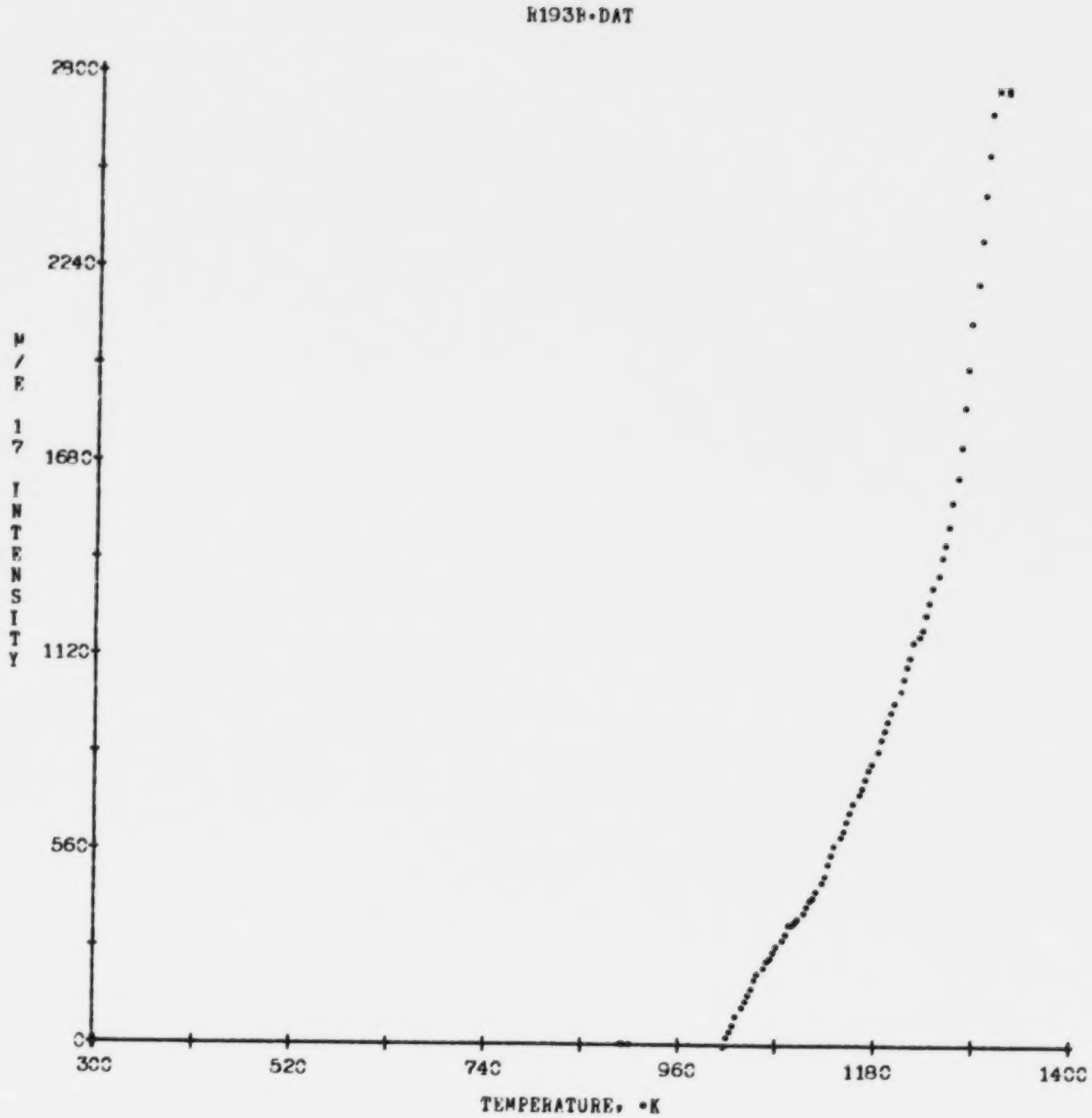

SYMBOL	NO.PTS.	LEGEND
•	79	CH5+ FROM SRI COAL #5, H2 CARRIER GAS AT 2000 CC/MIN, 40•/MIN, 10 ATM

Figure 105

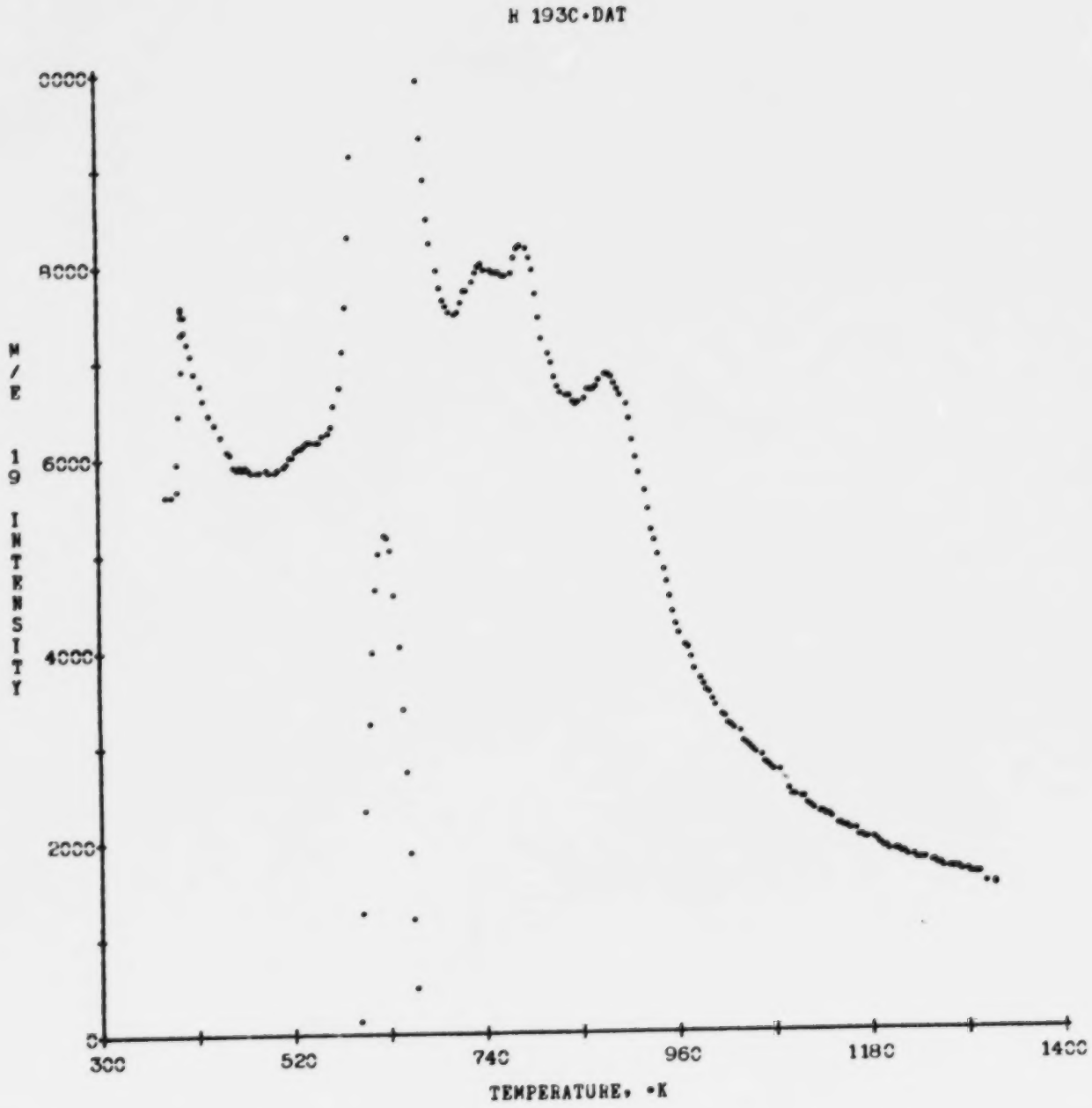

SYMBOL NO.PTS. LEGEND

. 234 H3O+ FROM SRI COAL #5, H2 CARRIER GAS AT 2000 CC/MIN, 40°/MIN, 10 ATM

Figure 106

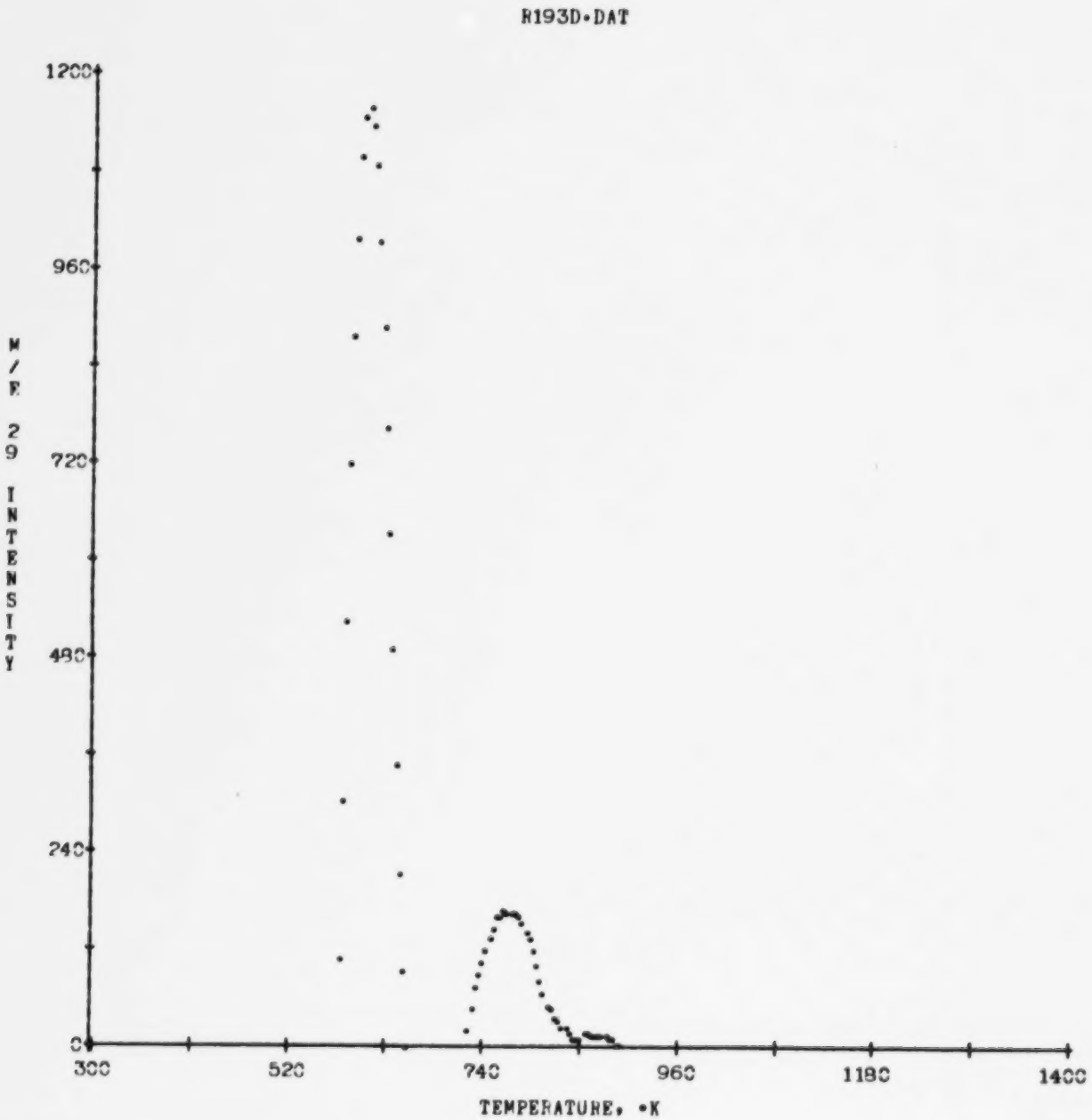

SYMBOL NO.PTS. LEGEND

. 63 C2H5+ FROM SRI COAL #5, H2 CARRIER GAS AT 2000 CC/MIN, 40°/MIN, 10 ATM

Figure 107

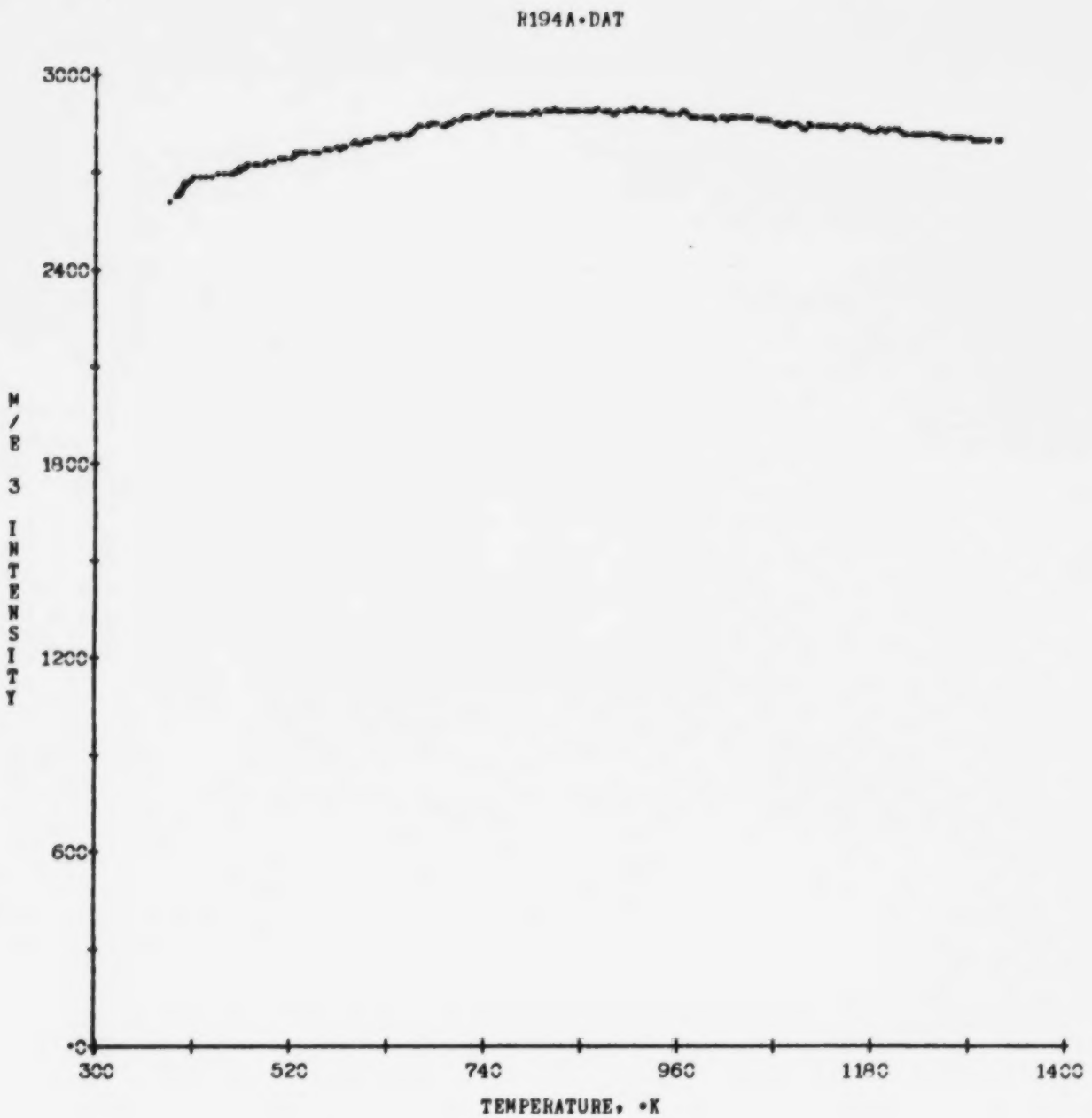

SYMBOL	NO.PTS.	LEGEND
.	235	H3+ FROM SRI COAL #7, H2 CARRIER GAS AT 2000 CC/MIN, 40°/MIN, 10 ATM

Figure 108

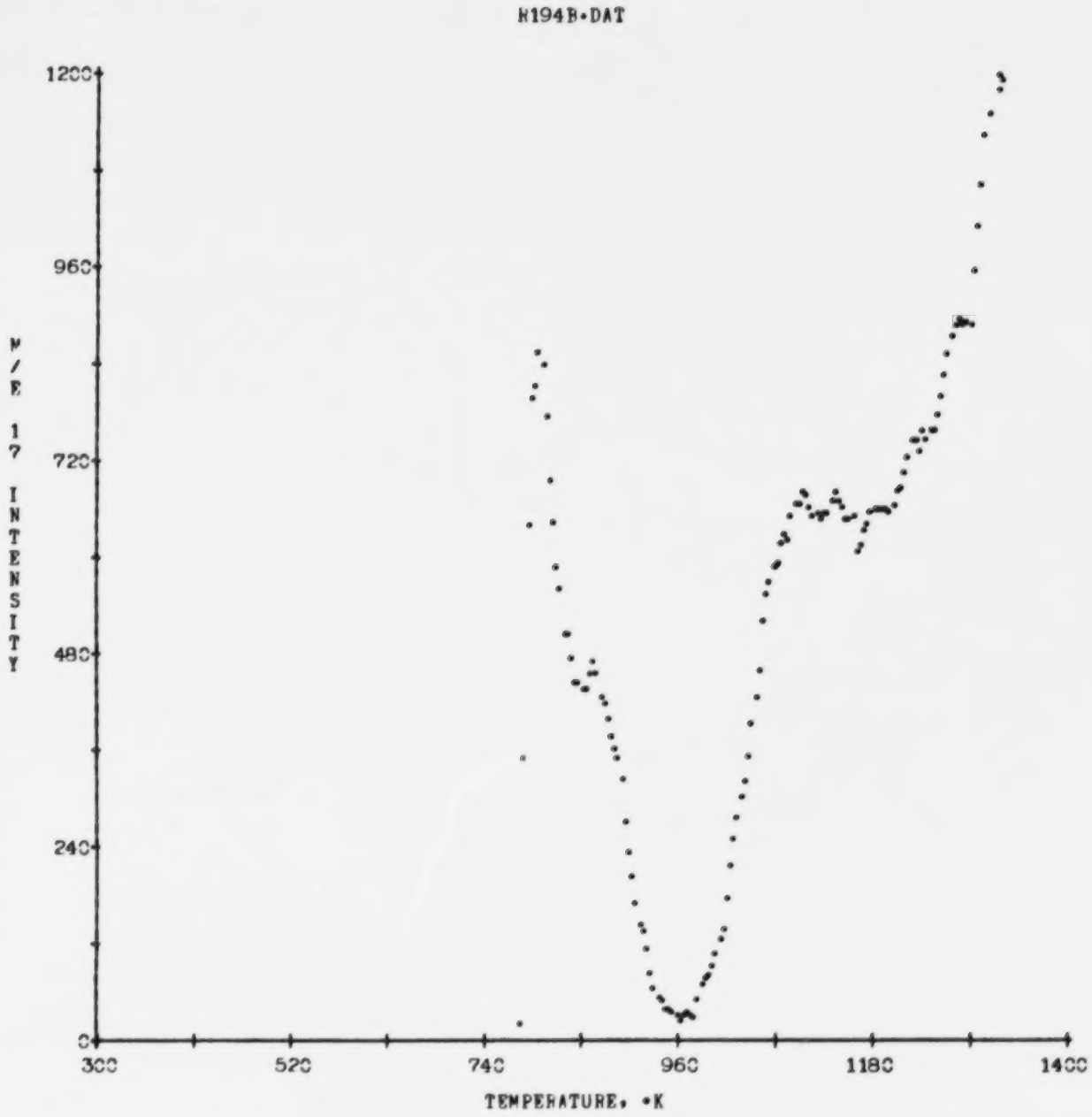

SYMBOL	NO.PTS.	LEGEND
.	134	CH5+ FROM SRI COAL #7, H2 CARRIER GAS AT 2000 CC/MIN, 40°/MIN, 10 ATM

Figure 109

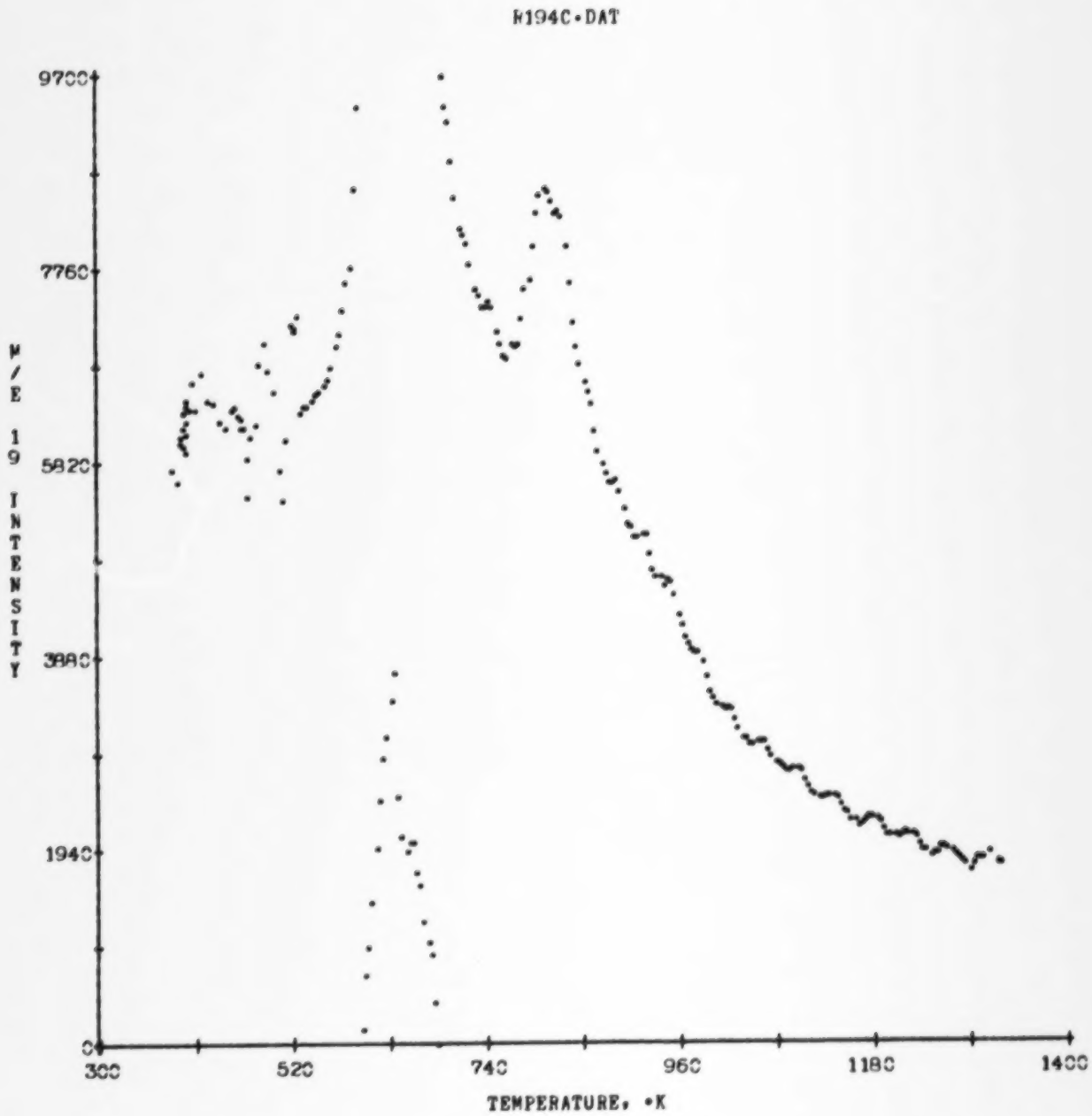

SYMBOL	NO.PTS.	LEGEND
.	234	H3O+ FROM SRI COAL #7, H2 CARRIER GAS AT 2000 CC/MIN, 40°/MIN, 10 ATM

Figure 110

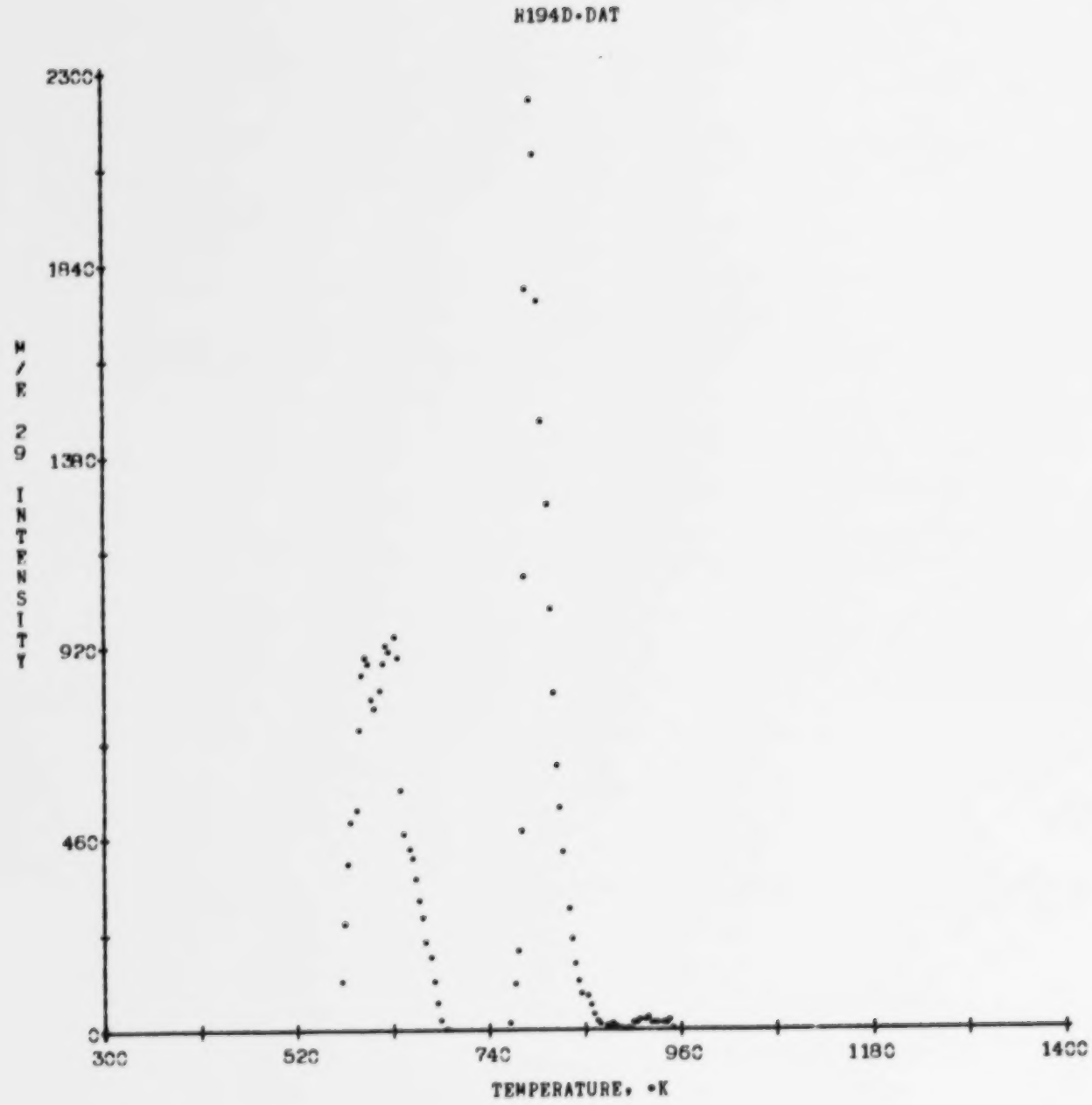

SYMBOL	NO.PTS.	LEGEND
.	77	C2H5+ FROM SRI COAL #7, H2 CARRIER GAS AT 2000 CC/MIN, 40°/MIN, 10 ATM

Figure 111

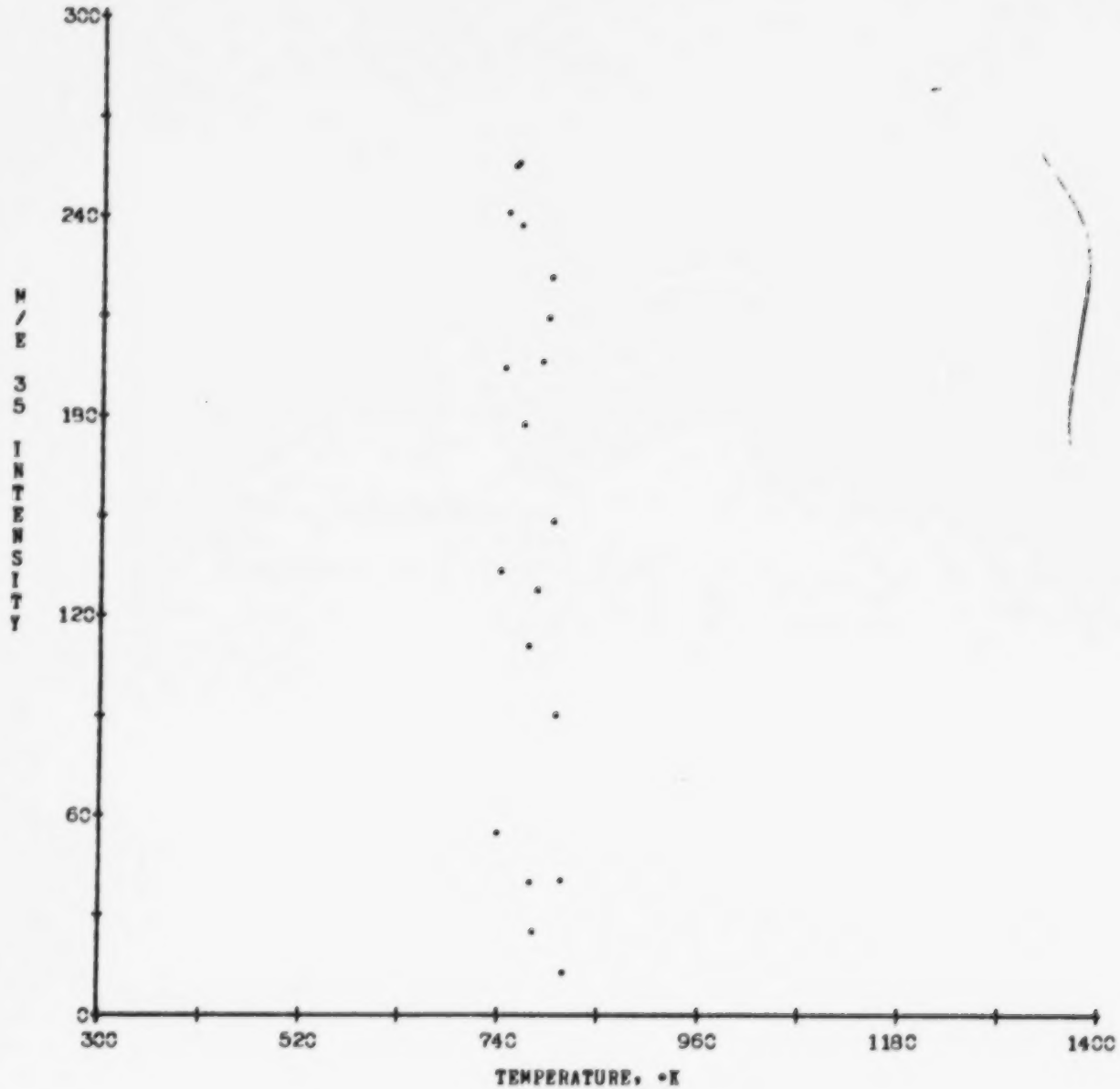

SYMBOL	NO. PTS.	LEGEND
•	19	H3S+ FROM SRI COAL #7, H2 CARRIER GAS AT 2000 CC/MIN, 40°/MIN, 10 ATM

Figure 112

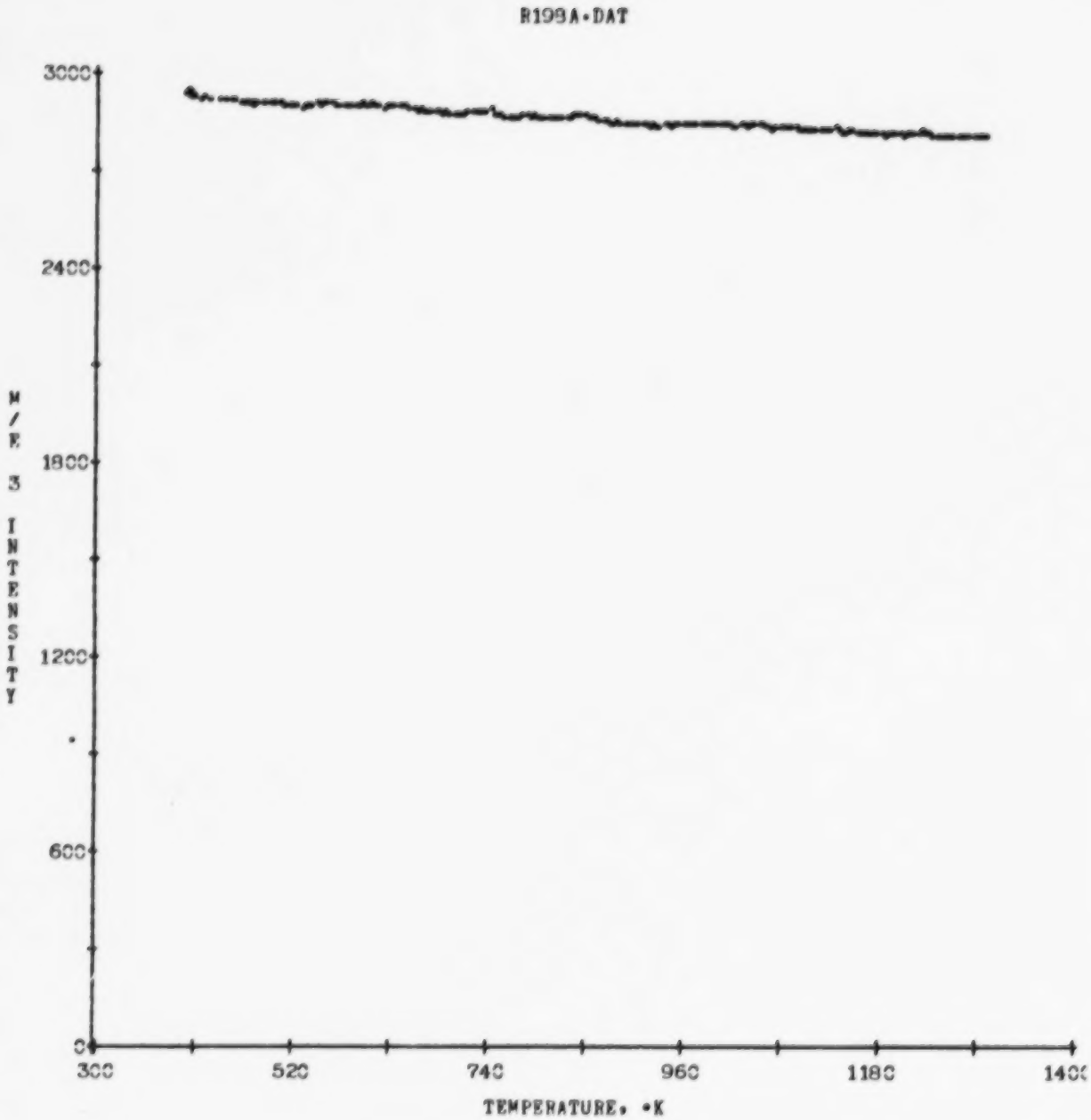

SYMBOL NO.PTS. LEGEND

. 231 H3+ FROM SHI COAL #10, H2 CARRIER GAS AT 2000 CC/MIN, 40°/MIN, 10 AT

Figure 113

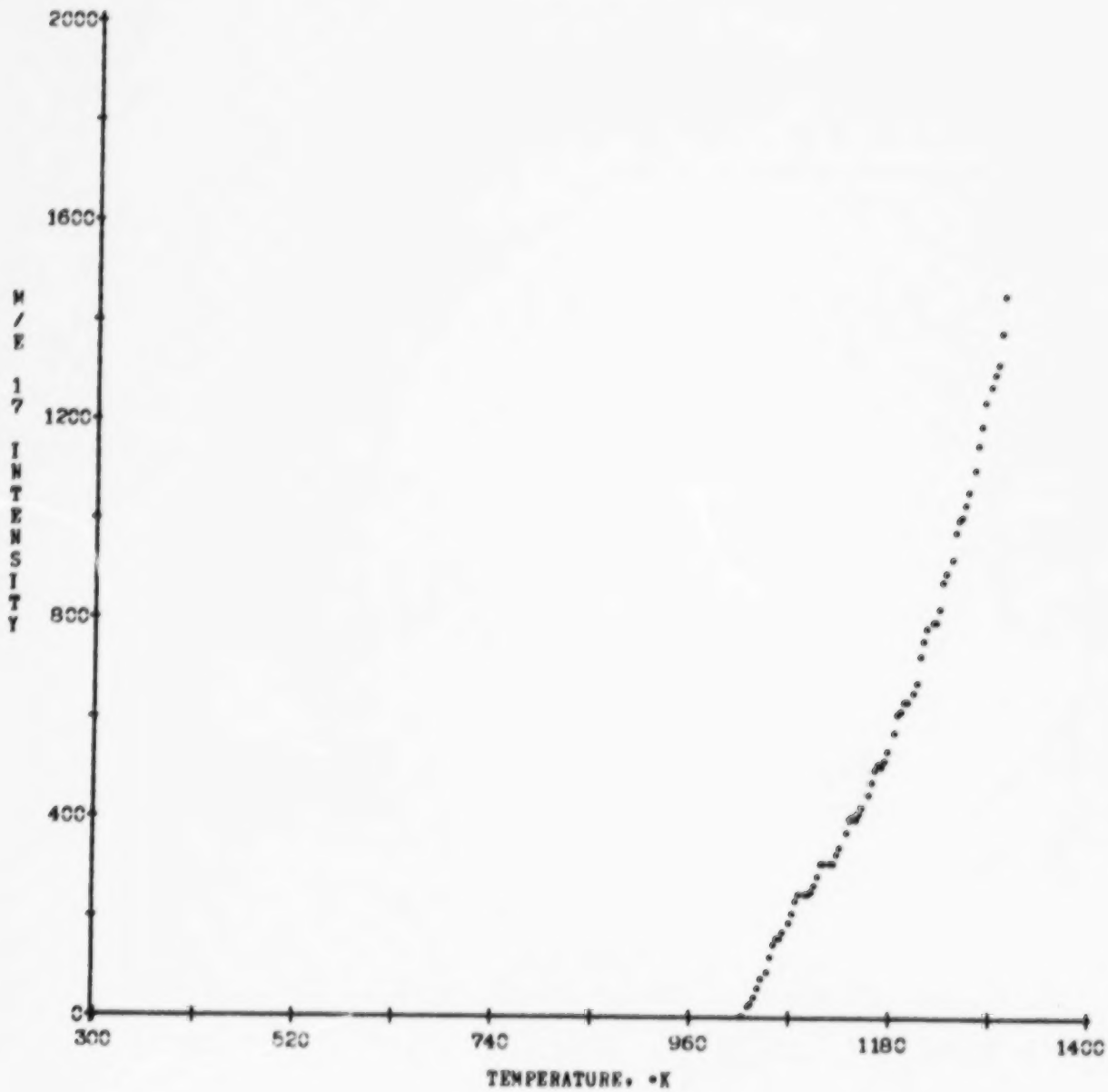

SYMBOL	NO.PTS.	LEGEND
•	70	CH5+ FROM SRI COAL #1C, H2 CARRIEN GAS AT 2000 CC/MIN, 40°/MIN,1C ATM

Figure 114

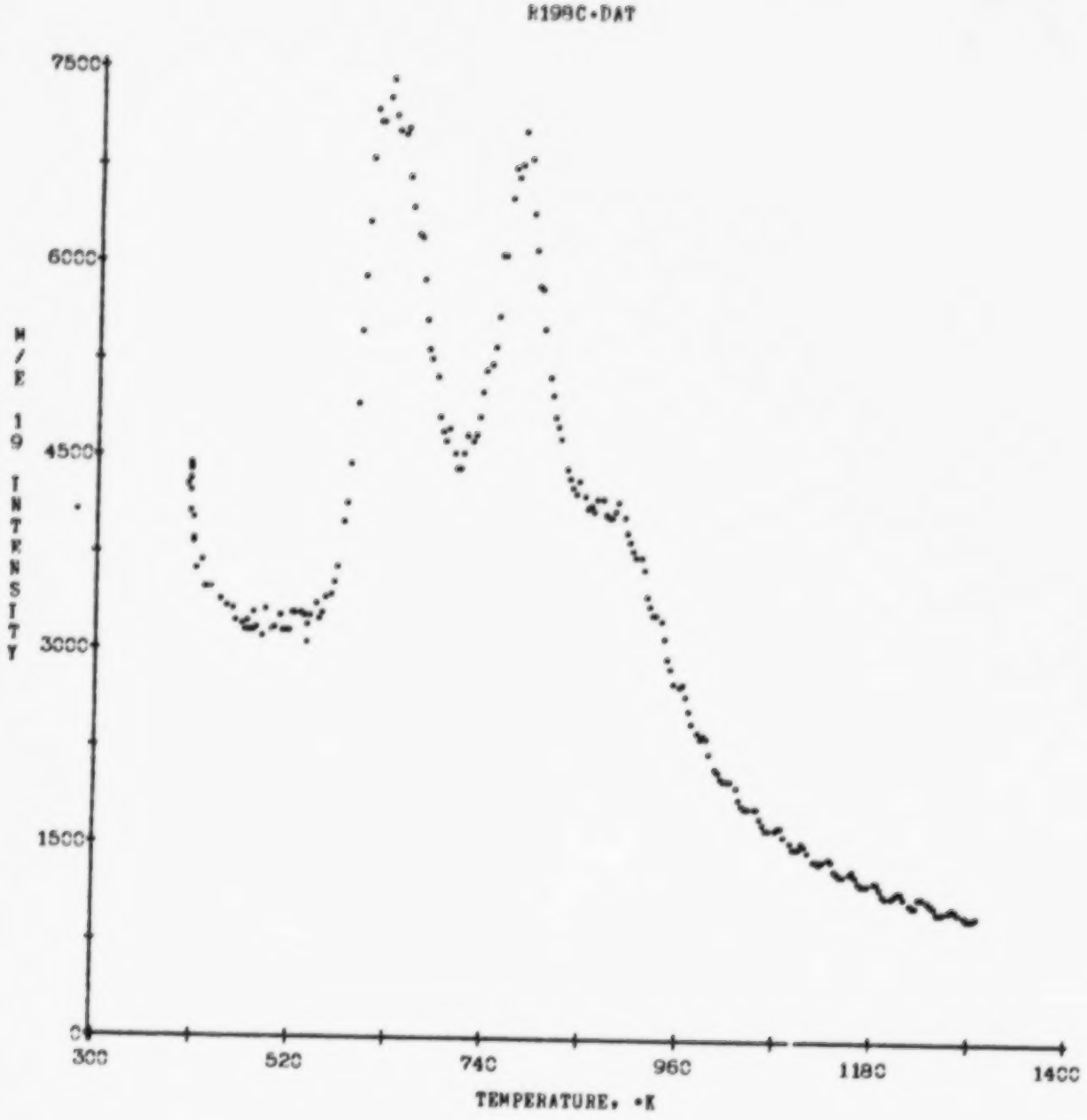

SYMBOL NO.PTS. LEGEND

. 231 H3O+ FROM SRI COAL #1C , H2 CARRIER GAS AT 2000 CC/MIN,4C°/MIN, 1C ATM

Figure 115

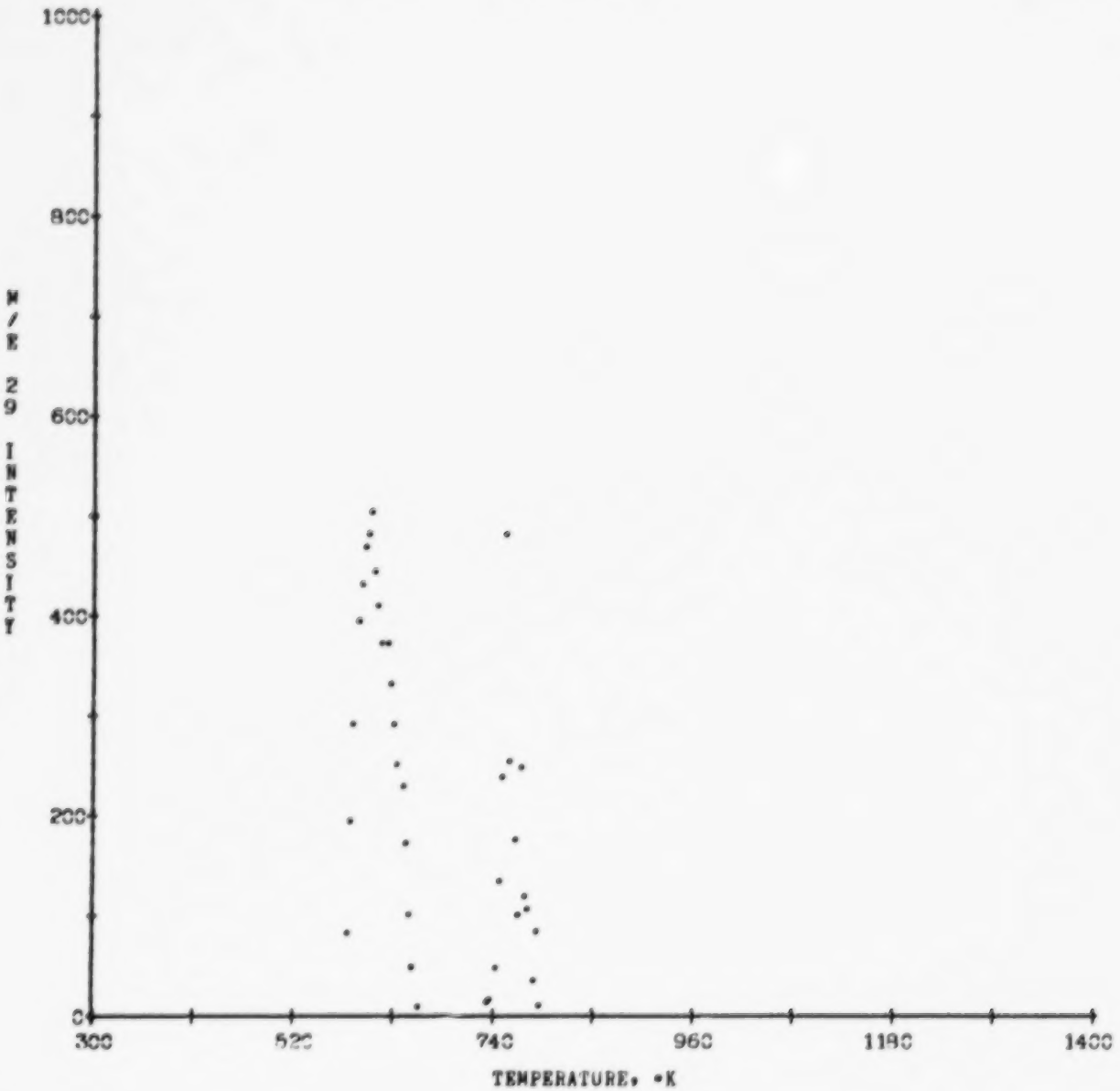

SYMBOL	NO.PTS.	LEGEND
.	35	C2H5+ FROM SRI COAL #10, H2 CARRIER GAS AT 2000 CC/MIN, 40°/MIN, 10 ATM

Figure 116

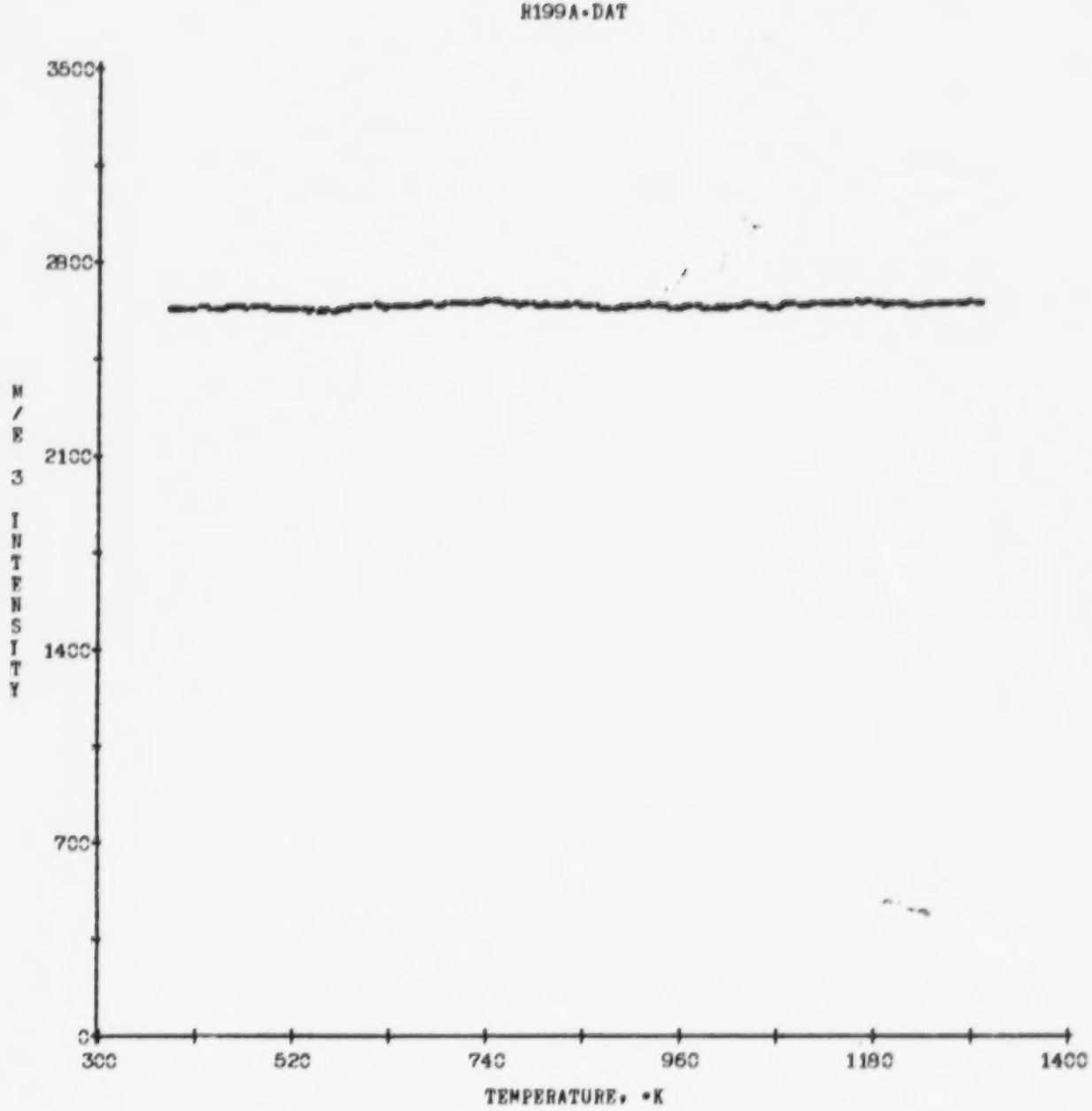

SYMBOL	NO.PTS.	LEGEND
.	230	H3+ FROM SRI ANTHR, H2 CARRIER GAS AT 2000 CC/MIN, 40°/MIN, 10 ATM

Figure 117

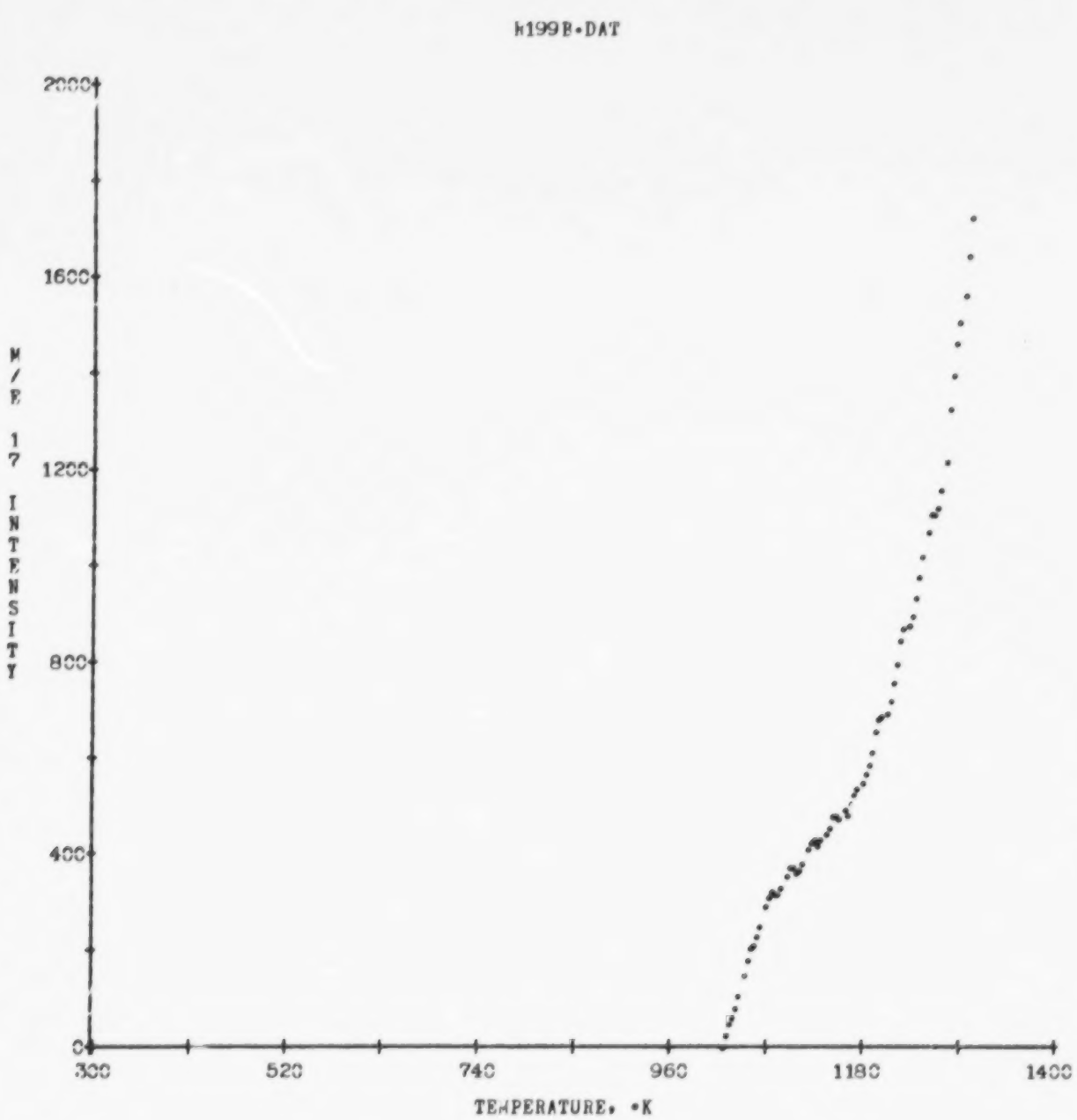

SYMBOL NO.PTS. LEGEND

. 70 CH5+ FROM SRI ANTHR, H2 CARRIER GAS AT 2000 CC/MIN, 40°/MIN, 10 ATM

Figure 118

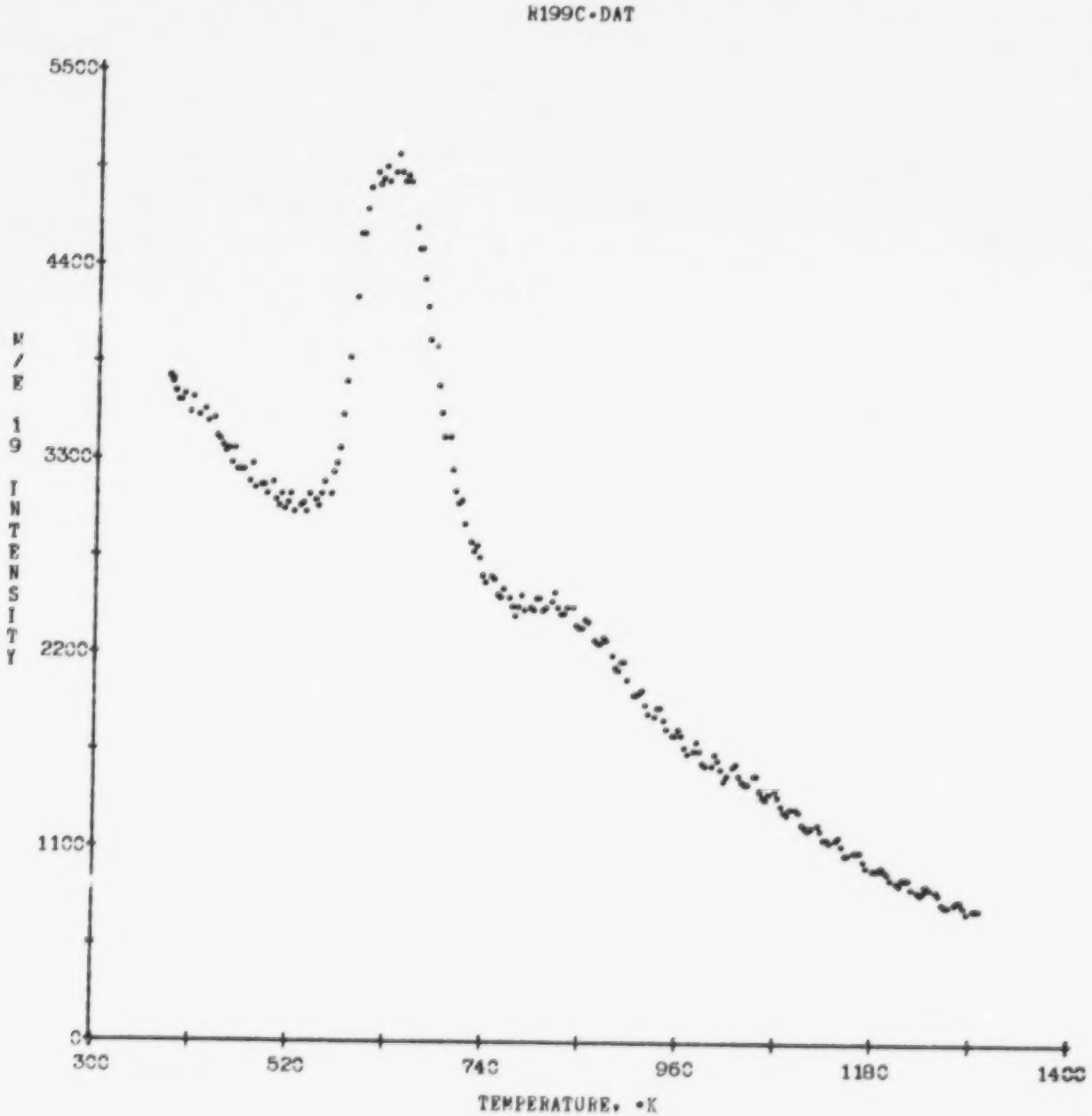

SYMBOL	NO.PTS.	LEGEND
.	230	H3O+ FROM SRI ANTHR, H2 CARRIER GAS AT 2000 CC/MIN, 40°/MIN, 10 ATM

Figure 119

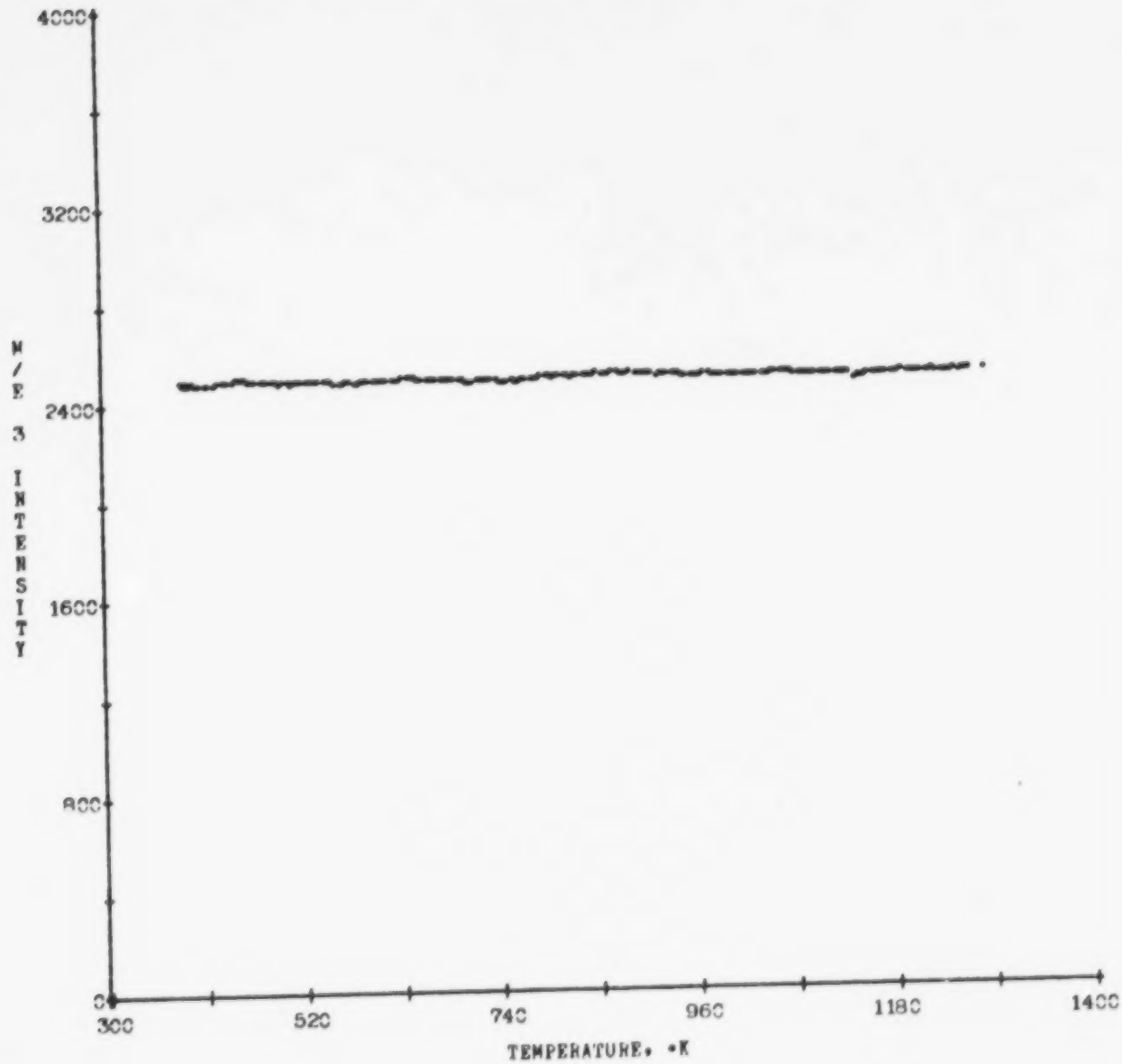

SYMBOL NO.PTS. LEGEND

. 216 H3+ FROM SHI LIG, H2 CARRIER GAS AT 2000 CC/MIN, 40°/MIN, 10 ATM

Figure 120

M201B.DAT

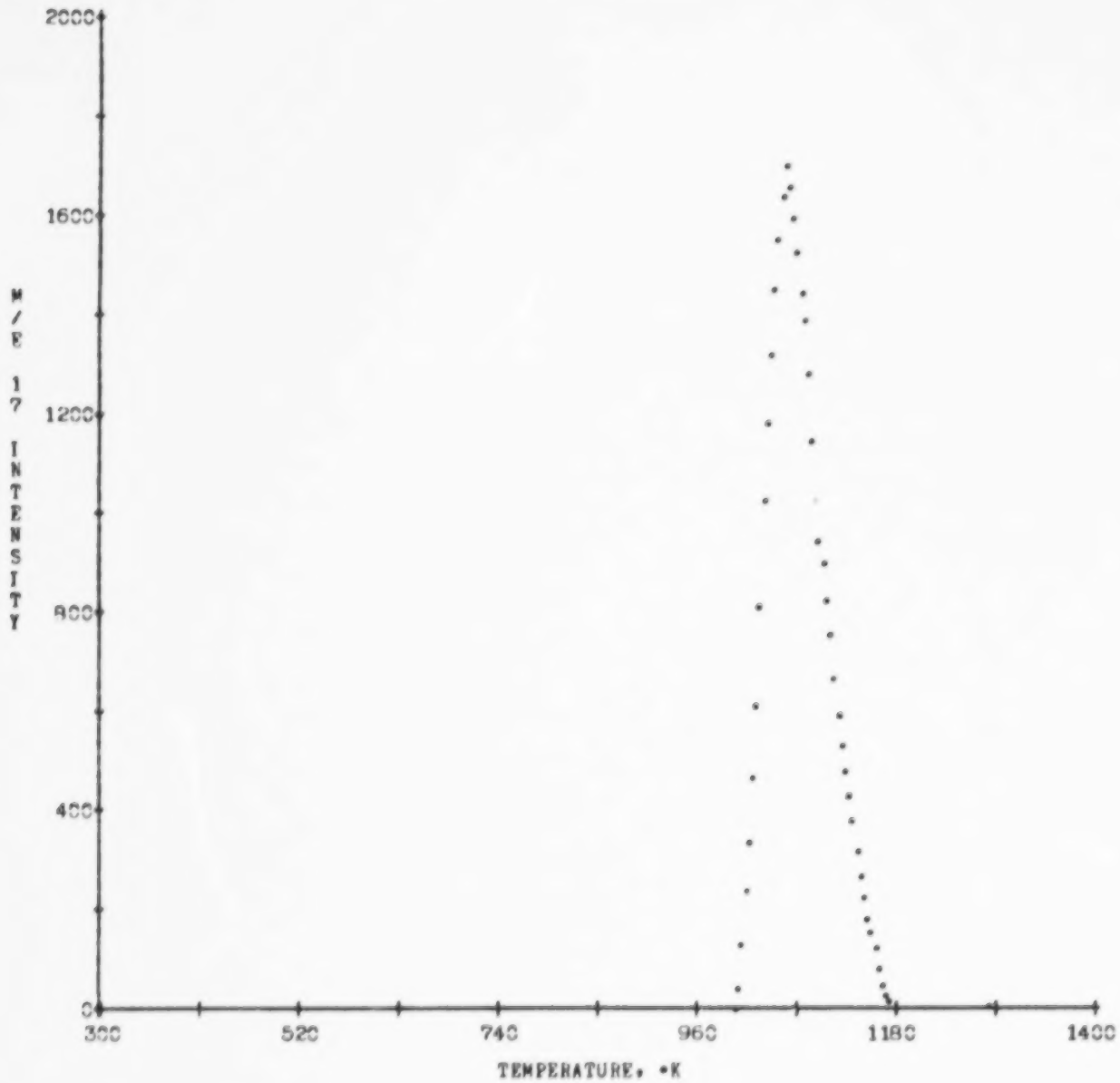

SYMBOL	NO.PTS.	LEGEND
.	44	CH5+ FROM SRI LIG , H2 CARRIER GAS AT 2000 CC/MIN, 40°/MIN, 10 ATM

Figure 121

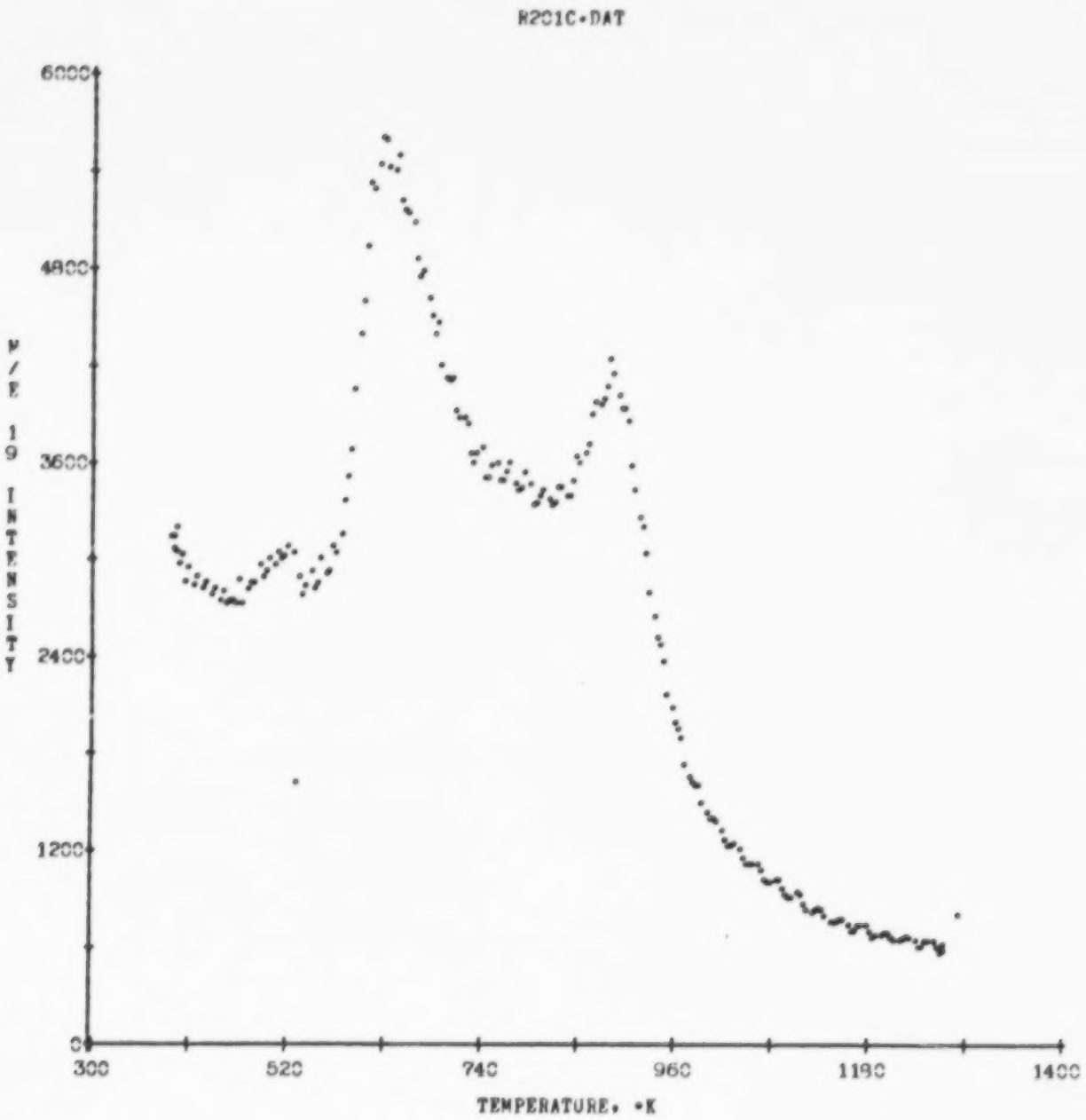

SYMBOL NO.PTS. LEGEND

. 216 H3O+ FROM SRI LIG, H2 CARRIER GAS AT 2000 CC/MIN, 40°/MIN, 10 ATM

Figure 122

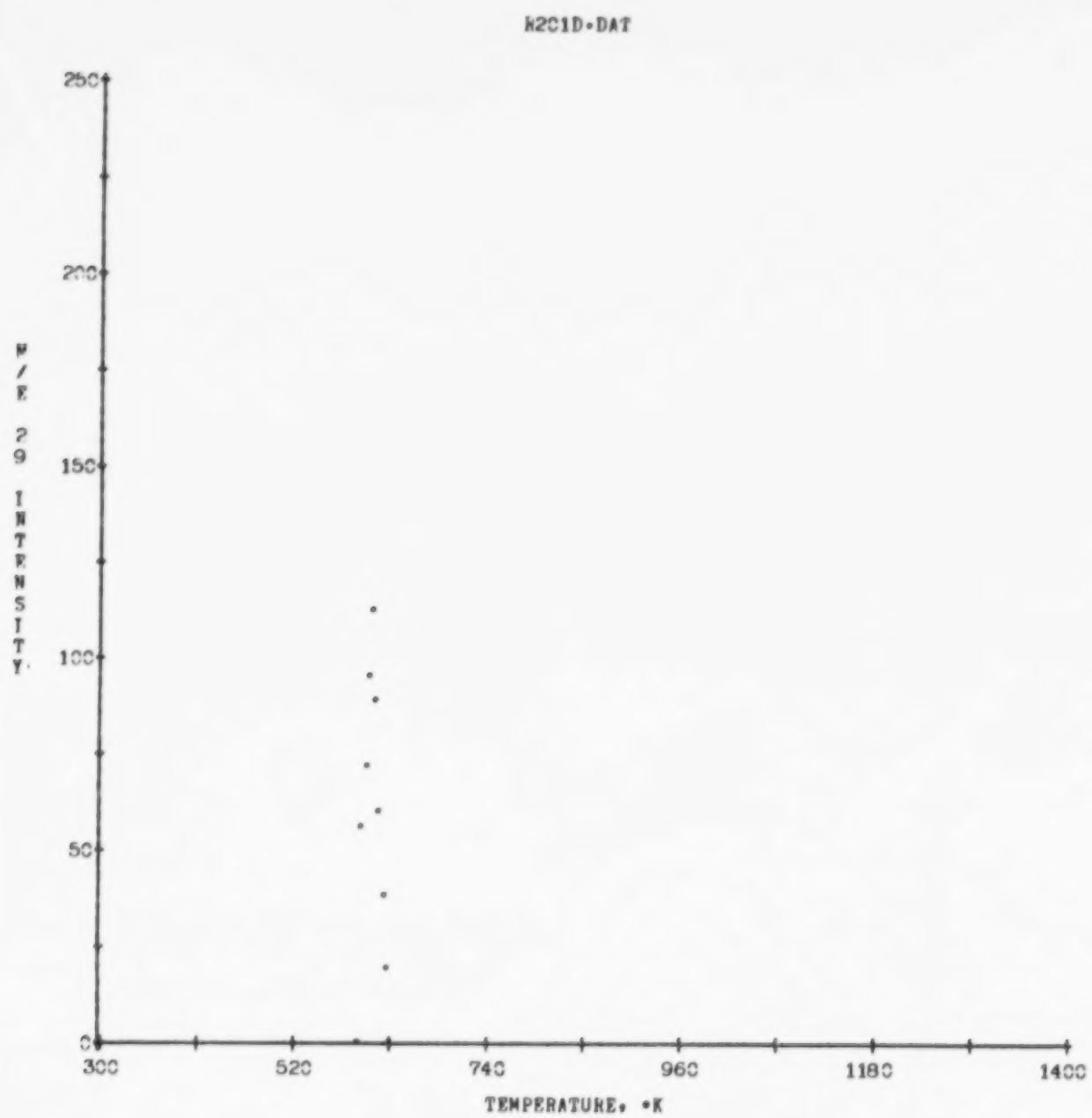

SYMBOL	NO.PTS.	LEGEND
•	10	C2H5+ FROM SRI LIG, H2 CARRIER GAS AT 2000 CC/MIN, 40°/MIN, 10 ATM

Figure 123

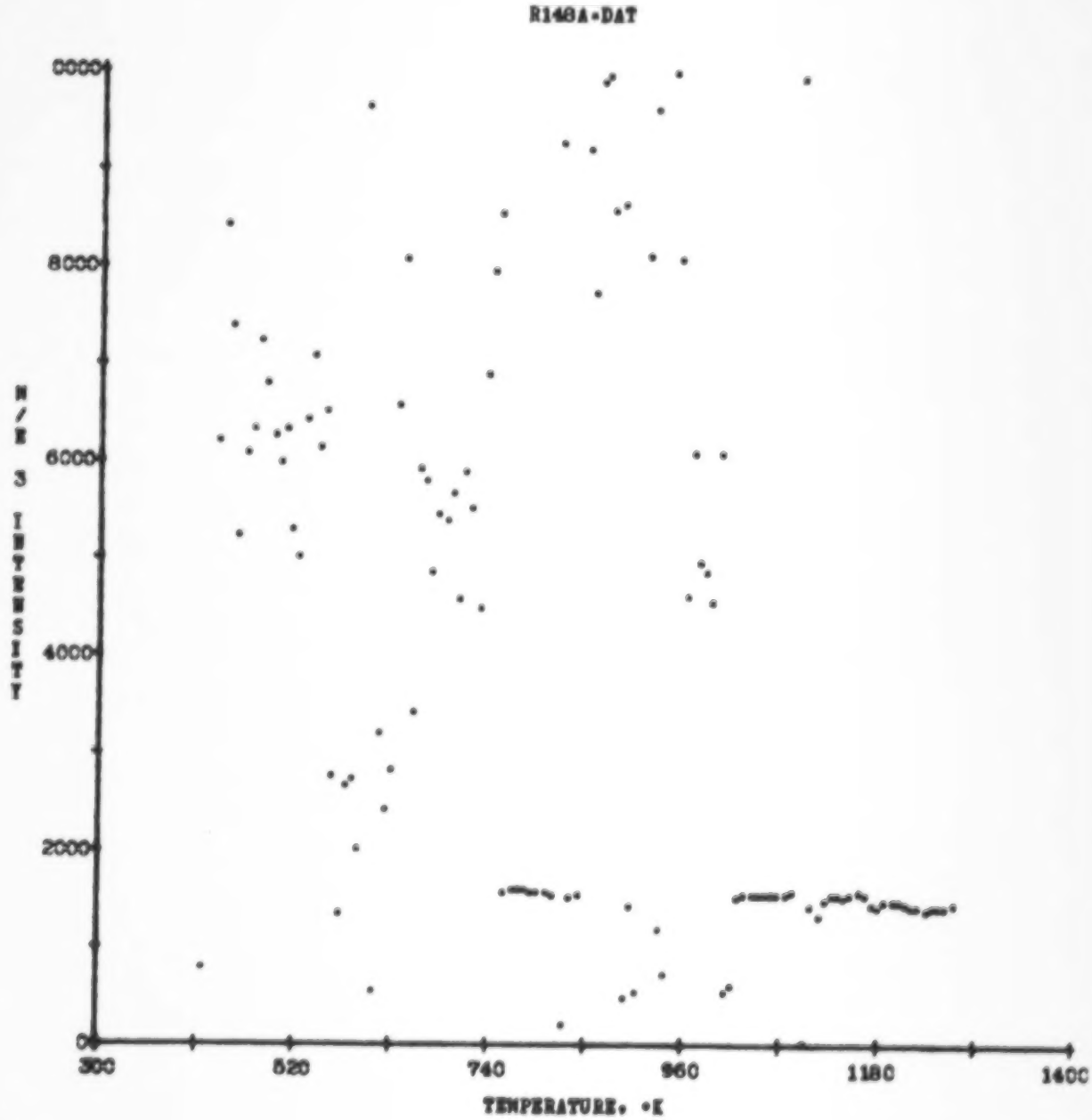

SYMBOL	NO.PTS.	LEGEND
.	112	H3+ FROM SRI COKE #7, H2 CARRIER GAS AT 2000 CC/MIN, 15°/MIN, 10 ATM

Figure 124

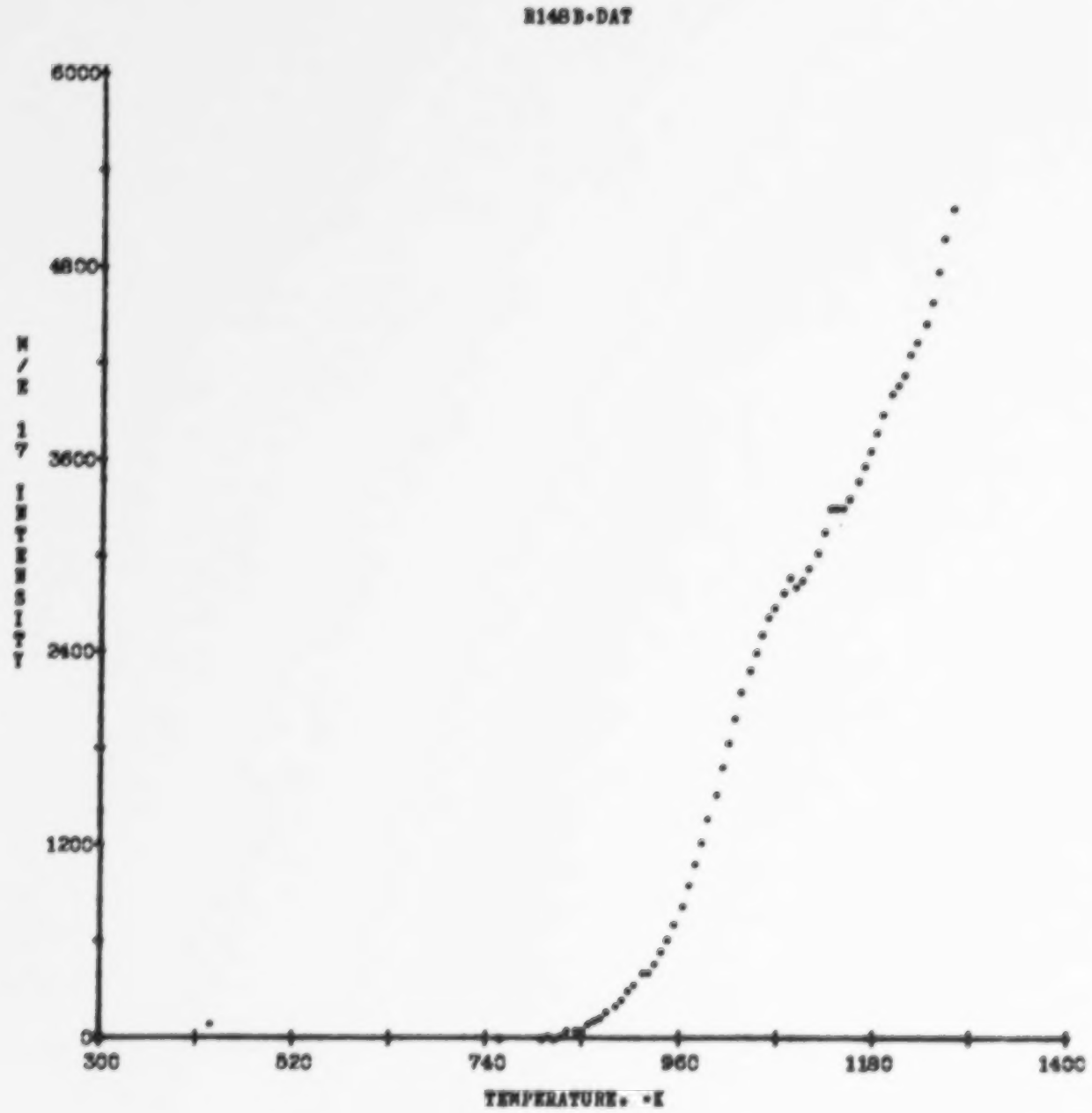

SYMBOL NO-PTS. LEGEND

• 64 CH5+ FROM SRI COKE #7, N2 CARRIER GAS AT 2000 CC/MIN, 15°/MIN, 10 ATM

Figure 125

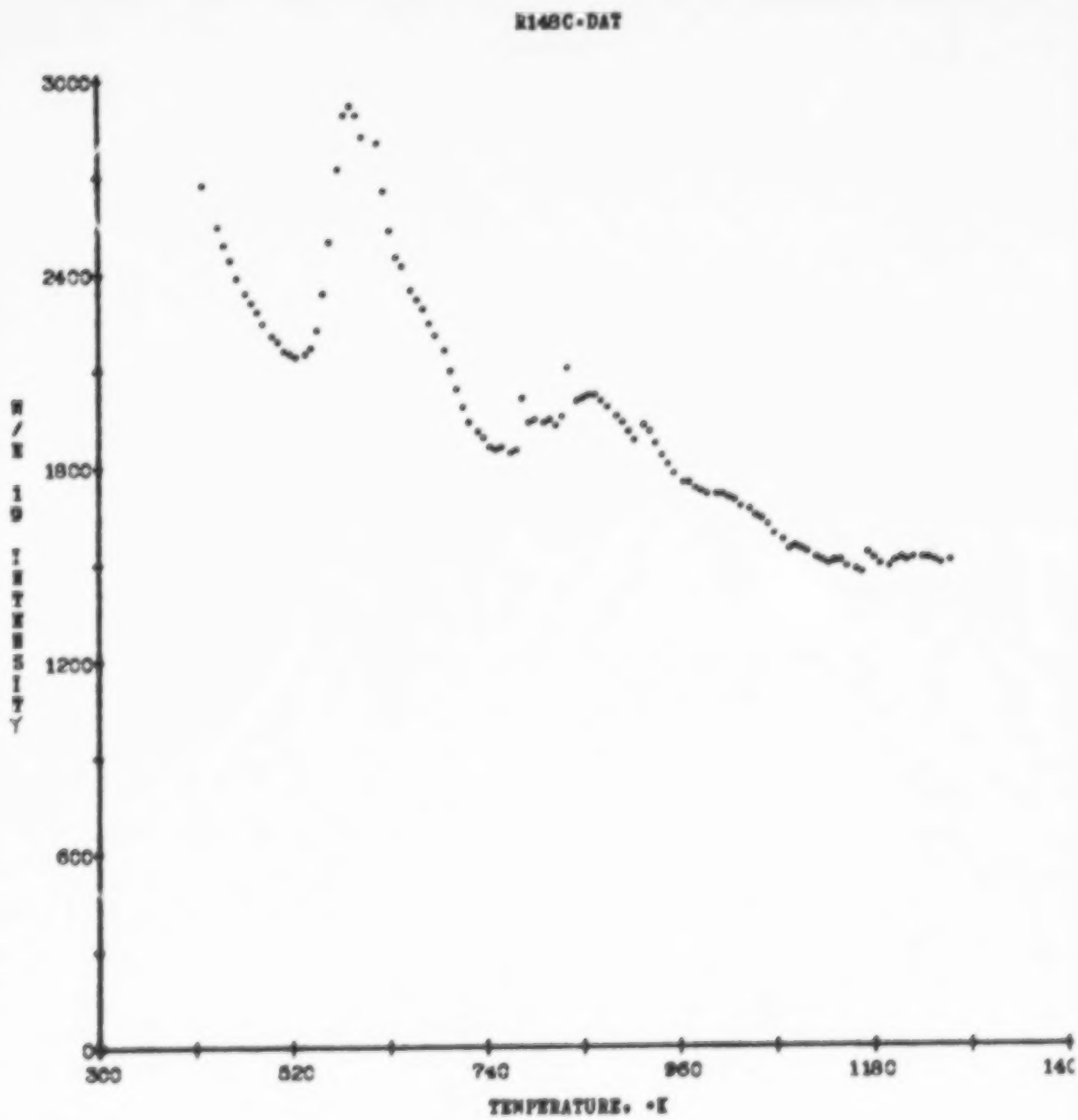

SYMBOL NO.PTS. LEGEND

. 112 H30+ FROM SRI COKE #7, H2 CARRIER GAS AT 2000 CC/MIN, 15°/MIN, 10 AT

Figure 126

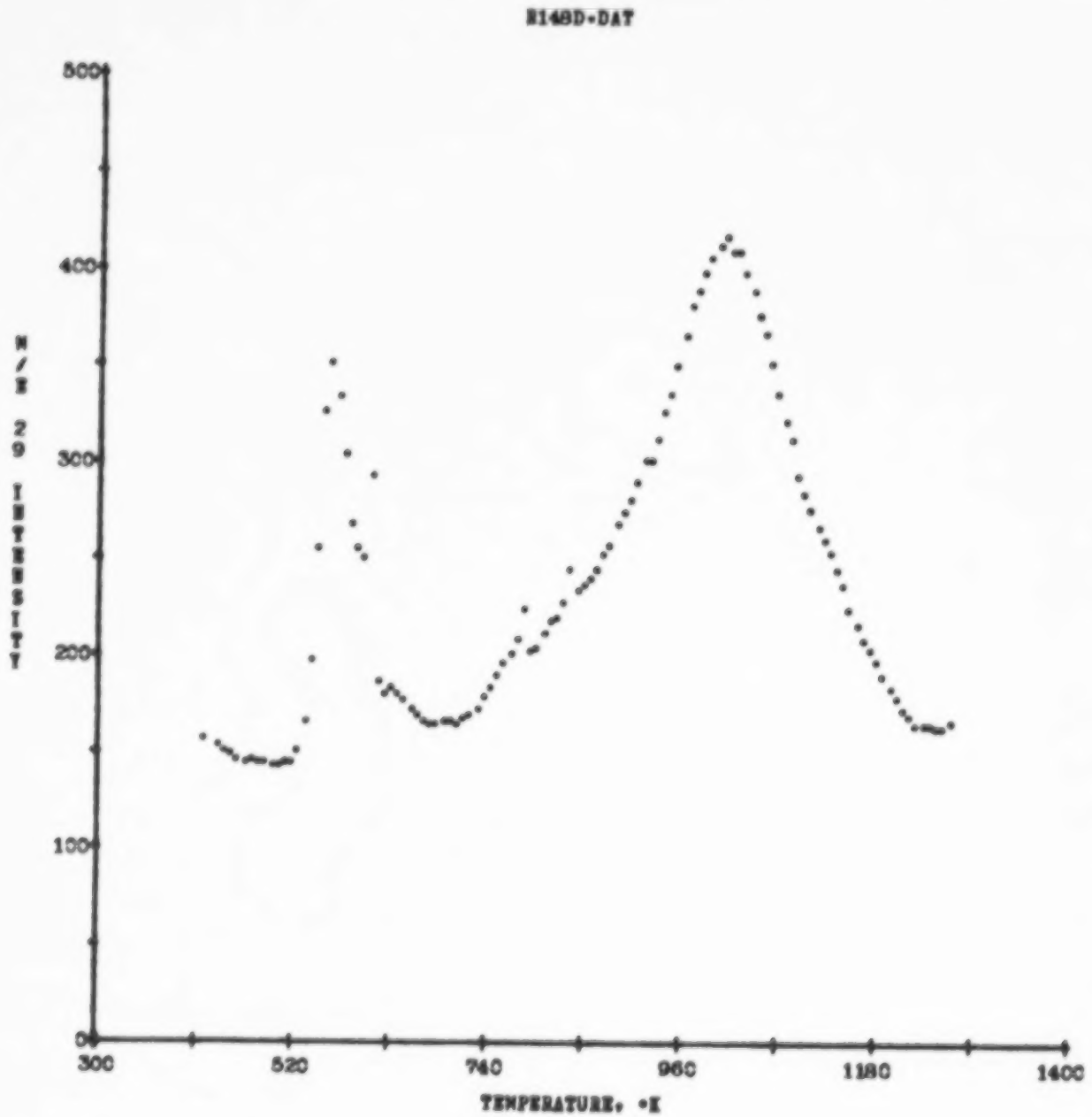

SYMBOL	NO.PTS.	LEGEND
•	113	C2H5+ FROM SRI COKE #7, H2 CARRIER GAS AT 2000 CC/MIN, 15°/MIN, 10 ATM

Figure 127

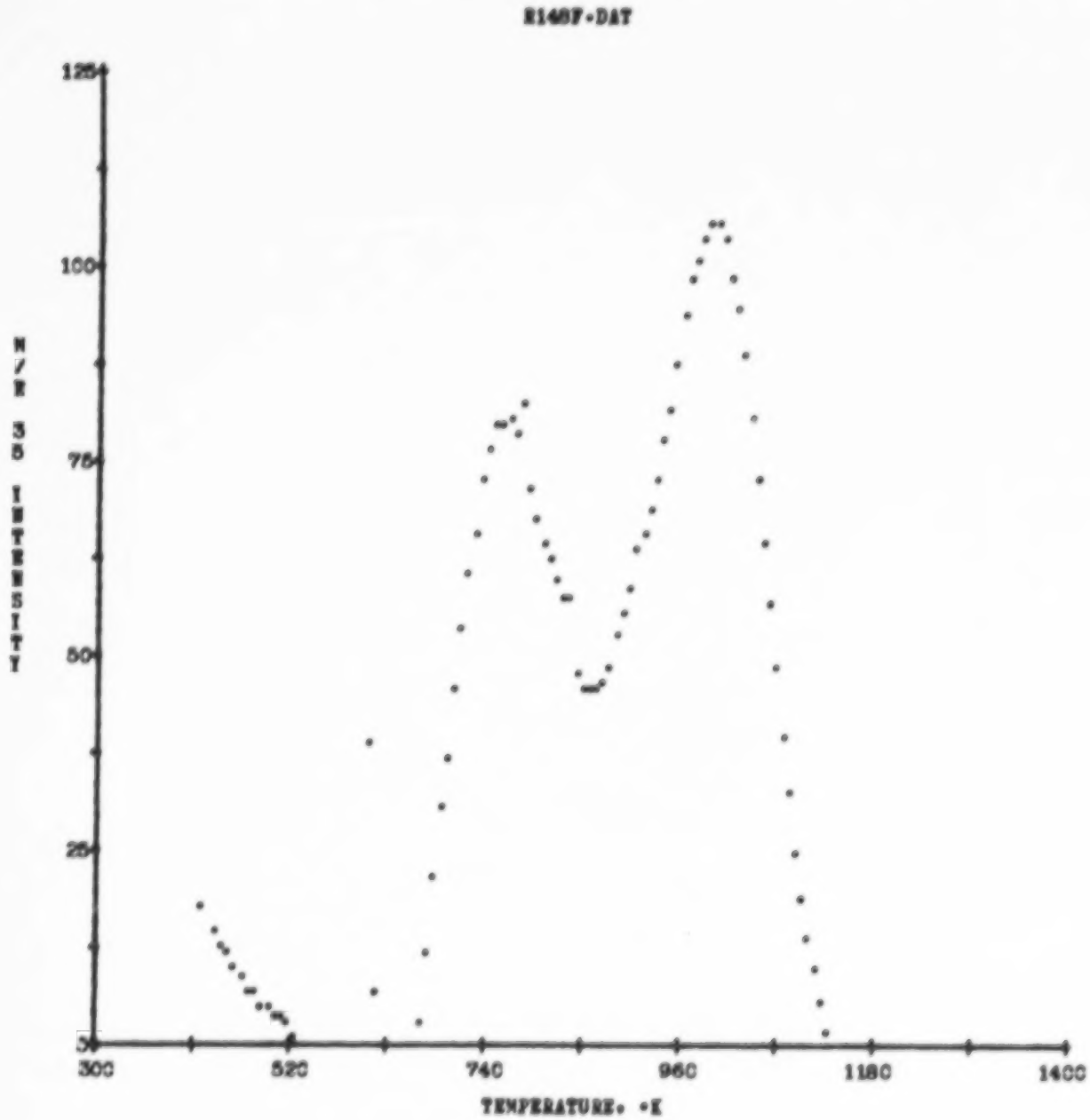

SYMBOL NO.PTS. LEGEND

. 78 H3S+ FROM SRI COKE #7, H2 CARRIER GAS AT 2000 CC/MIN, 15°/MIN, 10 ATM

Figure 128

APPENDIX D: Gaseous Evolution Data for ^{13}C Reactions

Figures: 129 - 132

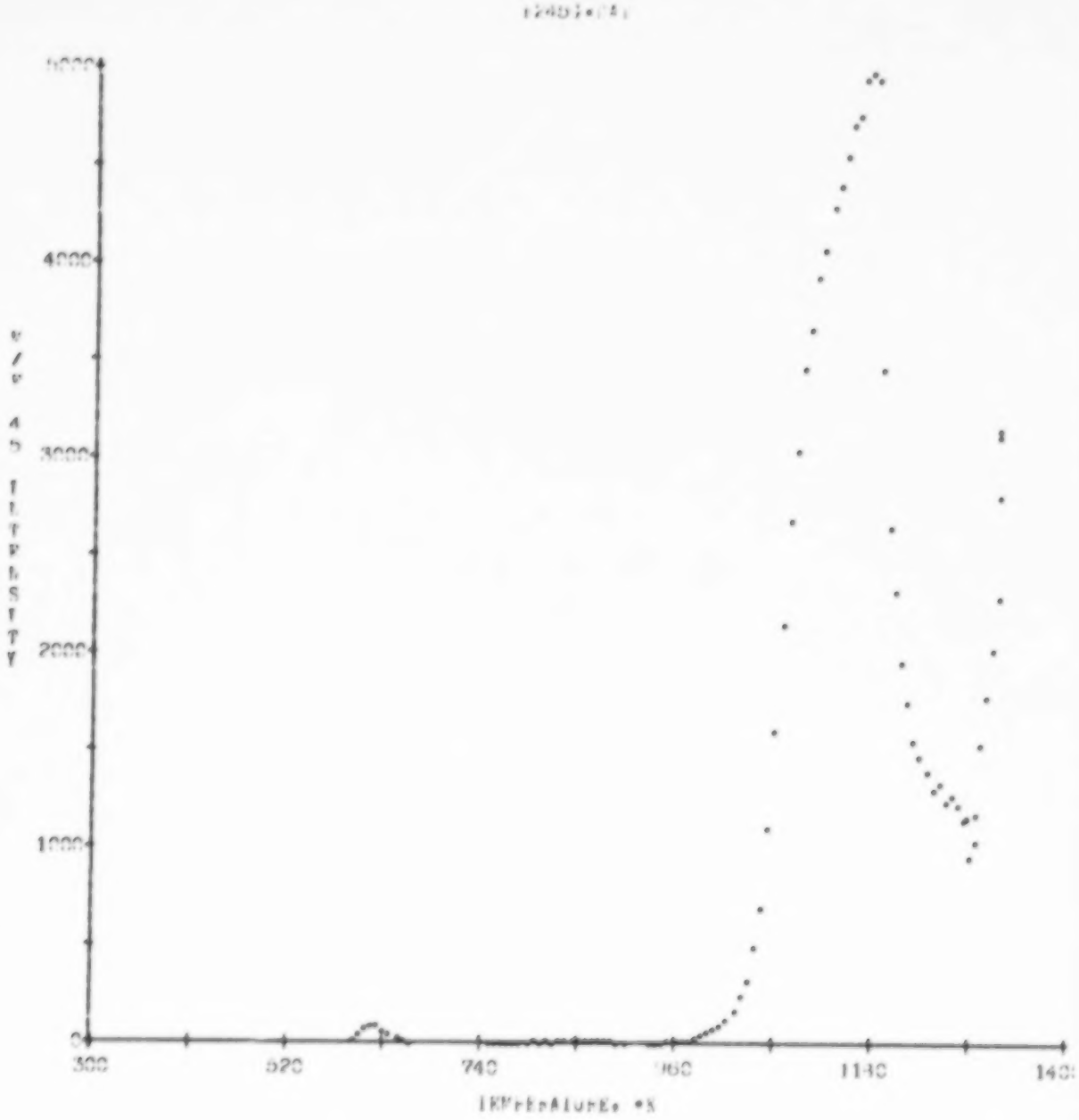

SYMBOL NO. OBS. REGRESSION

Figure 129

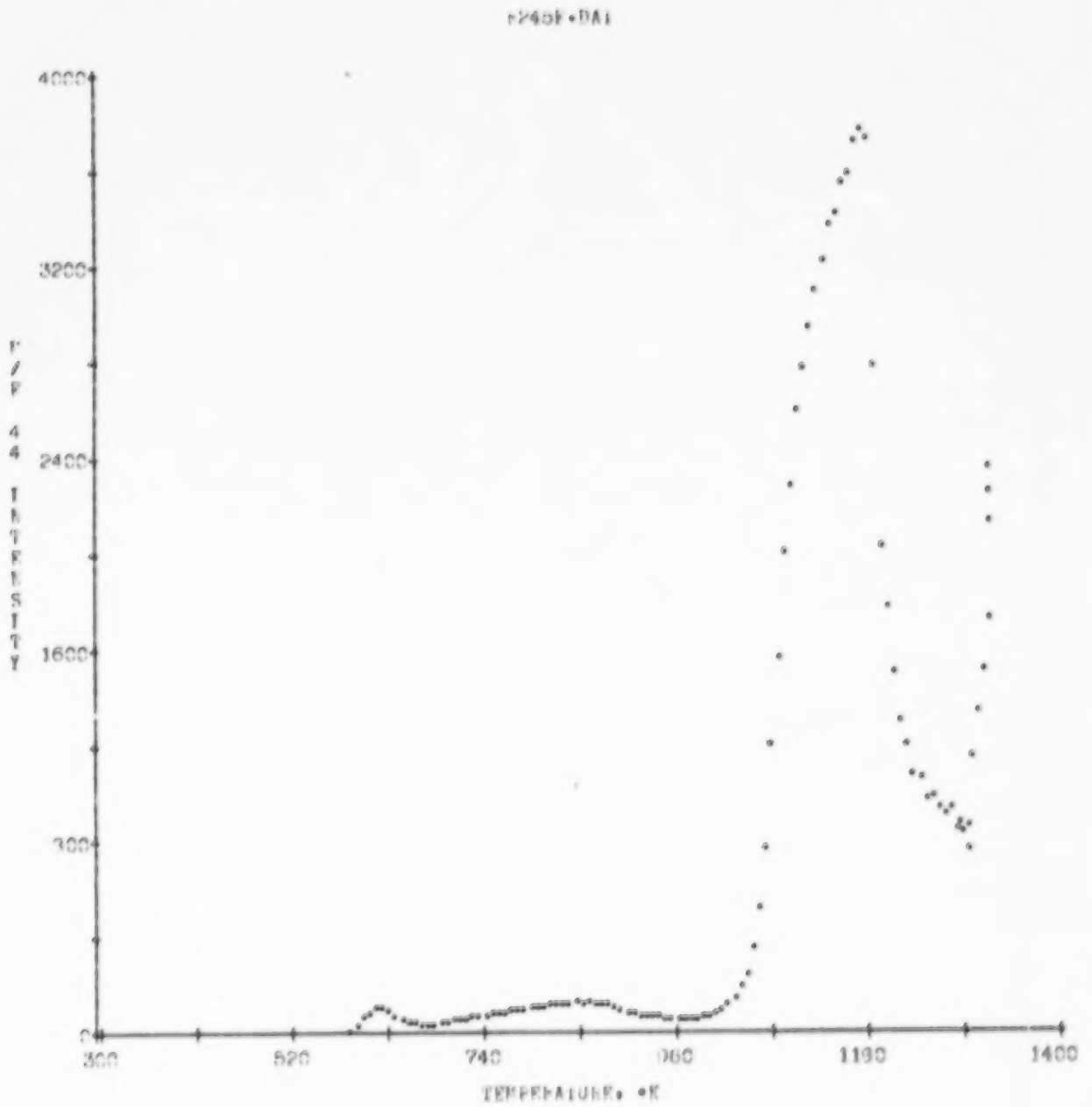

SYMBOL NO.PTS. LEGEND

. 107 C4121024 FLOW SAT C13, A1 + O2 AT 200 CC/MIN, 60°/MIN

Figure 130

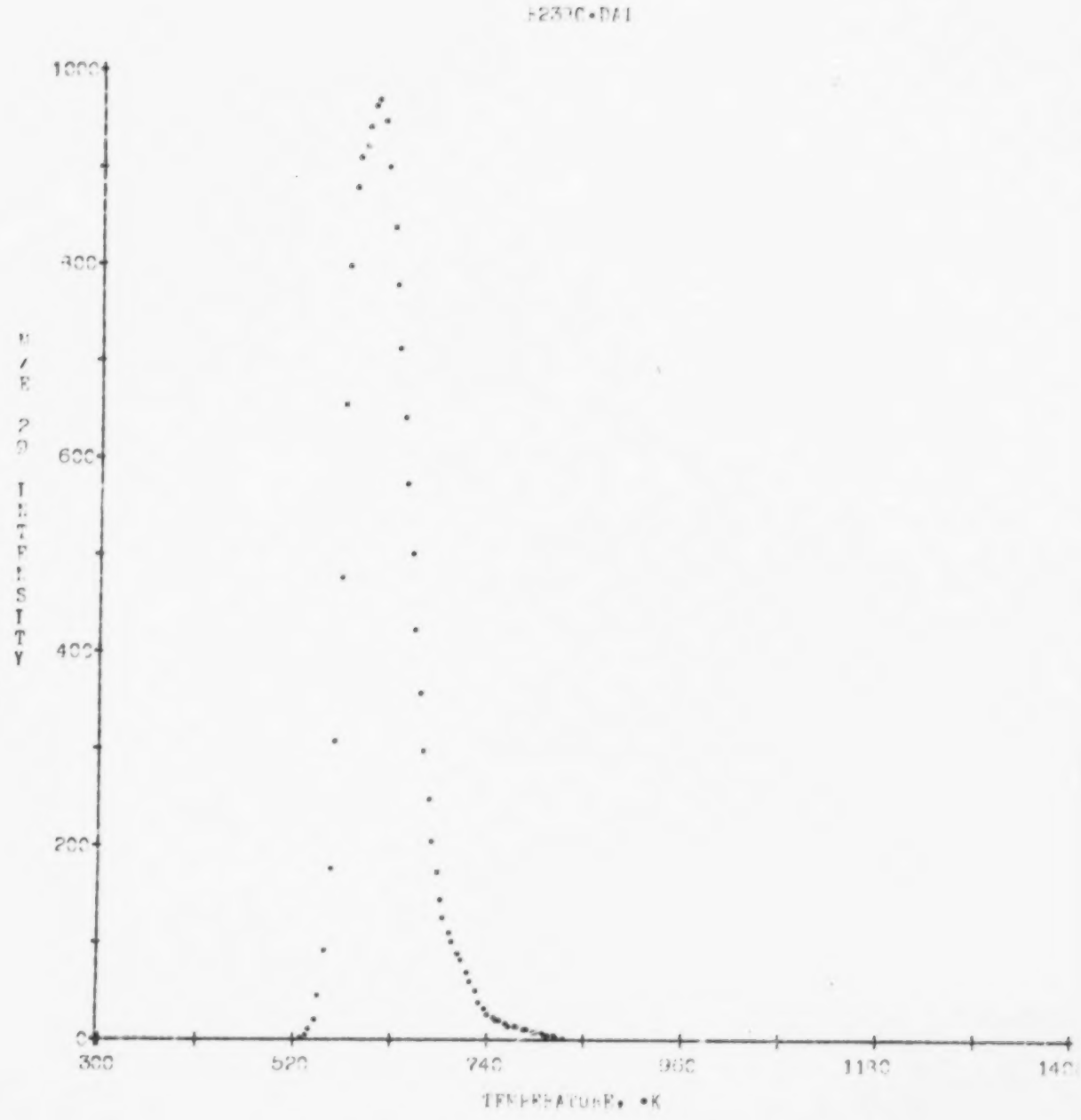

SYMBOL NO.PTS. LEGEND

• 60 C5230+ FROM SAT C13, AT + 14CO2 AT 200 CC/MIN, 30°/MIN

Figure 131

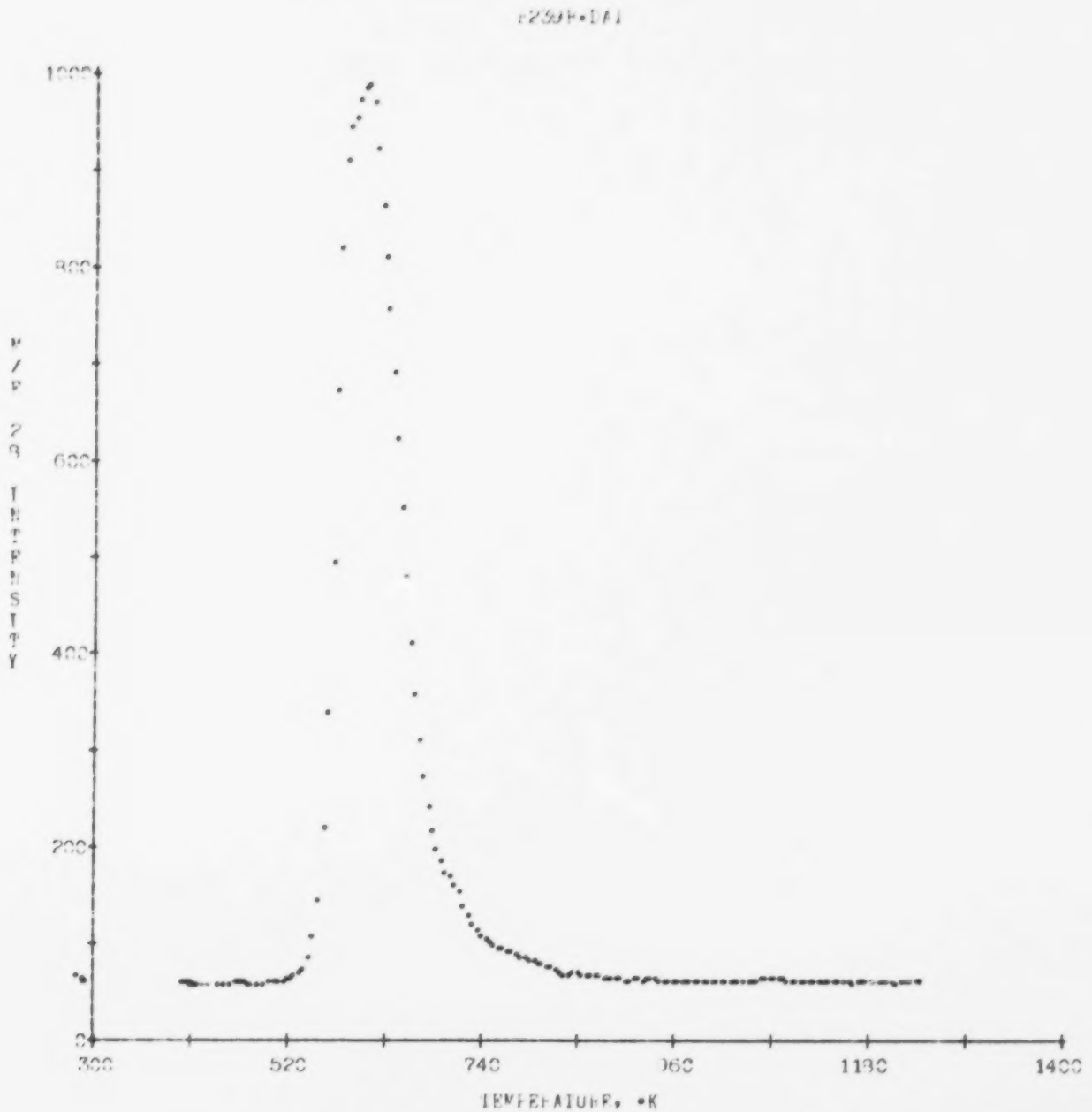

SYMBOL NO.PTS. LEGEND

. 179 C(13)O+ FROM SMI C13, AR + 1%CO2 AT 200 CC/MIN, 30°/MIN

Figure 132

APPENDIX E: Gaseous Evolution Data for Air Reactions

Figures: 133 - 134

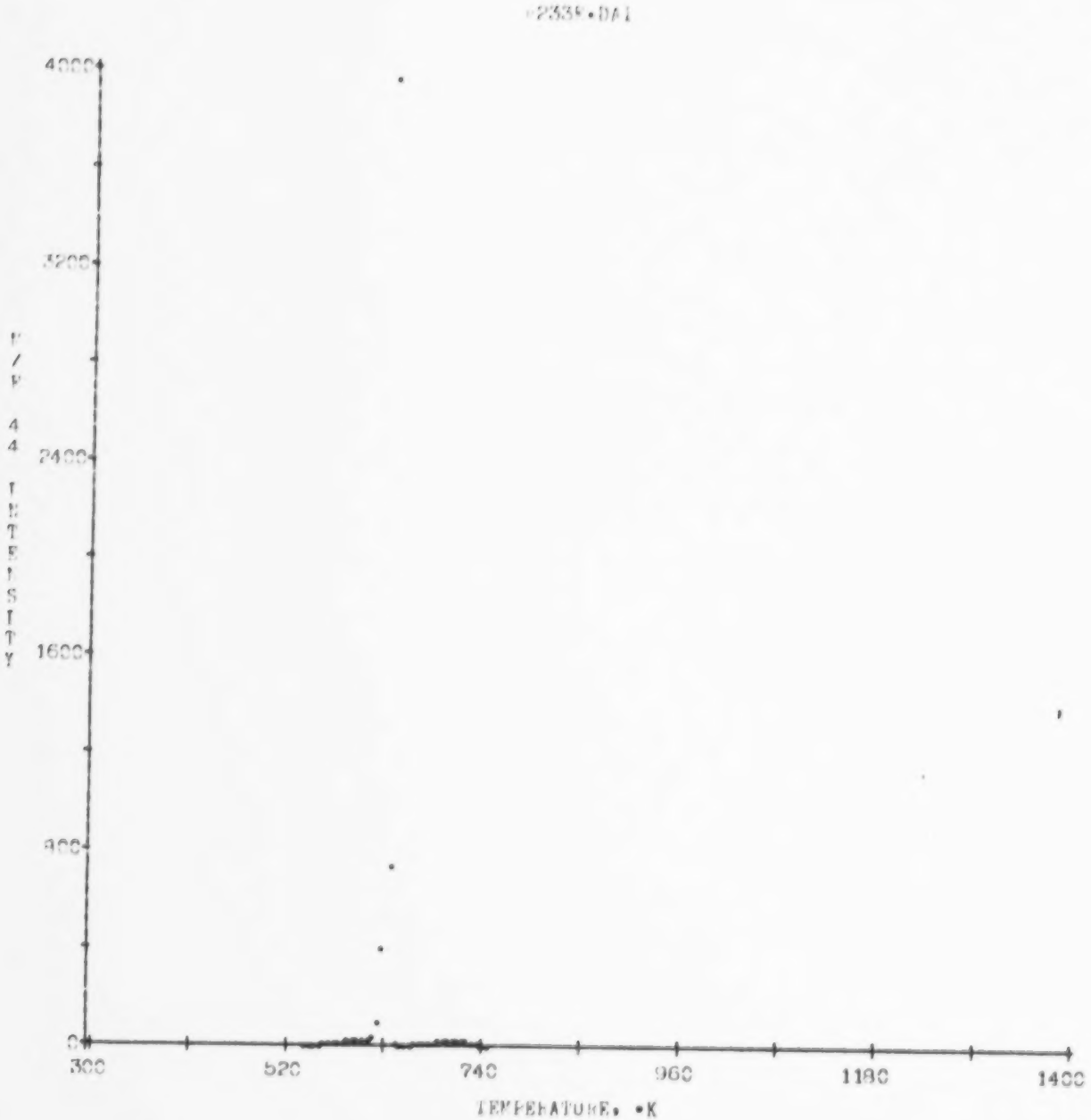

SYMBOL	NO. PTS.	LEGEND
•	39	CO2+ FROM SKI COAL #10, AIR AT 200 CC/MIN

Figure 133

1233C.DAT

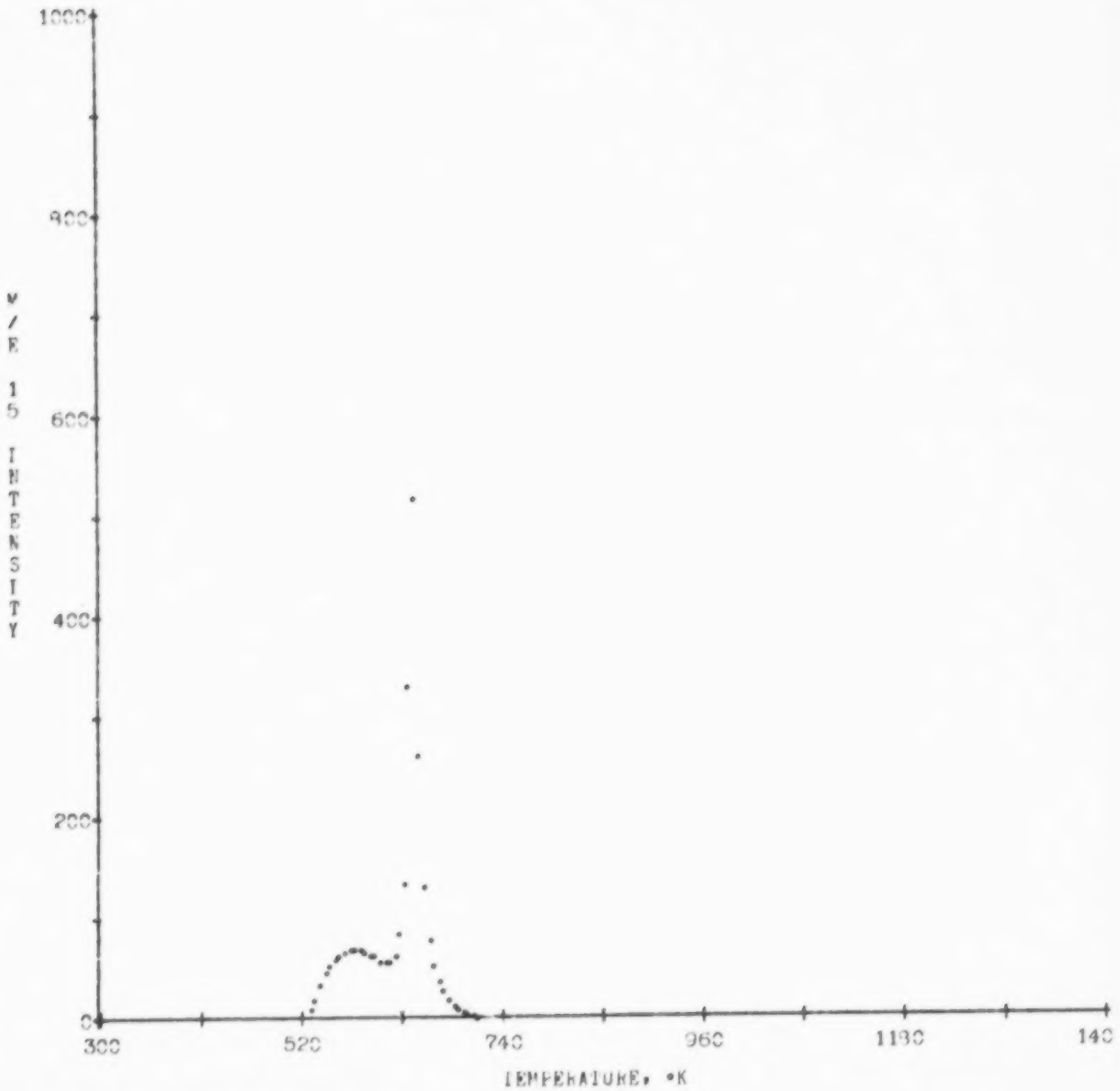

SYMBOL	NO.PTS.	LEGEND
.	35	H20+ FROM SRI COAL #1C, AIR AT 200 CC/MIN, 30°/MIN

Figure 134

BIBLIOGRAPHY

1. Scientific Research Instruments Corporation Report No. SRIC 71-15 (1971). NTIS No. PB 211481

2. Scientific Research Instruments Corporation Report No. SRIC 70-14 (1969). NTIS No. PB 211338

3. Operators Manual for Non-Isothermal Kinetics Laboratory, Scientific Research Instruments Corporation (1972).

4. A. L. Yergey, et al., (1972), Non-Isothermal Kinetic Studies of the Hydrodesulfurization of Coal, submitted for publication.

5. K. H. von Heek, H. Jüntgen and W. Peters, Ber. Bunsen Phys. 71, 113(1967).

6. F. H. Field, Acc. Chem. Research 1, 42(1968).

7. For example see C. Y. Wen, Optimization of Coal Gasification Processes, Vol. 1, U.S. Department of the Interior, Office of Coal Research, Chapter IV.

8. D. W. van Krevelen, Coal, Elsevier (1961) Chapters XII and XIII.

9. F. Bonner and John Turkevich, J. Am. Chem. Soc. 73, 561(1951).